UNIVERSITY OF LIVERPOOL

The Incidence of Cross-Linked Actin Networks (CLANs) in the Trabecular Meshwork of the Ageing Eye

---

Thesis submitted in accordance with the requirements of the University of Liverpool for the degree of Doctor of Philosophy by

Natalie Marie Pollock

May 2013

ABSTRACT

Cross-linked Actin Networks (CLANs) were first identified in bovine trabecular meshwork (BTM) cells in response to steroid treatment. Since then, work within our group has identified CLANs in human TM (HTM) cells and human tissue *ex vivo*. An alteration in the cytoskeleton of TM cells has been associated with changes in outflow facility and is a promising therapeutic target in glaucoma research. CLANs which are believed to make TM cells more rigid, were found in increase numbers in tissue from glaucomatous donors, but were also present in tissue from non-glaucomatous donors. This would indicate that CLAN formation is not merely a steroid response but may be triggered by changes within the outflow system.

The current work set out to identify CLAN inducing agents present within the normal outflow system and questioned whether age-related changes within the anterior chamber could influence CLAN number in a similar manner to glaucoma.

Investigating the influence of aqueous humor (AH) and some of its constituent growth factors on CLAN formation in both BTM and HTM cells revealed that AH itself was capable of inducing CLANs and that the main CLAN inducing agent present was TGF-β2. Conversely mitogenic growth factors (FGF and HGF) did not increase CLAN incidence and implicated that CLAN incidence was linked to cell shape change linked and therefore to function. I*n vitro* analysis of CLANs in reference to donor age revealed that TGF-β2 could induce a higher percentage of CLANs in HTM cells from older donors compared to HTM cells derived from younger donors. *Ex vivo* analysis run in parallel demonstrated that CLAN incidence increased with increasing donor age.In order to identify how age-related stress within the TM environment influenced CLAN incidence cells were treated with hydrogen peroxide. In BTM cells pre-treatment for 1 hour was sufficient to significantly increase CLAN incidence. In further experiments it would seem that CLANs are not associated with apoptotic cells nor with senescent cells.

The findings of this study indicate that CLANs can form when no glaucomatous pathology is detected and that changes in the extracellular environment can influence their formation. This is especial evident in older tissue.

ACKNOWLEDGEMENTS

I would like to thank my supervisors Prof. Ian Grierson and Dr. Luminita Paraoan. Thank you for giving me this wonderful opportunity and for your help; things have certainly changed since I first arrived in the department as an undergraduate student. Prof. Grierson, thank you for your guidance throughout my PhD and I have most definitely learned a lot from you.

Thank you to Age UK/ Research into Ageing for funding this work. To our continued collaboration with Dr. Clark and to Dr. Lane and Dr. Pang (Alcon Labs) for supplying the samples used in this study.

A big thank you to all my friends for putting up with my zombie like state and repetitive topic of conversation (my thesis). A special mention to a great friend and colleague, Laura Currie, for everything you've done for me. To everyone in Eye and Vision Science I had a great time working with you all and to the support staff in the institute for making my life a little easier.

To my boyfriend Ian, for all your support, love and for looking after me and his family for keeping me sane. I especially want to thank my Mum, my sister Vicki and brother Jason. Without your support throughout my life I know I wouldn't be where I am today. You have kept me going and kept me grounded. The mad scientist strikes again!!

PUBLICATIONS

Job, R., Raja, V., Grierson, I., Currie, L., O'Reilly, S., Pollock, N., Knight, E., Clark, A.F., 2010. Cross-linked actin networks (CLANs) are present in lamina cribrosa cells. The British journal of ophthalmology 94, 1388-1392

O'Reilly, S., Pollock, N., Currie, L., Paraoan, L., Clark, A.F., Grierson, I., 2011. Inducers of cross-linked actin networks in trabecular meshwork cells. Invest Ophthalmol Vis Sci 52, 7316-7324

Wade, N.C., Grierson, I., O'Reilly, S., Hoare, M.J., Cracknell, K.P.B., Paraoan, L.I., Brotchie, D., Clark, A.F., 2009. Cross-linked actin networks (CLANs) in bovine trabecular meshwork cells. Experimental Eye Research 89, 648-659

Hoare, M.J., Grierson, I., Brotchie, D., Pollock, N., Cracknell, K., Clark, A.F., 2009. Cross-Linked Actin Networks (CLANs) in the Trabecular Meshwork of the Normal and Glaucomatous Human Eye In Situ. Investigative Ophthalmology & Visual Science 50, 1255-1263.

PUBLISHED ABSTRACTS

Pollock N, Currie L, Paraoan L, Clark AF, Grierson I. Are cross-linked actin networks (CLANs) associated with age-related changes of th trabecular meshwork? *ARVO 2012.* Fort Lauderdale, Florida, USA; 2012

Pollock N, O'Reilly S, Paraoan L, Clark AF, Grierson I. Is TGF-b2 the component in aquesou humor responsible for induction of cross-linked actin networks (CLANs) in trabecular meshwork cells? , *ARVO 2011*

Grierson I, Heath A, **Pollock N**, Currie L. comparision between polygonal actin arrangements (PAAs) and cross-linked actin networks (CLANs) in cultured trabecular meshwork cells. *ARVO 2012*

Currie L, **Pollock N**, Paraoan L, clark AF, Grierson I. is transforming growth factor beta 2 an inducer of cross-linked actin networks (CLANs) in cultured optic nerve head cells (ONH)? , *ARVO 2012*

Grierson I, O'Reilly S, **Pollock N**, Currie L. cross-linked actin networks (CLANs) in cultured trabecular meshwork cell have an epitheliod shape and are immobile. *ARVO 2011*

TABLE OF FIGURES

LIST OF ABBREVIATIONS

NBF	Neutral buffered formalin
PBS	Phosphate buffered saline
PI	Propidium iodide
AH	Aqueous humor
IOP	Intraocular pressure
CLAN	Cross-linked actin network
PAA	Polygonal actin arrangement
TAPAS	Transient arrangement of polygonal actin structures
DMEM	Dulbeccos modified eagles medium
FCS	Foetal calf serum
TGF-β2	Transforming growth factor beta 2
HGF	Hepatocyte growth factor
FGF	Fibroblast growth factor
AGE's	Advanced glycation endproducts
POAG	Primary open angle glaucoma
TM	Trabecular meshwork
qPCR	Quantitative polymerase chain reaction
TC	Tissue culture

TABLE OF CONTENTS

1 Introduction

1.1 An ageing population

Ageing is a topic of much debate in the current climate as the populations of developed countries are experiencing a demographic shift in age according to united nations (United Nations. Department of and Social Affairs. Population, 2005). Data gathered during the 2001 census has shown for the first time that there are more 60 year olds than 16 year olds in the UK (Franco et al., 2007). Multiple factors have been implicated in the development of this shift (Crimmins, 2004). Improved health care and hygiene, in particular research and development in the early 20th C improved the childhood survival from infectious disease (Olshansky et al., 2001), thus reducing mortality rates (Christensen et al., 2009). More recently the influence of reduction in old-age mortality has led to an increase in life expectancy in developed countries. This increase in life expectancy has coincided with reduced fertility rates and has resulted in the ageing population (Baird et al., 2005). Some researchers have taken to dividing old age into 2 segments; young old age and "oldest old" (Bronnum-Hansen et al., 2009; Christensen et al., 2009; Suzman and Riley, 1985).

With this increase in life expectancy a major theme in research has been to improve the quality of those extended years (Nakasato and Carnes, 2006). "Conditions such as cognitive decline, arthritis and dysfunction of the senses may not be related to mortality rates but are highly associated with ageing" (Franco et al., 2007). Although advances in knowledge and health care have led to a postponement of limitations and disability in the population (Schoeni et al., 2008), data shows increases in chronic disease and conditions (Crimmins, 2004; Parker and Thorslund, 2007). Such considerations lead to the question (Vass, 2013); what is the point of surviving into old age if you can't live it?

1.2 Age-related loss of sight

One aspect of research which is tightly linked to improving the quality of life in the elderly is age-related loss of sight. Loss of sight in elderly persons can influence many aspects of life, as studies reveal mobility difficulties and reduced mobility among people with visual impairment (Nelson et al., 2003; Turano et al., 1999). The risk of falls is increased with age (Dolinis et al., 1997) leading to injury and increased hospitalization (Stevens et al., 2006). Several studies have shown that the risk of falling is associated with visual impairment (Black et al., 2011; Coleman et al., 2007; Freeman et al., 2007; Turano et al., 1999; Wood et al., 2011) and which may ultimately impact on a person's ability to remain in independent living (Tinetti and Williams, 1997). Loss of sight can also lead to increased feelings of isolation such that people with poor sight may begin to withdraw from society and are unable to interact with their environment (Weber and Wong, 2010).

According to the world health organisation 37 million people are registered as blind across the globe (Thylefors et al., 1995). While this value incorporates all age groups sub analysis revealed that 82% of this population were over 50 years old (Foster and Resnikoff, 2005; Resnikoff et al., 2004). Mean age of glaucoma onset was reported as 60 years with a progressive increase with increasing age (Mukesh et al., 2002; Quigley et al., 1994). Cataract (51%) was ranked as the primary cause of world blindness followed by glaucoma (8%) and age-related macular degeneration (5%) (Quigley and Broman, 2006; Resnikoff et al., 2004).

1.3 The anatomy of the human eye

The study of the human eye is not a new concept (Mark, 2010) and continued investigation into this fascinating organ has provided details of its internal structures and tissues, averaged dimensions of its structure, details of its various tissues and are still highlighting the function and dysfunction of its cells. The textbook diagrams illustrating the gross anatomy of the eye, such as that shown in Figure 1-1, are idealised drawings based on the human eye during its most stable period at 20-50 years (Adler et al., 2002; Davson, 1969; Forrester, 2008; Hogan et al., 1971; Oyster, 1999; Wolff et al., 1997), Most authors begin to describe the eye in one of two ways; as two fluid filled spheroids or as a series of layers with specific functions .Figure 1-1 is a diagram illustrating a sagittal section through the human globe and highlights the individual layers around the entirety of the globe, while identifying the chambers of the human eye and its main components.

The human eye is an enclosed system sheathed in three layers; the outer protective layer (green in figure) is composed of mainly collagen fibres which provide strength but still permit some degree of deformation. The opaque white scleral comprises most of this layer, except for the front where the orientation of the collagen is altered and so becomes the transparent cornea (Meller et al., 1997). The choroid layer (blue in figure) lies just beneath the sclera at the back of the eye but anteriorly protrudes into the globe in the form of the ciliary body and iris. This layer is highly vascularised throughout providing vital nutrients to the cells of the retina, ciliary body and iris. The final layer is the internal neural layer (red in figure) which is most prominent in the back of the eye where it exists as the retina. The internal neural layer extents anteriorly and forms the epithelium of the ciliary processes.

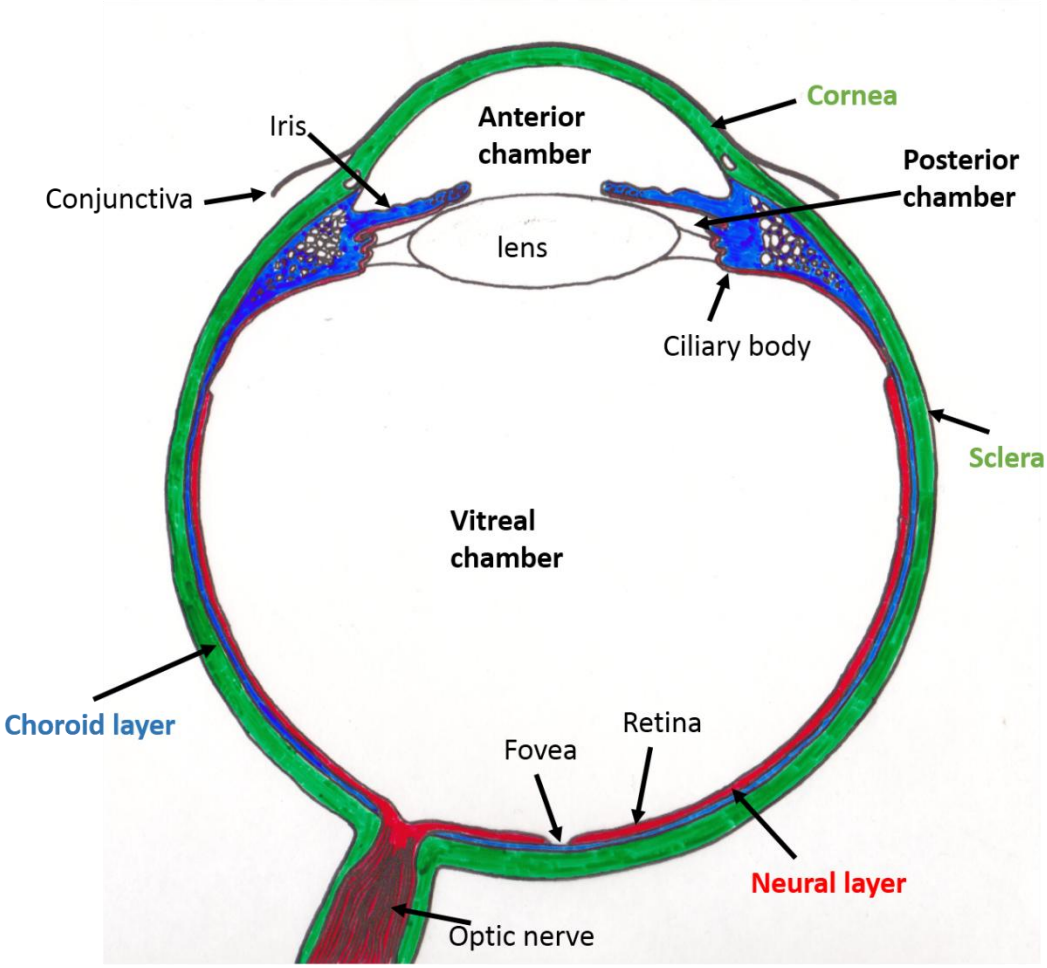

Figure 1-1. The gross anatomy of the human eye.

Diagram illustrates the main layers of the globe; green represents the outer protective sheath consisting of the opaque sclera and transparent cornea, the blue representing the choroid with the uveal extending from the back of the globe to the ciliary body and iris. The internal layer shown in red is the neural layer which includes the retina and continues as the ciliary epithelium. The main components of the globe are also labelled. (Altered from a drawing provided in house).

The protrusion of the iris and lens roughly demarcates the division of the internal space of the human eye into two fluid segments. The smaller anterior segment is separated from the larger posterior just behind the lens and iris where the vitreous attaches to the choroid layer, forming a physical barrier (Davson, 1969; Forrester, 2008; Hogan et al., 1971; Oyster, 1999; Snell, 1981; Wolff et al., 1997). The anterior segment consists of two chambers the anterior chamber is formed by the cornea, iris and anterior surface of the lens, while the posterior chamber is the small space between the lens and the iris into which AH is secreted.

Distinct tissues within these chambers carry out various functions which maintain the optimum conditions for sight (Adler et al., 2002; Ethier et al., 2004a). The vitreal chamber is demarcated by the presence of the retinal layer which begins just behind this barrier and extends toward the back of the eye and into the lamina cribosa region of the optic nerve (Ethier et al., 2004a). A major function of this chamber is the generation of clear neural signals which can be sent to the brain. The tissues of the anterior chamber are primarily used for the gathering and adjustment of light (Davson, 1969; Hogan et al., 1971; Wolff et al., 1997). Light must first pass through the layers of the cornea at the front of the eye, the amount of light which enters the posterior segment is modified by the pupillary aperture and refracted by the lens then passing through the internal space of the globe to the photosensitive receptors of the retina (Oyster, 1999). In order to gain sufficient information to create a clear image it is vital that the structures in this pathway are optically clear (Ethier et al., 2004a; Oyster, 1999). Blood vessels are therefore, not a practical means of supplying nutrients and removing waste to and from the tissues present in the light path (Mark, 2010). The role of the vascular system in the anterior and posterior chamber at the front of the eye is substituted to some extent by the aqueous humor (AH) (Davson, 1969; Forrester, 2008; Oyster, 1999; Wolff et al., 1997).

1.4 Aqueous humor formation

AH is a clear colourless fluid which is continually produced at a rate of approximately 2.4µl per minute (Davson, 1969) as a primarily energy dependant secretion from the non-pigmented epithelium of the ciliary processes (Macknight et al., 2000; McLaughlin et al., 2001) which extend outward from the ciliary body. As illustrated in Figure 1-1 the ciliary body and iris are extension of the uveal layer (chapter 7Adler et al., 2002) and are therefore populated by blood vessels which have long been known to have the numerous fenestrations which allows for solutes to pass easily across the capillary wall (Adler et al., 2002; Bill, 1975; Bill et al., 1980).

The early hypothesis that AH was simply a result of diffusion of the solutes from the vessels into the chamber was rejected with advancing insights that revealed several differences in composition (Kinsey, 1951; Mark, 2010), including relatively low concentration of proteins in AH (25mg/dL) compared with plasma (6g/dL) (Tripathi et al., 1989). Early investigations (Raviola, 1974) ruled that a physical barrier to solutes existed at the ciliary epithelium created by the nature of the epithelium as the processes are covered in a double epithelium (Raviola, 1977). The tight junctions between non-pigmented epithelial cells (Freddo and Raviola, 1982) physically block the passage of large molecules such as serum proteins. Freddo et al have suggested that the presence of proteins in the AH occurs not through entry into the posterior chamber but by direct entry into the anterior chamber (Freddo, 2001, 2013).

Energy dependent movement such as ion pumps (Jacob and Civan, 1996) are required for the passage of polar molecules such as glucose and charged ions such as K+ while water soluble molecules follow passively (Civan and Macknight, 2004; Macknight et al., 2000). Together these processes result in a fluid quite different from the plasma from which the components were derived (Brubaker et al., 2000; Civan and Macknight, 2004; Gaasterland et al., 1979). High concentrations of ascorbate in aqueous humor compared to blood plasma has been attributed to active transport (Brubaker et al., 2000; Ringvold et al., 2000) while the low mainly low molecular weight proteins are attributed to the physical barrier of the epithelium working as a molecular sieve (Bours, 1990).

The resultant fluid is sometimes referred to as “primary AH” as the composition of AH is altered through interactions with various tissues of the anterior chamber; the lens uses glucose, amino acids and potassium while releasing metabolites such as pyruvate (Allen et al., 1998; Bito, 1977). The central cornea takes in solutes and glucose while pumping out waste lactic acid (Joyce, 2003) so that the composition of AH is not uniform. Table 1-1 provides a range of constituents present in AH taken from various publications. These have been placed alongside the information that could be gathered relating to the constituents of culture media (mainly from the FCS) in which the cells are cultured (Thermo Scientific datasheet; Sigma datasheet; Aydin et al., 2005; Chowdhury et al., 2010; Freshney, 1992; Gryzunov et al., 1999; Jahn et al., 1983; Kim et al., 1992; Knisely et al., 1994; Lopatin et al., 1989; Tripathi et al., 1989).

Table 1-1. Comparison of the constituents of AH compared to those likely present in culture media.

Several publications have investigated the various constituents of AH and in some instances there has been great variation in the concentrations provided due to variations in techniques used and depending on donor health and species used. The use of FCS enriched medium, while a universally accepted method of culturing cells, does not always provide the same environment cells would experience in vivo. The exact constituents present are also not widely available as the components are purchased from commercial companies. From the information gathered here it is clear that the components available during cell culture are different to those in vivo. Those marked * have no data relating to concentrations.

Constituents	FCS	AH	
		cataract	glaucoma
Total proteins	40-80 mg/ml	125-500ug/ml	
Albumin	20-50mg/ml	290ug/ml	
Fibronectin	1-10ug/ml	5-100ng/ml	
Globulins	1-15mg/ml	5-10ug/ml	
Protease inhibitors	00.5-2.5mg/ml	*	
Transferrin	2-4mg-ml	0.5-1ng/ml	1-4ng/ml
Total growth factors	1-100ng/ml	*	
bFGF	37pg/ml	1.07 ±0.3	0.4-1.4ng/ml
TGF-β1	12.6ng/ml	0.2-0.5ng/ml	
TGF-β2	10-20ng/ml	0.9-1ng/ml	1-2ng/ml
HGF	*	0.02-0.9ng/ml	0.5-0.9ng/ml
IGF	100ng/ml	1-1.5ng/ml	
EGF	*	≤ 0.1ng/ml	
PDGF	*	≤0.3ng/ml	
Lipids	2-10mg/ml	16.4mg/dL	
Glucose	0.6-1.2mg/ml	2.8uM	
Lactic acid	0.5-2.0mg/ml	4.5uM	
Pyruvic acid	2-10ug/ml	10uM	
Urea	170-300ug/ml	6.1uM	
Ascorbate	*	1.06uM	
Calcium	4-7mM	2.5uM	
Chlorides	100uM	131uM	
Iron	10-50uM	0.97-1.05uM	
Potassium	5-15mM	3.9uM	
Phosphate	2-5mM	0.6uM	
Magnesium	1-2mM	1.2uM	
Sodium	135-155mM	152uM	
Zinc	0.1-1.0uM	0.62-1.10uM	
Hormones	0.1-200nM	*	
Hydrocortisone	10-200nM	18ng/ml	

1.5 Growth factors in the aqueous humor

Although the concentration of proteins in the AH is small in comparison to plasma the composition and quantity of the proteins present in AH has been investigated in some detail (Bours, 1990; Chowdhury et al., 2010; Dernouchamps, 1982; Tripathi et al., 1989). The composition of AH has been shown to be altered in many intraocular disorders, such as glaucoma (Duan et al., 2010; Kuchle et al., 1994) with a major focus on the presence and concentrations of many growth factors including transforming growth factor (TGF), hepatocyte growth factor (HGF), fibroblast growth factor (FGF), transferrin, epidermal growth factor (EGF), platelet-derived growth factor (PDGF) and vascular endothelial growth factor (VGF) (Benezra and Sachs, 1974; Cousins et al., 1991; de Boer et al., 1994; Inatani et al., 2001; Jampel et al., 1990; Klenkler and Sheardown, 2004; Tripathi et al., 1992) Although the concentrations of these growth factors has been found to differ across species , the relative abundance and conserved presence may indicate their importance in the system (Calthorpe et al., 1991; Hogg et al., 1995).

1.5.1 Transforming Growth Factor-beta (TGF-β)

TGF-β was first identified in 1980's (Sporn, 2006) and since this first discovery many other proteins have been identified and classed as belonging to the TGF-β family. All members of this family contain a dimeric structure and cysteine knot motif and are sub divided into TGF-β's, BMP's, GDF's, MIF's and activins (Massague, 2006). These proteins are known to illicit many cellular functions including cell proliferation, adhesion, migration, production of ECM and apoptosis (Massague, 2012; Roberts et al., 1990a; Sporn et al., 1986).

Of the 6 isoforms of TGF-β known to exist, three isoforms (TGF-β1, β2, β3) have been identified in mammalian cells including ocular cells (Agarwal et al., 1997; Pasquale et al., 1993; Roberts and Sporn, 1992) and in normal AH (Jampel et al., 1990). Of these isoforms, TGF-β2 is the most abundant in the AH of adult human eyes (Jampel et al., 1990). The main source of TGF-β2 is thought to be the secretions via the ciliary epithelium and the lens epithelium (Allen et al., 1998), where it is secreted as a latent complex (Annes et al., 2003). The majority of TGF-β2 present in AH is in this latent

form (Tripathi et al., 1994a) and requires activation by proteolytic processing (Annes et al., 2003).

TGF-β initiates various functions by binding to cell surface serine/threonine kinase receptors identified as TGFβR type I/ALKs and TGFβR type II (Attisano et al., 1994; Fanger et al., 1986; Massague, 2000; Massague and Gomis, 2006). This causes the formation of a receptor complex in which type II receptor phosphorylates the type I receptor (Wrana et al., 1992; Wrana et al., 1994). The intracellular signalling initiated by TGF-β2 is mediated through the Smad pathway which involves several Smad proteins. These proteins have two globular domains connected by a linker region (Wu et al., 2000); While one domain binds to DNA the other is responsible for binding of other molecules (Sigal, 2012). Smads are transcriptionally inert when non-phosphorylated but are capable of attaching to the receptor complex (Lutz and Knaus, 2002) and undergoing phosphorylation (Santibanez et al., 2011). Phosphorylated Smads undergo continual cycling and shuttling into the nucleus under TGF-β stimulation (Derynck et al., 1998). Once within the nucleus Smads are capable of altering gene expression (Massague, 2006; Shi and Massague, 2003). TGF-β2 can also activate Smad independent mediators such as ERK and JNK (Derynck and Zhang, 2003; Lutz and Knaus, 2002).

TGF-β is a molecule of interest for several reasons; TM cells are known to not only secrete TGF-β (Tripathi et al., 1994b) but express TGF-β receptors (Agarwal et al., 1997; Tripathi et al., 1993; Wordinger et al., 1998) and the concentration is increased in AH of glaucoma patients (Inatani et al., 2001; Ochiai and Ochiai, 2002; Ozcan et al., 2004; Tripathi et al., 1994a). Perfusion studies (Fleenor et al., 2006; Gottanka et al., 2004) and more recent animal models (Shepard et al., 2010) have demonstrated that TGF-β2 increases IOP and so has been implicated in the pathogenesis of glaucoma (Agarwal and Agarwal, 2010; Fuchshofer and Tamm, 2012; Lutjen-Drecoll, 2005).

TGF-β1 is induced by mechanical stress in TM cells (Liton et al., 2005b) and causes morphological changes in anterior chamber (Robertson et al., 2010) while TGF-β2 evokes many cellular changes in TM cells (Fleenor et al., 2006; Gottanka et al., 2004; Tamm et al., 1995) with HTM cells responding differently depending on the disease

state of the donor (Liu et al., 2003b). Perfusion with TGF-β2 has been shown to increase the expression of many ECM molecules including collagens, laminin, elastin, cochlin, fibronectin (Li et al., 2000), fibulin, versican, thrombospondin-1 and myocilin (Bollinger et al., 2011; Flugel-Koch et al., 2004; Sethi et al., 2011a). As well as increasing the expression of ECM molecules TGF-β2 alters the enzymatic degradation of the ECM. In vitro studies have shown the TGF-β2 induces plasminogen activator inhibitor (PAI)-I (Fuchshofer et al., 2003). TGF-β2 has also been shown to increase the expression of several enzymes in the TM. Transglutaminase (Tovar-Vidales et al., 2011; Welge-Lussen et al., 2000) and lysyl oxidase (LOX) (Sethi et al., 2011b) are increased by TGF-β2 treatment *in vitro*. The importance of these enzymes is that they cross-link components of the ECM (namely fibronectin, collagen and elastin) and reduce ECM turnover (Cao et al., 2002). Gene and protein expression are altered (Bollinger et al., 2011; Fuchshofer et al., 2009; Zhao et al., 2004) and *In vitro* studies have shown that TGF-β2 reduces the rate of cell proliferation even in the presence of mitogen EGF (Wordinger et al., 1998).

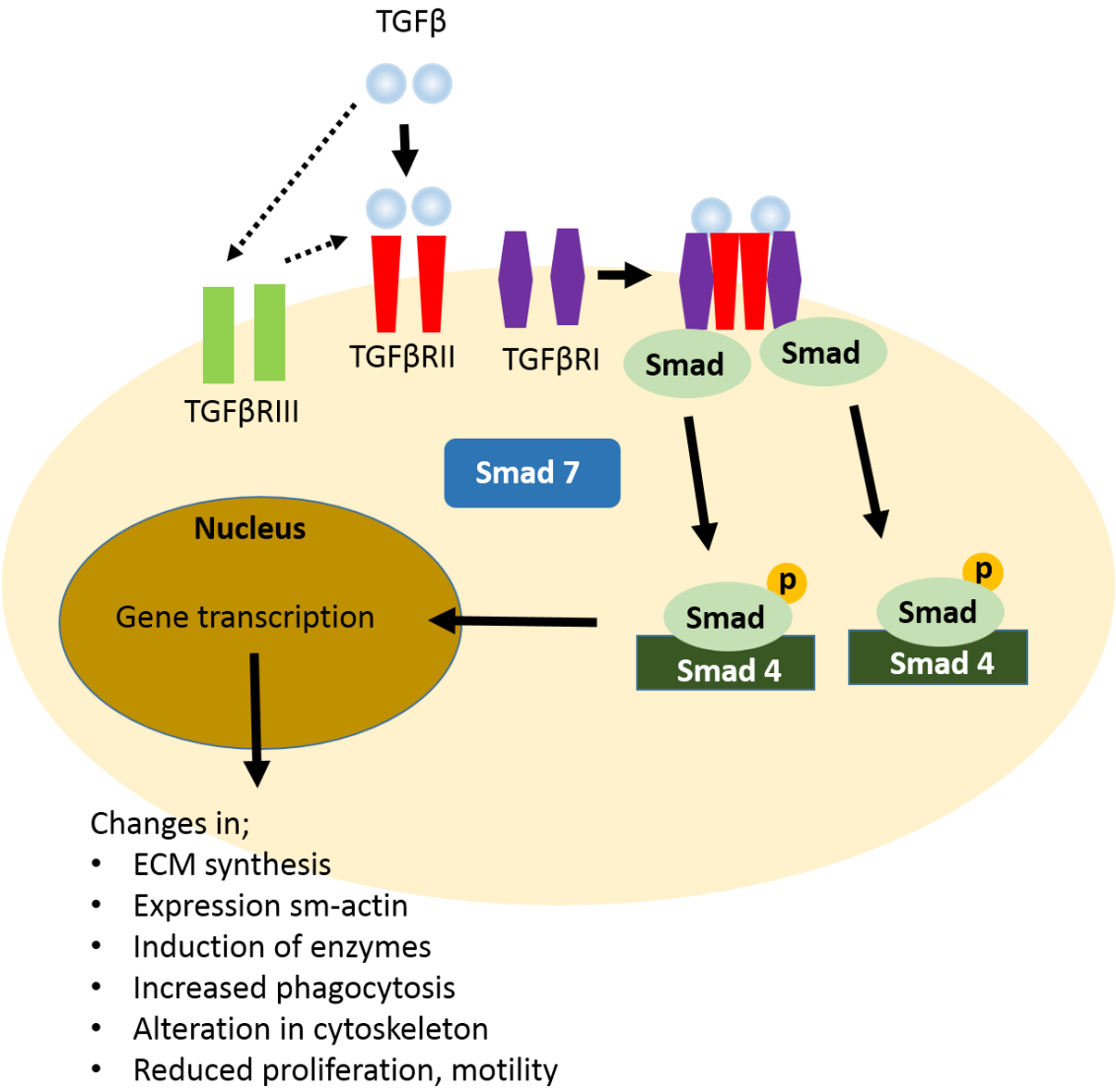

Figure 1-2. The TGF-ß pathway.

Diagram illustrating the basic signalling of TGF-ß. Three receptors for TGF-ß2 have been identified in the plasma membrane. TGF-ßRII and RI form a receptor complex upon the binding of a molecule. Activation of the receptor complex results in the phosphorylation of the Smad signalling cascade. Smad translocate to the nucleus where it alters gene transcription. In TM cells can lead to several alterations in cell function including increased expression of ECM components, alteration in cytoskeletal organisation and inhibition of proliferation.

1.5.2 Hepatocyte Growth Factor (HGF)

HGF was originally identified as a potent mitogen for hepatocytes (Nakamura and Mizuno, 2010; Nakamura et al., 2011) and found to be an identical molecule to scatter factor (Bhargava et al., 1992; Furlong et al., 1991), a fibroblast derived modulator of cell mobility (Nakamura and Mizuno, 2010; Nakamura et al., 2011; Stoker, 1989). Since its identification it has been found to initiate many cellular functions in a variety of cells (Nakamura et al., 2011; Takebayashi et al., 1995) including cell shape change in human RPE cells (Briggs et al., 2000) whereby the mainly epithelial cells became more spindle. In the eye HGF is produced by many cells including several which surround the anterior chamber such as corneal endothelium, lens and iris epithelium and trabecular cells (Grierson et al., 2000; Li et al., 1996; Weng et al., 1997). The cytokine is produced as an inactive precursor (Nakamura et al., 2011), upon activation it binds to trans membrane high affinity c-Met receptors (Weidner et al., 1993) which undergo a conformational change that initiates the signalling cascade (Matsumura et al., 2013; Stuart et al., 2000).

HGF has been identified in AH under normal conditions with values ranging from 0.02-0.93ng/ml (Araki-Sasaki et al., 1997; Hu and Ritch, 2001; Salom et al., 2010) and it is believed that its presence is due to the secretion from local tissues. Levels of HGF are found to be increased in AH of glaucomatous eyes (0.967ng/ml) (Hu and Ritch, 2001). TM cells were shown to express the c-Met receptor (Wordinger et al., 1998), and treatment with HGF can elicit a mitogenic response in TM cells (Grierson et al., 2000).

1.5.3 Fibroblast Growth Factor (FGF)

Another important growth factor present in AH is basic FGF which is found at concentrations ranging from 0.4-1.4ng/ml (Tripathi et al., 1992). The polypeptide was first isolated from the brain and found to be a potent mitogen for cultured fibroblasts (Bikfalvi et al., 1997). Since the identification of acidic and basic FGF, 22 different members have been assigned to the family (Itoh and Ornitz, 2011; Ornitz and Itoh, 2001).These structurally similar polypeptides have variable amino and carboxyl terminals and have been defined by their strong heparin affinity (Burgess et al., 1994; Powers et al., 2000; Seddon et al., 1991; Zhang et al., 1991). FGF is capable of initiating numerous cellular functions in a variety of target cells including cell proliferation, differentiation and angiogenesis (Bikfalvi et al., 1997; Coutu and Galipeau, 2011; Ornitz and Itoh, 2001). FGF can initiate these functions by binding to the extracellular surface of tyrosine kinase receptors (Powers et al., 2000). Once bound phosphorylation of the cytoplasmic region causes the recruitment of other signalling molecules and leads to signal transduction (Mohammadi et al., 2005; Ornitz and Itoh, 2001; Powers et al., 2000; Seddon et al., 1991).

Within the eye FGF plays a key role in lens development (McAvoy et al., 1991) and corneal wound healing (Rieck et al., 2001), it is also a potent mitogen of TM cells and was used as an essential proliferative stimulant of HTM cells from explants (Polansky et al., 1979).

1.6 The flow of Aqueous humor

The complex composition of AH illustrates that it is required to provide vital nutrients to avascular tissues in the anterior chamber and also remove waste products in order to maintain the optically clear conditions required for sight (Ethier et al., 2004a). It is the continual cycling of the AH, from its production at the ciliary processes in the posterior chamber into and around the anterior chamber that ensures the tissues are well maintained (Lutjen-Drecoll et al., 2001). The flow of AH is facilitated by the drainage of the AH via the outflow system, creating the continual turnover (Tan et al., 2006). The AH flows through the pupil into the anterior chamber where it circulates via convection currents (Canning et al., 2002) produced by the temperature difference created by the relatively cool cornea and the warmer vascular iris. As well as the nutritional role, the AH exerts a force on the globe creating an intraocular pressure (IOP) (Johnson, 2006; Overby et al., 2009) and maintains the shape of the globe for visual acuity (Adler, 1965; Ethier et al., 2004a). IOP is dependent on the rate of formation and the resistance produced by the outflow pathways and is relatively stable in healthy persons ranging from 15-21mmHg (McLaren, 2009; Toris et al., 1999) with diurnal fluctuations (Liu et al., 2003a).

The route of AH outflow has been explored in some detail, particularly by Bill et al (reviewed in Alm and Nilsson, 2009; Bill, 1993; Bill and Phillips, 1971). The use of dyes during these studies identified the site of aqueous drainage in the corneoscleral limbus region shown in Figure 1-3 and identified that AH could exit the chamber via two pathways in the anterior chamber angle commonly referred to as the conventional and unconventional (reviewed in Tamm, 2009).

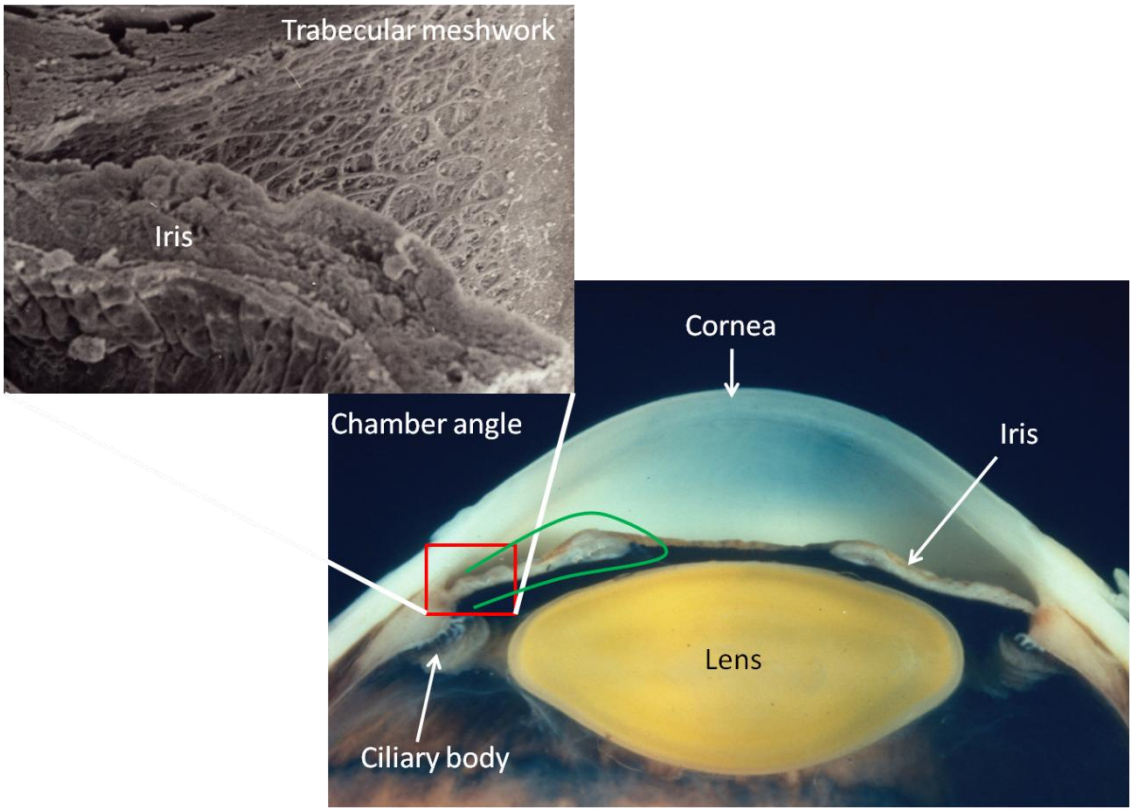

Figure 1-3. Composite image showing gross morphology of the anterior and posterior chambers.

The composite image demonstrates the morphology of the anterior chamber with the major tissues identified. AH is produced by the ciliary epithelium in the posterior chamber and as the green line illustrates it flows through the pupil into the anterior chamber. AH exits the eye via two pathways located in the chamber angle. The insert is an electron micrograph of chamber angle (images kindly provided by Prof. Grierson).

1.7 Outflow in the chamber angle

The chamber angle is created by the anterior portion of the ciliary body and protrusion of the iris away from the sclera into the centre of the globe at the corneal limbus region (Davson, 1969; Hogan et al., 1971; Oyster, 1999; Wolff et al., 1997). The limbus is the region in which the clear cornea meets the opaque scleral so that internally the peripheral corneal cells meet at schwalbe's line (transition zone). The trabecular meshwork begins at the transition region and extends towards the scleral spur and connects with the root of the iris (Tamm, 2009) (Figure 1-4).

1.7.1 The Unconventional outflow system (Uveoscleral)

Outflow via the unconventional occurs due to bulk flow forcing fluid through the intracellular spaces (Alm and Nilsson, 2009) which exist due to incomplete cellular coverage of the trabeculae and the anterior surface of the iris. Aqueous humor can therefore flow directly from the anterior chamber into the ciliary body. Work with monkeys showed that the connective tissue between muscle bundles was sparse and allowed for easy diffusion through the sclera (Inomata and Bill, 1977; Inomata et al., 1972).

There has been some debate over the exact percentage of outflow through the unconventional route as a direct method for measurement in humans is difficult (Toris et al., 1999). Investigations carried out by Bill et al (Bill and Phillips, 1971) reported uveoscleral outflow at 4% and 14% of the total outflow. The use of animal models (Green et al., 1977; Inomata et al., 1972; Pederson et al., 1977) has provided varying values. The physiological role of the unconventional outflow pathway is not clear and it has been stated that the trabecular route seems more equipped to deal with aqueous outflow. In a recent review by Alm and Nilsson, it was speculated that the outflow via the uveoscleral route could not be prevented, and as it has no negative consequences there has been no evolutionary alterations to prevent it (Alm and Nilsson, 2009). However, this pathway is important in glaucoma treatment, as it is the target of the most commonly used anti-glaucoma drugs (Cracknell and Grierson, 2009; Toris, 2010).

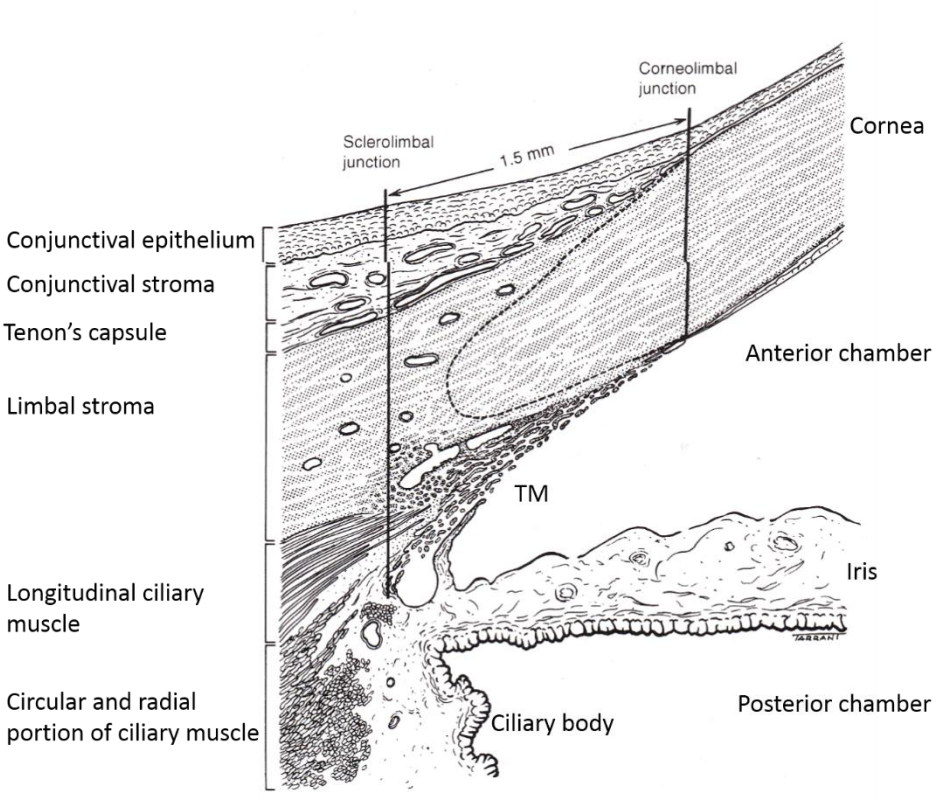

Figure 1-4. Schematic diagram showing the corneoscleral limbus region.

This illustration has been altered from Hogan (Hogan et al., 1971) and highlights the limbus region where the peripheral corneal endothelium transitions into the scleral. The chamber angle is created by the protrusion of the iris from the limbus region. The TM extends across the internal surface of the limbus from schwalbe's line back towards the ciliary muscle.

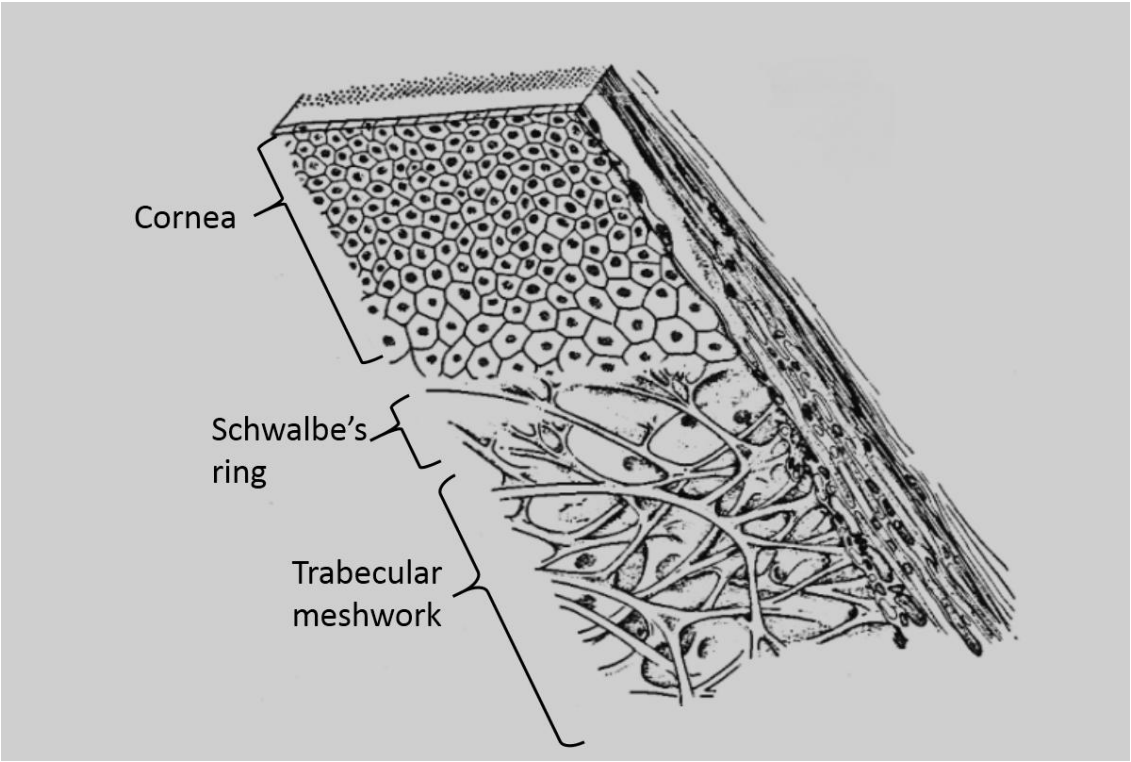

Figure 1-5. Schematic of transition from cornea to trabecular meshwork.

Schematic diagram modified from the human eye (Oyster, 1999), illustrating the transition region of the limbus. The peripheral corneal endothelium and TM both extend towards schwalbe's line/ring. The corneal endothelium is clearly distinguishable by the cobblestone appearance of the cells.

The majority of the AH flows through the conventional pathway which requires fluid to pass through the uveal and corneoscleral TM, the JCT and schlemm's canal before returning to the blood in the episcleral veins (Inomata et al., 1972; Lutjen-Drecoll, 1999b; Lutjen-Drecoll et al., 2001; Tamm, 2009).

1.7.2 The Conventional Outflow system

The first tissue that the AH encounters on the conventional pathway is the trabecular meshwork. This tissue is a complex meshwork of beams with a central core composed of collagen and some elastin (Gong et al., 1989). This scaffold is then sheathed in a monolayer of endothelial (Tamm, 2009) (Figure 1-6), smooth muscle-like cells (Wiederholt et al., 2000) which rest on a basement membrane containing collagen IV, laminin and fibronectin (Fuchshofer et al., 2006; Marshall et al., 1990; Ueda et al., 2002; Ueda and Yue, 2003) thus separating the cells from the central core (Rohen et al., 1993). Despite this basic organisation there are structural variations in the orientation of these beams, which has led to the TM being described as two regions (Hogan et al., 1971; Lutjendrecoll et al., 1981; Oyster, 1999; Tamm, 2009). Anteriorly the TM begins at the transition region where the meshwork cells meet the cells of the peripheral cornea at schwalbe's ring (Figure 1-5) (Davson, 1969; Forrester, 2008; Hogan et al., 1971; Oyster, 1999; Snell, 1981; Wolff, 1976). This uveal meshwork is the region furthest from schlemm's canal and therefore the first region through which the AH must pass. Extending posteriorly it attaches to the ciliary body and iris root (Davson, 1969; Hogan et al., 1971; Oyster, 1999; Wolff, 1976). The uveal meshwork is composed of chord-like structures (Figure 1-7) which weave and branch to form a maze of relatively large spaces, approximately 20-75 μm (Grierson, 1987; Tan et al., 2012; Wolff et al., 1997). The intra-trabecular spaces in this region offer virtually no resistance to flow and form 1-3 layers of the meshwork. Mathematical equations (Poiseuille's law) have been applied to the flow of AH through the various regions of the TM and have shown that pore size will influence the easy with which flow occurs and therefore influence pressure. "Pores of 100μm long and 20μm diameter could carry the entire AH flow (2μl/min) with a drop in pressure of 5mmHg" (Johnson, 2006). This suggested that the spaces in the uveal meshwork would offer no resistance to outflow; a finding that was proven experimentally by Grant et al (Grant, 1963; Overby

et al., 2009) The work of Barany (1959) was among the first to highlight that the passage of fluid through a pore may be retarded due to the “absorption of particles in the pores”(Barany, 1959). The diameter of free flowing materials is much smaller than the actual pore size given the presence of particles that have accumulated around the edges.

Passing further into the tissue the orientation of the trabeculae beams changes and the intra-trabecular spaces decrease in size (Davson, 1969; Oyster, 1999; Tan et al., 2012; Wolff et al., 1997). The images in Figure 1-8 show how the trabeculae continue to flatten until they form sheets which are perforated with pores. This organisation reduces the spaces through which AH can flow further and is called the corneoscleral region.

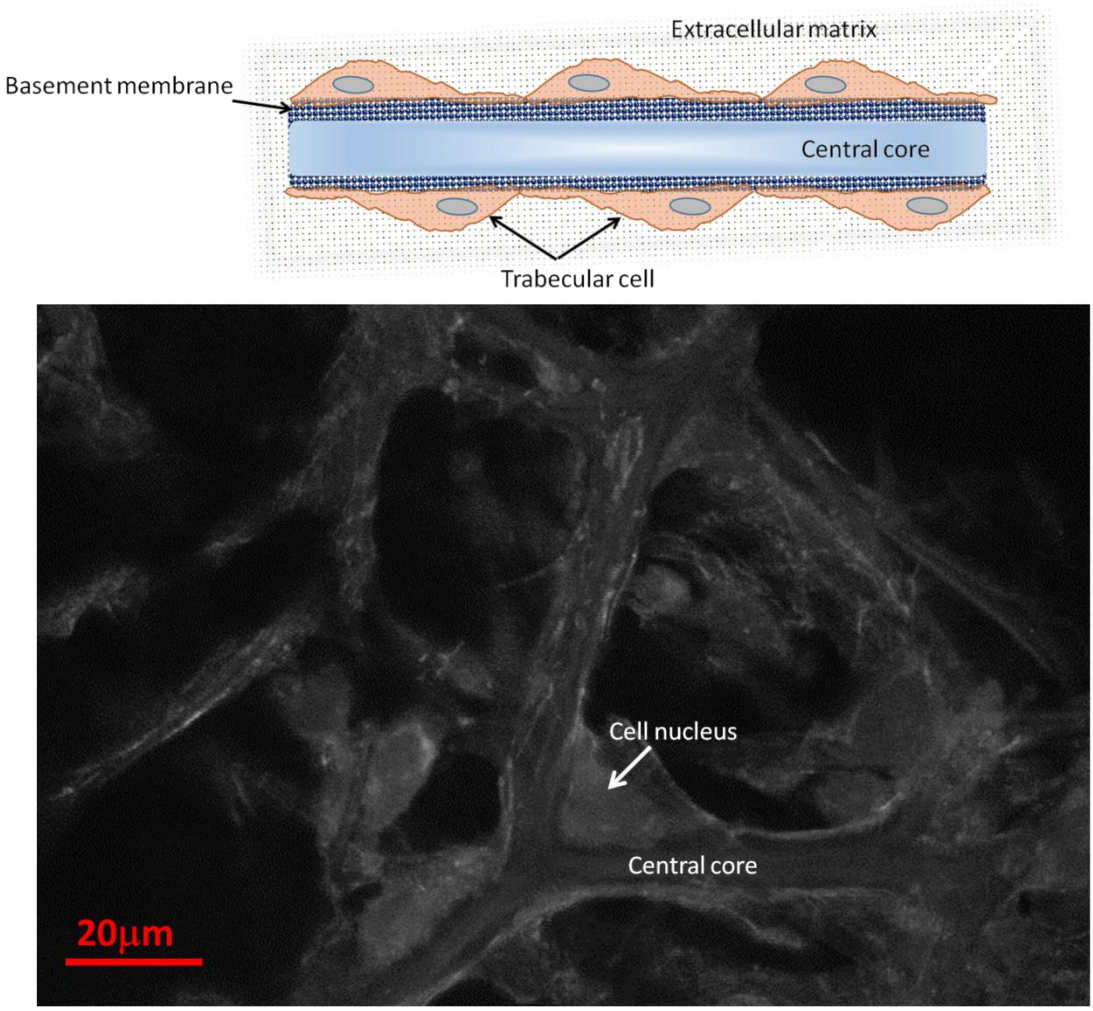

Figure 1-6. Structure of the uveal meshwork.

The top image is a schematic diagram of trabecular beams illustrating the structural components. The TM cells rest on a basement membrane which separated them from the central core. On the apical surface the TM cells are in contact with ECM. The appearance of the uveal meshwork in situ is demonstrated by the lower image; a confocal image of uveal meshwork showing auto-fluorescence of central core and the position of some TM cell nuclei.

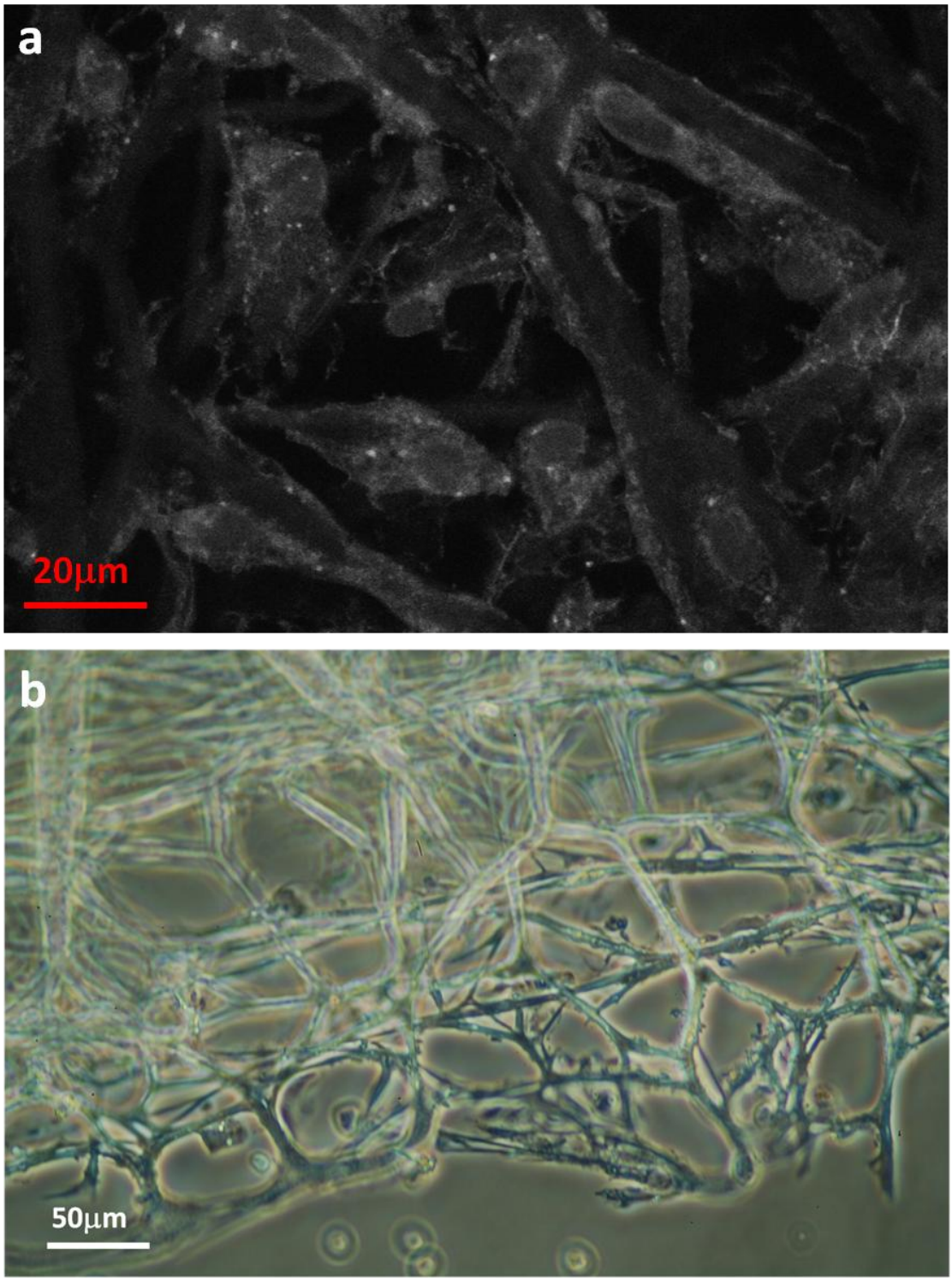

Figure 1-7. Confocal and phase contrast image of uveal meshwork.

Both images show the organisation of the trabecular beams in the uveal meshwork. Image a. was captured via confocal microscopy while image b. is a phase contrast image. The beams interlace and form large spaces through which the AH can pass.

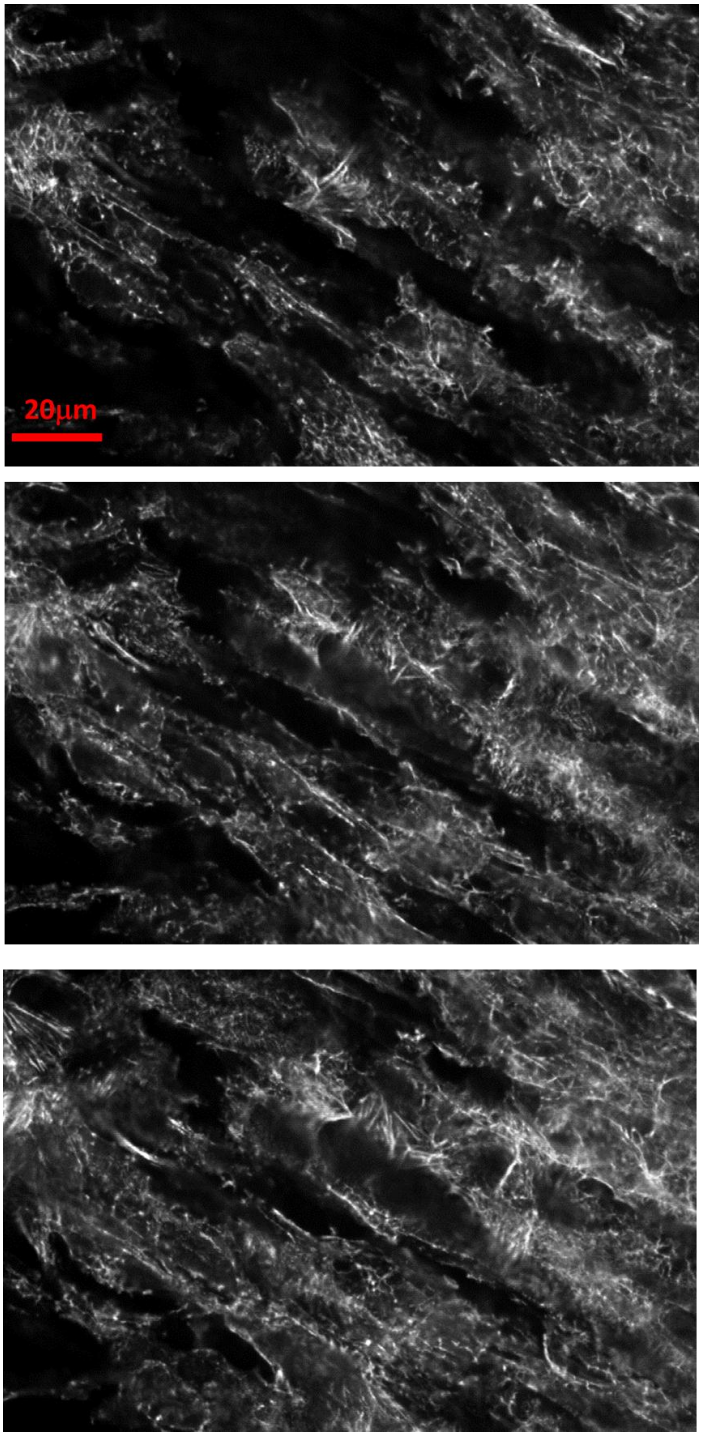

Figure 1-8. Confocal images of corneoscleral sheets.

The orientation of the corneoscleral region of the TM is unlike the interlaced beams of the uveal. In this region the trabecular beams are arranged in flat plate-like structures which are stacked. The actin orientation is dense and complex as is seen in these 3 consecutive confocal images through the TM tissue in situ.

The TM cells of the JCT have long processes which allows for cell-cell interactions as well as interaction with the ECM and with schlemm's canal (Grierson and Lee, 1974). Unlike the organised structure of the previous layers the cells of this region are embedded in a loose connective tissue of ECM that forms an irregular structure (Tamm, 2009) of narrow spaces through which the AH can flow (Davson, 1969; Forrester, 2008; Grierson, 1987; Hogan et al., 1971; Oyster, 1999; Wolff et al., 1997). The narrow spaces in the region are filled with extracellular materials (Acott and Kelley, 2008; Faralli et al., 2009; Keller et al., 2009; Rhee et al., 2009; Ueda et al., 2002) including matricellular proteins (Rhee et al., 2009), myocilin (Konz et al., 2009; Resch et al., 2010) and fibronectin (Faralli et al., 2009).The endothelial monolayer into schlemm's canal does not have a continuous basement membrane and relies on cell-to-cell contact (Ethier, 2002; Grierson and Lee, 1974). Features termed giant vacuoles were observed and reported as the way in which aqueous humor crosses the endothelial layer (Ethier, 2002; Grierson and Lee, 1973; Mcmenamin et al., 1983). Work since then has highlighted the presence of membrane lined pores (Ethier et al., 1998; Johnson, 1997; Johnson et al., 2002). Once in Schlemm's canal the aqueous flows into the episcleral venous network via collector channels (Davson, 1969; Hogan et al., 1971; Oyster, 1999; Wolff, 1976).

A lot of our knowledge of the outflow system comes from animal models (Gasiorowski and Russell, 2009) including non-human primates (Clark et al., 1996; Epstein et al., 1986; Gabelt et al., 2003; Grierson and Lee, 1977; Inomata and Bill, 1977; Kaufman and Barany, 1977b; Lutjen-Drecoll, 1999a), porcine (Bachmann et al., 2006; Camras et al., 2012; Mcmenamin and Steptoe, 1991) and bovine (Calthorpe and Grierson, 1988; Johnson et al., 1993; Lu et al., 2008; Mao et al., 2011; Wiederholt et al., 1995). The anatomical organisation of the TM and outflow pathway varies between species. In the bovine eye there is an extensive meshwork but only 50% of this occurs as organised trabeculae. The region with minimal organisation is equivalent to the JCT of the primate eye as it is composed of loose connective tissue (Flugel et al., 1991; Grierson et al., 1985a). Regardless of the structural dissimilarity, cattle do demonstrate ocular hypertension following steroid treatment (Gerometta et al., 2004) and made them a useful model in glaucoma research.

1.8 Function and Dysfunction of the TM

It had been assumed that many functional activities of the TM cells had been lost after embryological development (Grierson, 1987) and cells were mere trabecular "covers" (Anderson et al., 1980). The establishment of meshwork cell cultures in the 1980's, (including human (Alvarado et al., 1982; Grierson et al., 1983; Polansky et al., 1979) and bovine (Calthorpe and Grierson, 1988; Grierson et al., 1985a; Grierson et al., 1985b)) combined with a wide range of advancing technologies, including genetics, proteomics and advances in microscopy revealed TM cells to be metabolically active (Gasiorowski and Russell, 2009) and implicated their dysfunction in ageing and the pathogenesis of glaucoma (Ferrer, 2006; Gabelt and Kaufman, 2005; Grierson, 1987; Lutjen-Drecoll, 2000, 2005; Stamer and Acott, 2012).

Pressure within the episceral veins into which AH drains is 9mmHg while the pressure within the anterior chamber ranges from 10-21mmHg (Adler et al., 2002; Allingham, 2005). The difference in pressure was postulated to occur due to resistance in the outflow pathway, mainly in the JCT and schlemm's canal (Ethier, 2002; Ethier et al., 1995; Johnson, 2006; Overby et al., 2009; Zhou et al., 2012). The endothelial cells of schlemm's canal are the last site of resistance to outflow (Allingham et al., 1992; Ethier et al., 1995; Johnson et al., 1992; Zhou et al., 2012). These cells have been shown to have separate characteristics to TM cells (Alvarado et al., 2004). Changes in schlemm's canal have been described to reduce outflow (Boldea et al., 2001) while the purposed resistance in the JCT has been placed with the ECM. There is a vast amount of evidence showing that meshwork cells are able to synthesize a wide range of extracellular materials in vitro and in vivo (Acott and Kelley, 2008; Schachtschabel et al., 1977; Schachtschabel et al., 1989). Cultured TM cells are capable of synthesising collagen I IV V, glycoproteins such as fibronectin and laminin as well as glycosaminoglycan's (GAG's) including hyaluronic acid, chondroitin sulphate and dermatan sulphate (Gong et al., 1994; Tschumper et al., 1990; Yue and Elvart, 1987) and proteoglycans (Wirtz et al., 1997).

The ECM of the TM is not a static scaffold but is regulated by several signalling molecules (Fuchshofer and Tamm, 2009; Keller et al., 2009). TM cells are capable of secreting growth factors and chemokine's (Shifera et al., 2010; Takai et al., 2012) as

well as wide range of matricellular proteins (Rhee et al., 2009) which modulate the amount of ECM deposited and its composition through a dynamic system of production and degradation of its components (Acott and Kelley, 2008; Keller et al., 2009). TGF-β2 induced changes in ECM are modulated by BMP's (Fuchshofer et al., 2007), while secretion of MMP's (Alexander et al., 1991) ensure a constant balance in the production and degradation of the ECM (Bradley et al., 1998; Fuchshofer and Tamm, 2009; Keller et al., 2009). Perfused organ cultures (Ericksonlamy et al., 1991; Wiederholt et al., 1995) have demonstrated that outflow can be modulated in response to changes in IOP.

These alterations are achieved through mechano-regulation of the TM (Acott and Kelley, 2008; Borras et al., 2002; Bradley et al., 2001; Keller et al., 2009; WuDunn, 2009) through the ECM and cytoskeleton (Wiederholt et al., 1998; Wiederholt et al., 2000. The change in pressure leads to stretching of the cells which activates changes in gene expression (Luna et al., 2009; Vittitow and Borras, 2004), secretion of various proteins (WuDunn, 2001) and therefore alteration of ECM components (Ramos and Stamer, 2008). Interactions between the ECM and cytoskeleton result in changes in the actin cytoskeleton (Borras, 2003; Fuchshofer and Tamm, 2009; Keller et al., 2009; Ramos and Stamer, 2008; Tumminia et al., 1998; Vittitow and Borras, 2004). TM cells contain alpha smooth muscle actin (Dekater et al., 1992) and thus have contractile abilities (Inoue et al., 2010b; Lepple-Wienhues et al., 1991) Perfusion experiments have shown that cytoskeletal altering agents can alter aqueous outflow by targeting the cytoskeleton of TM cells (Epstein et al., 1999; Ericksonlamy et al., 1992; Ethier et al., 2006; Kaufman, 2008; Kaufman and Rasmussen, 2012; Khurana et al., 2003; Liu et al., 2001; Tian et al., 1998). Although the exact mechanism through which there agents functions is unknown it has been suggested that the disruption of the cytoskeleton leads to relaxation of the TM cells. While contraction of the TM cells pulls the intra-trabecular spaces together, relaxation means that the pathways through the meshwork are more open. This will therefore allow the passage of AH with reduced resistance (Overby et al., 2009). The pattern of AH flow has also been noted to be disrupted (Lu et al., 2008) from the funnelling pattern observed in untreated TM. It is also possible that the disruption of the cytoskeleton causes changes in the ECM

composition therefore reducing the amount and/or charge of the material accumulated in the TM. Different components of the ECM can retard the flow of particles and therefore alterations induced by cytoskeletal changes could reduce resistance.

The ECM of the JCT was reported to increase with both age and glaucoma (Acott and Kelley, 2008; Lutjen-Drecoll et al., 1986; Lutjendrecoll et al., 1981; Rohen et al., 1993) but the extent to which these materials influence resistance was of some debate. The increase in ECM components with age is well documented and is suggested to lead to a thickening of the trabeculae that might therefore influence the functional properties of the TM (Lutjen-Drecoll, 1999a). These changes include elastin localising to the core (Gong et al., 1989) and an accumulation of wide-spacing (curly) collagen (Marshall et al., 1991). McMenamin et al suggested it was not simply an increase in ECM but an alteration in its composition from fine fibril-granular material to gross fibril-granular material that was of importance (McMenamin et al., 1986). Changes in the factors that regulate ECM turnover are implicated with glaucoma as reduced turnover could lead to the build-up of ECM described (Wordinger et al., 2007).

GAGs within the TM have been of particular interest for many years since the work of Barany and Francois (Acott and Kelley, 2008; Yue, 1996; Yue et al., 1984) as their long repeat chains and negative charge makes them ideal resistance material. The GAGs present in the TM form a coating along the apical surface of the cells. These are highly charged and so are considered “sticky” molecules as they attract other molecules, of positive charge towards them. In the confined spaces of the TM the GAGs serve to further reduce the available space through which molecules can flow. As intra-trabecular spaces are reduced in size then the proximity of the molecules is increased allowing for stronger interactions and increased resistance to flow. These interactions were clearly demonstrated in perfusion studies (Keller et al., 2008; Keller et al., 2012; Tschumper et al., 1990). The specific composition of GAGs in the TM has also been greatly studied (Schachtschabel et al., 1977; Tschumper et al., 1990) with various techniques employed to determine the localization of GAGs within the TM (Keller et al., 2009; Keller et al., 2008).

TM cells have been shown to be actively phagocytic capable of ingesting melanin from the iris (Cracknell et al., 2006) and synthetic particles used in various studies (Buller et al., 1990; Grierson et al., 1986; Zhou et al., 1999a). Phagocytic challenge has been shown to have a detrimental effect on TM cells and resulted in detachment from the substrate (Zhou et al., 1995; Zhou et al., 1999a) and up regulation of ECM remodelling genes (Porter et al., 2012).Once ingested TM cells appear to have capabilities of breaking down ingested materials (Liton et al., 2009; Yue et al., 1987) which allows them to digest materials such as mis-folded and damaged proteins and to neutralise potentially damaging molecules such as oxygen free radicals (De La Paz and Epstein, 1996; Russell and Johnson, 1996) and H_2O_2 (Nguyen et al., 1988). Lysosomal dysfunction with age (Caballero et al., 2004; Cuervo and Dice, 2000; Kiffin et al., 2006) and chronic oxidative stress (Caballero et al., 2003; Liton et al., 2008) results in an accumulation of material in lysosomes which cannot be broken down (Liton et al., 2008).

Protective mechanisms (Wang et al., 2001) such as glutathione and methionine are decreased with age (Costarides et al., 1991) and the level of antioxidants have been shown to be decreased in glaucoma patients (Ferreira et al., 2004). Together these changes would result in increased damage in TM cells which is known to lead to apoptosis or senescence, depending on the severity. It is well established that there is a progressive loss of TM cells with age. Alvarado stated that 43% of cell density is lost between the ages of 20 to 80 from the filtration region of the meshwork (Alvarado et al., 1981), while Grierson indicated that cellular loss is at a constant rate of approximately 6,000 cells per year. It also indicated that this loss was associated with all regions of the meshwork and the endothelium of schlemm's canal (Grierson and Howes, 1987; Grierson et al., 1984) and was greater in glaucoma (Alvarado et al., 1984; Grierson and Howes, 1987). This loss in total number of TM cells is suggested to influence IOP as the loss of cells means there are fewer cells to carry out basic maintenance of the TM tissue, such as remove debris that is washed into the TM. As hypothesised by Grierson et al(Grierson, 1987), a reduced ability to remove material by phagocytosis could lead to an accumulation. These particles may block the narrow passages themselves but could also damage the TM cells further by altering the TM

microenvironment. This may also hold true for accumulating ECM. Without enough viable TM cells the ECM will not be undergoing continual turnover and could lead to the accumulation of mature and highly stable ECM such is seen with increasing age(Keller et al., 2009). As the TM cells are known to have strong contact inhibition and a limited capacity for replication (Alvarado et al., 1982), these factors combined with no mechanisms which occur naturally to replace cells means that cell populations cannot be replaced once lost. Compromised TM cells have been shown to be removed by apoptosis (Agarwal et al., 1999; Baleriola et al., 2008; Sibayan et al., 1998) and there appears to be an increase in senescence in glaucoma (Liton et al., 2005a).

1.9 Cellular stresses cause ageing

Ageing for the higher level multicellular organism has been described as an inevitable fate; a multifactorial process of intrinsic, progressive loss of function and physical deterioration that occurs over time, beginning about the time of reproductive maturity accompanied by increased morbidity and decreased fertility (Hayflick, 2000; Kirkwood and Austad, 2000). There has been much debate about the science of ageing and theories such as the biological clock (programmed) (Salvi et al., 2006) and wear and tear theory (Masoro, 1990) have been published. It is likely that the alterations observed are a combination of genetic and environmental stresses leading to an accumulation of damaged intracellular molecules (Wei and Lee, 2002) leading to an internal breakdown of cellular processes that would result in cells which are unable to function as normal. Several key influences which are postulated to result in cell dysfunction are reactive oxygen species (ROS) (Harman, 1992) and a build-up of aggregates such as advanced glycation end-products (AGE) (Stitt, 2001).

1.9.1 ROS

Reactive oxygen species have long been the focus of ageing (Finkel and Holbrook, 2000; Harman, 1992) but under normal conditions small quantities are used as messengers locally within the cell (Tezel, 2006). Due to the potential harm these molecules can cause, any excess ROS is captured by antioxidant enzymes, which convert these potentially harmful products to non-toxic products (Tezel, 2006). H_2O_2 normally present in AH (Rose et al., 1998; Spector et al., 1998) does not increase with age or glaucoma but there is a decline in antioxidants present in AH in glaucoma

patients (Ferreira et al., 2004) while the level of oxidative DNA damage has been shown to increase (Izzotti et al., 2006; Majsterek et al., 2011). Oxidative damage can lead to the alteration of cell function in the anterior chamber and degeneration of TM cells (Aslan et al., 2013; Caballero et al., 2003; Izzotti et al., 2006; Sacca and Izzotti, 2008; Zhou et al., 1999b). Mitochondrial abnormalities were detected in TM cells (He et al., 2008a) and have been implicated in POAG.

1.9.2 AGE's

Advanced glycation end products have been implicated in many diseases ranging from diabetes (Stitt, 2010; Vlassara and Palace, 2002), Alzheimer's (Munch et al., 1998; Srikanth et al., 2011) and age-related dysfunction of ocular cells (Stitt, 2001) including RPE (Glenn et al., 2009; Ishibashi et al., 1998) and optic nerve head cells (Tezel et al., 2007). AGEs are a heterogeneous group of molecules that form via the same complex rearrangements to form structurally different molecules. The first step in the formation of AGEs occur through the non-enzymatic condensation of sugars (Stitt, 2005). This reaction leads to the formation of unstable Amadori products. These molecules form readily and are irreversible meaning that they reach equilibrium depending on the availability of sugars. These products then undergo further modifications which produce AGEs.

AGEs accumulate on long-lived molecules within the cell (Schmidt et al., 2000) and slowly cause damage. These modified molecules include proteins and lipids which will impair cell function. AGE receptors have also been identified (Schmidt et al., 2000; Zong et al., 2010). The binding of AGE can promote altered cell function including inappropriate release of growth factors, initiation of apoptosis and increased ECM (Singh et al., 2001). Within the anterior chamber AGEs receptors are present on corneal endothelial cells and the binding of AGE resulted in increased ROS production and apoptosis (Kaji et al., 2003). AGE's have been linked with the pathogenesis of glaucoma but only in relation to the optic nerve (Tezel et al., 2007); there is no published data relating to AGE's and the outflow system. The increased levels of ROS and accumulation of AGE's are interrelated with the formation of AGE generating ROS while increased oxidative stress leads to AGE production (Tezel et al., 2007). This synergistic relationship leads to increasing numbers of dysfunctional cells. Cellular

dysfunction can evoke the activation of the apoptotic pathway; however, damage does not always result in cell death.

1.9.3 Senescence

Replicative senescence is a state in which normal cells maintain their metabolic functions but become non-replicative *in vitro* following several divisions (Hwang et al., 2009) due to the shortening of telomeres following every division (Patil et al., 2005). While high degrees of stress can lead to cell death, low levels of stress causes another type of senescence known as stress-induced premature senescence (SIPS) in several cell types (Toussaint et al., 2002) including TM cells (Caballero et al., 2004). Much work has focussed in the influence of chronic oxidative stress; in the case of TM cells a significant factor seems to be exposure to the oxidant environment of the AH (Rose et al., 1998; Spector et al., 1998).

The arrest in cell proliferation *in vitro* is accompanied by morphological changes. Cells have a reduced rate of growth, become rather flattened and larger in size and become tightly bound to the substrate (Hwang et al., 2009). A commonly used biomarker for senescence is the presence of β-gal (Dimri et al., 1995). Senescence has also been detected in the TM, with increasing levels in glaucomatous samples (Babizhayev and Yegorov, 2011; Liton et al., 2005a).

1.9.4 Apoptosis

Apoptosis is a an important physiological process involved in development, wound healing and differentiation (Kerr et al., 1972) by removing unwanted or damaged cells. Apoptosis can be initiated by many factors which function via the activation of plasma membrane receptors or by the down-regulation of survival factors. Regardless of induction, apoptosis is a highly regulated series of changes; cytoplasmic shrinkage follows the condensation of nuclear material, followed by membrane blebbing at which point cell to cell contact is lost from neighbours. The nucleus begins to break down and the final stage is the degradation of the entire cell into apoptotic bodies (Hall, 1999; Steller, 1995; Wyllie et al., 1980). TM cells are known to express mRNA for several mediators of apoptosis (Agarwal et al., 1999) and the loss of cells with age and

glaucoma has been attributed to apoptosis (Baleriola et al., 2008; Kerrigan et al., 1997; Li et al., 2011).

1.10 Glaucoma

The original definition of glaucoma was based on a raised intraocular pressure (IOP) which resulted in cupping of the optic nerve and in the death of ganglion cells leading to progressive loss of peripheral vision (Quigley et al., 1994). Normal IOP was accepted as 15-20mmHg (Allingham, 2005) and patients presenting with IOP higher than this showed evidence of optic nerve cupping and were therefore reported as having glaucoma. More recently, however, the definition has shifted (Shields and Spaeth, 2012) and increased pressure is considered a significant risk factor rather than an indication of the disease itself (Coleman and Miglior, 2008; Foster et al., 2002; Quigley, 2005, 2011). This distinction was required as some patients with loss of visual field and optic disc cupping presented with IOP that was accepted as normal (Lee et al., 1998).

Glaucoma is now considered an umbrella term (Agarwal et al., 2009) used to describe a group of neuropathies and not a single disease (Foster et al., 2002; Quigley, 2005, 2011). There are two main distinctions in glaucoma; angle closure or open angle and whether the disease is caused by primary or secondary factors.

Multiple variations in the pathophysiology of the disease all result in ganglion cell death leading to the continued loss of peripheral vision (Foster et al., 2002; Quigley, 2011). Glaucoma is diagnosed based on visual field tests and assessing the appearance of the optic nerve (Batterbury et al., 2009; Khaw and Elkington, 1999; Quigley, 2011). As retinal ganglion cells are lost there is increased excavation of the cup due to deformation of the supportive connective tissue (Quigley et al., 1981; Quigley et al., 1991), therefore increasing the cup to disc ratio (Crawford Downs et al., 2011; Yang et al., 2011). Increased IOP has been linked with increased loss of retinal ganglion cells in animal models (Howell et al., 2008; Roberts et al., 2010) as the pressure is translated from the cornea to the point of optic nerve exit (Coudrillier et al., 2012; Gerometta et al., 2011; Sigal and Ethier, 2009) resulting in loss of retinal ganglion cells which is correlated with deteriorating vision (Kerrigan-Baumrind et al., 2000). The optic nerve is

not the only site of dysfunction in glaucoma, increased IOP results from dysfunction in the anterior chamber.

The exact mechanisms involved in the pathogenesis of glaucoma are still being uncovered (Clark, 2012). Many changes have been cited including increased deposition of ECM (Lutjen-Drecoll et al., 1986; Lutjendrecoll et al., 1981), genetics (Allingham et al., 2009; Gould et al., 2004) and the cytoskeleton (discussed in detail as follows). Glucocorticoids (GC) have been shown to reduce AH outflow to a point where damage caused by pressure resembles that of glaucoma (Clark and Wordinger, 2009; Kersey and Broadway, 2006). TM cells are known to express GC receptors (Weinreb et al., 1981) and GC have been shown to cause several changes in TM cells including decreased phagocytosis (Matsumoto and Johnson, 1997), as well as modifying the secretion of glycoproteins (Allingham, 2005; Steely et al., 1992; Wordinger and Clark, 1999; Yun et al., 1989). During *in vitro* experiments the presence of DEX caused a striking change in the actin cytoskeleton of the TM cell (Clark et al., 1994).

Any cell biology textbook will note that the cytoskeleton is vital to normal function of the cell; providing a means of movement, both of the cell itself and of the components within the cell, maintaining cell shape and structural stability (Alberts and National Center for Biotechnology, 2002; Fletcher and Mullins, 2010; Lodish, 2008). Alterations in the cytoskeleton of a cell would therefore impair its normal function.

1.11 Cytoskeleton

The main constitutes of the cytoskeleton are three 3 filamentous proteins; microfilaments, intermediate filaments and microtubules. The composition of each filament is based on different subunits and so infers unique properties to each. The filaments also localise in specific regions of the cell allowing for the different functional aspects of the cytoskeleton (Alberts and National Center for Biotechnology, 2002; Fletcher and Mullins, 2010; Lodish, 2008).

The intermediate filaments are rope-like structures which provide tensile strength to the filaments. These filaments are present in large numbers just below the membrane and concentrate at the sight of cell interactions, allowing the cells to withstand the pressure and strains of their environment. The role of internal organisation falls to the

microtubules. These hollow tubes of protein serve as tracks along which organelles can move (Alberts and National Center for Biotechnology, 2002; Fletcher and Mullins, 2010; Lodish, 2008). The third filamentous element of the cytoskeleton is actin which is responsible for cell motility and shape change and is the main focus of this work (Tian et al., 2000).

Actin is one of the most highly conserved proteins discovered and one of the most abundant in eukaryotic cells (Dominguez and Holmes, 2011). Actin exists in two forms within the cell; the globular protein is the individual units which polymerise to form long filamentous chains (F-actin) (Dominguez and Holmes, 2011). The dynamic nature of the actin cytoskeleton is dependent on the ability of the filaments to assemble and disassemble quickly as and when required, this is made possible by the many actin associated proteins which are involved in processes such as polymerisation, capping and dissolution of the F-actin (Ballestrem et al., 1998; dos Remedios et al., 2003; Fletcher and Mullins, 2010; Lee and Dominguez, 2010). Proteins such as alpha-actinin are bundling proteins, which organise actin into bundles which are visible in the form of stress fibres (Pellegrin and Mellor, 2007). These proteins are also responsible for organising the actin into various structures which allow the different functions in which actin is involved. Much work has identified how the organisation of the actin allows cell locomotion through attachment with myosin (Mitchison and Cramer, 1996; Stricker et al., 2010).

The activity of these actin binding proteins can be modulated by the extracellular signals via Rho proteins which allow the cytoskeleton to reorganise in response to changes in the environment (David et al., 2012). Integrin's are heterodimeric transmembrane glycoproteins which are responsible for not only tethering cells to the ECM but allowing communication which can regulate the cytoskeleton (Brakebusch and Fassler, 2003; Faralli et al., 2011).

1.12 Actin cytoskeleton of TM cells

Staining of the conventional outflow illustrated that TM cells contained alpha smooth muscle actin (Dekater et al., 1992; Ethier et al., 2004b). Further examination of TM cells from various species, revealed a complex network of filaments (Gipson and Anderson, 1979; Grierson and Rahi, 1979; Ryder et al., 1988; Weinreb and Ryder, 1990). The actin cytoskeleton of TM cells as seen via florescent linked probes showed that the main actin arrangement within the TM cell is normally straight stress fibres spanning across the length of the cell (Grierson and Rahi, 1979; Ryder et al., 1988; Weinreb and Ryder, 1990) as seen in Figure 1-9. Stress fibres are bundles of 10-30 actin filaments bound -together by alpha-actinin (Cramer et al., 1997; Lazarides, 1976). Stress fibres have been shown to have contractile properties and form in response to mechanical force such as hydrostatic pressure and cyclic stretch (Franke et al., 1984; Pellegrin and Mellor, 2007). The presence of stress fibres in TM cells imparts contractile properties on these cells (Lepple-Wienhues et al., 1991; Wiederholt et al., 1996).

Experiments exploring the use of cytoskeletal altering agents within the outflow system (Cai et al., 2000; Ethier et al., 2006; Inoue et al., 2010a; Kaufman, 2008; Kaufman and Barany, 1977a; Liu et al., 2003c; Tian et al., 2009; Tian et al., 1998) highlighted the cytoskeleton as a potential therapeutic target for reduction of IOP as increased rigidity of TM cytoskeleton resulted in increased resistance to AH outflow (Ericksonlamy et al., 1992; Rao et al., 2001; Tian et al., 2000). Therefore if the cytoskeleton of the TM was impaired then the cells would not function normally and this could influence outflow as illustrated in many experiments (Epstein et al., 1999; Kumar and Epstein, 2011; Rao et al., 2001).

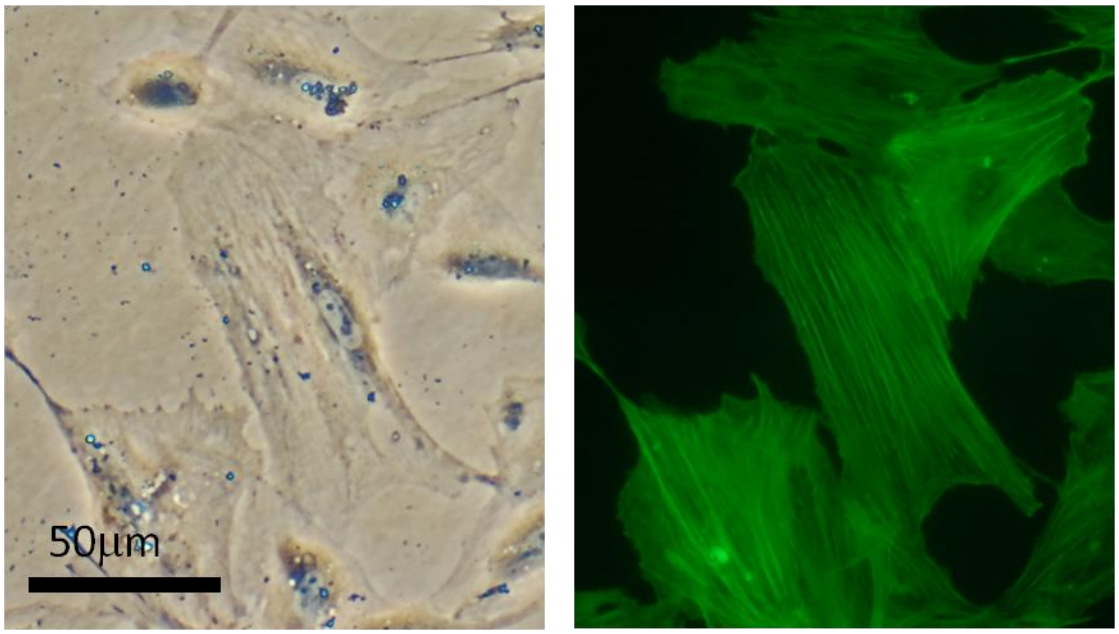

Figure 1-9. Phase contrast image of TM cell with fluorescent image providing an example of a stress-fibre pattern.

The left hand image is a phase contrast image of TM cells on tissue culture glass substrate. Cells are expressing normal TM cell morphology and although not in a confluent culture, processes are making cell to cell contacts with neighbours. The right hand image is the same field of view but taken via fluorescence. The actin has been stained with Alexa 488 phalloidin and can be seen most clearly in the central cell as straight stress fibres running the length of the cell.

1.12.1 Cross-linked Actin Networks (CLANs)

As previously stated steroids such as DEX were known to cause many changes in TM cells, Clark discovered that the cytoskeleton of some TM cells was also influenced (Clark et al., 1994). Following treatment with DEX the normal F-actin arrangement of straight stress fibres spanning across the length of the TM cell were now accompanied by geodesic structures termed cross-linked actin networks (CLANs) (Clark et al., 1994) as seen in Figure 1-10. We have previously defined a CLAN as a "polygonal structure composed of hub points connected by actin spokes which are arranged in triangulated units to form a polygonal shape. The minimum inclusion requirement for a CLAN is that it has at least 5 hub points that form a minimum of 3 linked-triangulated units".

Since this initial discovery much work has focussed on these structures especially within our group. CLANs have been identified in TM of perfused globes (Clark et al., 1995) BTM cells (Wade et al., 2009) in organised TM tissue (Hoare et al., 2009) and the optic nerve head (Job et al., 2010). It was interesting to discover that there were more CLANs in glaucomatous TM cells (Clark et al., 2005) and tissue (Hoare et al., 2009). CLANs are no longer considered another side-effect of steroids, nor can they be an artefact of the culture environment. Structures similar in appearance to CLANs were identified in many cells (Ireland and Voon, 1981; Lazarides, 1976) and were reported as having a role in cell settlement and spreading (Ingber, 2003; Lazarides, 1976; Maguire et al., 2007). The actin spokes are connected at hub points where alpha-actinin and syndecan-4 form a complex (Filla et al., 2006). Earlier studies demonstrated the presence of tropmyosin and filamin in these structures that form under the apical cell surface(Ireland and Voon, 1981; Lazarides, 1976).

The influence of these structures within the cell has not yet been shown, however, based on tensegrity models of the cytoskeleton (Ingber, 2003), the presence of CLANs was hypothesised as making the TM cells more rigid (Clark et al., 2005). Increased rigidity of the TM cytoskeleton could result in increased outflow resistance (Ericksonlamy et al., 1992; Rao et al., 2001; Tian et al., 2000). Actin fibre rearrangement can be triggered by shear stress and mechanical stretch (Franke et al., 1984; Tumminia et al., 1998).

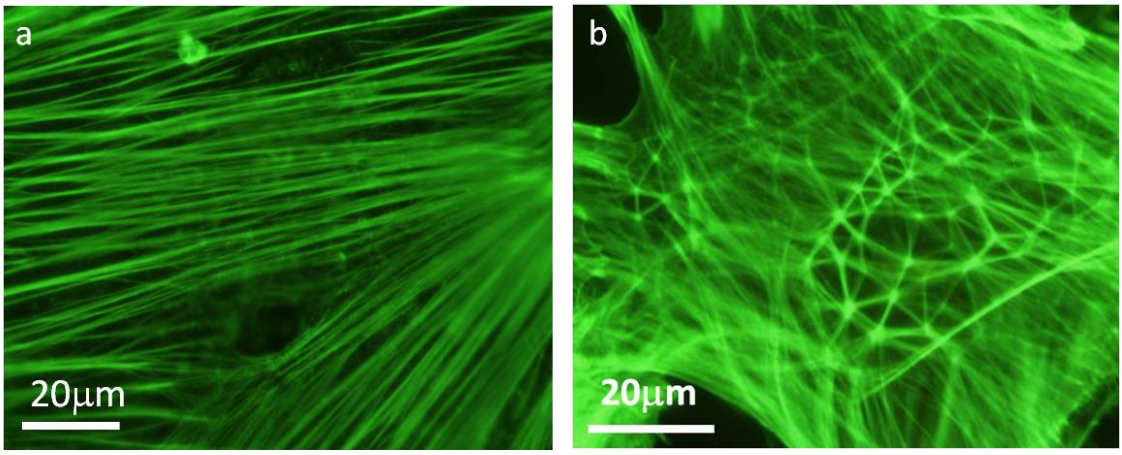

Figure 1-10. Fluorescent images providing an example of a stress-fibre and CLAN in TM cells.

Both images are taken from cultures of BTM cells incubated for 7 days in either maintenance medium only (image a) or with 2ng/ml TGF-β2 in maintenance medium (image b). Following treatment the actin was visualised using Alex-488 phalloidin. The actin arrangement in image a. is straight stress fibres running in parallel, while the organisation in image b is very different. Stress fibres are just visible but are obscured by the presence of a CLAN. The actin is now arranged in short spokes which connect at hub points and form triangulated units.

1.13 Aims

Alterations of the cell cytoskeleton are indicative of changes in cell function and the presence of CLANs is suggested to alter the contractile nature of TM cells to a point where it is implicated in reduced AH outflow. The presence of CLANs in tissue and cells without steroid treatment suggested the existence of CLAN inducing agents under normal physiological conditions. The current work was undertaken to identify whether these changes could be linked with ageing and age-related stresses within the TM.

This firstly required defining these structures and lead to chapter 3 questioning; **Can CLANs be clearly defined and distinguished from other actin structures?**

- Evaluate masked images of actin structures and establish a working definition of a CLAN.
- Obtain measurements of actin structures and compare between these structures.

As CLANs were present in non-glaucomatous TM tissue the inducing agent must also occur under normal conditions. As the TM is continual bathed in AH, a complex mixture of growth factors it became our primary focus. **Do factors present in the aqueous humor influence the formation of CLANs in TM cells?**

- Assess the influence of aqueous humor on CLAN incidence
- Determine how growth factors known to be increased in patients with glaucoma (TGF, HGF, FGF) affect CLAN incidence when added singularly and in combination

Glaucoma is an age-related disease and so normal ageing processes may provide early indications of the disease process. **Is the incidence of CLANs in TM cells associated with donor age?**

- Quantify the presence of CLANs in TM cells from donors of various ages.
- Quantify the presence of CLANs in TM tissue from human donors of various ages.

Ageing is a complex process and many cellular changes and dysfunctions are associated. We questioned; **Can various stresses associated with ageing influence CLAN formation?**

- Assess TM cell cultures for senescence and apoptosis markers and quantify the coincidence with CLANs.
- Impart an oxidative stress on TM cells with hydrogen peroxide and evaluate CLAN incidence under these conditions.
- Measure general oxidative stress levels of TM cell and how this compares to CLAN incidence.
- Assess CLAN incidence in TM cells grown on AGE-modified matrigels.

2. Materials and methods

2.1 General techniques

2.1.1 Media

Human (HTM) and bovine trabecular meshwork (BTM) cells were incubated with Dulbecco's Minimum Eagles Medium (DMEM) (Sigma) containing various concentrations of fetal calf serum (FCS) (Biosera). All media had added L-glutamine (2mM), penicillin-streptomycin solution (100U/ml and 100μg/ml respectively) and amphotericin B (2.5μg/ml) (all from Sigma). Throughout the work media containing various concentrations of FCS were used as indicated. Growth medium contained 10% FCS and was used for routine cultivation of cells. Maintenance medium contained 1% FCS to minimise the influence of factors present and maintain monolayers. Finally enhanced medium contained 30% FCS and was used when freezing cells or when cells were initially defrosted.

2.1.2 Maintaining cells

All TM cells were maintained by incubation at 37^{o}C with 5% CO_2 in growth medium in standard tissue culture (TC) flasks (Greiner). Growth medium was replenished every 3-4 days by removing two-thirds of the medium and replacing it with fresh growth medium. Cells were monitored and photographed on an inverted phase microscope (Nikon Optiphot) at regular time points for changes in cell morphology, evidence of proliferation or any signs of infection.

2.1.3 Passaging cells

Cells were maintained in this manner until 70% of the TC flask area was covered with a monolayer of cells. Once at this level of confluence the growth medium was removed, cells were washed in sterile phosphate buffered saline (PBS) and incubated with up to 5mls of trypsin solution (0.5g porcine trypsin and 2g EDTA in 0.9% NaCl) (Sigma) until all cells had detached from the flask (as determined by inverted phase microscopy). The trypsin was quenched by the addition of twice the volume of growth medium. The cell suspension was removed from the flask, placed in a suitable centrifuge tube and centrifuged at 1000 revolutions per min (rpm) for 5mins.

The supernatant was discarded and the resulting pellet re-suspended in growth medium. A cell count was performed using a haemocytometer and the volume of suspended cells was divided into volumes to maintain a working stock, for frozen stocks or for experimental evaluation and assays.

2.1.4 Culturing cells

To maintain a working stock of cells the volume of cell suspension calculated to contain 10,000 cells per cm^2 was placed in a new TC flask with fresh growth medium and the process of cell proliferation continued. This concentration of cells was found to be optimum so that primary BTM cells usually reached a 70% confluent level within 4-5 days however, primary HTM cell growth was not so uniform across donors with some cell cultures taking up to 7 days to reach a 70% confluent level.

2.1.5 Freezing cells

Stocks of cells were frozen at various passages for future use. Cells were re-suspended in 900µl of enhanced medium and placed in a cryo-tube. To this 100µl of dimethyl sulphoxide (DMSO) (Sigma) was added and the cryo-tube placed in a specialised container which immersed the tubes in propan-2-ol (Fisher Scientific) at room temperature. This was then placed in -80^{o}C freezer for up to 5 hours before the cryo-tube was removed and placed in a liquid nitrogen store.

2.1.6 Cells for experimentation

TM cells were only used for experimental purposes after passage 3 as before this they were still pigmented (Grierson et al., 1985b) and cells undergoing phagocytic challenge display altered cellular functions (Day et al., 1986; Porter et al., 2012). Cell health and growth were continually monitored via morphological evaluation and observing the time which lapsed between passages. Primary BTM cells were not used beyond passage 15 in our experiments as cells exhibited slowed growth, an increased number of giant cells and cells containing high numbers of vacuoles. Some HTM cells showed these signs by passage 10 and so were not used past this.

TM cells were seeded on labtek chamber slides at a density of 10,000 cells per cm^2, which was found to be optimum for experimentation purposes (as shown in chapter 4). The chambers were filled with growth medium and placed in the experimentation incubator at 37^{o}C with 5% CO_2 for 7 days. By 7days the surface of the well was covered in a monolayer of cells and so experiments could commence.

2.1.7 Fluorescent staining *in vitro*

Once the appropriate experimental time had passed the labtek chamber slides containing the TM cell monolayers were removed from the incubator. The medium was removed from the wells and each well was slowly washed with PBS at room temperature. Cells were then fixed in 10% neutral buffered formalin (NBF) for 20 minutes at room temperature. The fixative was removed and disposed of and any residual NBF removed from the cells with careful washes in PBS.

In order to visualise the f-actin, TM cells were stained with Alexa-phalloidin-488 (Sigma) and counterstained with propidium iodide (PI) (Sigma) to visualise the nuclei as previously described (Wade et al., 2009). Cells were firstly permeablised using 0.1% triton-X (Sigma) for 5mins; following two washes in PBS-tween, 250µl of Alexa-phalloidin-488 (1:40) was added to each well and allowed to develop for 40 minutes. After removing the phalloidin the cells were rinsed with PBS before counterstaining with 250µl of PI (10µg/ml) for 15 minutes at room temperature. Excess PI was removed by further washes in PBS. Throughout this process care was taken not to expose the samples to excess light (during the development of both dyes wells were

wrapped in foil). As this protocol requires the removal and addition of solutions at multiple stages it is vital that this is done slowly so as not to disturb the cell monolayer.

Using the device provided with the labtek chamber slides, the wells were removed from the labtek slide and any excess glue which remained pulled from the slide. A small amount of fluorescent mounting media (Dako) was added to each well and a glass coverslip applied. The mounting media was allowed to set overnight at room temperature prior to beginning microscopy.

Using a fluorescent microscope with a 450-495nm bandpass filter, each well was examined firstly on an x4 and x10 objective. From this notes were made on the status of the cell monolayer; whether there was any cell loss due to processing, the shape of individual cells, the presence or absence of cell to cell contact, whether the population appeared homogeneous across the well, whether there was any distinct overall actin pattern and finally whether staining was satisfactory.

After this initial evaluation, the monolayers were imaged on higher power objectives (x25 and x40) and notes were made detailing the actin patterns present. Representative images were taken on every objective using a camera attached to the microscope.

The use of labtek chamber slides meant that multiple treatments and controls could be run on the same slide without contamination of solutions. CLANs were identified and counted through the eye pieces of the microscope so that CLAN incidence was expressed as the percentage of CLAN containing cells in the population counted in a field of view. A total of 10 fields of view were counted at x60 for each well and the values obtained were averaged and taken as 1 biological replicate. The number of cells in the field of view was variable, depending on treatment, species and donor, and so was also considered when presenting results as a substantial decrease in cell number in one replicate may indicate a detrimental external influence. Statistics were carried out using ANOVA analysis with Tukey's range method on Minitab software.

2.2 Samples

This study involved the use of both TM tissue and primary TM cell cultures from human and bovine specimens.

2.2.1 Bovine samples

Bovine eyes were obtained with permissions from a local abattoir (G & G.B Hewitt Ltd) and transported to the lab on ice, where the excess tissue was removed and the globes placed in a solution of phosphate buffered solution (PBS) containing penicillin-streptomycin solution (100U/ml and 100μg/ml respectively) and amphotericin B (2.5μg/ml). The globes retrieved were used to provide BTM cells and bovine aqueous humor (AH) as expanded on subsequently.

2.1.1.1 Bovine TM (BTM) cells

BTM cells used in this study were primary cells isolated in the lab from fresh bovine eyes. A class II biological cabinet was thoroughly cleaned using virkon solution and 70% ethanol prior to dissection. Holding the globe firmly (exerting a small amount of pressure) an incision was made using a no. 15 scalpel approximately 1cm posterior to the limbus. Care was taken to ensure the incision cut through all layers of the globes anterior to the vitreous sack. Once made, the incision was extended around the circumference of the globe using curved scissors and the posterior segment was disposed of.

The lens was removed from the anterior segment, thus exposing the posterior surface of the iris. The anterior segment was then divided into quadrants using no. 21 scalpel along a horizontal/ medial cut and taking hold of each quadrant in turn, the iris was carefully peeled back, revealing the limbus region. Using fine forceps the meshwork (seen as the heavily pigmented line in Figure 2-1) was separated from the anterior segment.

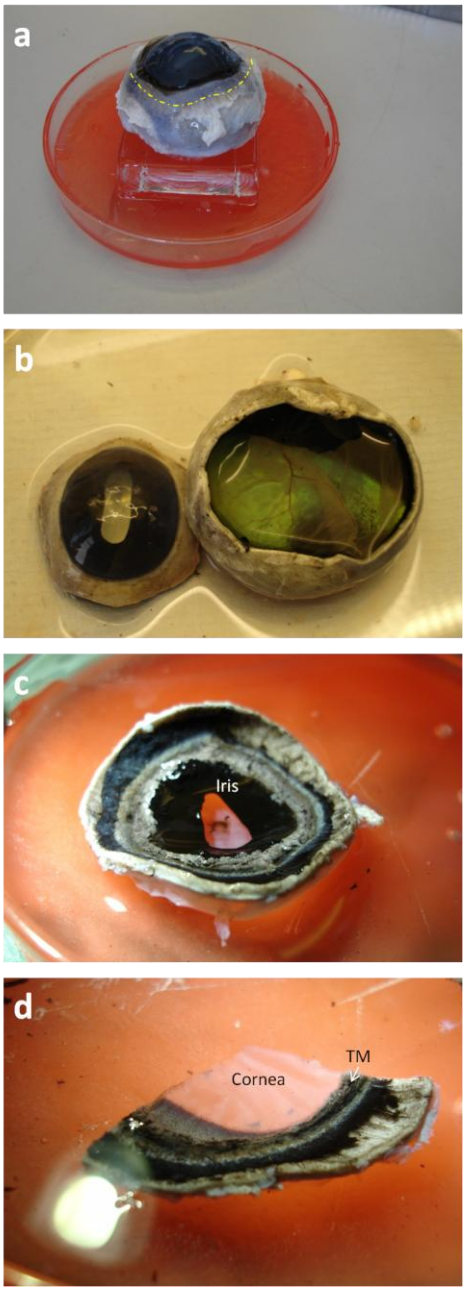

Figure 2-1 Photographs detailing the dissection of bovine globes into quadrants

A set of photographic images demonstrating the different stages of bovine globe dissection. Image a. is a whole bovine globe, with the yellow line added to demarcate how the anterior and posterior segments are separated. Image b. shows the interior of the posterior segment and the exterior of the anterior segment. With the posterior segment disposed of the lens is removed so the iris is visible (c). The anterior segment is then divided into quadrants like the one seen in image d. The iris has been peeled away to reveal the pigmented TM.

Once separated from the quadrant small sections of the TM explants were placed in standard 12cm^2 TC flasks and a small amount of growth medium added so to just cover the tissue but insuring it remained attached to the surface of the flask. Each sample was date stamped, given a three digit number based upon the globe from which it was obtained and letters were used to identify the multiple sections of meshwork taken from each globe. All excess bovine material was disposed of by incineration at the animal house following University guidelines for containment of prions.

The flasks containing explants were placed in a dedicated primary culture incubator at 37^{o}C with 5% CO_2 and left undisturbed for 5 days. Flasks were examined for cell growth and records were made to accompany phase images taken. If cells had begun to protrude from the tissue explant (Figure 2-2) then fresh growth medium was added, others without growth were discarded. Following another 5 days in the incubator the cells were again examined and the tissue explants removed and disposed of. Once cells reached 70% confluence they were dissociated from the flask using trypsin solution and transferred to a fresh 25cm^2 flasks with growth medium. These cells were then placed in the culturing incubator (37^{o}C and 5% CO_2) and the process of proliferation and passage continued as previously explained. Cultures were successful obtained from 6 bovine donors and these primary cultures were used throughout this study.

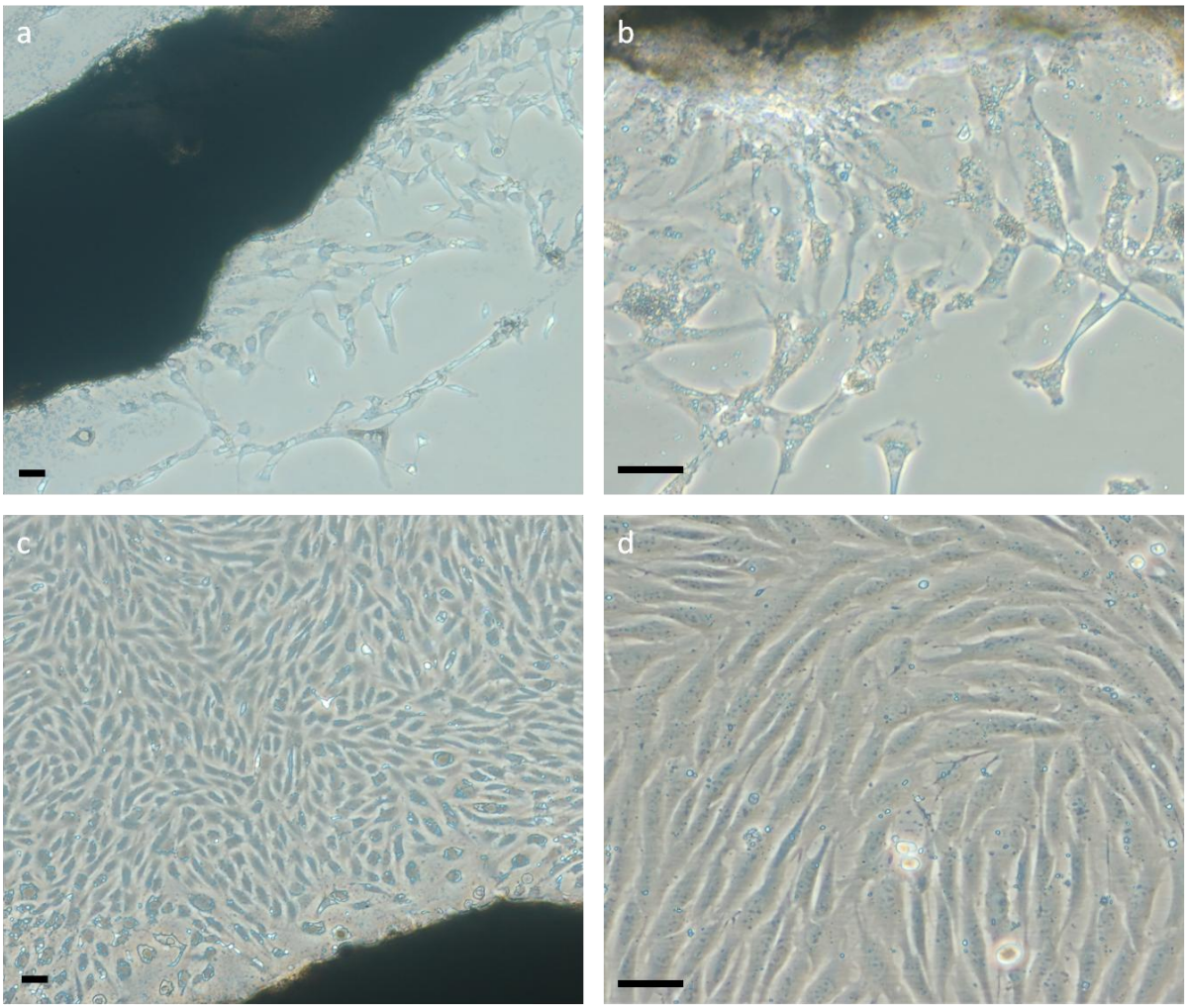

Figure 2-2 Phase contrast images of BTM cells growing from TM tissue explant.

The above phase contrast images show the growth of BTM cells from a section of TM tissue removed from fresh globes and placed in standard culture flasks. Images a & b. illustrate TM cell growth after 5 day with image b taken on higher magnification. Images c & d demonstrate TM cell outgrowth following 2 weeks. Confluent areas of TM cells are present across large areas of the culture flask and will soon be dissociated from the substrate and split to first passage. Scale bar represents 20μm.

2.1.1.2 Bovine Aqueous humor (AH)

Separate bovine globes were used to collect aqueous humor (AH). These globes were kept separate as removal of AH could affect the structure of the TM and/or could cause the release of growth factors. A 1 inch 25 gauge needle, attached to a 1cm syringe was used to extract the AH by inserting through the cornea, bevel upward, 0.5cm anterior to the limbus. Once the tip of the needle was visible at the pupil 500-800µl of AH was removed slowly to minimise the risk of disturbing the internal structures. The volume of AH from each globe was placed in separate vials and immediately frozen until required.

2.2.2 Human Samples

2.1.1.3 Human Tissue

Human samples were provided by Alcon Research Laboratories (Fort Worth, Texas, USA) or were obtained from the Royal Liverpool University Hospital Mortuary. Human globes kindly provided by Alcon Research Laboratories were obtained and consented from various Eye Banks across the United States by Alcon Laboratories according to ethical approval. Globes were retrieved and fixed at the eye banks; suitable globes were then assigned to our study based upon our inclusion criteria. Globes from the Royal Liverpool University Hospital Mortuary were consented by National Health Service Blood and Transplant team and retrieved by an in-house team of qualified eye retrievers. For inclusion in this study globes had to be from non-glaucomatous patients. All other ocular diseases were acceptable but needed to be recorded in medical history. Donor age, sex and ethnic origin were required but were not selective parameters. After enucleation globes were fixed by making an incision approximately 2cm posterior to the limbus region and immersed in 10% NBF for 24 hours. Globes were then washed in PBS before being stored in an air tight container of PBS. Samples were then shipped with donor information to Liverpool where they were immediately transferred into a container of fresh PBS and stored at 4^{o}C. Upon arrival each sample was provided with a new unique code, therefore masking the samples. Donor information relating to medical history, age, sex and ethnicity were recorded on forms which were stored in a secure filing cabinet.

Table 2-1. Identifies globes received from Alcon Laboratories.

Following arrival into our laboratory globes were assigned unique identifying numbers. Each globe used in the study is presented along with donor age, sex and ethnicity.

Identifying number	Age	Sex	Ethnicity
1110	0	Male	Other
1116	11	Female	Caucasian
1102	16	Male	African American
987	35	Male	Other
1106	46	Male	Caucasian
1091	65	Male	Caucasian
1081	73	Male	Other
1099	74	Male	Caucasian
1087	78	Female	Other
1097	86	Female	Caucasian
1100	90	Female	Caucasian

2.1.1.4 Human TM cells

Primary human TM cells were kindly provided by Dr. Pang and Dr. Lane at Alcon Research Laboratories (Fort Worth, Texas, USA). The cells were shipped frozen in DMSO in individual vials to the University of Liverpool. Cells were thawed on arrival, as temperature fluctuations during transit may have resulted in partial thawing.

The contents of each vial were re-suspended 9mls of enhanced medium and centrifuged to remove DMSO. The cell pellet was re-suspended in enhanced fresh medium and placed into an appropriate TC flask (based on cell counts). Cells were incubated at 37^{o}C with 5% CO_2 and examined after 48 hours. Once at 70% confluent level the cells were removed with trypsin and transferred to a larger TC flask with growth medium and cultured as outlined in the previous section (adapted from Pang et al., 1994).

All vials were shipped with specific information relating to passage number and donor information. To prevent bias the cells were assigned random numbers by another member of the group (Laura Currie). Throughout experimentation the human cells were only identified by the code HTM HAS and a three digit number. In all HTM cells from 33 donors were received, of which 26 were used in various investigations. Three vials were found to be infected upon arrival in our lab and a further 4 were not robust enough to recover from freezing and so had to be disposed of. A summary of the cells obtained is presented in Table 2.2.

Table 2-2. Details of primary HTM cell received from Alcon Laboratories.

HTM cells were randomly assigned a donor number for the study (HTM HAS). Of the 33 cultures obtained 26 were used in different investigations throughout this work. Donors marked with an (*) were not used in any of the investigations as they were not robust enough following thawing. The donor cells used in each experiment is detailed in the specific methods.

Donor Number (HTM HAS)	Sex	Age
001*	M	3
002*	F	83
003*	M	73
004*	M	72
005*	F	0
006*	M	80
007	F	2 months
008	M	81
009	M	57
010	M	80
011	F	4
012*	M	88
013	M	73
014	M	91
015	F	58
016	F	51
017	M	67
018	F	83
019	M	6 months
020	M	36
021	M	23
022	M	48days
023	F	92
024	M	0
025	F	61
026	F	6
027	F	5 days
028	M	72
029	F	89
030	F	0
031	F	2
032	F	4
033	M	3

2.3 Defining actin patterns in the TM

The literature provides details on multiple actin patterns in TM cells and tissue (Clark et al., 2005; Clark et al., 1994; Filla et al., 2004a; Grierson et al., 1986; Hoare et al., 2009; Read et al., 2007; Wade et al., 2009). Alongside the normal straight stress fibres, transient arrangements of polygonal actin structures (TAPAS) and actin tangles have been described. In order to further refine our definition of a CLAN a series of experiments were carried out.

2.3.1 Formation of TAPAS

In experimental work set up by Jacinta Lee, confluent cultures of BTM cells were treated for 7 days with either maintenance medium or maintenance medium plus DEX (10^{-7}M). Cells were then dissociated from the substrate using trypsin, centrifuged for 5 minutes, after which the supernatant was discarded and the cells re-suspended in medium. Following introduction onto fresh TC wells the cells were fixed and imaged at 2 hours, 4 hours, 8 hours, then at 24 hours and 48 hours following introduction to the well. The number of polygonal structures present was counted and individual cells were characterised as being round, intermediate or flat in shape.

2.3.2 Morphological analysis

From a large cohort of in-house images, 25 images were handed over in a masked fashion to 3 experienced observers. These images represented 10 of the early polygonal structures (PAAs) imaged in TM cells settling onto a glass substrate within the first 7 hours and 20 CLANs induced following 7 days treatment with various agents including TGF-β2, DEX, decorin and those formed under control conditions.

In separation each observer was asked to place the images into groups based solely on their appearance. Observers were allowed to create as many groups as they wanted and were not provided with any headings.

2.3.3 Measurement of actin structures

In an attempt to further define these structures we conducted computer based measurements of the actin arrangements. In total 25 images were assessed by myself

and Andrew Heath (a person not involved in the initial morphological analysis), consisting of 17 CLANs and 13 PAAs.

Each image was viewed using Image J software and the scale set using the scale system of the program and the values obtained from the calibration of the microscope. The following parameters were then measured using the tools present in image J following a set of previously agreed guidelines.

2.1.1.5 Territory measurements

Using the free-hand tool, a line was drawn along the most peripheral spokes that were involved in a clear triangulated unit. This measurement excluded any hubs or spokes that were not attached to the main body of the structure via a triangulation regardless of whether they were involved in another triangulation. Similarly for analysis purposes any components which were out of focus were excluded.

Given the variation in structure and that the centre of most PAAs were not visible it was necessary to take two territory measurements for PAAs. The first was termed total territory; this included any hub and spoke visible throughout the structure and was used for the size comparison of CLANs and PAAs. Two smaller areas were selected from within the total territory and provided the observable territory. The areas were selected from opposite ends of the structure and in a position where the hubs and spokes were in focus. It was from within the observable area that all other measurements were made. The software calculated several parameters based on these drawings (*Figure 2-3*).

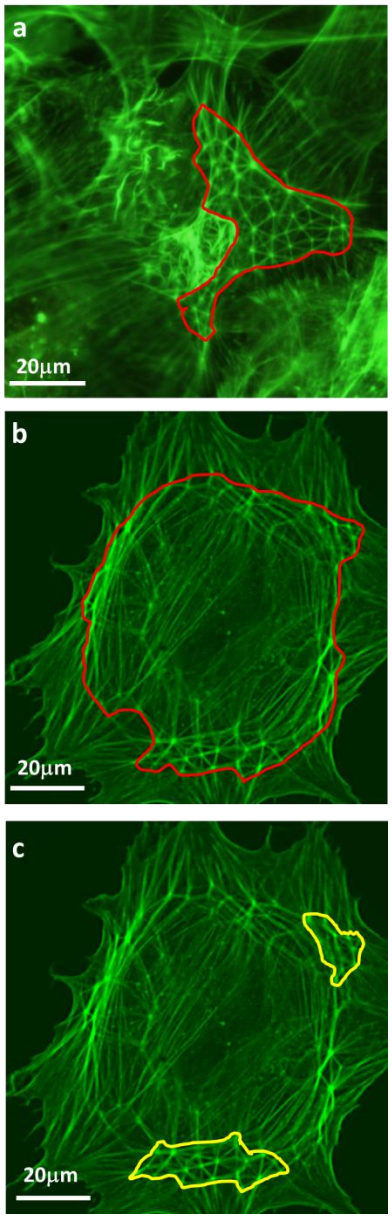

Figure 2-3. Examples of a CLAN (a) and a PAA (b&c)

CLAN territory was achieved by drawing around the peripheral hubs and spokes that were involved in clear triangulated units to the main structure. PAA's however had much greater variation with regards to the spread of triangulations. As seen in image b & c the triangulations do not continue in a uniform pattern around the circumference, therefore 2 measurements were taken on PAA's. The first seen in image b was called the total territory and was compared to the measurement taken for CLANs. The second measurement seen in image c was called observable territory and focused on areas of clear triangulations. Measurements relating to hubs and spokes were obtained from within this area

Using the counter tool present on the software, the number of hubs which fell within the previously set territory were marked and counted. From this the number of spokes radiating from each hub was noted, so that as each hub was counted in turn; the same spoke may have been involved with several hubs. These values were recorded as the frequency of spokes per hub. Separate to this, the boundary of each hub identified was drawn around using the free-hand tool. The software then calculated the area of each hub.

Following these counts, the number of individual spokes present within the territory were marked and counted. This included those which made the periphery of the structure and marked the territory. A single spoke began at one hub and terminated at another. Using the straight line tool of the software the pointer was positioned in the centre of a hub and extended, following the line of the spoke, to the centre of the terminating hub.

As with spoke length the straight line tool was used to measure across the thickness of the spokes. To achieve this it was necessary to use the zoom function on the software. Each image was magnified to the same level and the central band of pixels exhibiting the same grey level (fluorescence level) was included in the measurement.

Measurements were carried out three times and averaged to adjust for any variation in how the lines were drawn. After each image was completed the data was transferred to an excel spread sheet (Microsoft). As well as considering the parameters in respect to the individual images the measurements were pooled together to give average values for both PAAs and CLANs.

2.4 Characterisation of TM cells

2.4.1 Morphological assessment of TM cells

Prior to beginning any experimental work the cells which were used throughout this investigation were observed under standard cell culture conditions. Cells in TC flasks with growth medium were imaged using x4, x10 and x20 objectives on a phase contrast microscope. These images were taken throughout the growth of cells and accompanied notes on cell morphology. By assigning codes to the cultures this assessment was undertaken in a masked manner.

2.4.2 Cell seeding density

As these experiments required the cells be at a confluent level before treatment which could be as long as 7 days an appropriate seeding density was vital. TM cells were seeded onto glass labtek chamber slides at the following densities; 5,000 cells per cm^2, 10,000 per cm^2 or 30,000 per cm^2. At days 1, 3, 5, 7 and 10, images were taken to evaluate cell confluence and cell morphology. After microscopic examination TM cells were dissociated from the substrate and counted via a haemocytometer.

2.4.3 Growth curves

TM cells were seeded at 10,000 cells per cm^2 into 6 wells of a 12 well plate and incubated with growth medium for up to 14 days with medium replenished every 3 days. Growth curves for BTM cell cultures established from 6 donors and a panel of HTM cells were produced by performing haemocytometer counts at day 1,3,5,7, 10 and 14. The influence of maintenance medium, maintenance medium plus 2ng/ml TGF-β2 or maintenance medium mixed 1:1 AH was assessed in the same manner.

2.4.4 Can media affect CLAN formation?

Previously published results obtained from the current work (O'Reilly et al., 2011) demonstrated that CLANs were present to some degree in all cultures. These experiments were carried out in order to assess the influence of FCS on TM cell CLAN formation. Confluent cultures of HTM cells from donors HAS 007, 011, 015, 010 and BTM cells established from multiple donors were incubated with DMEM containing 0%, 0.5%, 1% 10% or 30% FCS for 7 days, with the media replenished at day 3.

Dextran charcoal can be used to remove factors from FCS (Dang and Lowik, 2005). The dextran coated charcoal (DCC) suspension was prepared by adding 2.5g of DCC (Sigma) to 20mls of 10mM tris-buffer at pH 8.0.The solution was centrifuged at 1000rpm for 10 minutes after which the supernatant was removed and the DCC was re-suspended in 20mls of 10mM tris-buffer. The centrifugation step was repeated and the pellet was again re-suspended and the resulting solution was autoclaved.

In order to strip the FCS, 2mls of DCC suspension was added to 100mls of FCS and was incubated overnight at 4^{o}C on a rocker for gentle agitation to allow for the binding of steroids in FCS. The solution was then centrifuged at 3000rpm for 20 minutes followed by incubation at 56^{o}C for 40 minutes with agitation to allow adsorption of molecules. Any remaining particles were removed from the solution by multiple cycles of centrifuging at 4,500rpm for 5 minutes. Finally the solution was passed through a 0.2mm filter membrane and stored in frozen aliquots until needed. Commercially available stripped FCS was also purchased from Sigma. When required the stripped FCS was thawed and added to DMEM with L-glutamine (2mM), penicillin-streptomycin solution (100U/ml and 100μg/ml) and amphotericin B (2.5μg/ml) (Sigma).

In further experiments BTM cells which had been grown to a confluent level in growth medium had all the media removed and replaced with maintenance medium for 24 hours prior to incubation with either growth medium, maintenance medium or 2ng/ml TGF-β2 for 7 days.

2.5 Do factors present in the aqueous humor (AH) influence the formation of CLANs in TM cells?

As TM cells are constantly bathed in AH *in vivo* any components which could influence TM cells would be present in the fluid making it an obvious starting point to investigate possible inducers of CLANs under normal physiological conditions.

2.5.1 Effect of fresh and frozen AH on BTM cells

Given the nature in which AH was collected, cells could not always be treated with fresh AH and so to ensure that the freezing process did not alter the AH, a comparison was made between BTM cells grown in fresh AH and frozen AH. This was achieved by treating BTM cells with either fresh or frozen AH for 7 days. Cells were examined visually every 24 hours via phase microscopy until they were fixed using 10% NBF. These visual records of cell health and the final analysis of the fixed cells were used to assess any differences between treatments.

2.5.2 Optimising AH media

Under normal circumstances AH is in continuous production and motion ensuring TM cells are constantly bathed with appropriate growth factors and waste products are removed. During our investigations, however, the use of undiluted AH was quickly identified as an unreliable cell culture medium. It was suggested that it was not sufficient to maintain cell health when stagnant. Given the limited supply of AH available it was deemed impractical to replace the AH regularly and so the decision was taken to supplement the AH with medium containing FCS. To minimise the effect of additional factors in the FCS the percentage added was kept below 2%. BTM cells grown to a confluent level on labtek chamber slides were treated with AH mixed 1:1 with DMEM containing 0.5%, 1% or 2% FCS. Different ratios of AH to DMEM were also investigated so that cells were treated with 1:3, 1:1 or 3:1. Cells were treated in this manner for 7 days with a media change on day 3. Cells were imaged every 24 hours throughout the 7 days experimentation period to assess cell health and attachment.

2.5.3 TM cells treated with aqueous humor

Based on the optimising experiments, BTM cells were treated with AH mixed 1:1 with maintenance medium for 7 days after which they were fixed and CLAN incidence was assessed. The same procedure was also conducted on HTM cells from 5 donors spanning the age range available.

2.5.4 Treatment of TM cells with growth factors

Three growth factors found to be increased in the AH of glaucoma patients were added to TM cells in concentrations ranging across the physiologically measured concentrations.

2.1.1.6 Growth factor dose response

The growth medium was removed from confluent cultures of BTM cells in labtek chamber slides and replaced with fresh maintenance medium containing varying doses of the following human recombinant growth factors (all from Invitrogen); hepatocyte growth factor (HGF) (0.2-1ng/ml),basic fibroblast growth factor (FGF) (0.2-1ng/ml) or transforming growth factor beta 2 (TGF-β2) (1-8ng/ml). Medium was replenished at day 3 and the experiment terminated at day 7.

2.1.1.7 Combined growth factor effect

In further experiments, cells were incubated for 7 days in maintenance medium containing the following combinations of the growth factors to assess their overall effect:

HGF plus FGF,

HGF plus TGF-β2,

FGF plus TGF-β2,

FGF plus HGF plus TGF-β2

Based on the previous dose response curves BTM cells were treated with maintenance medium containing 0.8ng/ml FGF 0.8ng/ml HGF or 2ng/ml TGF-β2 for 7days.

2.5.5 Is TGF-β2 the main CLAN inducing agent in Aqueous humor (AH)

Given the promising CLAN induction evoked by the addition of TGF-β2 to TM cells, the effects of this growth factor were further explored by the addition of neutralising antibody specific to TGF-β2 to either medium containing 2ng/ml TGF-β2 or to AH.

A solution of maintenance medium was prepared containing 2ng/ml TGF-β2 and a TGF-β2 specific neutralising goat polyclonal antibody at varying concentrations (0.8μg/ml, 1.6μg/ml, 3.2 μg/ml and 6.4μg/ml). This was then added to confluent cultures of BTM cells and incubated in the manner for 7 days with media replenished as always at day 3. Fixed cells were then assessed for cell morphology and CLAN incidence in comparison to TGF-β2 treated cells. Data collected from the dose response curve indicated that an antibody concentration of 1.6μg/ml was sufficient to reduce CLAN incidence without having an adverse effect on cell morphology.

In neutralisation experiments, the TGF-β2 antibody was added to a solution of 2ng/ml TGF-β2 in maintenance medium. In a separate well, an IgG control was added at the same concentration (1.6μg/ml) to the maintenance medium containing TGF-β2 (2ng/ml) and served to highlight any non-specific response in CLAN incidence by the presence of the antibody. As an assay control the IgG control was also added with maintenance medium only. Confluent monolayers of BTM cells were treated with TGF-β2 (2ng/ml in maintenance medium) to serve as a positive control for CLAN induction while cells treated with maintenance medium only, were used to show baseline CLAN incidence. All conditions were extended for 7 days, with a change in media at 3 days.

These experiments were also carried out with aqueous humor.

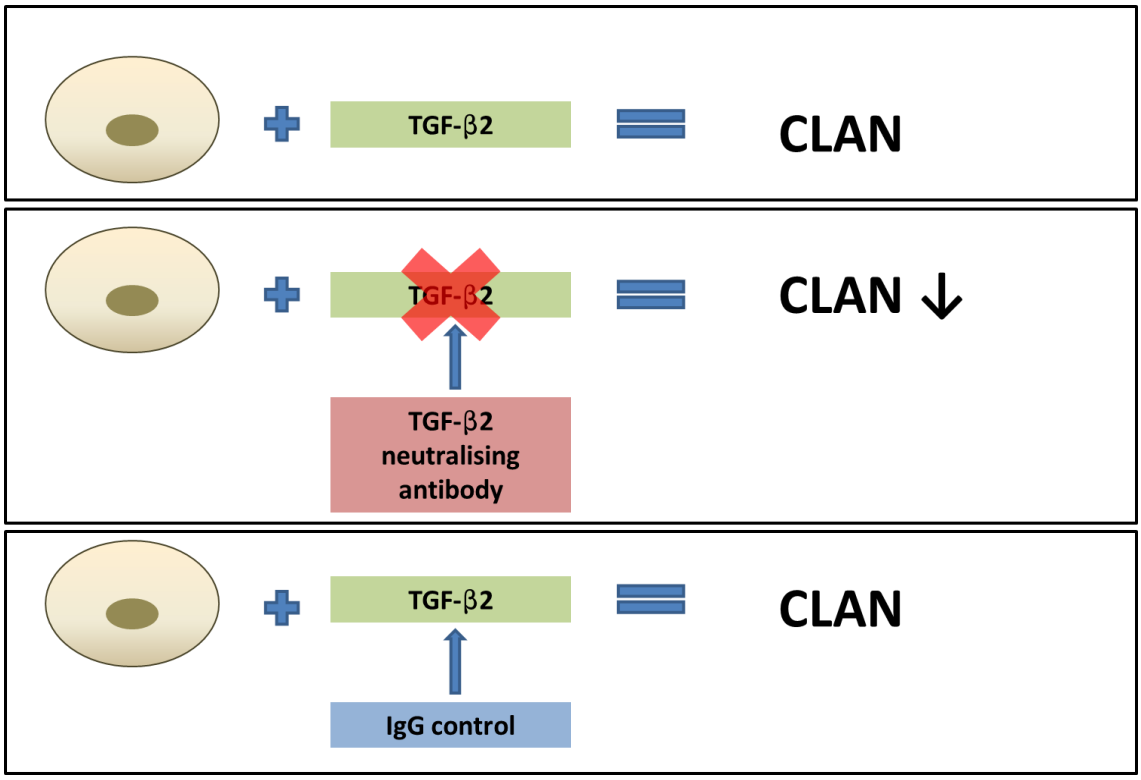

Figure 2-4 Diagram illustrating the TGF-β2 neutralisation experiment.

The addition of TGF-β2 to TM cells in vitro was shown to produce CLANs. If TGF-β2 was the main CLAN inducing agent then removal of this cytokine would result in baseline levels of CLANs. The action of TGF-β2 was blocked by a specific neutralising antibody and if TGF-β2 was the sole inducer then the CLAN induction would be negated. In order to test the specificity of the antibody an IgG control was added to TGF-β2 treated cultures of BTM cells. As this should not influence TGF-β2 (to any great effect) the incidence of CLANs should remain consistent with TGF-β2 treatment.

2.6 Can donor Age influence CLAN incidence?

2.6.1 *In vitro* experiments

HTM cells (passage 5-8) from 26 donors of various ages (5 days – 91 years old), were seeded onto glass labteks at 10,000 cells per cm^2. Cultures were incubated for up to 7 days in growth medium until cultures were almost confluent. The growth medium was removed and cells in each labtek were treated with either: maintenance medium, growth medium or 2ng/ml TGF-β2 in maintenance medium. At the end of the 7 days cells were fixed and stained to allow CLAN incidence to be assessed.

2.6.2 *Ex Vivo* Experiments

2.1.1.8 Human TM tissue dissection

The human globes were orientated based upon muscle position and the superior point marked. Curved scissors were used to extend the incision made during the fixation process and to cut around the globe 0.5cm posterior to the limbus (to avoid the attachment point of the vitreous humor). This resulted in a separate anterior and posterior segment (*Figure 2-5*). The lens was carefully removed from the anterior segment by cutting the zonules. Based on the earlier orientation the anterior chamber was divided into quadrants (Figure 2-5). The temporal quadrant was always used for whole tissue analysis while the other quadrants are retained for other techniques; the nasal for cryo-sectioning or immunohistochemistry, the inferior for quality control and the superior was held in reserve. In order to visualise the TM the iris had to be removed. This was achieved by holding the end of the cornea and gently peeling the iris back toward the ciliary body using blunt forceps. Using a sharp blade the boundary of the meshwork was scored along and using fine pointed forceps (Agar Scientific) the meshwork was gently peeled free. The individual sections of meshwork were floated onto PBS in a 12 well plate.

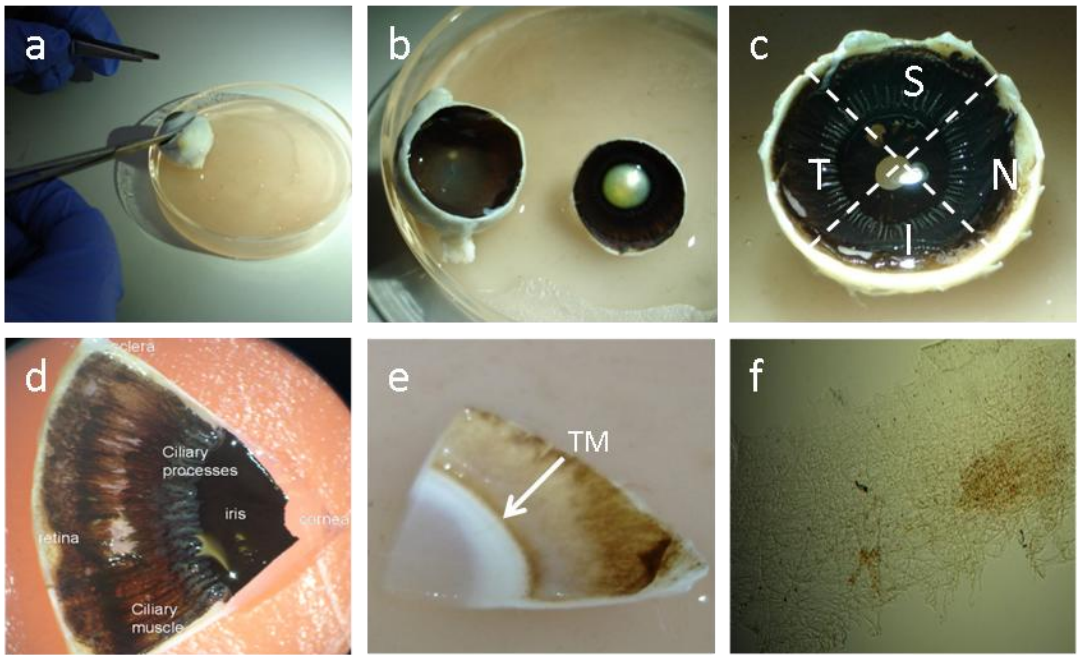

Figure 2-5. A series of photographs showing key steps in dissection of a human eye.

Human globes that had been previously fixed in NBF were dissected to provide a section of trabecular meshwork for in situ analysis of the actin structure. The incision made during fixation was extended using curved scissors to produce a posterior and anterior segment. The lens was removed and the anterior segment divided into quadrants. The iris and ciliary body were removed from the temporal quadrant to reveal the trabecular meshwork which could then be removed with fine forceps and floated out onto PBS for staining.

2.1.1.9 Human TM tissue processing

Once removed from the eye all temporal sections of TM (floated on PBS) were examined and imaged under light microscopy (Nikon Optiphot) so that the condition of the tissue could be evaluated and selected for further processing.

In a fresh 12 well plate the selected TM section was firstly permeablized using Triton-X for 5 minutes, following two washes in PBS tween the section was then stained using Alexa-phalloidin-488 (1 in 40) for 20 hours. After further washes in PBS the section was submersed in PI (10μg/ml) for 4 hours at room temperature. Once excess PI had been removed by further washes in PBS, the tissue section was transferred to a glass slide. Fluorescent mounting media (Dako) was used to cover the section and a glass cover slip applied. The mounting media was allowed to set overnight at room temperature before imaging was carried out.

The stained TM section was firstly imaged by x10 objective on a Nikon Diaphot microscope with fluorescent band pass 450-490nm filter to provide overlapping images that covered the entire area of the tissue section. Combining the images provided a montage to allow for orientation and sample area selection (Figure 2-6).Using x60 oil objective on confocal microscopy system (Biorad), a z-series stack was captured at each of 20 areas identified as containing TM. In each area 16 images at an increment of 1μm were captured on both red and green filters (Brotchie et al., 1999).

Images collected via the green channel were phalloidin and each image in a z-stack was examined using Image J program. Once a CLAN was identified its boundary was marked using the drawing option. Once all images in the stack were examined the z-series was converted to a single merged image. As CLANs could transcend multiple z-images this allowed for identification of actual CLAN number as we could clearly see which individual areas were part of a larger CLAN. Nuclei were captured separately via the red channel and quantified by merging z-images to be counted manually using cell counter application of Image J.

Figure 2-6. Montage of phalloidin images showing extent of TM tissue.

The individual images were capture on a Nikon camera attached to a Nikon Diaphot microscope using a 450-490nm filter to excite the phalloidin. A montage like that shown was created for all pieces of tissue analysed and was used for orientation purposes when viewing the tissue on higher objectives on confocal microscope.

2.7 How do age-related stresses influence CLAN incidence?

2.7.1 β-galactosidase staining

Confluent cultures of BTM cells at passage 6 and 11 were maintained on labtek chamber slides for 4 weeks to increase cell adhesion to the substrate and induce a state of senescence. These cells were used to optimise the β-galactosidase (β-gal) staining protocol of a commercially available senescence kit (Sigma). Following the manufacturers guidelines, the medium was removed and cells were washed in PBS prior to the addition of fixation buffer, provided with the kit. An optimum fixation time was found to be 6 minutes. Following further washes 500µl of the staining mixture (prepared following the manufacturers guidelines) was added to each well and allowed to incubate for 6 hours at 37^{o}C without CO_2 (Yu et al., 2010).

Following the evaluation of BTM cells, a panel of HTM cells from various donors were stained with β-gal following 7 days incubation with either maintenance medium or 2ng/ml TGF-β2 in maintenance medium. In order to investigate CLAN coincidence in senescent cells the monolayers were counterstained with Alexa-phalloidin 488 and PI as previously described. A microscope with both bright field and fluorescent capabilities was used to capture images from 10 fields of view in each well. Areas were selected randomly moving across the well and images were captured via x40 objective using a Nikon camera attached to the microscope. Images were firstly collected from the bright field to show the β-gal staining, the microscope was then adjusted for fluorescence and images were captured using the 450-495nm and 520-560nm filters.

When all areas were captured, the images were viewed using Image J software. The PI stained nuclei provided the total number of cells present in a field of view. Comparing the phalloidin and β-gal images allowed for the identification of the number of β-gal positive cells in the field of view and the number of β-gal positive cells that contained a CLAN. From these values the following could be calculated: the level of senescence in different cultures, the percentage of CLAN containing cells in the culture and the percentage of cells which were categorised based on β-gal staining and the presence of CLANs.

2.7.2 Apoptosis staining

Confluent cultures of TM cells were assessed for apoptosis using Click-iT TUNEL staining kit (Invitrogen). Following the specification guidelines, cells previously fixed with NBF and permeabilised using Triton-x were washed in deionised water and incubated for 10 minutes in TdT reaction buffer. Following this, cells were again washed and incubated in TdT reaction cocktail for 60 minutes at 37^{o}C. After further washes in 3% BSA the cells were incubated in Click-iT reaction cocktail for 30 minutes at room temperature. Cells treated with DNase served as an experimental control while cells treated with staurosporine served as a positive control.

2.7.3 Oxidative stress

Confluent cultures of BTM cells and a panel of HTM cells (HAS 030, 032,020,015,028) were treated with 200, 400, 600 or 800µM of hydrogen peroxide (H_2O_2) in maintenance medium for 1 hour (adapted from Yu et al., 2008). The short term influence of H_2O_2 on TM cells was assessed by fixing cells immediately. In further experiments the media was removed and replaced with either maintenance medium or 2ng/ml TGF-β2 in maintenance medium. Cells were allowed to recover for 7 days with media replenished at day 3. Cells were then fixed and stained as previously described.

BTM cells treated for 1 hour with increasing concentrations of H_2O_2 were stained using a commercially available general ROS probe, CM-H_2DCFDA (Invitrogen). Cells were incubated with 10µM of probe (in PBS containing 2% FCS) for 20 minutes at 37^{o}C after which the cells were washed in warmed PBS containing 2% FCS. Cells were then imaged on an inverted microscope with both phase and florescent capabilities using x20 objective and 450-490nm band pass filter for fluorescence.

The probe was also utilised for flow cytometry to assess any baseline variations in ROS. Confluent cultures of BTM and HTM cells incubated with maintenance medium or 2ng/ml TGF-β2 for 7 days were re-suspended in PBS containing 2% FCS plus 10µM CM-H_2DCFDA. A proportion of cells from each donor were left unstained to adjust for auto-fluorescence and allow for efficient gating of cells if any variation in cell shape or size existed between donors. Cells were treated for 1 hour with 800µM H_2O_2 prior to

addition of CM-H_2DCFDA served as a positive control for fluorescent levels. Cells were run through a FACScalibur instrument using FL-1channel as the emission/excitation spectrum for this product was excitation 492-495nm and emission 517-527nm. The thresholds for forward and side scatter were set to 52 using detection E00 and a total of 10,000 counts were performed for each sample.

2.7.4 Advanced glycation end-products (AGE)

As variation in substrate can influence functionality, TM cells were grown on glass or plastic labtek chamber slides as well as unmodified matrigels and AGE-modified matrigels. Cells were seeded onto the substrates and monitored daily until a level of near confluence was reached. Cells were then incubated with maintenance medium or 2ng/ml TGF-β2 for 7 days after which the cells were fixed, stained and assessed for CLAN incidence.

The matrigel was AGE modified following the previously published protocol (Glenn et al., 2009; Stitt et al., 2004) as described. Commercially available matrigel (BD bioscience) was thawed at 4^{o}C overnight before being diluted 1 in 10 with DMEM only over ice. 300 µl of the resultant solution was then gently aspirated (avoid introducing air bubbles) over the surface of a 3.5cm^2 diameter dish (Iwaki) to form a thin layer. The dishes were then incubated for 1 hour at 37^{o}C, during which the dishes were occasionally rocked to ensure an even coverage of the surface. Any excess liquid remaining after this time was removed and 2 mls of 100mM glycoaldehyde (Sigma) in PBS was added to the dish. The matrigel coating was incubated with this solution for 4 hours at 37^{o}C, after which the reaction was terminated by adding 50mM sodium borohydride in PBS (Sigma). The termination mixture was incubated for 1 hour at 37^{o}C before being removed and the coating washed in PBS. The modified matrigel was covered in PBS and returned to the incubator overnight. Unmodified matrigels were set-up at the same time as the modified with PBS used for incubation period. The cells were fixed with NBF and stained using Alexa-488 phalloidin. Round coverslips were placed in the centre of the wells and imaging was performed using an upright microscope with both bright field and fluorescent capabilities.

3. Defining actin structures in the TM

While this work has focussed on whether CLAN formation in TM cells is related to age, we as a group have worked to establish more clearly a definition of what a CLAN is and how we quantify their presence. The literature has identified several actin patterns in TM cells (Clark et al., 1994; Filla et al., 2004a; Wade et al., 2009) and in TM tissue (Hoare et al., 2009; Read et al., 2003; Read et al., 2007). Broadly these are polygonal actin structures which will be referred to as transient arrangements of polygonal actin structures (TAPAS), straight stress fibres, tangles and CLAN-like structures. This section is focused on distinguishing between actin structures present in TM cells and illustrating the structures on which this work is based. This involved reviewing work previously carried out and re-assessing the findings in line with the current literature and discoveries.

3.1 Formation of TAPAS

The initial work of (Clark et al., 1994) and work published by our group (Wade et al., 2009) reported that DEX could induce CLANs in confluent cultures of BTM cells. Data published by Wade, represented in Figure *3-1*, illustrates the increase of polygonal structure from around 20% at 3 days exposure to DEX to almost 50% following 14 days. These structures remained present while the treatment was maintained but were subsequently lost when the treatment ceased, falling to within baseline levels by day 7.

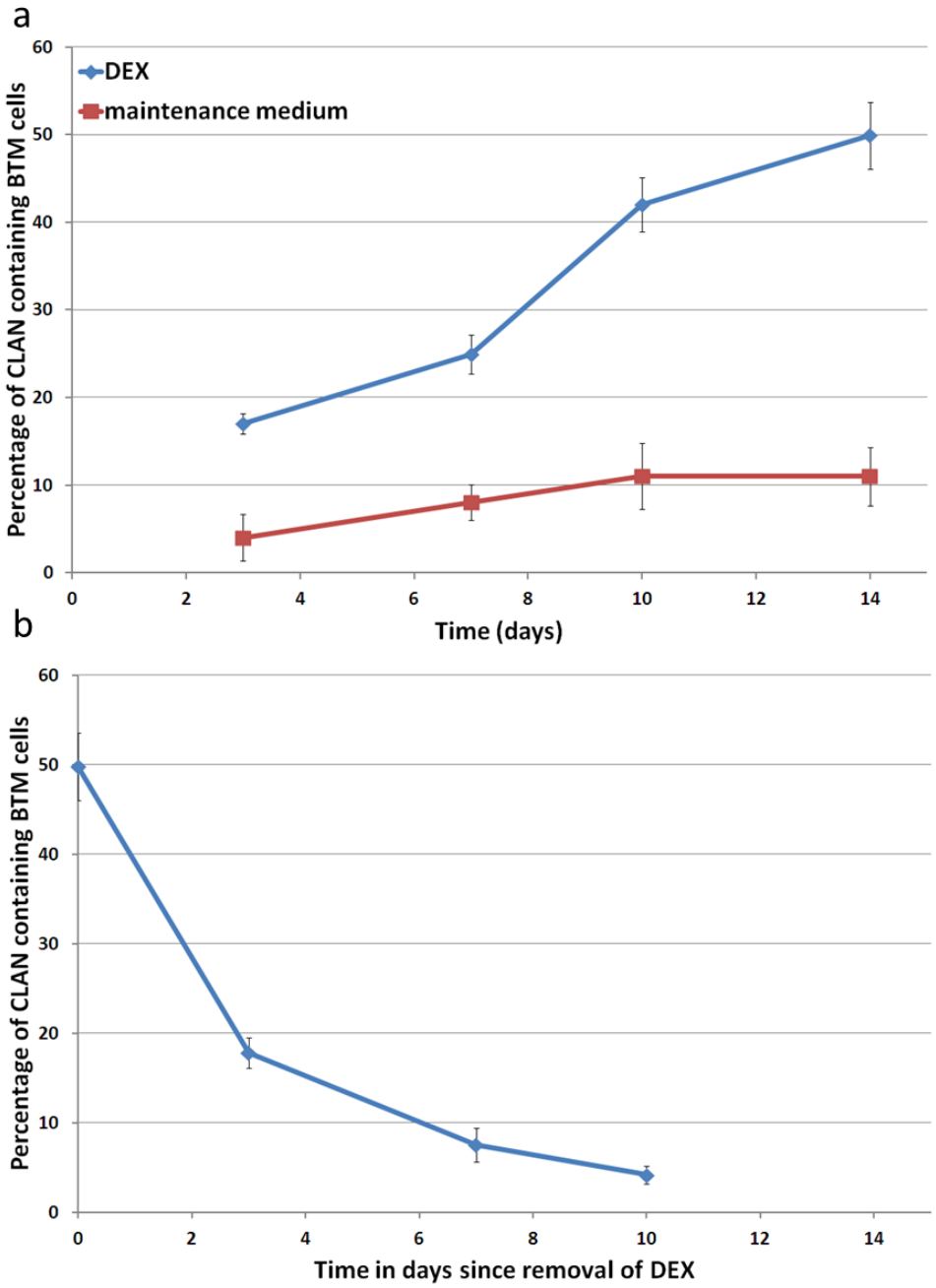

Figure 3-1. Percentage of CLAN containing cells produced by DEX treatment over 14 days and after removal of DEX.

Data adapted from Wade et al, exploring the presence of TAPAS in BTM cells. (a). Line graph showing the increasing incidence of CLANs in BTM cell cultures in the presence of DEX (x10^{-7}) compared to medium over a 14 day period. The incidence increases with time but to a much greater extent in the presence of DEX. (b). Scatter plot of percentage of CLAN containing cells following the removal of DEX (replacing with medium). The percentage of cells containing these structures decreases until the numbers are similar to baseline by 7 days. (n=3, error bars represent standard deviations).

Others investigating CLANs have used polygonal structures formed during settlement (Filla et al., 2004a). The current work demonstrates the formation of these structures. The percentage of BTM cells containing TAPAS in the hours following the introduction of cells to a fresh TC substrate exhibited a sharp increase rising from less than 2% to 15% in the first 4 hours. The initial increase was followed by a decline, and by 48 hours there was little evidence of polygonal structures (Figure *3-2*).

Characterisation of BTM cell phenotype as round, intermediate or flat was used as an indication of the degree to which cells had attached to the substrate. As cells settle onto a fresh substrate they begin to slowly stretch out and flatten. Figure *3-2* provides a graphical account of the percentage of BTM cells in each category. At 2 hours most BTM cells were categorised as intermediate (49.5%), however as time passed the percentage in this category decreased so that by 4 hours 35% and by 8 hours 20% were intermediate. By 8 hours 76% of cells exhibited a flatten phenotype with only 4% as round, this trend continued as at 24 hours 91% of the cell population had a flattened shape and only 1.5% round. There was however a small shift at 48 hours, with a decrease in the number of flat cells (79%) and increased in the intermediate category.

BTM cells previously treated with DEX were dissociated into cell suspension and introduced to a fresh TC substrate. Under these conditions a similar pattern was observed to cells settling without pre-treatment, however, the highest incidence of these structures took longer to form (Figure *3-3*). After 2 hours almost 3% of BTM cells contained TAPAS, increasing to 7% at 4 hours and to a maximum of 21.5% at 8 hours. Following this the numbers began to decrease until at 48 hours approximately 1% of cells contained TAPAS.

Analysis of cell phenotype revealed the greatest numbers of cells were classed as intermediate (58%) at the 2 hour time point. whereas almost half the cell population was categorised as flat (44%) by 4 hours, increasing to 66% at 8 hours. By 24 hours the number of round cells was 1.3% while flat cells accounted for 89% of the population, however, by 48 hour there was a shift in cells from flat to intermediate.

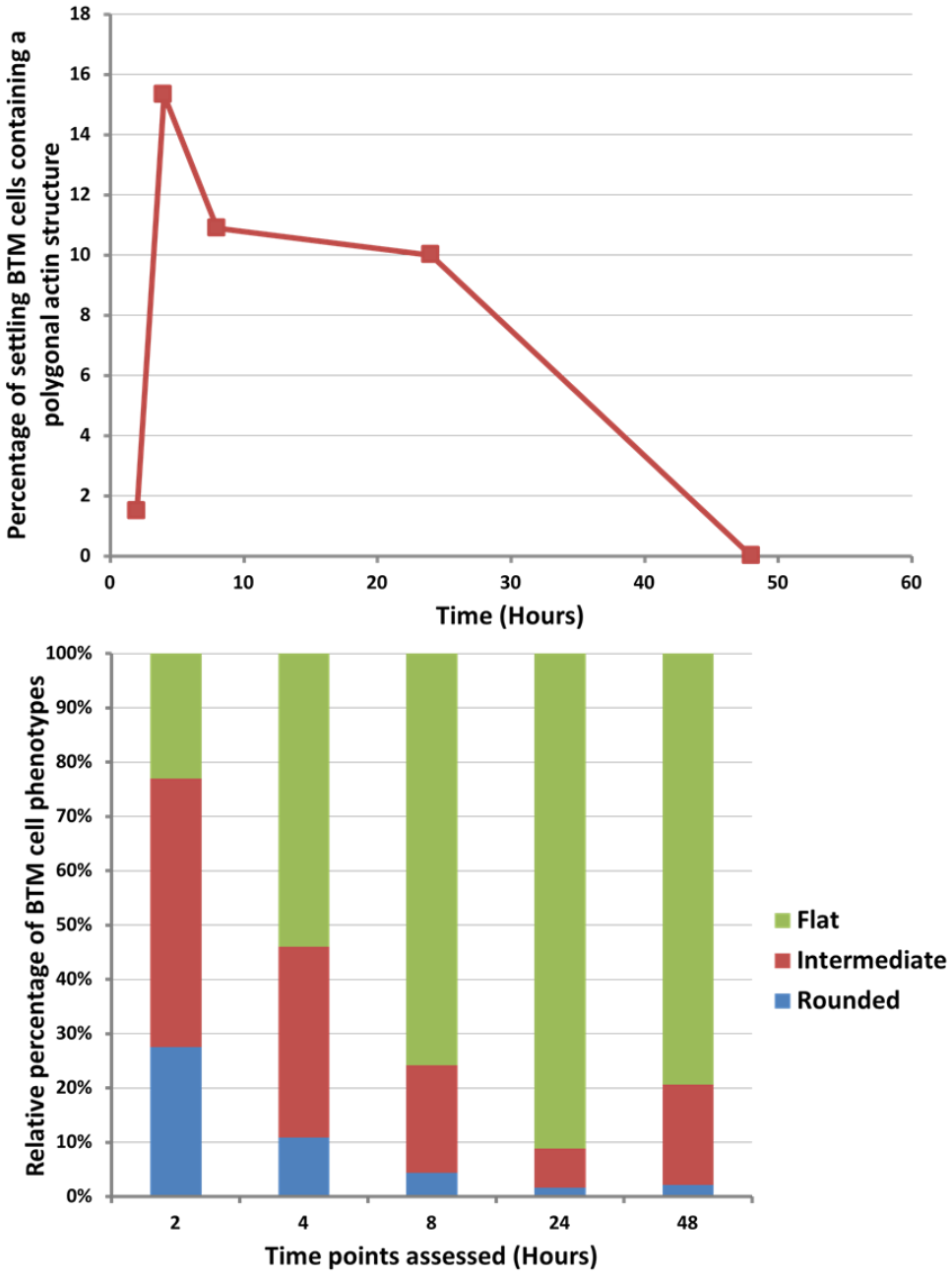

Figure 3-2. The percentage of TAPAS in settling cells alongside cell phenotype.

Analysis of data obtained in conjunction with Jacinta Lee, exploring the formation of TAPAS during BTM cell settlement. Scatter plot showing the change in the percentage of BTM cells containing a polygonal actin structure at various time points following addition of cell suspension to TC substrate. Bar chart representing the percentage of the BTM cell population that falls within three categories; rounded, intermediate and flat, used to describe how well cells have settled onto substrate. (Average percentage where n=3).

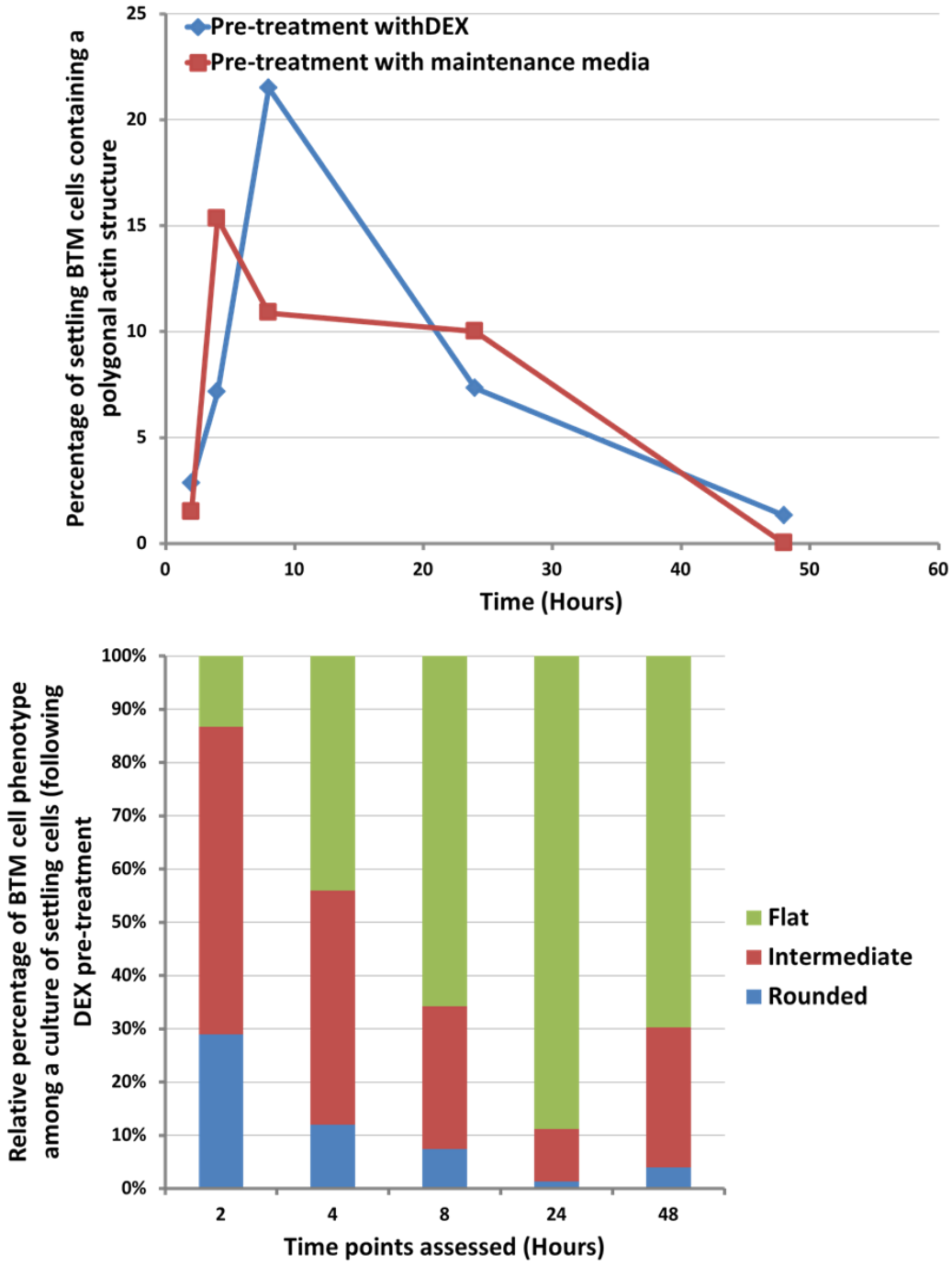

Figure 3-3. Percentage of BM cells containing TAPAS during settlement following DEX treatment.

Analysis of data provided by Jacinta Lee, exploring the formation of TAPAS during BTM cell settlement. a. Scatter plot showing the change in the percentage of BTM cells containing a polygonal actin structure at various time points following addition of cell suspension to substrate. b. Bar chart representing the percentage of the BTM cell population that falls within the three categories; rounded, intermediate and flat, used to describe how well cells have settled onto substrate. (n=3)

3.2 Defining TAPAS

As TAPAS were formed during settlement and following treatment of stable cultures with DEX and TGF-β2 we wished to address whether their morphology was identical regardless of inducement. Experienced observers reported that all TAPAS were composed of hub points connected by straight actin spokes which were arranged in triangulated units to form polygonal shapes. However, upon unmasking, it was found that all observers had placed those TAPAS formed during settling in a separate group from those formed in confluent cultures. For the purposes of clarity we have therefore referred to TAPAS formed during settlement, polygonal actin arrangements (PAAs) and have reserved the term cross-linked actin network (CLAN) for the structures induced in stable cultures, in keeping with our previous publications.

Our previous definition of a CLAN stated that the minimum inclusion criteria for a CLAN to be counted was 5 hub points connected by spokes to form 3 linked triangulated units as illustrated in Figure *3-4*. While it is clear that both PAAs and CLANs fit within this definition it seemed to the observers that CLANs and PAAs occupied different locations within the cell. PAAs occurred around the periphery of the cell and were large in overall size. PAAs were also noted as being less uniform with regards to the spread of triangulated units around the cell, while CLANs had more compact and regular spread of triangulated units. CLANs were recorded as being smaller structures that were localised to the centre of the cell (Figure *3-4*). CLANs also appear to occur higher in the cell than the stress fibres and in some instance their 3D nature is clearly obvious

No observer was able to distinguish between CLANs formed under the various treatments in confluent cultures.

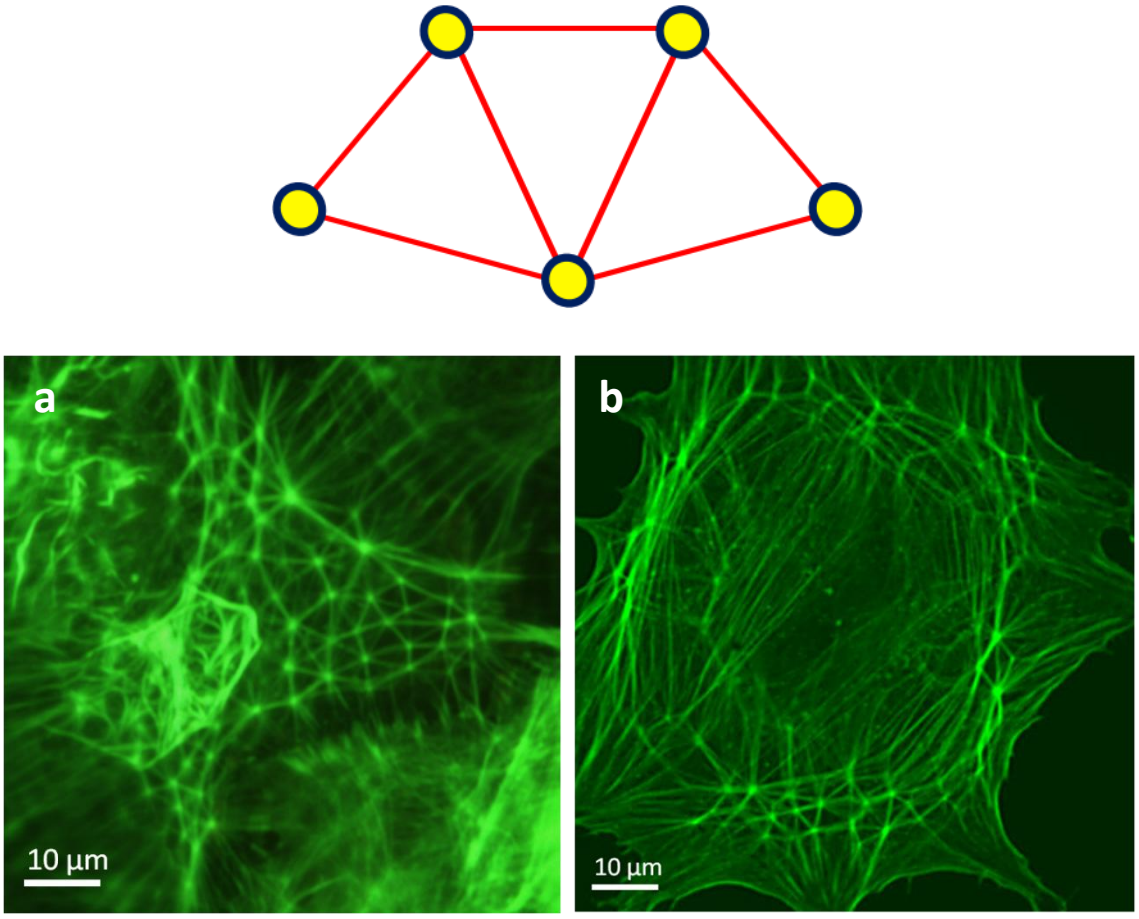

Figure 3-4. Example of a CLAN and a PAA in BTM cells illustrating the localisation of the structures.

The diagram demonstrates the minimum criteria previously set for inclusion of CLANs in quantitative analysis. For inclusion in our counts the actin structure must contain 5 hub points connected via straight actin spokes to form 3 distinct triangulated units. Clearly this structure fits with both CLAN and PAAs as seen in the fluorescent images. Image a. is an example of a typical CLAN formed in TM cells while image b. demonstrates a typical PAA formed in BTM cell. While the CLAN occurs in the centre of the cell the PAA forms close to the cell periphery. The triangulated units of the PAA are not clearly visible around the entirety of the cell. The scale bars also provide an idea of the relative size difference between these structures.

3.3 Measurement of actin structures

In order to quantify the morphological observations made a series of measurements were carried out on masked images of TAPAS formed under different circumstances. These measurements included the overall size of the structures as determined by area and the number of hubs and spokes within.

Morphological assessment reported that CLANs were smaller than PAAs. Measurements revealed that CLAN area was variable ranging from 550μm^2 to almost 3000 μm^2 in the extremes, however, the majority of the values fell between 600-1000μm^2 with a mean value of 830μm^2. In comparison, PAAs were consistently larger than CLANs with total territory ranging from 4000-9000μm^2. There were some larger than average PAAs with 3 measuring above 8000μm^2 ,however, most were found to measure between 4000 to just above 6500μm^2.

A difference in overall shape was also discovered when territory circularity was evaluated. PAAs seemed to be much rounder (average value of 0.8 +/-0.09, where 1 is a perfect circle) compared to CLANs (average value 0.4+/-0.14). The circularity of CLANs was more varied than that observed in PAAs, with values ranging from 0.3-0.7. Comparing cell surface area to the area of these structures would have been informative as it would place a numerical value on how much of the cell was potentially compromised by the structure.

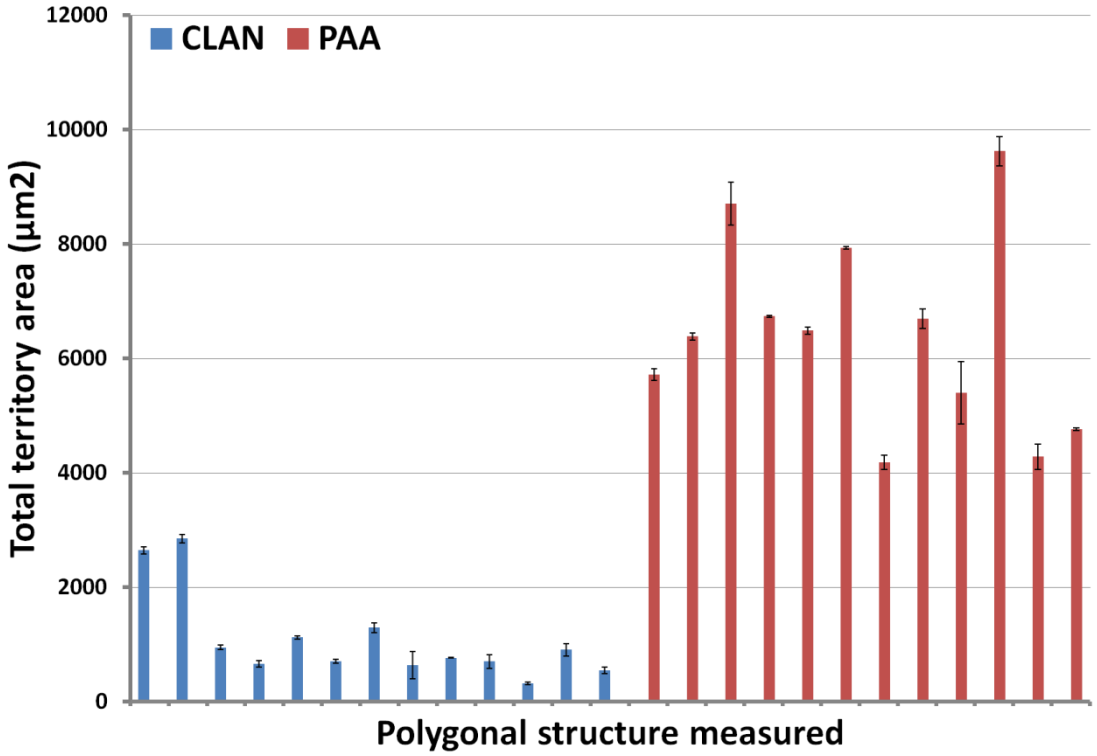

Figure 3-5. Graph showing variation in territory measurements of CLANs and PAAs.

The above areas were obtained by drawing around the perimeter of each structure. The territory area of CLANs was significantly lower than that of PAA's despite the variation observed in both groups.

As well as considering the area of the structures the components from which they were composed were carefully examined. The number of hubs and spokes within the territory revealed that the average CLAN contained approximately 30 hubs. The few large CLANs included in the investigation contained 70-150 but CLANs of this size were not frequently observed. PAAs had on average 50 hubs ranging from 22-70 (Figure 3-6). The number of spokes present in CLANs was calculated as 55 on average but could reach around 150 in larger CLANs. PAAs tended to have more spokes (average 85) ranging from 60-120, this was not an unexpected finding as PAAs tended to have more hubs. The number of spokes per hub was found to be 4 on average for CLANs and 3.5 for PAAs. This value was viewed with caution however as many of the spokes were believed to be out of the plane of focus.

Despite differences in overall size and shape, measurements of the basic components (triangulated units) of CLANs and PAAs revealed that they were almost identical. Hub area for both structures was found to be comparable with an average of 2.2μm^2 calculated for both structures. Measurement of spoke width was found to be problematic and produced variable results. Regardless of CLAN size there was good consistency in spoke length measured. The average spoke length for all CLANs in the series was found to be 6μm (+/- 1) while spoke length in PAAs was found to be slightly shorter (5μm+/-1.1) (Table 3-1).

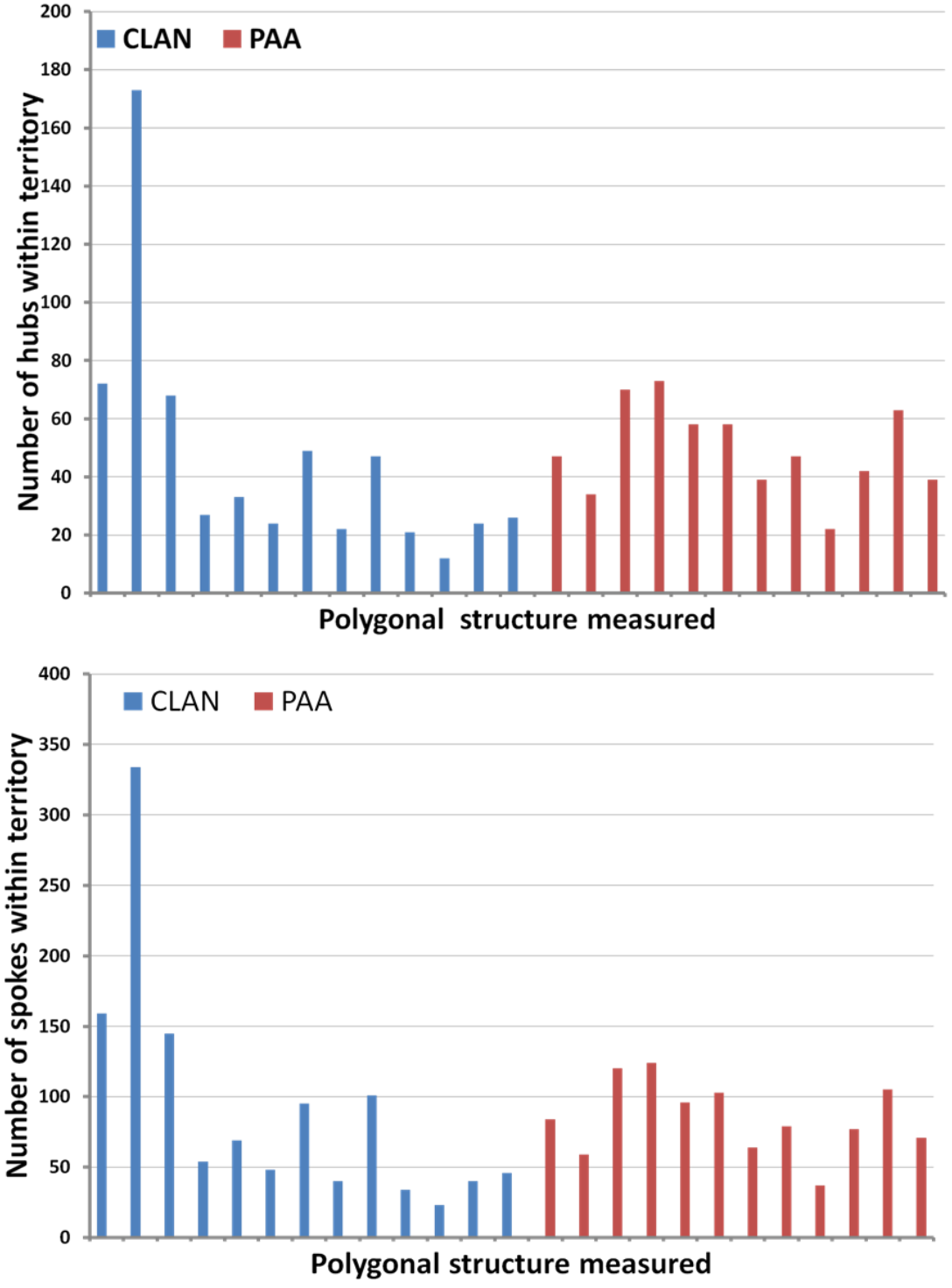

Figure 3-6. Histograms demonstrating the number of hubs and the number of spokes in CLANs and PAAs.

Image analysis measurements revealed that the number of hubs and spokes in each structure was variable regardless of whether it was classified as a CLAN or PAA. Despite a few very high values in some CLANs no difference was observed between averaged CLAN and PAA values.

Table 3-1. Average measurements of PAAs and CLANs present in BTM cells in vitro

As seen from the averaged values, PAAs tended to have a larger territory than CLANs and were more rounded in their overall shape; however, the basic units that compose both structures were very similar in both groups.

Measurements	PAAs	CLANs
Area	5794	1183
Circularity	0.81	0.49
Territory Height	8-3	1-3
Hub Area	2.19	2.2
Spoke Length	5.25	6.04
Spokes per hub	3.63	3.9
Hub circularity	0.91	0.92

The final aspect of these structures that was investigated was the incidence of hubs in the territory. It was noted that CLANs appeared to have a more regular pattern while PAAs were more variable and that the triangulations could not always be observed across the territory the structure was assumed to occupy. As shown in Figure 3-7 there was fair correlation (R^2=0.4) between the number of hubs within the total territory and the area measurement, confirming that with an increasing number of hubs the size of the structure increased. In contrast the same correlation was not observed in PAAs in relation to total territory (R^2=0.09) or observable territory (R^2=0.0) (Figure 3-8). CLANs therefore appear to have much greater organisation.

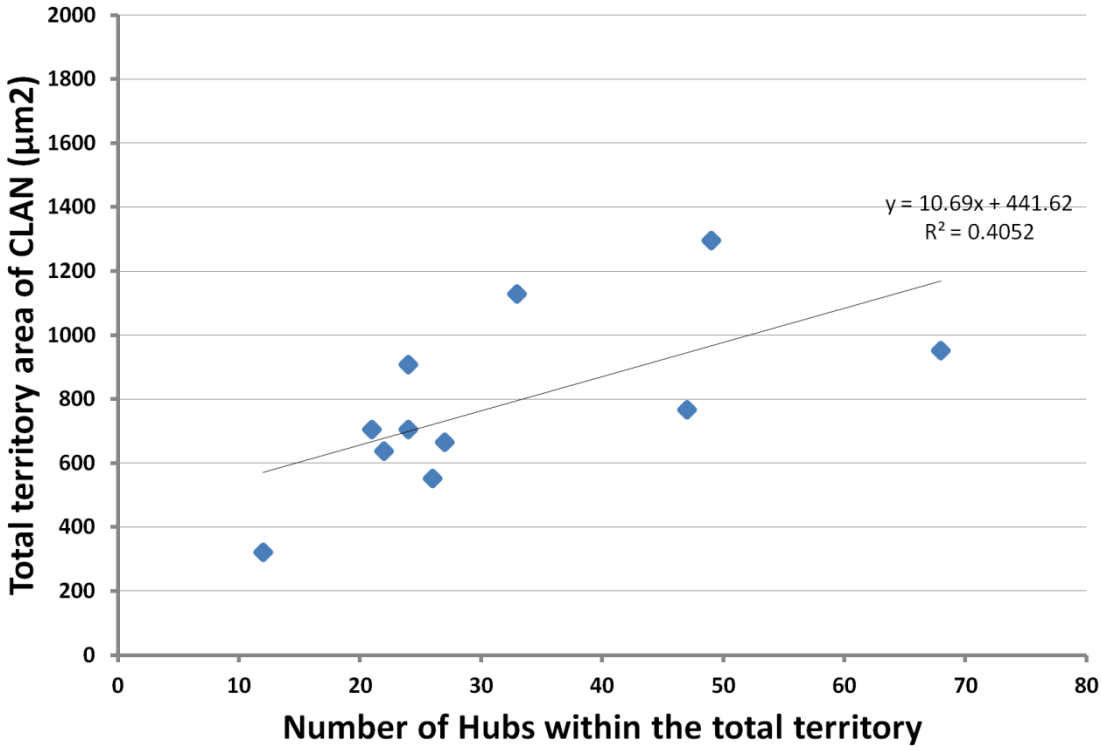

Figure 3-7. Scatter plot of total CLAN territory against the number of hubs within.

By plotting the number of hubs against the total area it is clear that the number of hubs increased with increasing size of the CLAN structure. Although several of the points clustered between 20-30 hubs there was a good linear relationship (R^2=0.4052).

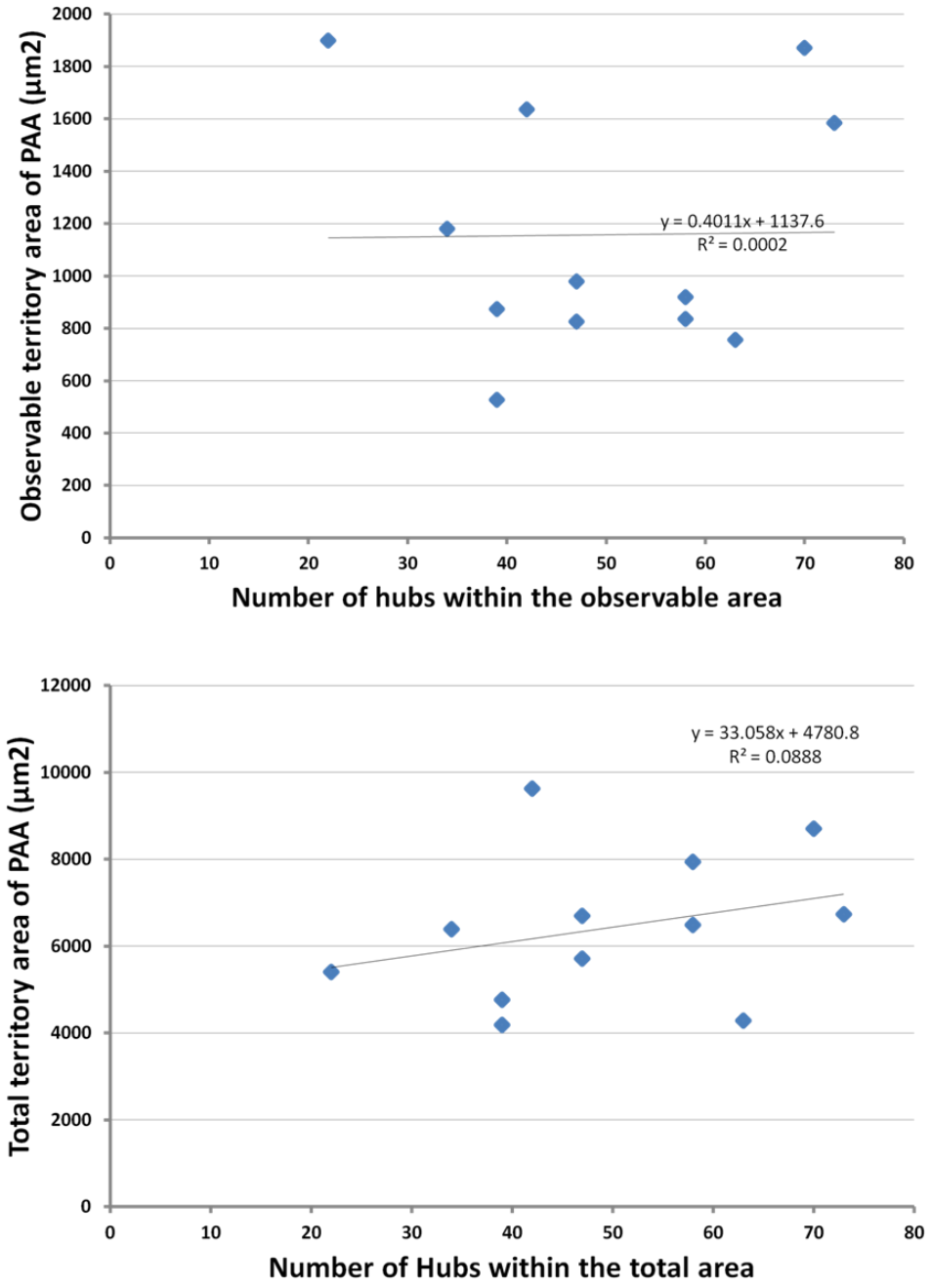

Figure 3-8. Scatter plot illustrating the relationship between PAA territory and the number of hubs within.

Unlike with CLANs the linear relationship between the number of hubs and PAA area was poor. Unsurprisingly there was no relationship between hub number and observable territory as this was a randomly sampled area used for the analysis of the basic units. There was also limited correlation (R^2=0.088) between total area and the number of hubs. This would indicate that larger PAAs did not necessarily have the largest number of hubs and is in keeping with the morphological observation that the pattern of basic units is not evenly spread throughout the area.

3.4 Discussion

The normal actin arrangement present in TM cells is straight stress fibres running in parallel along the axis of the cell (Grierson et al., 1986). As TM cells are known to have contractile properties (Stumpff and Wiederholt, 2000; Wiederholt, 1998) this arrangement would allow for muscle-like contraction and relaxation (Pellegrin and Mellor, 2007). Investigation of the cytoskeleton *in vitro* and *ex vivo* under various conditions has identified geodesic arrangements of actin (Clark et al., 1994; Filla et al., 2004a; Hoare et al., 2009; Read et al., 2003; Wade et al., 2009). The manipulation of TM cell cytoskeleton has been implicated in the regulation of AH outflow (Cai et al., 2000; Ferrer, 2006; Gabelt et al., 2006; Honjo et al., 2001; Johnson, 1997; Kaufman, 2008; Liu et al., 2001; Shimazaki et al., 2004; Tian et al., 2009; Tian and Kaufman, 2007) and is therefore a potential target in glaucoma research. CLANs were initially believed to be a unique TM cell response to DEX treatment and a potential therapeutic target (Clark et al., 2005; Clark et al., 1994). The induction process seemed to take some time as the incidence of CLANs increased slowly following exposures of 3 to 14 days (Wade et al., 2009). While not permanent, CLANs did take 10 days to return to baseline levels following the removal of DEX.

Before the identification of CLANs, polygonal actin arrangements were described in settling cells in culture (Ireland and Voon, 1981; Lazarides, 1976; Rafferty and Scholz, 1985). The presence of these polygonal structures in multiple cell types indicated a functional role associated with cell spreading and actin stress fibre formation (Maguire et al., 2007). During settlement, TM and optic nerve head cells (data not shown) formed polygonal structures within the first few hours. These structures were no longer present at 48 hours, by which time the cells were fully settled on the TC substrate. Given the differences in formation those polygonal structures formed during settlement were termed polygonal actin arrangements (PAAs) as a means of distinguishing them from CLANs identified in stable cultures by Clark et al (Clark et al., 1994).

Measurements conducted on a selection of CLANs and PAAs illustrated that PAAs were consistently larger in “total territory”, such that the largest CLANs where only approximately half the size of the smallest PAAs measured. This measurement was

entirely consistent with our general qualitative observations. It was also our opinion that PAAs tended to occur around the periphery of the cell and their overall shape was more uniform than the many different shapes of CLAN. The observation was confirmed by PAA circularity reading of 0.81 compared to 0.49 for CLANs.

Although there were distinct differences between the gross appearance of CLANs and PAAs this was lost almost entirely when it came to comparison of the hubs and spokes arrangements. The hubs were circular in both and of almost identical area (as far as we could tell although accurate measurement was problematic). The numbers of spokes radiating from each hub were counted, and were found to be between 3 and 4 for both structures. This is likely to be an underestimation, as the actual numbers presumed from design principles of geodesic domes is between 5 and 6 spokes per hub in order to achieve the polygonal curved arrangements these structures are taken to have. It is presumed that the "undercount of spokes" was because some spokes were not in the plane of counting. The visible spokes were also measured and spoke length was found to be 5-6μm in both structures. Spoke width was attempted but given their size and the variation in staining and plane of view their thickness could not be measured accurately.

Despite the identical nature of their basic components the spread of these units is different as illustrated by the correlation between incidence of hubs and territory. While there is positive correlation between the number of hubs and the size of the structure in CLANs the same correlation does not exist within PAAs. CLANs and PAAs also appear to occupy different cytoplasmic spaces with PAAs in ring-like structures (the presence of the top of the dome is not yet concrete), with a circumference not much smaller than the cell it occupies. CLANs from our measurements are smaller in overall size, are normally centrally located within the cell close to nucleus.

Stress fibres in different cytoplasmic spaces evoke different responses within cells (Pellegrin and Mellor, 2007), so it may be that the different TAPAS arrangements also evoke different responses. TM cells are capable of sensing and responding to changes in their environment including mechanical stresses from fluid flow and changes in IOP (Luna et al., 2009; Schlunck et al., 2008; Tumminia et al., 1998; WuDunn, 2001, 2009;

Zhou et al., 2012). Ingber proposed that specialised structures maintain cellular tensegrity (Ingber, 2003), while Clark et al suggested that the presence of CLANs would decrease the contractile abilities of TM cells by making them more rigid (Clark et al., 2005). As the actin cytoskeleton is known to be directly involved in regulating cellular activity (Ballestrem et al., 1998; Dominguez and Holmes, 2011; Mseka and Cramer, 2011), TM cells containing TAPAs may produce different cellular responses which could impact on outflow facility (Epstein et al., 1999; Kaufman, 2008; Lu et al., 2008; Tian et al., 2000; Wiederholt et al., 2000).

At least one group (Filla et al., 2004a) have studied polygonal structure which formed soon after re-settlement and reported DEX induction of TAPAS even at the early stage of sparse cell distribution. Our own initial data indicated that pre-exposure to DEX before passage and settlement may cause a marginal increase in cells with TAPAS but these were thought by us to be PAAs based on their large size, circularity and their temporary nature (virtually none left at 2 days with a half-life of only a few hours). While they have called these structures CLANs in their publications our studies would suggest that they belong to the group of TAPAS we have called PAAs. Certainly because they are rapidly forming PAAs are easier to study than CLANs which require many days for each assay and experiment to be conducted. It may well be that PAA investigation has a lot to tell us about actin network formation and the pathways that regulate their formation (Filla et al., 2004b; Filla et al., 2005; Filla et al., 2006). However, the gross differences in shape and cellular orientation coupled with their temporary nature could make them a problematic substitute for CLANs.

Previous publications from our group (Hoare et al., 2009; Wade et al., 2009) worked towards providing a definition of what constituted a CLAN stating that “A CLAN is a polygonal structure composed of hub points connected by actin spokes which are arranged in triangulated units to form a polygonal shape. The minimum inclusion requirement for a CLAN is that it has at least 5 hub points that form a minimum of 3 linked-triangulated units”. The definition artificially defined a CLAN as having a minimum size for the purposes of quantification as it excluded the smallest polygonal structures likely to cause confusion in the quantitative evaluation of CLAN numbers.

The emphasis was placed on the geometric arrangement of hubs and spokes as it would distinguish a CLAN from the CLAN-like structures and tangles that could complicate identification particularly in the organised TM tissue (Hoare et al., 2009; Read et al., 2007). The definition was unable to distinguish between the two polygonal structures which we call CLANs and PAAS. In the current work we have introduced another term; transient arrangement of polygonal actin structures (TAPAS), which is inclusive of all polygonal actin structures (PAAs and CLANs) but not those in which straight spokes cannot be identified, therefore, excluding tangles of actin.

In cell culture, the temporary nature of PAAs and their tendency to be found in sparse cultures for only the first day or so eliminate them as a potential artefact in the outlined investigations of this thesis and from our quantification of CLANs.

4 Characterisation of TM cells

The purpose of this chapter was to investigate the morphological and functional features of the TM cells used throughout this work. As primary TM cell cultures are heterogeneous in nature and are limited in passaging number (Alvarado et al., 1982; Polansky et al., 1979) it was vital to observe the health of the cultures and any changes throughout the experimentation period to reduce variability as much as possible. In this study there was the added variability of using cells from multiple donors.

4.1 Morphological assessment of TM cells

The general morphology of TM cells in vitro has been well documented (Alvarado et al., 1982; Grierson et al., 1985b) and throughout this work TM cell morphology was closely monitored from pre-confluence to the termination of the experiment. During the process of settlement, cells initially had a very round morphology when first introduced to a new substrate, as discussed previously in chapter 3. Once attached to the surface of the substrate the cells began to alter in size and shape becoming more elongated and spindle shaped. As the cells began to settle the phenotype changed and in this pre-confluent state 3 distinct cell shapes were identified (work lead by Prof. Grierson); spindle, kite and epithelioid (Figure 4-1).

In early pre-confluent cultures, represented in Figure 4-2a, there was ample space for cells to attach and space for proliferation. Many cells were classified as kite shaped while other cells were elongated and seemed to be slightly detached from the surface of the plate, represented by the halo effect surrounding them. A slightly more populated field of view was observed with a culture time of approximately 3 days. By this point cells had begun to form clusters as cell proliferation was enhanced. As time on the substrate continues the cells pack together in “islands” which are connected by multiple protrusions of cells to a neighbouring island. As proliferation continues the spaces in the cultures diminish and cells at this stage of growth (Figure 4-2c) are passaged before all spaces are filled because as space on the culture plastic becomes sparse, proliferation rates slow to account for this reduction in available space initiated by cell to cell contact inhibition. By this stage cells in the culture were of a fatter spindle shape and even towards the epithelioid. However, if further growth was

permitted BTM cells formed very densely packed monolayers, cell boundaries were impossible to detect but given the close proximity of the nuclei it seems cells have reduced cytoplasmic area to allow for continued proliferation. Interestingly the cultures at this confluent monolayer stage exhibited an overall pattern in the culture. As seen in Figure 4-2 d cells in close proximity have a level of alignment and a wave-like pattern was visible.

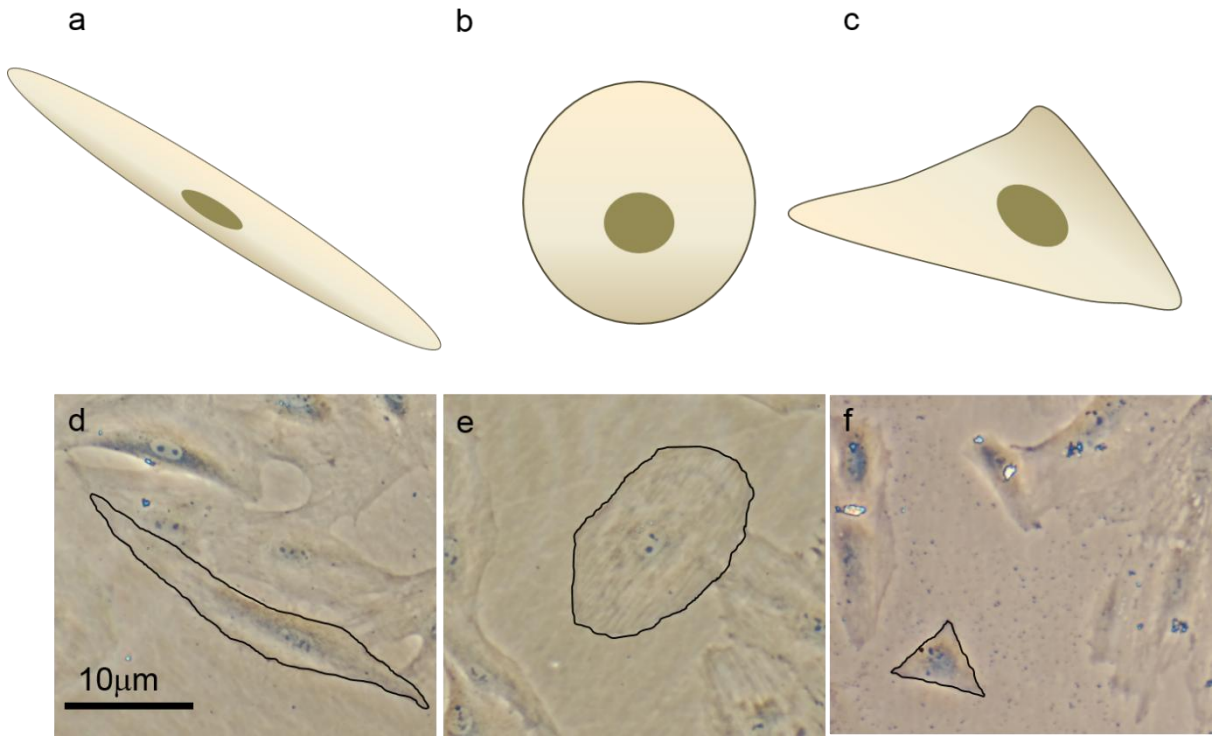

Figure 4-1. Idealised images of 3 distinct cell shapes found in TM cell cultures.

Images a-c are computer generated diagrams explaining the idealised cell shapes used for classification. Images d-f are phase contrast images of BTM cells in pre-confluent culture and one cell has been selected to provide an example of the cells placed in each category. a & d are spindle representations, b & e are epithelioid, while c & f show kite shaped BTM cells. Phase contrast images were cropped from larger images Scale bars represent 10μm.

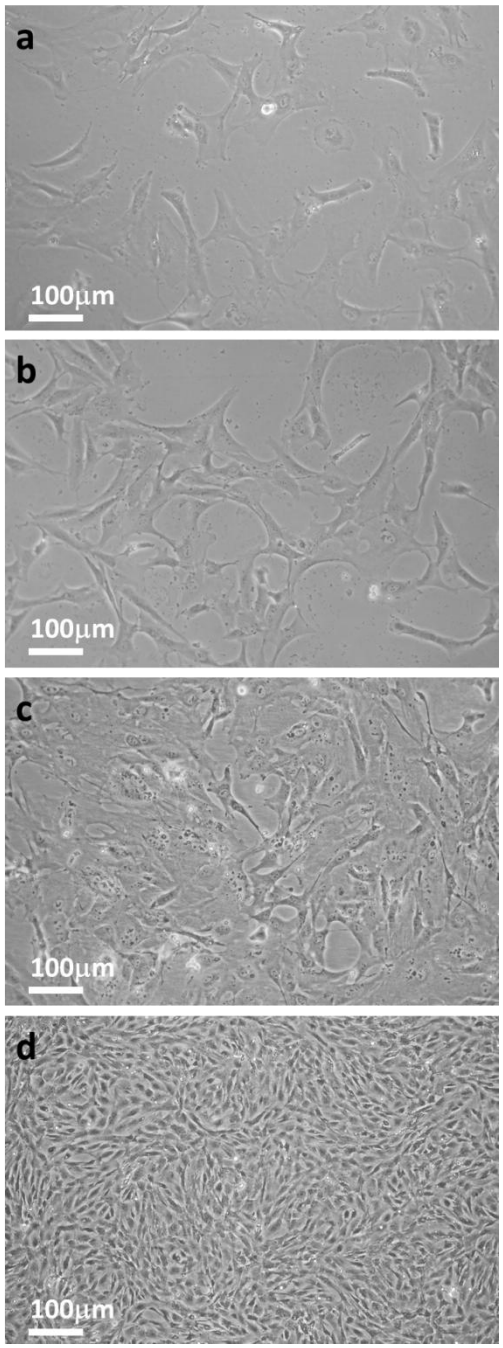

Figure 4-2. Representative phase contrast images of BTM cell culture morphology over time.

The changes in BTM cell morphology in the presence of growth medium were monitored over time via phase microscopy. As seen in image a, the number of BTM cells in a pre-confluent environment was sparse but even by 3 days there was clustering of cells with spindle and kite morphologies (b). Continued proliferation resulted in diminished space on the culture substrate as seen in image c and demonstrated increased cell to cell contact with cells exhibiting a less elongated phenotype. Cultures that were not passaged when 70% of the substrate was covered have now formed a complete monolayer with cells very tightly packed together.

In general, the growth of HTM cultures was phenotypically similar to BTM cells, however, HTM cells exhibited a greater degree of variation in both cell and culture phenotype. Figure 4-3 is an example of HTM cells from 4 different donors at the same time point following introduction to the same type of substrate. The observed differences were taken to indicate that proliferation rates between some cultures were much faster than others. For example, cells in Figure 4-3a. were packed very tightly together, obscuring cell boundaries. Cells were spindle shaped but the most striking feature was the high level of alignment observed amongst the cells. Unlike in very confluent BTM cells, the alignment was not in small clusters forming waves but rather large areas of cells were in complete alignment.

Cell morphology within a culture could be very heterogeneous (Figure 4-3b). In some areas cell morphology resembled the highly compact and aligned arrangements of figure a, but this was not complete and did not occur across such extensive areas. These areas were instead interrupted by areas of un-aligned cells with greater space available between them. Although a similarly heterogeneous cell phenotype can be seen in Figure 4-3c, there was no discernible alignment across much of the culture substrate. There was an increased number of large and often “giant” cells between small areas were cells retained the spindle morphology. Finally a number of cultures exhibited morphology much more comparable with those observed in BTM cells, with no discernible alignment and cells that were more epithelioid rather than elongated (Figure 4-3d).

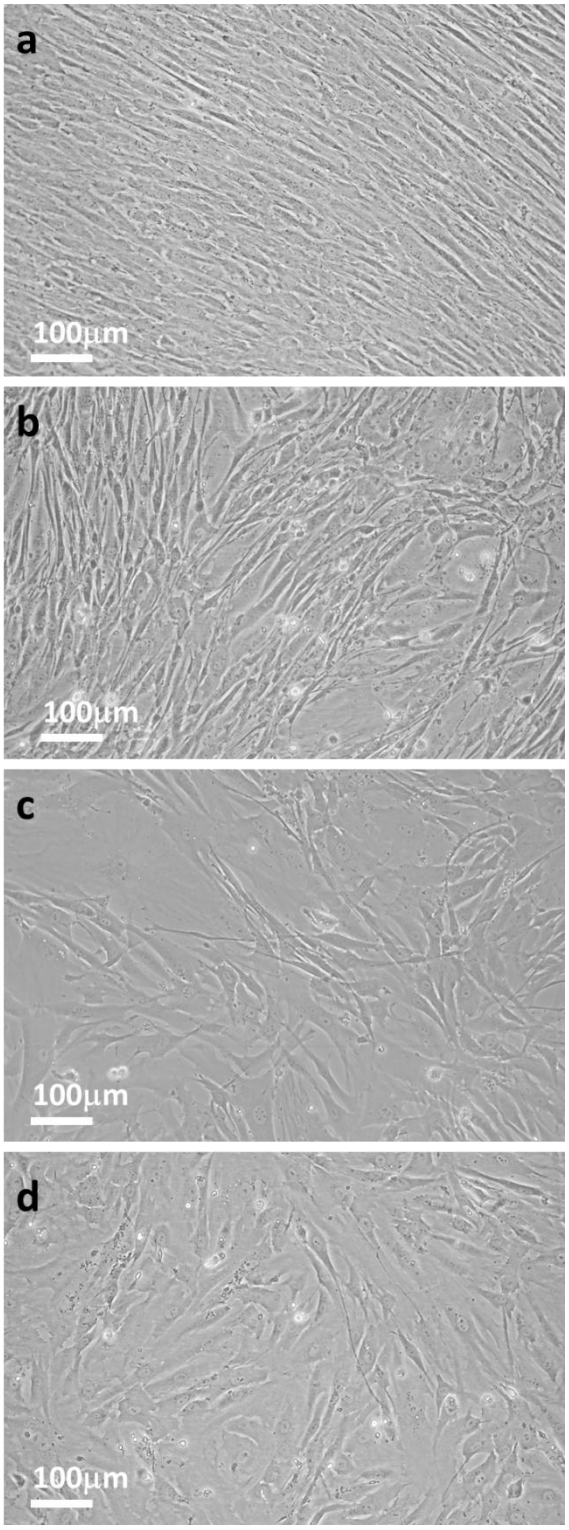

Figure 4-3. Representative phase contrast images of HTM cell morphology.

Phase contrast images of HTM cell cultures from 4 different donors at 7 days after plating illustrated the different culture morphologies. While some cultures exhibited cells of a similar phenotype (a) most were heterogeneous in nature exhibiting varying percentages of spindle and epithelioid cells.

4.2 Cell seeding density

Investigating cell seeding density was vital as it could impact greatly on final CLAN counts. If cultures were too densely packed by the end of the experimental period then counts would be more difficult and could produce falsely low numbers. By seeding too few cells, the risk of minimal cell growth could affect cell functioning and the increase plating time prior to beginning treatment would extend experimental time unnecessarily.

Upon morphological analysis of cultures seeded at different densities it was discovered that cells seeded at 5,000 per cm^2 were not sufficient to form a complete monolayer and so was dismissed as a possibility. Cells seeded at 10,000 and 30,000 per cm^2 grew very well and within 7 days had covered a large area of the well in a uniform manner. Growth curves revealed that BTM cells seeded at 30,000 per cm^2 exhibited a sharp decline in cell numbers within the first 5 days of seeding before seeming to reach equilibrium (Figure 4-4). Interestingly cells seeded at 10,000 per cm^2 showed a steady increase in cell number within the first 5 days and then reached a steady level comparable to that of 30,000 per cm^2.

Cells seeded at 10,000 per cm^2 showed normal cell morphology was maintained throughout the experimentation period and based on visual assessment and growth curves cultures were deemed at a suitable level of confluence at day 5-7 to begin experimentations. At this seeding density cells were also found to form a stable monolayer when time was extended to 10 days. These parameters meant that experimentation could be started within 7 days of introduction to the substrate and could be extended without overcrowding or loss of cell viability. For these reasons a seeding density of 10,000 per cm^2 was used throughout experiments, with treatment initiated at day 7 following plating.

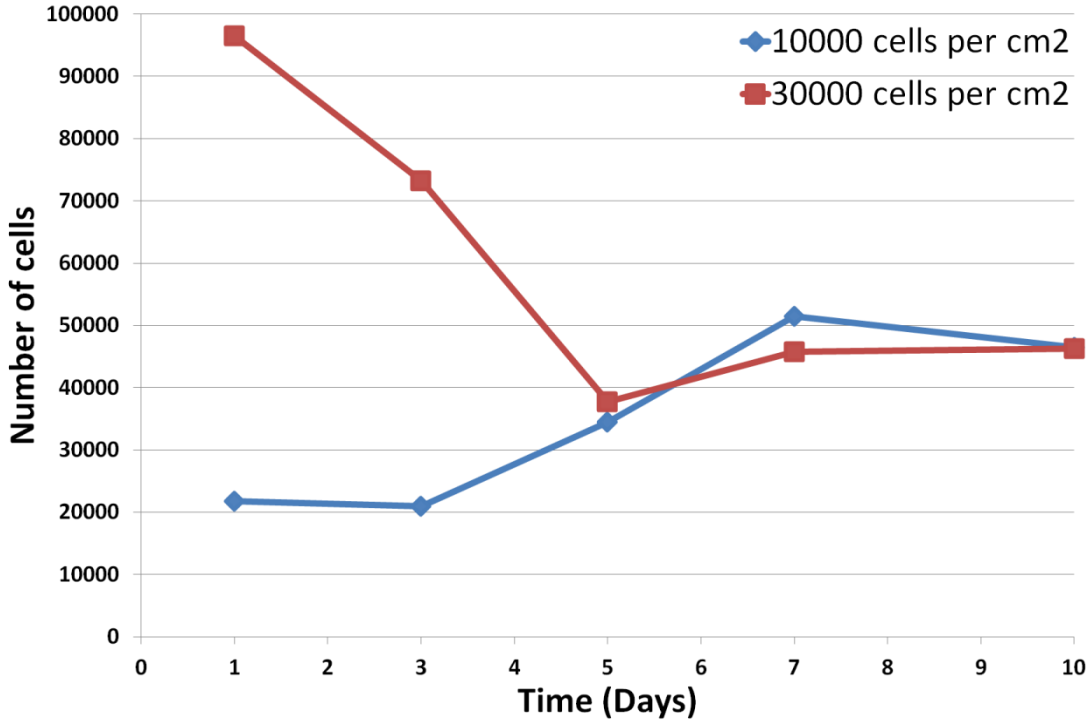

Figure 4-4. Line chart showing BTM cell number over time following different seeding densities.

The number of BTM cells, at 1, 3, 5, 7, and 10 days was assessed by haemocytometer counts following seeding of BTM cells at 10,000 per cm^2 and 30,000 per cm^2.When seeded at 30,000 per cm^2 there was a sharp decline in cell number until day 5 when values plateau. In contrast cells seeded at 10,000 per cm^2showed a steady increase in cell number up to day 7. Points represent values obtained from counts at specific time points where n=2. Connecting lines predict how values would have changed between the time points.

4.3 Growth curves

4.3.1 BTM cells

The effect of cell passage number of growth rates could be quite variable as seen in Figure 4-5. Cells of passage 3 demonstrated a sharp increase in cell number within the first 5 days followed by a short plateau of 5 days and sharp decline, with cell number almost returning to starting values. In contrast, BTM cells of passage 17 showed a steady increase in cell number throughout the assay. BTM cells of passage 5 and 8, showed little variation in actual number and followed the same pattern throughout; following a slight increase up to day 5, cell number began to fall away but the decrease was not significant. The results for passage 10 were unexpected as cell counts showed inconsistencies between consecutive time points.

In order to account for individual variation, BTM cells cultivated from 6 different donors within passage 4-10, were used throughout this work. While cultures from different donors showed some variation in the actual number of cells counted at each time point, they exhibited the same general trends in growth. Higher cells counts within the first 5 days after seeding were followed by a plateau or slight decrease in cell number so that by day 10 cell numbers were comparable between all donors. Even at day 7, all but 1 donor had a cell count of between 28,000 and 39,000 (Figure 4-6). Non-viable cells were found to account for less than 5% of total cell counts via trypan blue exclusion assay

On occasion cultures of BTM cells were found to have consistently low cell counts across 14 days (in some cases too low to count via haemocytometer). The morphology of these cells was different to other cultures in that cells were much larger and flatter. Cells also appeared to produce a lot of debris and had evidence of vacoulation. When trypsin was added to these cultures it was discovered to take an excessive amount of time to cause cell detachment. Any culture found to be exhibiting these altered features was excluded from experimentation.

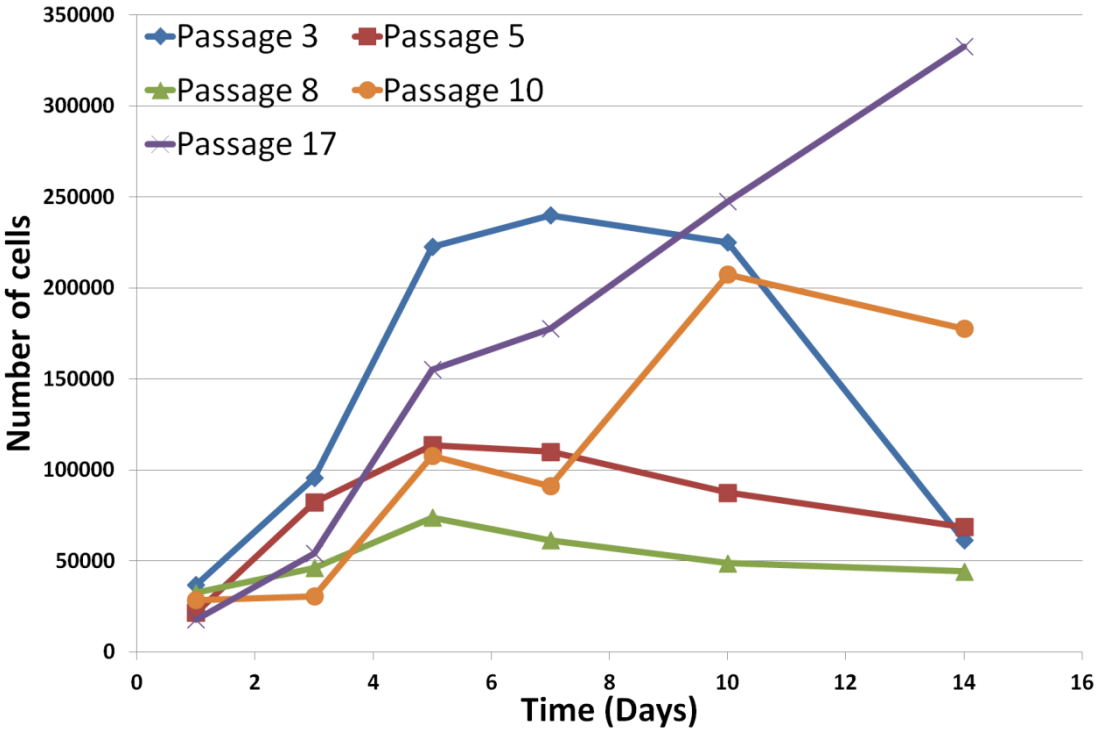

Figure 4-5. Growth curves of BTM cells at increasing passage number.

BTM cells from one donor in growth media provided the above growth curve. Cells from individual wells were removed with trypsin and counted at the time points 1, 3, 5, 7, and 10 days following seeding. At passage 17 cell numbers continues to increase throughout the experimental period and does not follow the expected growth of cells in cultures. Cells are expected to proliferate until there is no available space remaining, and then as they are contact inhibited will plateau as they enter the lag phase of growth and if left undisturbed cell loss will be observed as nutrition diminishes and waste products accumulate. BTM cells at passage 5 and 8 follow this pattern as does passage 3, however, the number of cells present reach much higher levels. The growth pattern of passage 10 is unusual and may demonstrate a loss of normal cell function. Coloured points are averaged values where n=2 and coloured lines have been used to predict the change in cell number between the time points assessed.

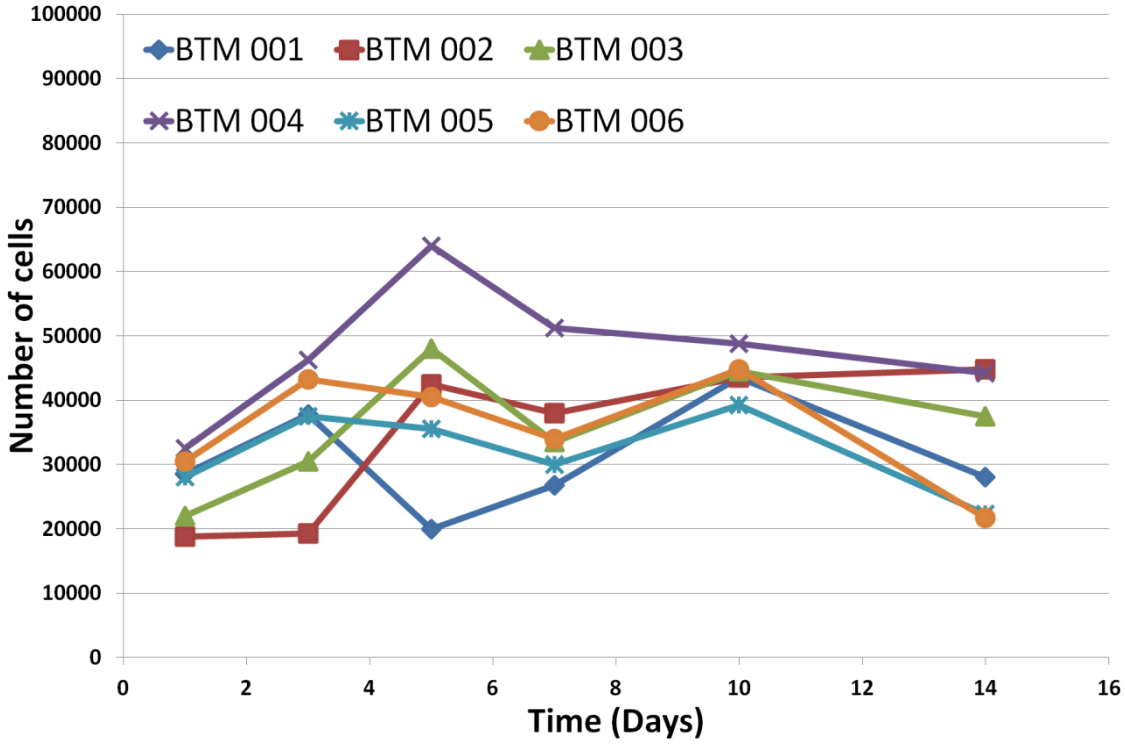

Figure 4-6. Growth curves of BTM cells from multiple donors.

BTM cells from 6 different donors at passage 6-7, plated in medium provided the growth curves above. Cells from individual wells were removed with trypsin and counted at 1, 3, 5, 7, and 10 days following seeding. Despite some fluctuations in cell number there was little variation across the experimental period or between donors. By day 7 cell number was almost identical across all donors. Coloured points are averaged values where n=2 and coloured lines are used to demonstrate how cell numbers may fluctuate between the time points assessed.

4.3.2 HTM cells

As with BTM cells, the comparative growth of HTM cells from different donors was investigated using cultures from 6 donors of different ages. As seen in Figure 4-7 cells obtained from younger donors (4, 6, 36 years) had a rapid, almost exponential increase in cell number over the first 10 days, in contrast, cells from older donors (>50 years) showed a much more depressed increases over the same period.

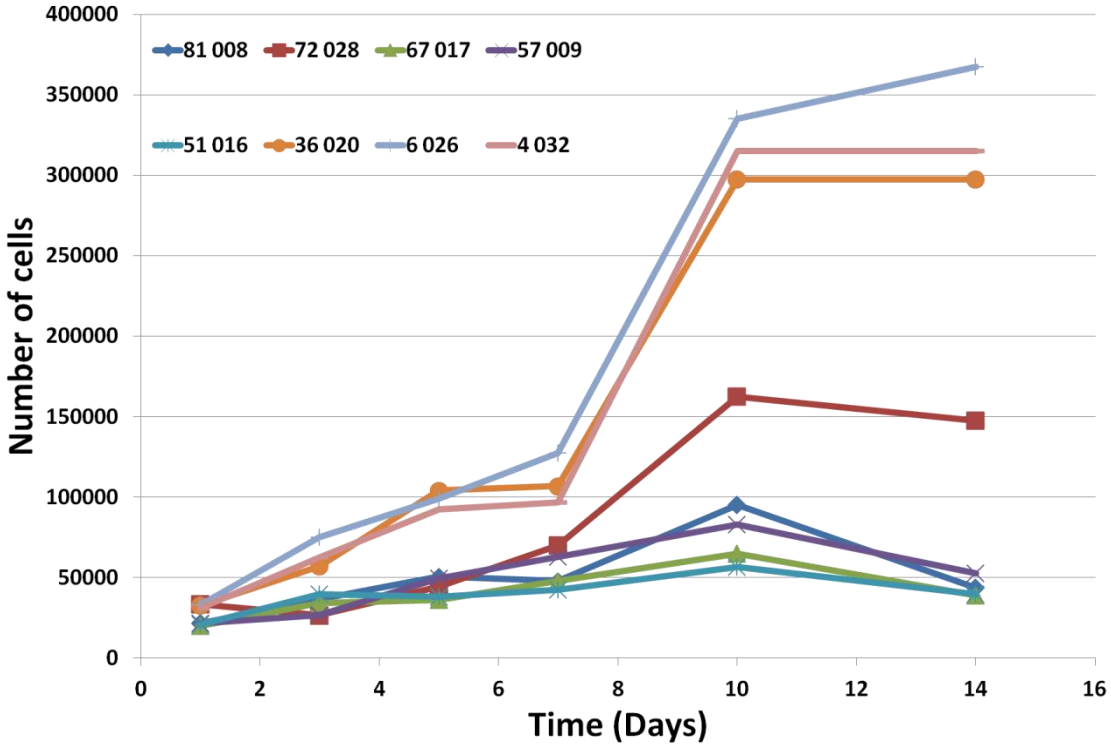

Figure 4-7. Growth curves of HTM cells from 8 donors of various ages.

The rate of HTM cell proliferation was assessed by counting the number cells present at various time points spanning 14 days. As demonstrated by the line graph cell number increased until day 10 after which there was either a decline or plateau. The most striking feature is the difference in the rate of cell increase between young donors (4, 6, 36 years old) and older donors. While young donors increase almost exponentially the older donors only increase marginally. Each coloured line represents a different donor which are arranged in increasing donor age (n=2).

4.4 CLANs incidence in culture medium

Previously published work (O'Reilly et al., 2011), derived from the current research has shown that even under control conditions cells contain a percentage of CLANs. Therefore before beginning any experiments that could alter the cell environment we needed to investigate whether the medium used under standard cultures conditions was influencing CLAN formation.

The percentage of FCS added to medium can have a drastic influence on TM cells as demonstrated by growth curves. Incubation with growth medium caused an increase in cell number within the first 10 days after which the number of cells decreased. Incubation in maintenance media, unsurprisingly, produced little change in cell proliferation with only small fluctuations in cell number. BTM cells were found to be more resilient to lower serum concentrations compared to HTM cells. The FCS content of medium could also influence the cell cytoskeleton as demonstrated by incubating HTM and BTM cells with medium containing 0%, 0.5%, 1% or 10% FCS. When examined under fluorescence, the percentage of CLAN containing cells in BTM cultures was found to be consistently higher than in HTM cells under the same conditions. BTM cells treated with medium containing 0% FCS and 0.5% FCS induced CLAN formation in 2.5% and 2.8% of the population. Observation revealed that HTM cells began to deteriorate in media with a FCS concentration of less than 1%, and so there was limited data on the cytoskeletal arrangement present. HTM cells incubated in 1% medium produced CLANs in approximately 4% of cells and increasing the concentration of FCS to 10% failed to have a significant influence on CLAN incidence (3%). In contrast BTM cell cultures incubated with 1% FCS had a CLAN incidence of almost 6 %, a value that increased to 12% in the presence of 10% FCS. Further increasing the FCS content to 30% did not further increase CLAN incidence (Figure 4-9).

Given the consistent nature of the finding across multiple donors a baseline level of CLANs was established for both BTM and HTM cells. The BTM baseline in growth medium was 10% while it was 6% in maintenance medium. The baseline for HTM cells was set at 5%.

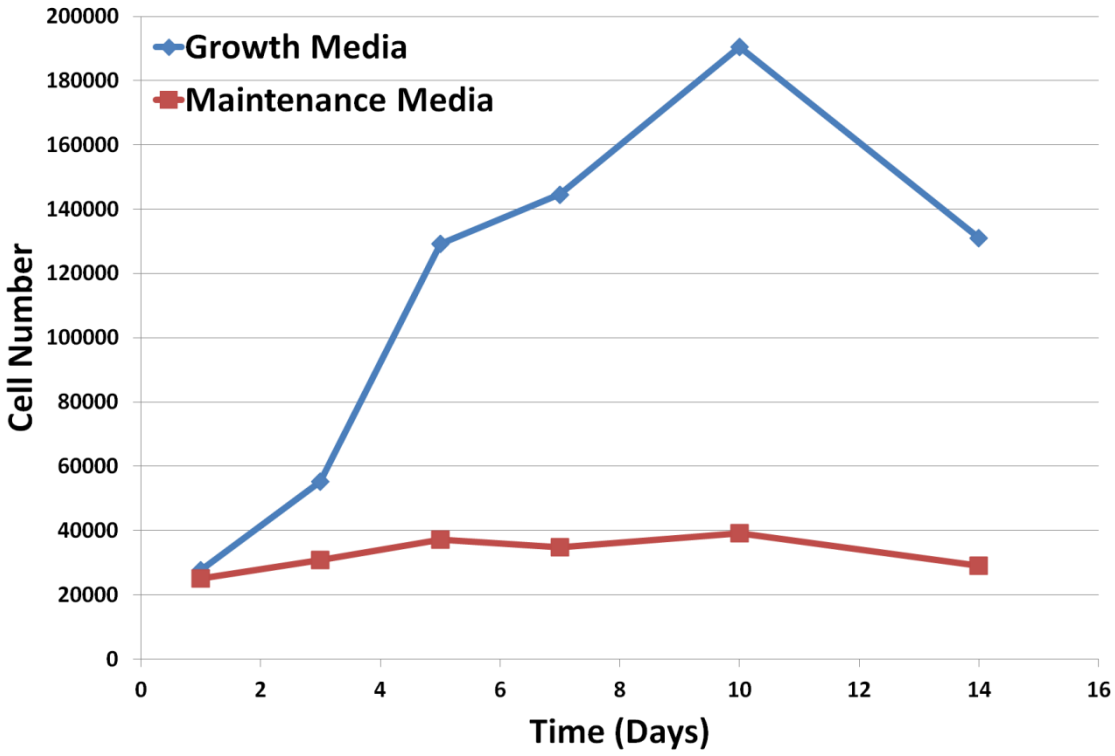

Figure 4-8. Line graphs demonstrating growth curves of BTM cells grown in either growth or maintenance medium.

Incubation in growth medium resulted in a rapid increase in BTM cell number over the first 10 days. This was followed by a sudden decrease in cell numbers at day 14. The presence of maintenance medium did not cause a significant change in cells number across the time frame examined. Coloured points represent the averaged values where n=4.

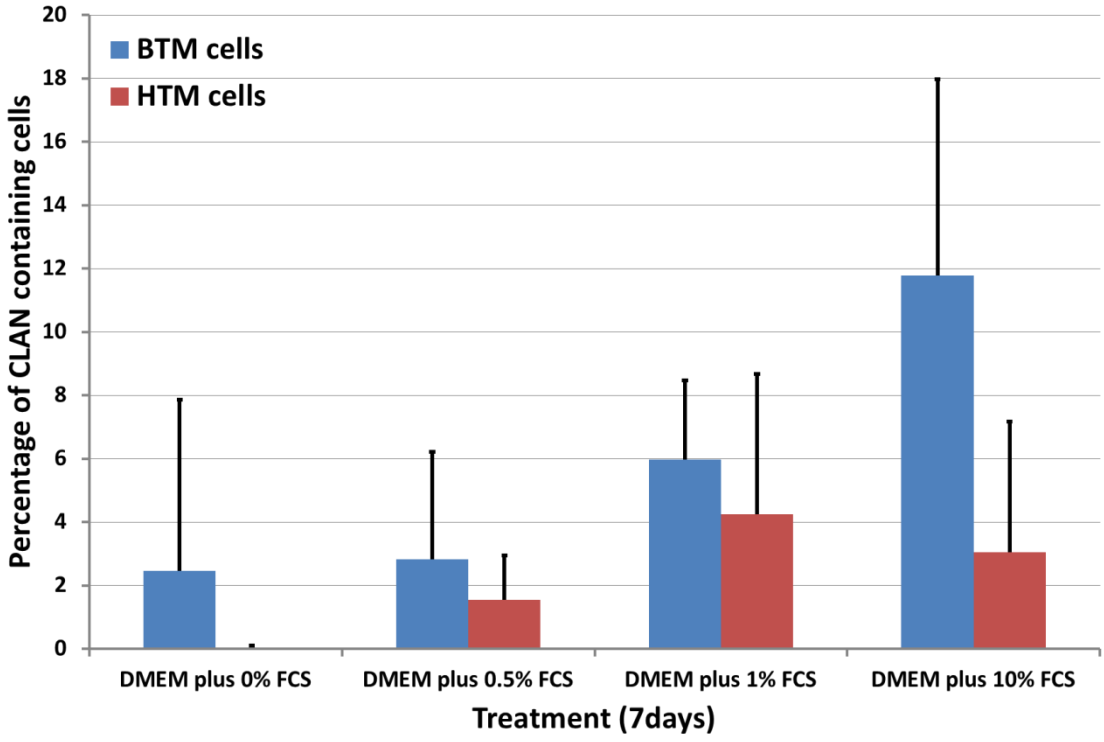

Figure 4-9. Percentage of CLAN containing cells in HTM and BTM cells with varying concentrations of FCS.

Blue bars represent the percentage of CLAN containing BTM cells while red bars are HTM cells. It is clear that BTM cell cultures consistently contained more CLANs than HTM cells. HTM cells were found to be sensitive to concentrations of FCS less than 1% and so there was limited data, however, concentrations of 1% produced CLANs in 5%. Increasing the concentration of FCS up to 10%, caused an increase in the percentage of CLAN containing cells in BTM cells (12%). Bars represent average values obtained when n=3 and error bars represent the standard deviation.

In order to address variation in protocols between labs BTM cells were transferred to maintenance medium for 24 hours prior to beginning treatment. As shown in Figure 4-10, reducing the concentration of FCS present in medium for 24 hours prior to beginning treatment produced no significant differences in CLAN incidence. BTM cells treated for 7 days with maintenance media produced a CLAN incidence of 5%, which was comparable to those observed under normal experimental conditions ($p=0.793$). A similar result was found under growth medium conditions with a percentage of CLAN containing cells of 10% following 24 hours starvation and 12% without ($p=0.602$). However, the percentage of CLANs following treatment with TGF-β2 did show some variation with 24% of cells containing a CLAN following starvation compared to 33% in the unaltered condition. The difference did not reach significance with a p value of 0.128.

In order to deduce the potential CLAN inducing agent present in FCS, BTM cells were treated with dextran charcoal stripped FCS. BTM cells showed no alteration in cell morphology over the experimentation period as confirmed by morphological evaluation and by cell counts. Cell morphology resembled that of other untreated cultures with no evidence of vacuolation or alterations in nucleus and cell numbers remained unaltered across all media, averaging 37.7-49 nuclei per field of view ($p=0.124$).

As previously mentioned a baseline level of 10% was set based on findings from multiple experiments. Two similar methods for stripping FCS were used as well as a commercially available product and as seen in Figure 4-11, no significant difference ($p=0.555$) was observed between the different stripped media. All stripped media resulted in CLAN incidence between 7-9% which was comparable to BTM cells treated with unaltered medium ($p=0.631$).

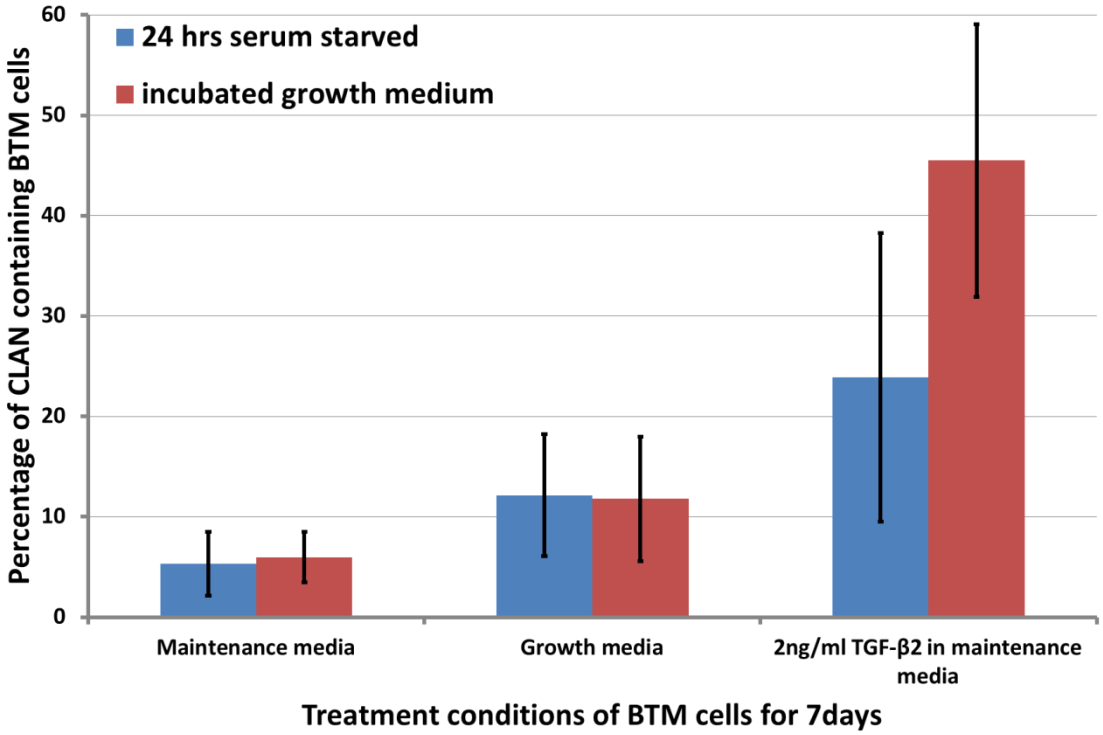

Figure 4-10. CLAN incidence in BTM cells following 24 hours serum starvation.

Bar chart of the percentage of CLAN containing BTM cells incubated with maintenance medium, growth medium or 2ng/ml TGF-β2 following 24 hours serum starvation. Depriving BTM cells of FCS before treatment did not significantly influence CLAN incidence in comparison to cultures that were treated in an identical fashion but without the initial serum starvation. Coloured bars are averaged values taken from 2 cultures. Error bars are representative of standard deviation.

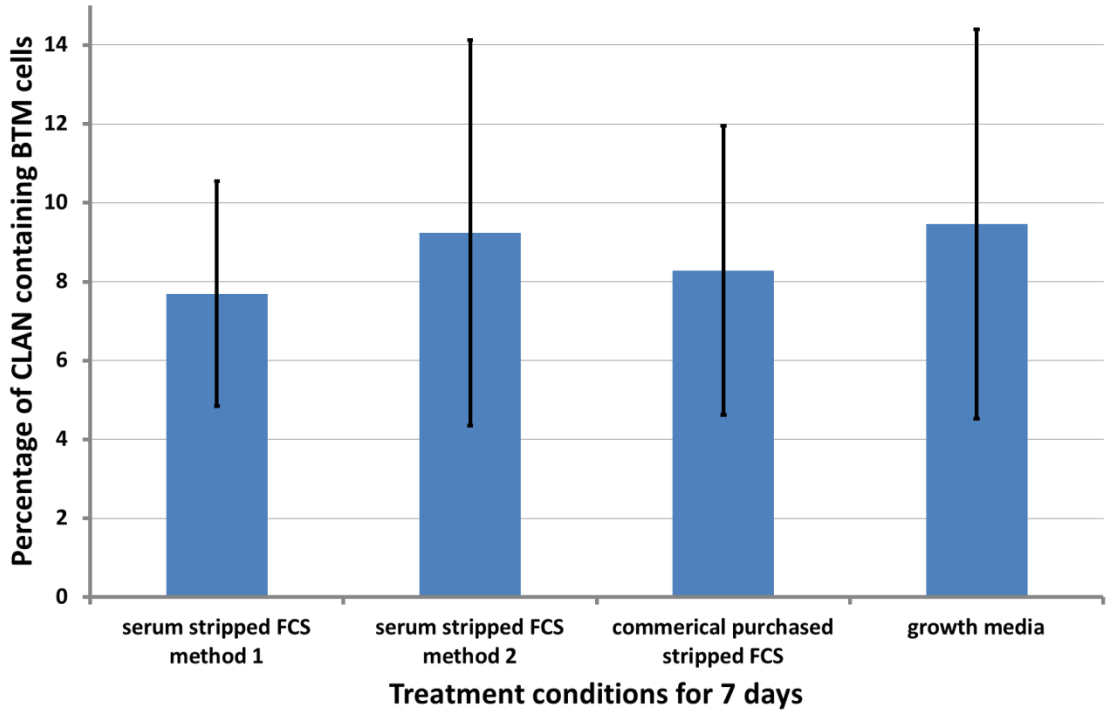

Figure 4-11. Incidence of CLANs in BTM cells treated with charcoal stripped media.

The percentage of CLAN containing BTM cells are represented in the bar chart. It is clear that CLAN incidence was not altered by stripping the FCS as the percentage of CLANs ranged from 7-9%.The coloured bars are the averaged values based on n=2, error bars demonstrate standard deviation.

4.5 Discussion

The use of multiple donors throughout this thesis was anticipated to increase the variability in experiments, it was therefore vital that the cells used were well characterised and monitored to reduce variability from external factors such as passage or variation in proliferation rates. TM cells *in vitro* have been well characterised (Alvarado et al., 1982; Grierson et al., 1985a; Polansky et al., 1979) and monitoring of the cells used in the current study demonstrated that the cells were identical to the published descriptions. In pre-confluence 3 distinct cell shapes were identified which were later linked with cell motility as described in Steven O'Reilly's thesis (O'Reilly, 2010).

BTM cell cultures derived from different donors demonstrated little variation in cell morphology or culture phenotype, a finding also confirmed by growth curves, highlighting the benefit of using these cells. Cultures within passage 3-10 demonstrated similar log phase growth periods (as monitored by length of time between passage), which was normally 5 days until 70% confluent at which point the cells were split. Cell number on labtek chamber slides more than doubled within the first 5 days after which time it stabilised or declined. By passage 10 however cell numbers did not appear contact inhibited and passage 17 there was continued proliferation. A recent publication reported how BTM cells became spontaneously immortalised (Mao et al., 2012) which may help to explain the continued proliferation of cells at passage 17.

HTM cell morphology proved more variable than BTM cells ranging from highly aligned compact cells to larger epithelioid cells. Evaluation of growth curves demonstrated that cells derived from older donors had a much smaller increase in cell number across 14 days while younger donors (below 40 years) demonstrated extremely high increase in cell number, increasing to a point where the effectiveness of cell to cell inhibition was questioned. HTM cells from much younger donors seemed to be able to compact very close together, while cells from older donors appeared more epithelioid and did not compact. TM cells treated with growth medium were unsurprisingly forced into proliferation, while cell number in cultures in maintenance medium did not change significantly.

No culture was found to be entirely without CLANs and increasing the concentration of FCS from 1-10% increased CLAN incidence in BTM cells at least. HTM cells proved much more sensitive to FCS concentrations and healthy cultures could not be maintained in medium containing less than 1% FCS. The species difference may be accounted for by the use of bovine serum as HTM cells may not be receiving optimal growth factors therefore any alterations would visibly impact upon cells.

As the percentage of CLAN containing cells was never above 10%, this was set as a baseline for BTM cells while a value of 5% was set for HTM cells. Previous work carried out in-house (data not shown) failed to demonstrate the presence of steroids in medium. The concentration and composition of growth factors present in FCS is not documented and is variable. Treatment of FCS with dextran coated charcoal strips out (Dang and Lowik, 2005) serum factors but did not influence CLAN incidence.

Several other groups consistently serum starved cells for 24 hours (Filla et al., 2006). While HTM cells were not subject to this treatment, as it was felt they were not robust enough, BTM cells appeared unaffected. Cells treated with maintenance, growth medium and TGF-β2 produced a percentage of CLAN containing cells identical to those without starvation. The purpose of serum starvation was to reduce proliferation rates induced by FCS, and remove any interference by other factors. As our cells are approaching 100% confluence when treatment begins starvation may not significantly alter these conditions.

Based on these findings we were satisfied that the cells to be used in this study were comparable and expressed normal phenotype. The established baseline for CLANs was considered in all future work.

5 Do factors present in the aqueous humor (AH) influence the formation of CLANs in TM cells?

The presence of CLANs in the organised TM tissue of elderly and glaucomatous eyes (Hoare et al., 2009) led us to search for non-steroidal inducing agents. As TM cells are continually bathed in AH, it was an obvious choice when searching for a CLAN inducer present *in vivo*. We firstly examined the influence of AH itself on TM cells and then expanded our studies to investigate specific components within the AH.

5.2 Effect of AH on TM cells

5.2.1 TM cell phenotype

Bovine AH could only be obtained fresh from the abattoir on specific days so it was not always possible to synchronise our experiments to when the aqueous was fresh or even a few hours post-mortem. Morphological comparison of BTM cells grown in fresh and frozen AH showed no visible difference in cell morphology throughout the treatment period. Cells exhibited normal TM cell morphology of flat slightly elongated cells with processing extending and making contact with neighbouring cells (Figure 5-1).

Cultures of BTM cells maintained in AH exhibited a constant level of confluence throughout the treatment period compared to cultures treated with growth media. Growth curves of BTM cells incubated in fresh and frozen AH varied little across the 14 day treatment period, with values comparable to those produced by treatment with maintenance medium (Figure 5-2).

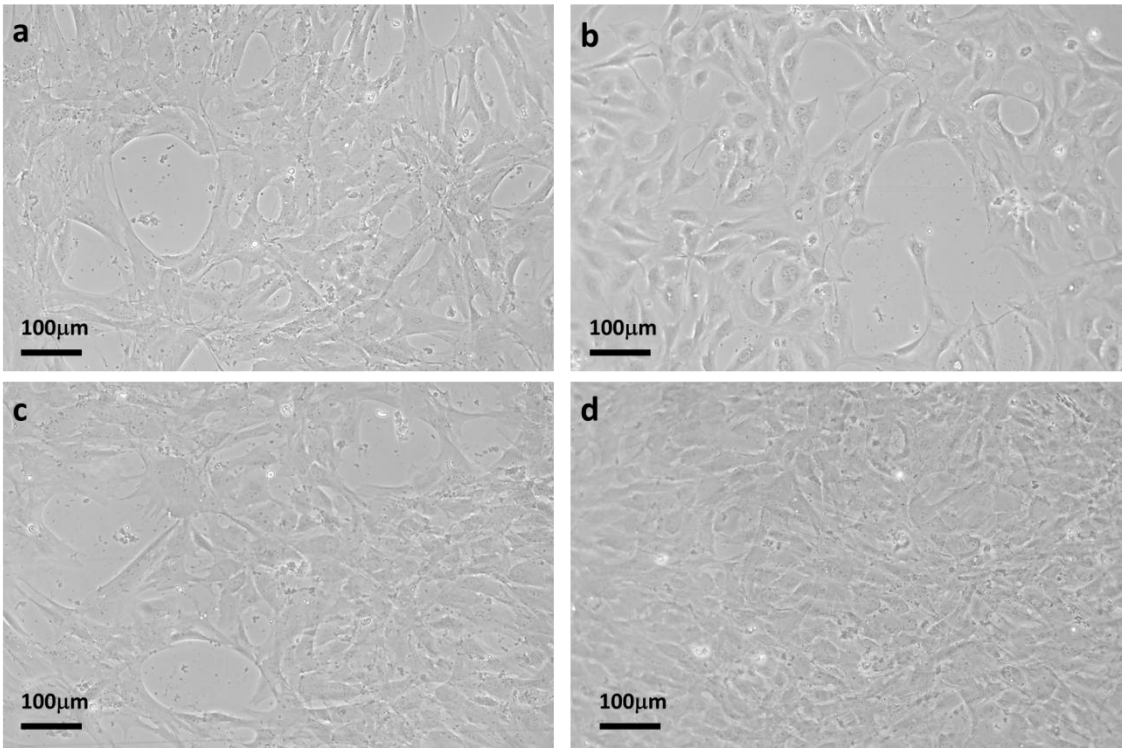

Figure 5-1. Phase contrast images of BTM cells treated with fresh and frozen AH.

Phase contrast images of BTM cells following treatment with frozen AH shown in a & c and in fresh AH shown in b & d (AH mixed 1 to 1 with medium containing 1%FCS). These are representative images illustrating that both were capable of maintaining normal BTM cell monolayers. Images a & b were taken at 3 days and images c & d were taken at 7days.

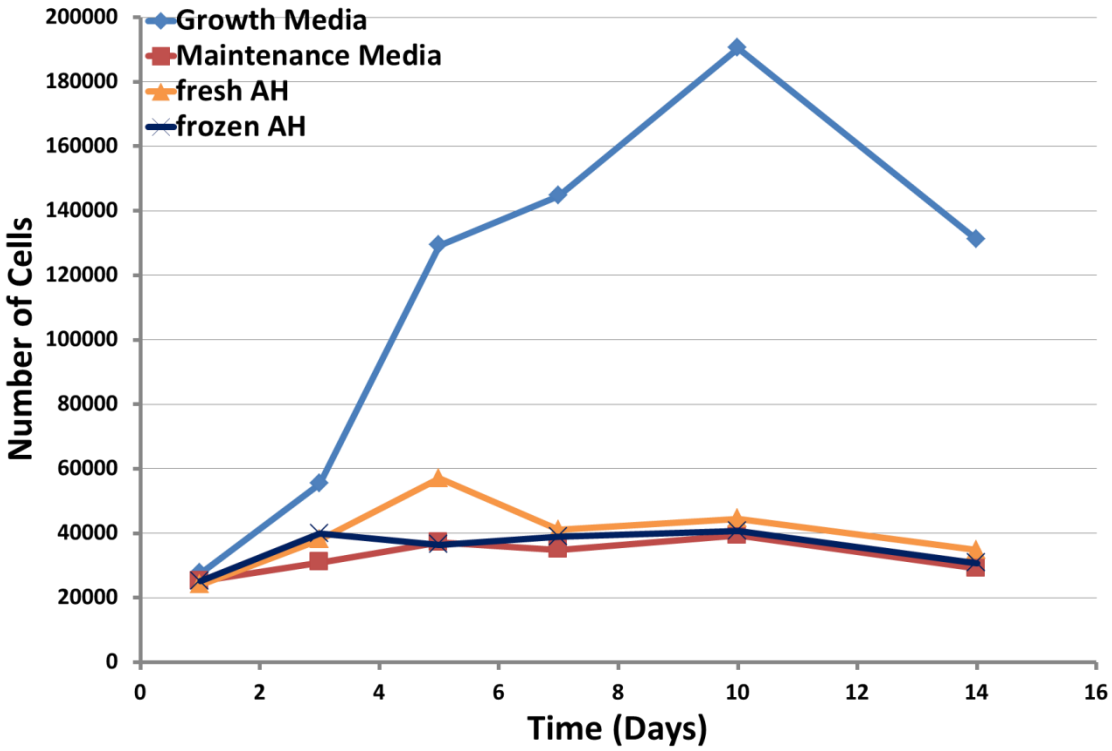

Figure 5-2. Growth curve of BTM cells cultured in fresh and frozen AH compared to growth and maintenance media.

Line graph representing the number of BTM cells present at 1, 3, 5, 7, 10 and 14 days, following initial settlement onto plastic substrate. The averaged values for growth and maintenance media used across all growth curves are represented by the blue and red lines. BTM cells cultured with fresh and frozen AH showed little increase in cell number and across the time period were comparable to values obtained with maintenance media. There was no difference in cell numbers obtained between fresh and frozen. (Coloured points represent averaged values taken from 3 separate BTM cell cultures).

AH could be an unreliable media, producing variable results in relation to cell morphology/survival, regardless of whether it was fresh or frozen. In some instances cells exhibited a normal morphology with little evidence of stress, however, in other experiments under experimentally identical conditions, cells showed signs of distress within 24 hours including shrunken cytoplasm and cell detachment and by 48 hours no viable cells remained attached to the substrate (Figure 5-3a).

By mixing AH with medium containing FCS it was possible to improve the morphology of cells for extended treatment times (Figure 5-3b). Altering the ratio at which medium was mixed with AH illustrated that 1:3 was not sufficient to maintain normal cell morphology but ratios of 1:1 and 3:1 produced healthy monolayers. The concentration of FCS present in these mixtures also influenced cell health and survival. AH mixed with medium containing 0.5% FCS showed no improvement in TM cell morphology while increasing the FCS content to 1% and 2% showed improved cell morphology (Figure 5-3). Based on the observations made throughout these initial experiments the optimum condition selected was AH mixed 1:1 with medium containing 1% FCS, here after referred to as AH-DMEM.

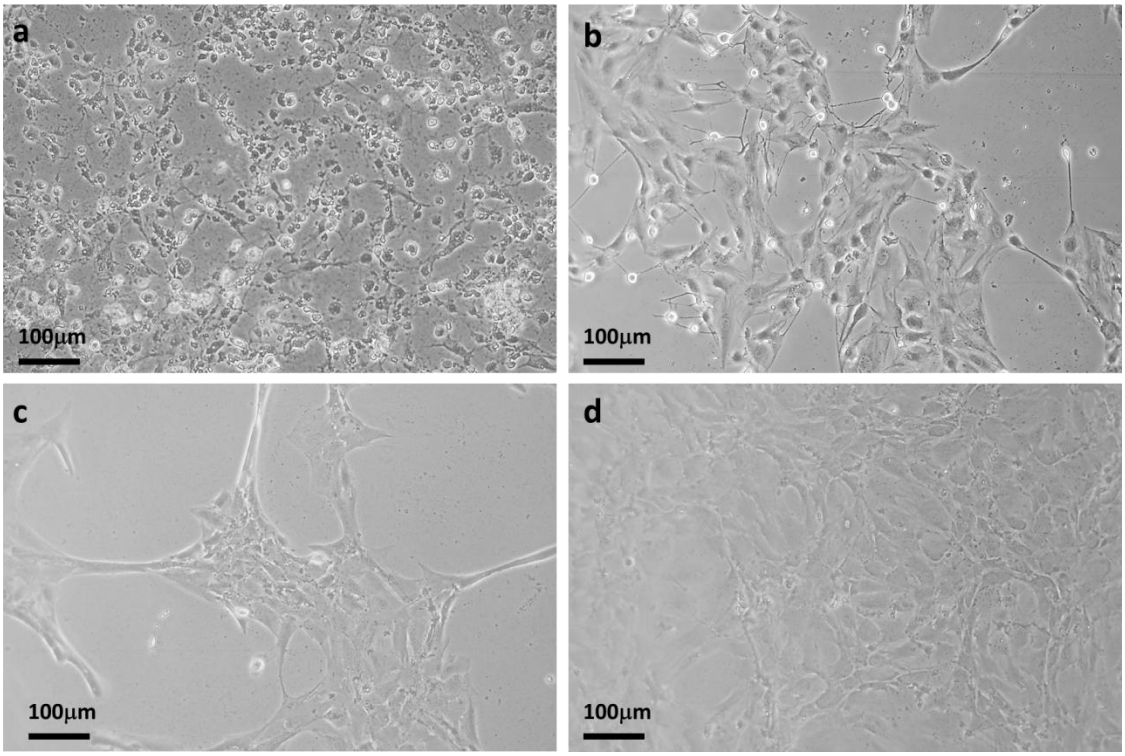

Figure 5-3. Phase contrast images illustrating BTM cell morphology during optimisation of AH.

Phase contrast images of BTM cells under various conditions during optimisation of AH experiments. In image a one batch of AH has resulted in complete cell death after 3 days treatment. BTM cells in figure b have been treated with 900μl of AH with 100 μl of maintenance medium (1% FCS). Cells have begun to shrink and detach from the substrate by 5 days treatment. Mixing AH 1 to 1 with media containing FCS was found to enhance cell health even at 7 days treatment as shown in images c & d. The FCS concentration in figure c was 0.5% compared to 1% in image d.

5.2.2 CLAN incidence

The percentage of CLAN containing BTM cells in cultures treated with AH-DMEM for 3 days (5%) showed no significant difference when compared to control cultures (maintenance medium only) (4.5%) (p=0.608). While CLAN incidence in control cultures following 7 days incubation (7%) was found to be comparable to the value obtained at 3 days, 7 days exposure to AH-DMEM significantly increased CLAN incidence to 37% (p=0.003) (Figure 5-4).

As human AH could not be obtained, a panel of HTM cells were treated with bovine AH-DMEM, under the same conditions as BTM cells. The incidence of CLANs in HTM cell cultures treated with maintenance media was variable between the donors, ranging from 4% to 21%, although most baseline levels were found to be below 5% (21% was the highest baseline value observed in any HTM cell culture). This variability was also present following treatment with AH, with the percentage of CLAN containing cells ranging from 14 to 34%. As with BTM cells, the presence of AH increased CLAN incidence after 7 days exposure, as seen in Figure 5-5. Despite the variability CLAN incidence in the presence of AH was significant increased in all instances (p=0.001, 0.032, 0.001, 0.015, 0.001).

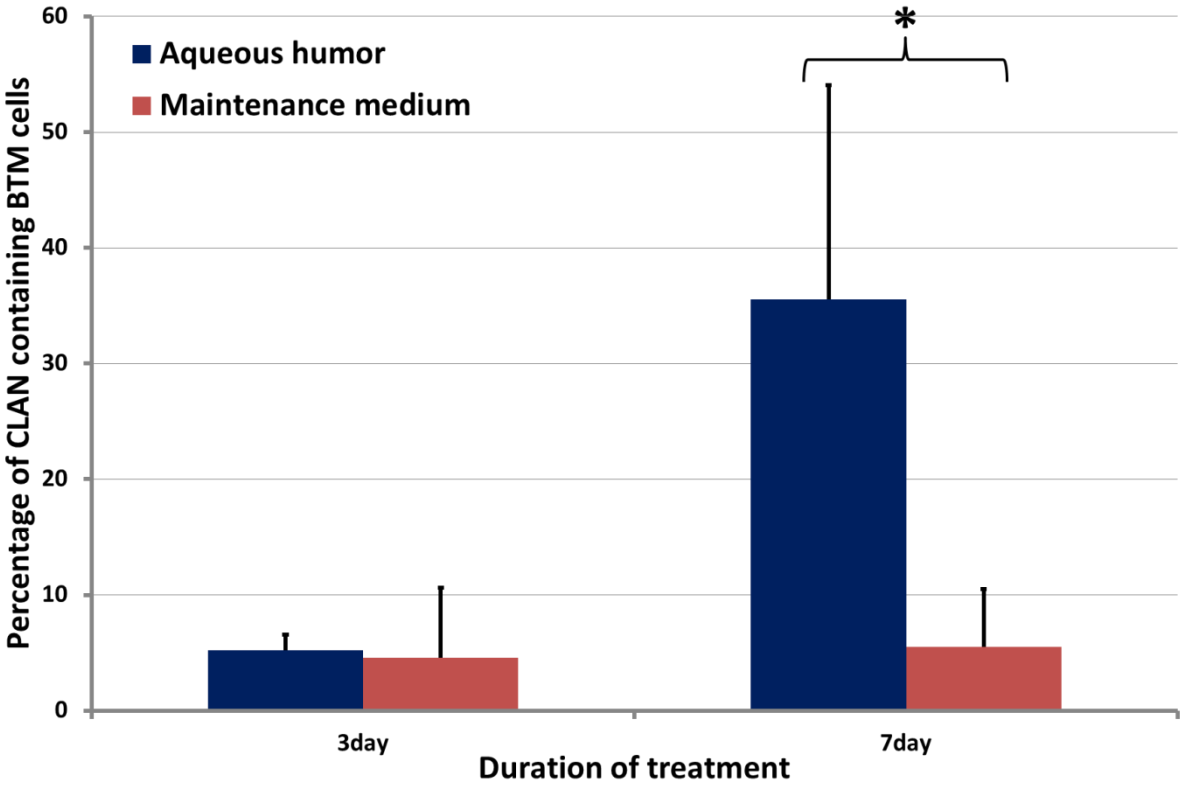

Figure 5-4. CLAN incidence in BTM cells treated with AH for 3 and 7 days.

Bar graph shows the incidence of CLANs following 3 and 7 days treatment with AH mixed with maintenance media compared to maintenance media only. While CLAN incidence is increased at both time points compared to control (maintenance medium) the difference only reaches significance following 7days treatment when values increase from 7% in the control to 37% when AH is present. Coloured bars represent the averaged values from 7 different experimental repeats. Error bars represent standard deviation and those marked with a * show a statistically significant difference (p=0.003).

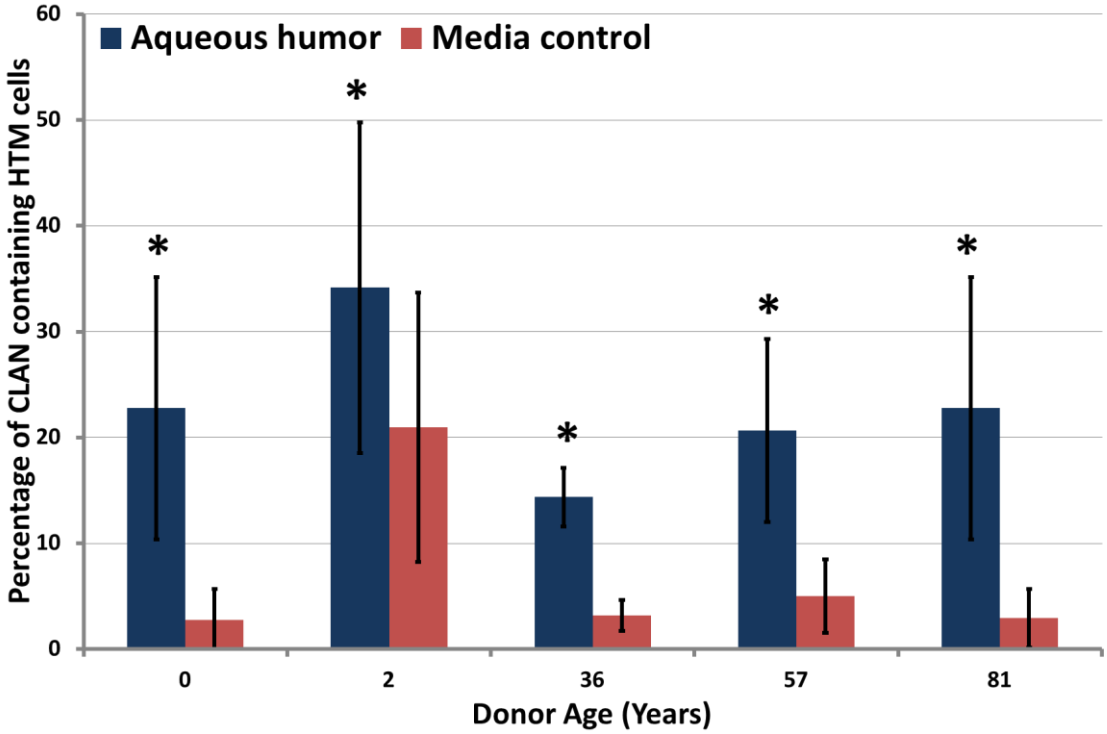

Figure 5-5. Histogram showing CLAN incidence in HTM cells from 4 donors in presence of AH compared to maintenance media.

Bar chart shows the percentage of CLAN containing cell observed in confluent cultures of HTM cells from 5 different donors. CLAN incidence was variable between donors in both control and treatment. Despite this the addition of AH resulted in a significant increase in CLAN incidence compared to control conditions in all donors. Coloured bars represent the averaged values where n=2. Error bars represent standard deviation and those marked with a * show a statistically significant difference compared to the relative control (p=0.001, 0.032, 0.001, 0.015, 0.001).

5.3 Influence of growth factors on TM cells

The ocular content and distribution of growth factors is known to be altered in several diseases including glaucoma (Jampel et al., 1990; Ozcan et al., 2004; Tripathi et al., 1998). Therefore, we explored the influence of 3 key growth factors reported to be increased in the AH of glaucoma patients. The three growth factors investigated in this work were HGF, FGF and TGF-β2. Each was added in isolation to BTM cells for exposure times of 7 days at various concentrations and thereafter cell morphology and cytoskeleton were assessed.

The addition of each individual growth factor produced growth curves not dissimilar to cultures treated with maintenance medium only. As shown in Figure 5-6, addition of TGF-β2 resulted in a slow reduction in cell number over the 14 day period while both HGF and FGF values were consistently higher. Treatment with HGF resulted in a sharp increase in cell number between day 5 and 7 with values remaining at this slightly elevated level until the termination of the experiment, while FGF lead to a more progressive increase in cell number up to 7 days. After this time point the numbers slowly fell, but were consistently higher than maintenance medium only.

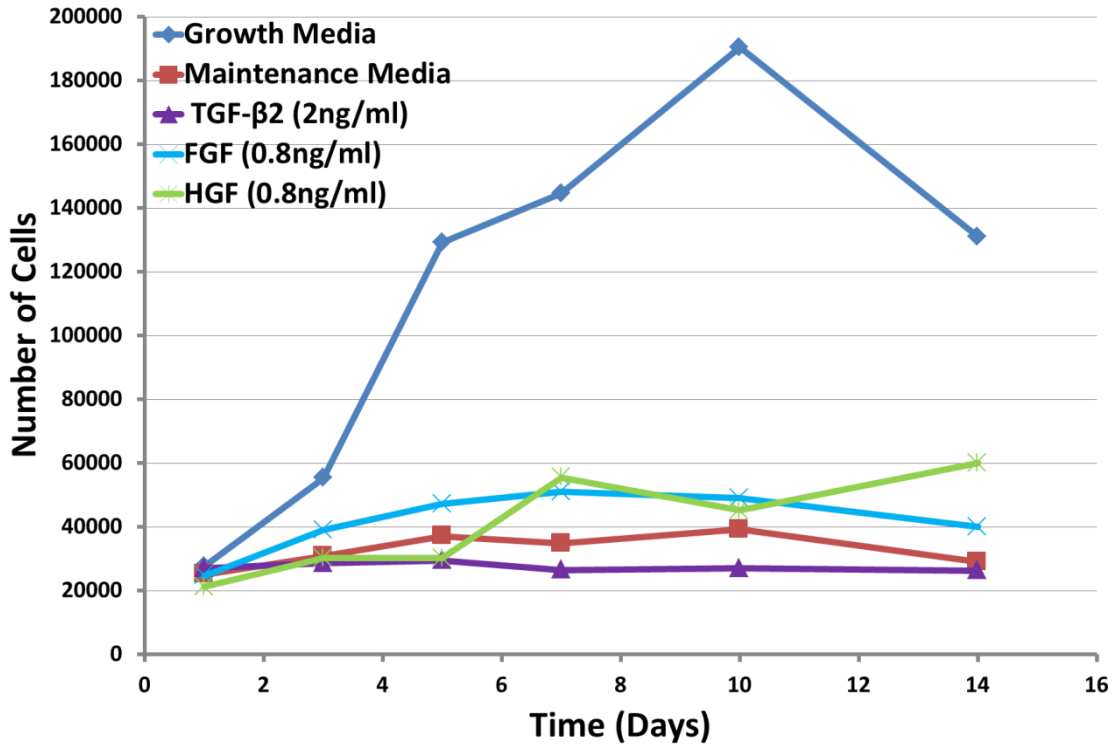

Figure 5-6. Line graph of BTM cell number at various time points when treated with media supplemented with HGF, FGF or TGF-β2.

Line graph shows the standard curves produced in the presence of growth and maintenance medium which provide comparison across all BTM growth curves in blue and red respectively. Treatment of BTM cells with maintenance medium containing one of the three growths factors resulted in minimal changes to cell proliferation as represented by cell number.

5.3.1 HGF and FGF

Monitoring of cells demonstrated that BTM cells retained normal cell morphology throughout the experimental period. Figure 5-7 is representative images of BTM cells following 7 days treatment with increasing concentrations of HGF. The cells in all cultures showed good contact with neighbouring cells which seemed more evident at concentrations of 0.5 and 0.8ng/ml. This observation was in keeping with the growth curves obtained. The cytoskeleton of these cells was observed to be mainly stress fibres running parallel across the cell. Concentrations of 1ng/ml HGF were found to produce cell morphologies in which cells had more cytoplasmic protrusions and cell to cell contact was reduced.

Treatment with FGF for 7 days did not significantly alter BTM cell morphology, as seen in Figure 5-8 cells expressed a normal cell shape and had close contact with neighbouring cells. Concentrations of 0.5 and 0.8ng/ml produced cultures that were more closely connected and appeared to have increased cell numbers. The cytoskeleton consisted of stress fibre arrangements running parallel across the cells. In cultures treated with concentrations of 1ng/ml the cytoskeleton of cells seemed less defined.

The addition of rhHGF, at concentrations ranging from 0.2-1ng/ml in maintenance media, resulted in a CLAN incidence of between 7-9% in BTM cell cultures following 7 days exposure. Increasing the concentration of HGF across this range did not result in a dose dependant variation in CLAN incidence ($p=0.59$), however, values were just significantly higher than maintenance medium only values ($p=0.045$). While higher than the control cultures the values obtained were comparable to the baseline level of CLANs observed with growth medium (Figure 5-9).

As with HGF treatment, increasing the concentration of FGF (0.2-1ng/ml) had no significant influence ($p=0.97$) on CLAN incidence. The percentage of CLAN containing BTM cells ranged from 5-9% (Figure 5-9) and so was not significantly different to control cultures ($p=0.95$).

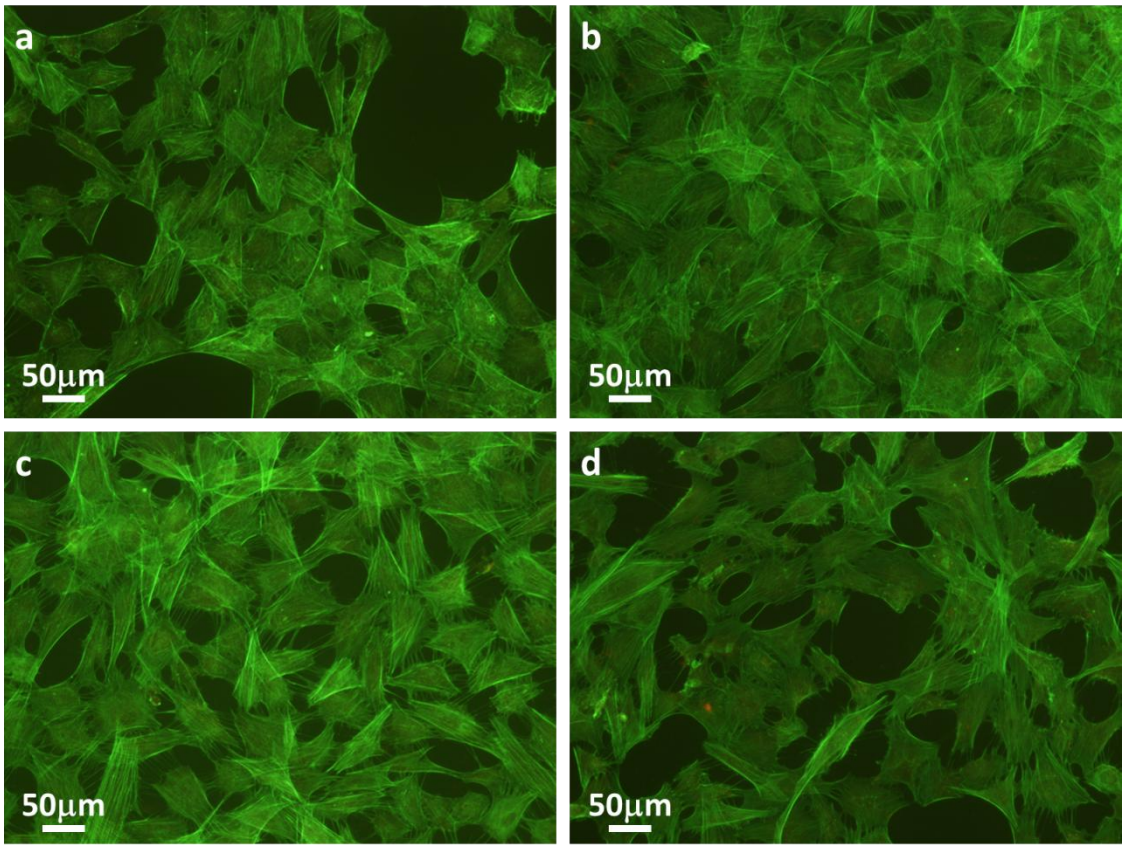

Figure 5-7. Fluorescent images of BTM cell cultures treated for 7 days with increasing concentrations of HGF.

Increasing concentrations of HGF had no great influence on BTM cell morphology following 7 days treatment as shown in the fluorescent images a-d. BTM cells in figure a. were exposed to 0.2ng/ml HGF. BTM cell morphology was found to be unchanged in comparison to maintenance medium treated cells and this was true when concentrations of HGF were increased to 0.5ng/ml (b) and 0.8ng/ml (c). BTM cells in figure b and c appeared more densely populated with more cell-cell interactions. Cells treated with concentrations of 1ng/ml (d) exhibited reduced cell-cell contact. Throughout all treatment concentrations the predominant cytoskeletal arrangement remained straight stress fibres.

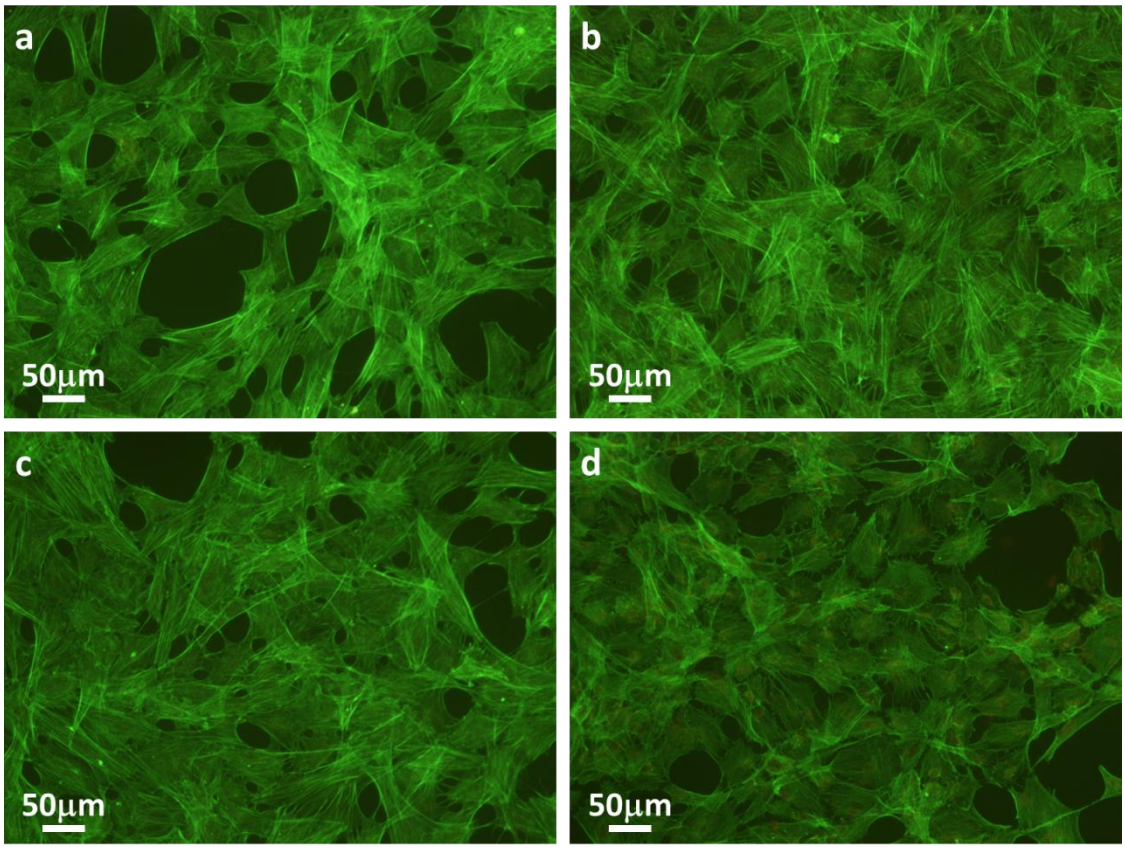

Figure 5-8. Fluorescent images of BTM cell cultures treated for 7 days with increasing concentrations of FGF.

Fluorescent images of BTM cells following treatment with a. 0.2, b. 0.5, c. 0.8 and d. 1ng/ml of human recombinant FGF for 7 days. Cell morphology was not significantly altered with concentrations of FGF. Cells maintained their characteristic shape and had good cell-cell contact with the majority of the culture surface covered. The cytoskeletal arrangement in the majority of cells was stress fibres.

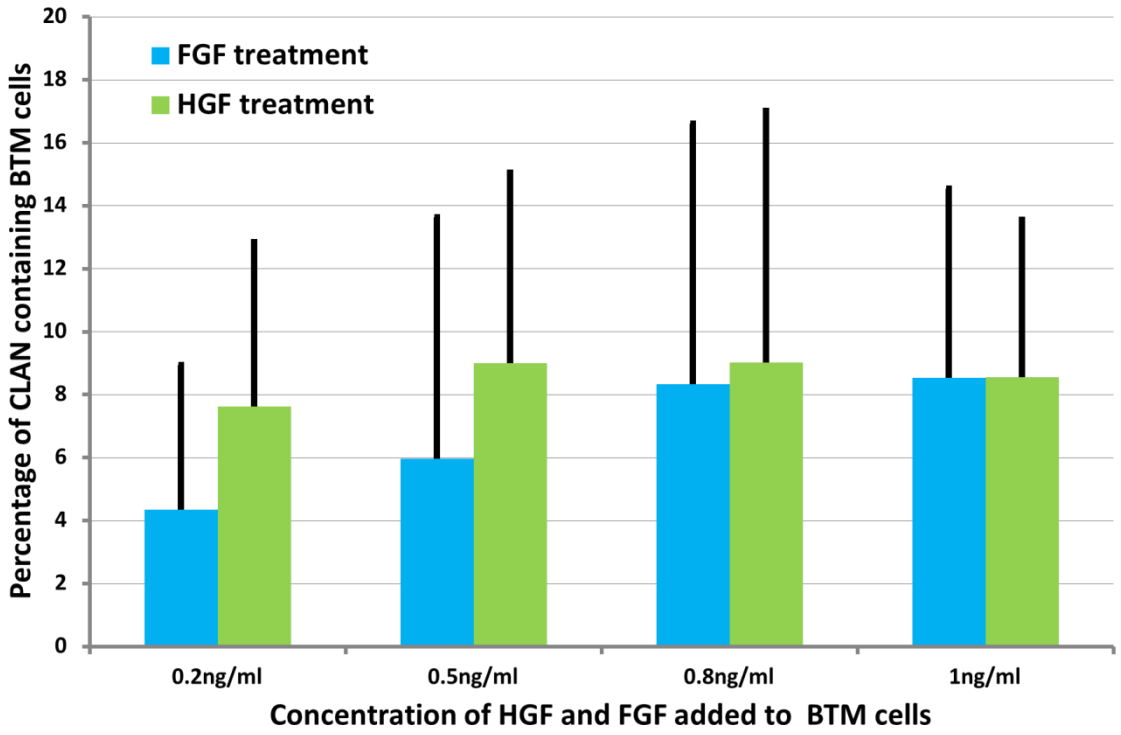

Figure 5-9. Percentage of CLAN containing cells with treatment of HGF and FGF.

Graph showing the percentage of CLAN containing BTM cells at 7 days with an increasing concentration of HGF or FGF added to maintenance media. No significant increase in CLAN incidence was observed with increasing levels of either growth factor. The baseline level of CLANs observed in BTM cells treated with growth media for 7 days was 10%. Results from the 2 growth factors do not exceed the serum only baseline and there is no statistically significant difference (p=0.95). (Coloured bars represent the averaged values where n=4. Error bars represent standard deviation).

5.3.2 TGF-β2

The addition of TGF-β2 to maintenance medium produced quite different results from those found with HGF and FGF treatment. CLAN formation in cultures of BTM cells treated with rhTGF-β2, at concentrations ranging from 1-8ng/ml, was 23-43%. 1ng/ml TGF-β2 induced CLAN formation in 23% of BTM cells while doubling the concentration to 2ng/ml resulted in 43% of cells containing CLANs, a significant increase compared to 1ng/ml ($p=0.001$). Concentrations above 2ng/ml produced no further increase ($p=0.081$) in CLAN formation (Figure 5-10), as values reached a plateau of 32% and 30% with 5ng/ml and 8ng/ml respectively. The percentage of CLAN containing cells at all concentrations of TGF-β2 was found to be significantly increased over control levels ($p=0.001$).

Cell morphology was monitored throughout and the fluorescent images shown in Figure 5-11 are representative of BTM cell cultures treated with increasing concentrations of TGF-β2. The presence of TGF-β2 did not appear to significantly alter the BTM cell morphology at concentrations below 5ng/ml. Cell coverage of the substrate and cell to cell contact was good until the concentration was increased to 8ng/ml. At this concentration cell coverage was incomplete although cell morphology was not greatly altered. Even with a low power x10 objective the cytoskeleton was observed to contain polygonal arrangements of actin.

Figure 5-12 is an example of a CLAN induced in a BTM cell in a culture treated with 2ng/ml TGF-β2 for 7 days. The polygonal structure of the CLAN is clearly visible and it is positioned just over the nucleus, visible in red. From this image it is clear that the cells are in a confluent state with good cell to cell contact. The surrounding cells contain mainly straight stress fibres, although anther CLAN is just visible in the bottom right hand corner. The main CLAN in Figure 5-12 provides some evidence of the 3D nature of the CLAN itself and of the cell culture. Identifying CLANs within cell cultures required the continual adjustment of the fine focus because, as Figure 5-13 illustrates different portions of the CLAN may be visible at slightly different depths.

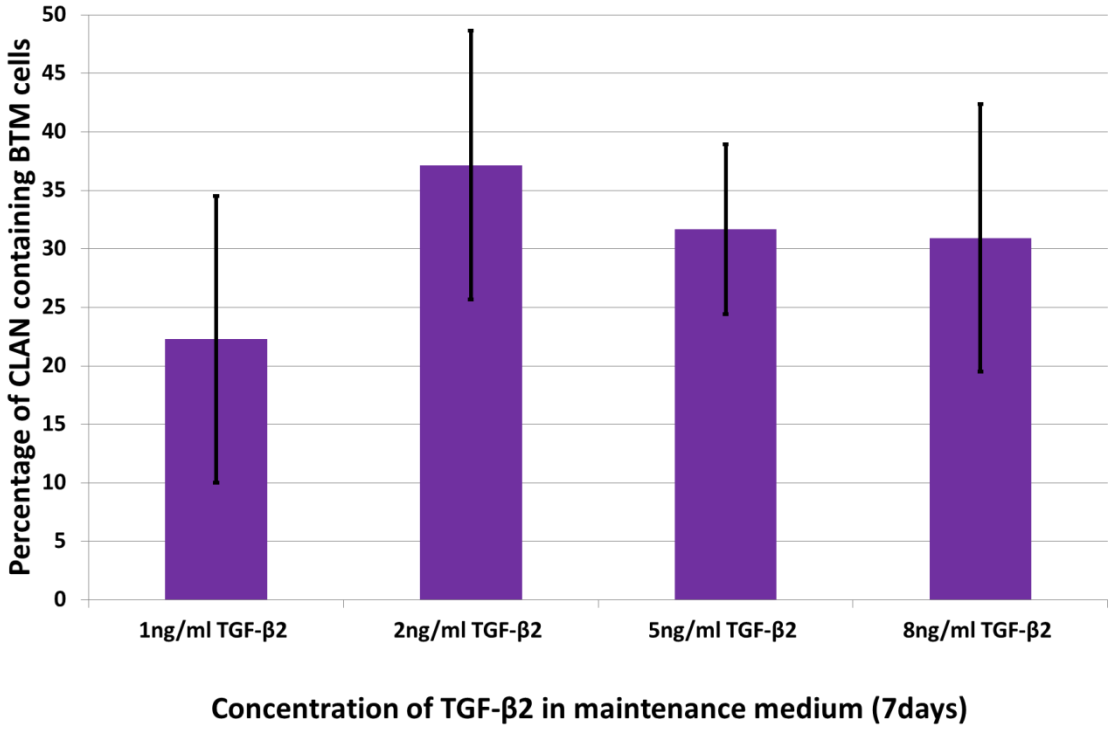

Figure 5-10. CLAN incidence with increasing concentration of TGF-β2.

Bar chart illustrating the percentage of CLAN containing BTM cells present in confluent monolayers following 7 days exposure to varying concentrations of TGF-β2. The initial increase observed from 1ng/ml to 2ng/ml is a significant increase (p=0.081) which plateaus and does not significantly increase further, even when concentrations are increased as high as 8ng/ml. Bars represent average values where n=3. Error bars are standard deviations and all values show a statistically significant difference compared to the control levels of 7% (p=0.0001).

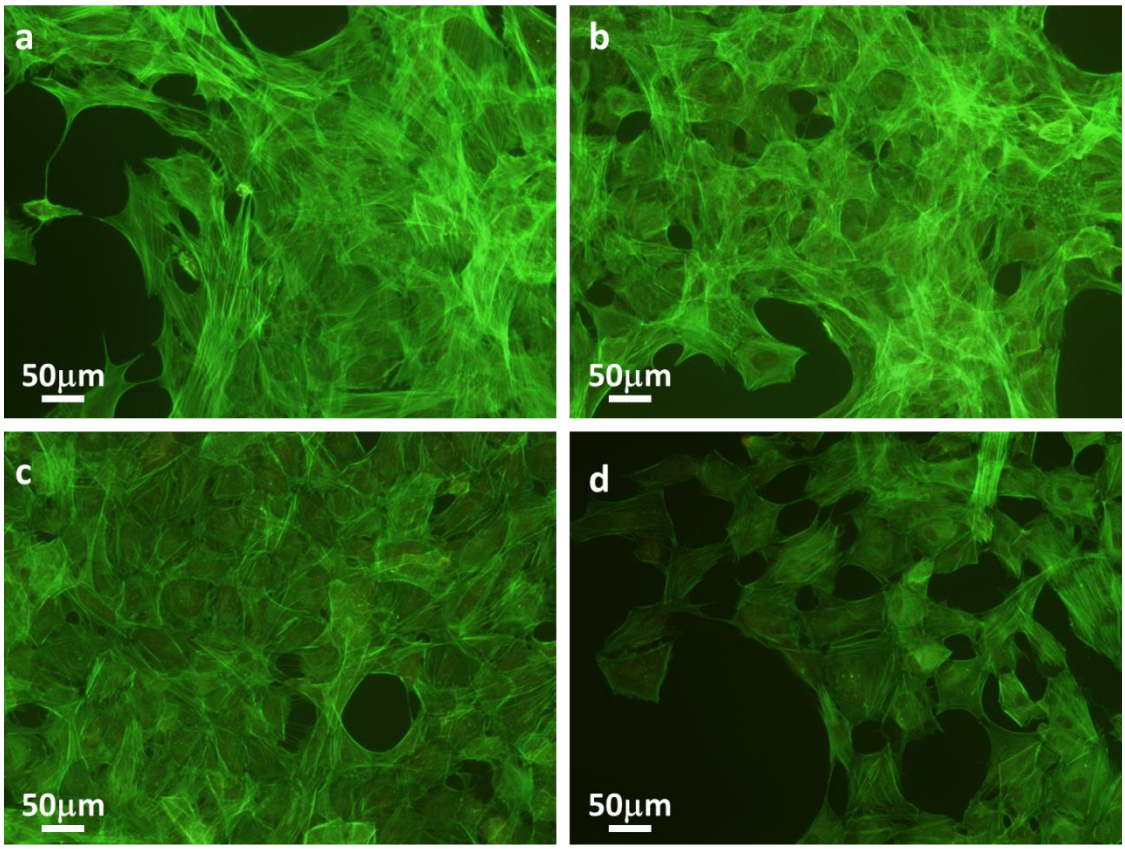

Figure 5-11. Fluorescent images of BTM cells treated with increasing concentrations of TGF-β2.

Fluorescent images captured via x4 objective following 7 days treatment of BTM cells with a. 1ng/ml, b. 2ng/ml, c. 5ng/ml and d. 8ng/ml TGF-β2 in maintenance medium. Cell morphology remains normal throughout but there is evidence of cell loss in cultures treated with 8ng/ml. In all cultures BTM cells have close contact with neighbouring cells and the characteristic TM culture morphology with small spaces which are remnant of pores in the 3D structure of TM.

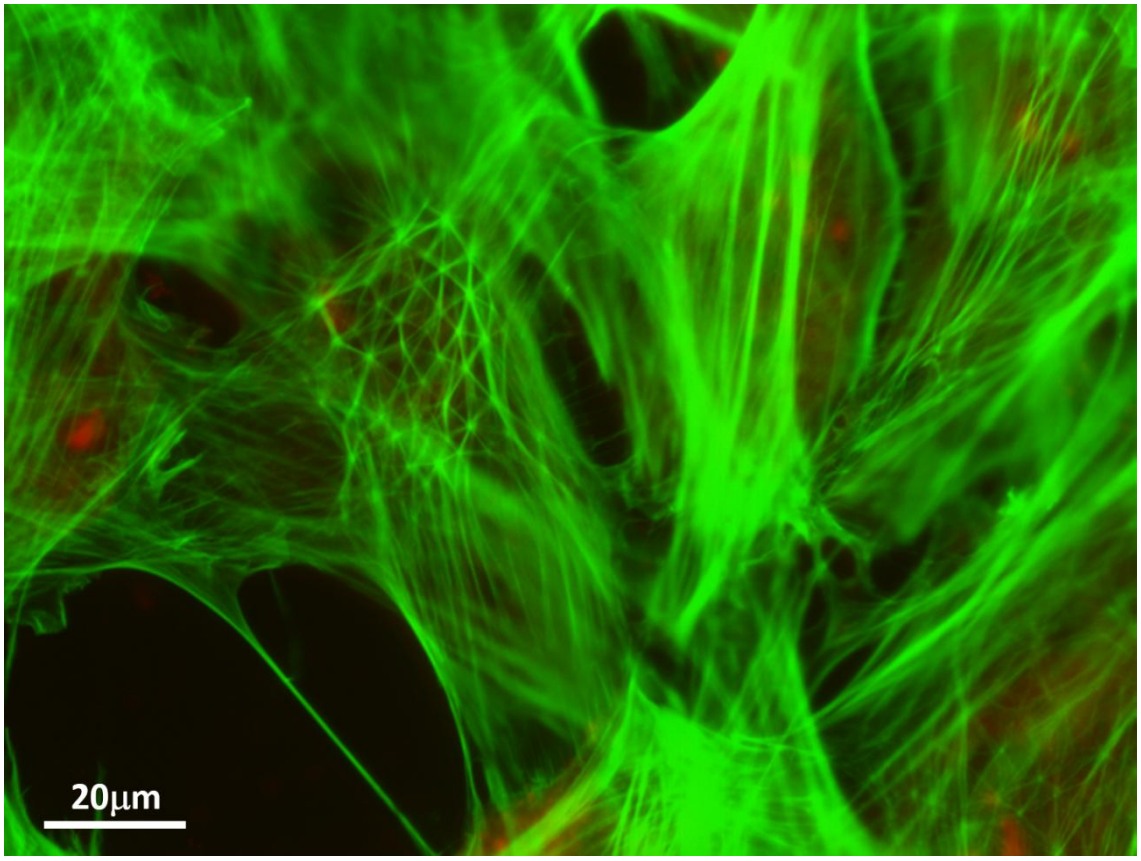

Figure 5-12. CLAN identified in BTM cells treated for 7 days with TGF-β2.

This fluorescent image is an example of a CLAN formed in BTM cells treated for 7 days with TGF-β2. The actin was seen as green following incubation with Alexa-488 phalloidin while the nuclei fluoresced in a red colouration with PI. In most cells present the actin is arranged in straight stress fibres however one very clear and regular CLAN is observed.

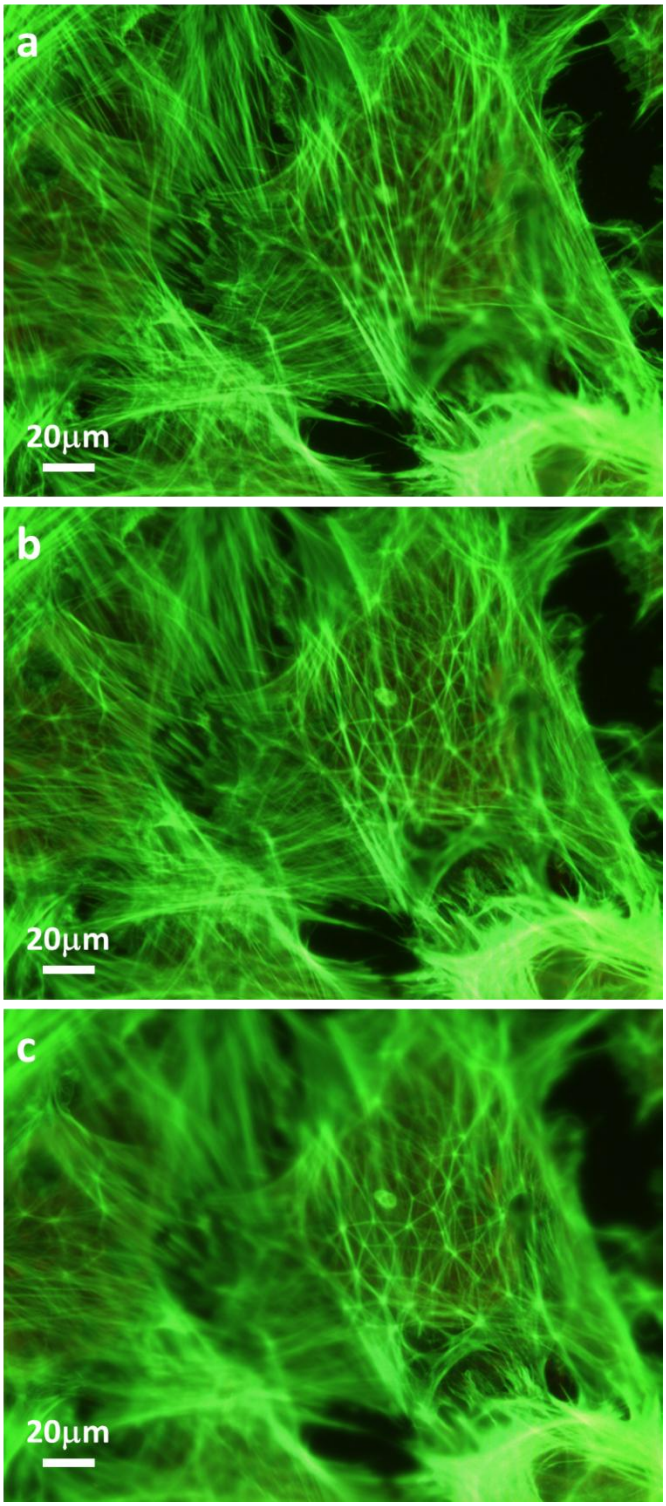

Figure 5-13. Fluorescent images illustrating the 3D nature of a CLAN identified in BTM cells treated for 7 days with 2ng/ml TGF-β2.

Identifying CLANs in vitro is carried out via the eye pieces of the microscope and not from images because the cytoskeleton of cells is not 2-dimensional. The series of 3 fluorescent images, taking via conventional fluorescence microscopy, reveals how the cytoskeleton is a 3-dimensional structure with CLANs tending to be higher in the cell than stress fibres.

HTM cells treated with 2ng/ml TGF-β2 demonstrated an increase in the percentage of CLAN containing cells, however, there was variability with values ranging from7-37%. The average CLAN incidence induced by TGF-β2 treatment in the 26 HTM cell cultures was 22%, compared to an average 5% under control conditions (the individual changes observed in HTM cultures is expanded upon in chapter 6).

It was observed that the percentage of CLAN containing TM cells following 7 days incubation with AH and TGF-β2 was similar. In BTM cells, 2ng/ml TGF-β2 resulted in 37% of cell containing a CLAN while AH resulted in 35% (p=0.909). The same comparison was made between a HTM cells from 5 donors. As shown in Figure 5-14 the incidence of CLANs produced in HTM cells by treatment with TGF-β2 was comparable to those induced by AH in 3 of the 5 donors. Despite some individual variation within donors, the average CLAN incidence was 22% (p=0.711) for both treatments.

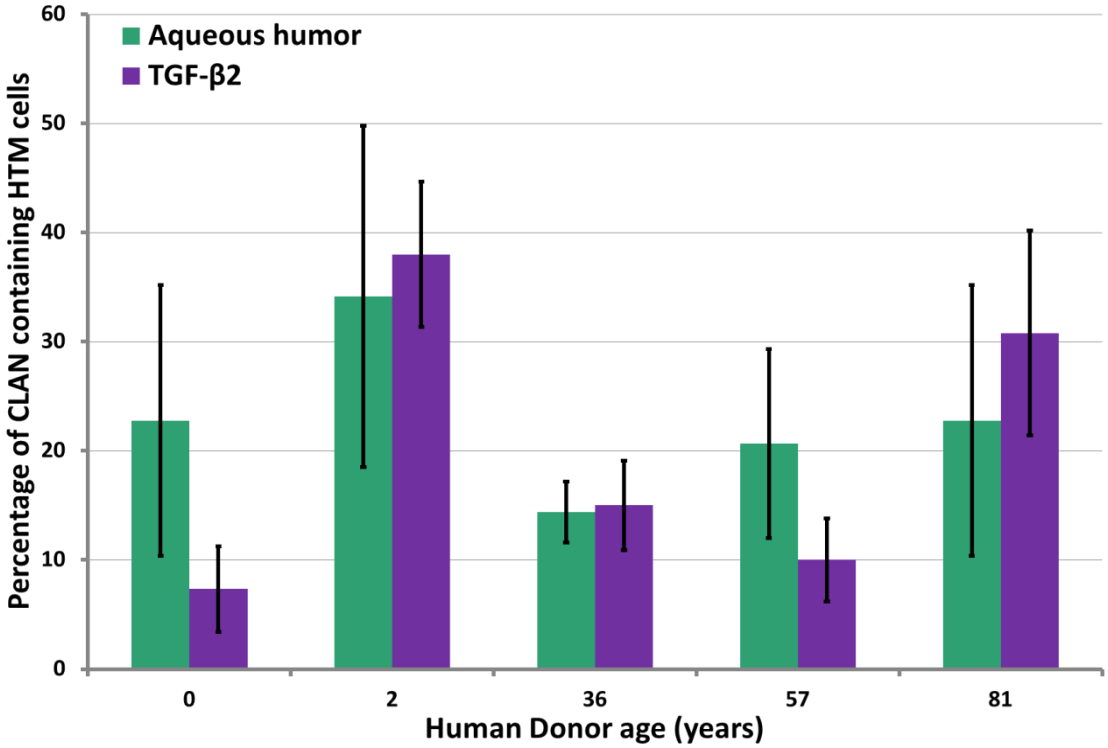

Figure 5-14. Bar chart of relative CLAN incidence induced with TGF-β2 and AH in HTM cell cultures.

Bar chart shows the percentage of CLAN containing HTM cells in a panel of HTM cells treated with TGF-β2 or AH-DMEM. While CLAN incidence across the different donors ranged from 10-37% both treatments were found to produce comparable levels of CLAN containing cells within each culture. Coloured bars represent the averaged values where n≥2 for AH and n≥4. Error bars represent standard deviation.

5.3.3 Combined growth factor effect

The growth factors previously added in isolation do not exist in this manner within the eye but are part of the complex mixture of components that make up the AH. The growth factors were therefore added in combination with one another to investigate their combined influence on TM cells.

The addition of HGF with TGF-β2 resulted in a CLAN incidence of 16%, a value higher than the baseline but lower than that expected from previous experiments with the addition of TGF-β2 only. The addition of FGF with TGF-β2 caused a similar result but the percentage of CLAN containing cells was much lower under these conditions averaging 10% and was not statistically different to control ($p=0.497$). Not unexpectedly, the addition of HGF and FGF together failed to induce a CLAN incidence of above 8%, a value almost identical to control levels ($p=0.99$). Combining all three growth factors resulted in an average CLAN incidence of 14% following 7 days exposure. This value was found to be significantly different to both control and TGF-β2 treatment ($p=0.009$) (Figure 5-15).

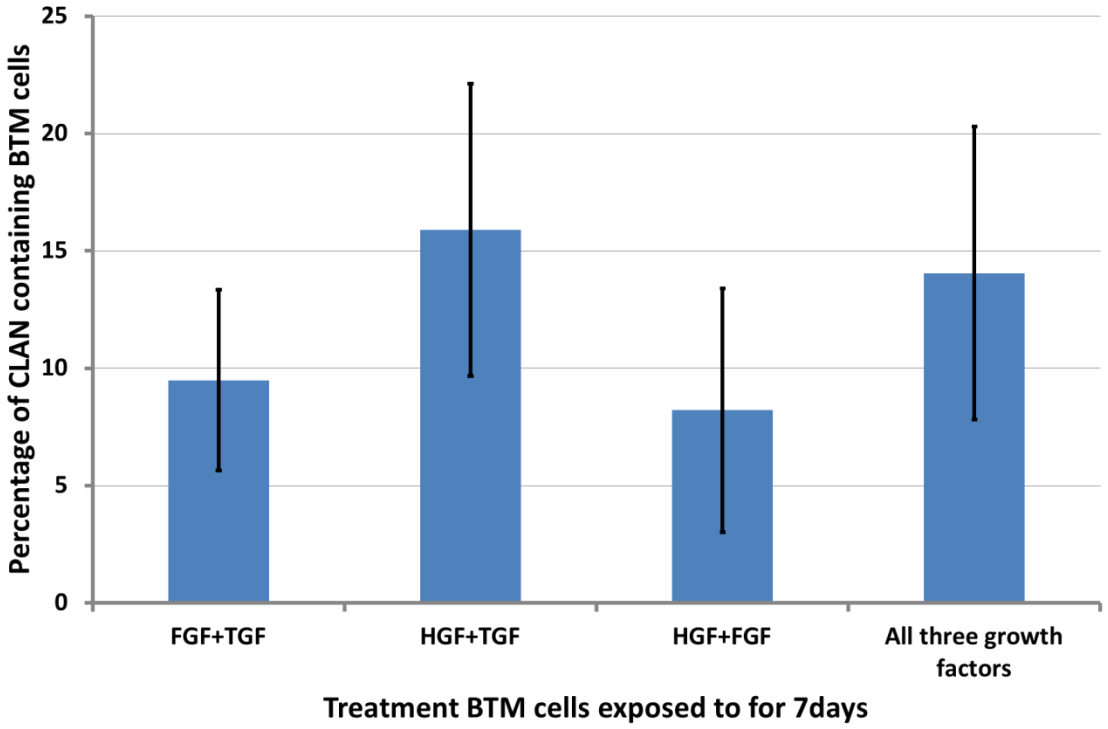

Figure 5-15. CLAN incidence with growth factor combinations.

Graph showing the effect of adding a combination of three growth factors (HGF, FGF and TGF-β2) to BTM cells. Given the data from our previous experiments, we would expect the presence of TGF-β2 to significantly induce CLAN formation above the baseline 10%. While treatment with HGF & TGF-β2 and all three resulted in CLAN incidence above 10% the value failed to reach significance. The CLAN inducing ability of TGF-β2 is negated by the presence of the HGF and FGF. (Bars represent an average percentage of CLAN containing cells at 7 days where n=3. Error bars are standard deviations).

5.4 Is TGF-β2 the main CLAN inducing agent in Aqueous humor (AH)?

Although both AH and TGF-β2 were capable of inducing CLANs to a similar level in both HTM and BTM cells this was not proof that TGF-β2 in AH was responsible for the induction. In order to investigate whether TGF-β2 was responsible for the CLAN promoting influence of AH the following experiments were conducted.

Addition of a TGF-β2 specific neutralising antibody to a solution of 2ng/ml TGF-β2 in maintenance media significantly reduced CLAN incidence ($p=0.0001$) following 7 days exposure from 46% to 4.2%. CLAN incidence was reduced to within baseline levels ($p=0.089$) representing a percentage decrease of 90%. The addition of an inappropriate IgG control to 2ng/ml TGF-β2 in maintenance media also resulted in a decrease in CLAN incidence (from 46% to 28%). The decrease observed was not significantly reduced from TGF-β2 treatment ($p=0.141$) and was taken to represent the level of non-specific binding, accounting for a reduction of 38%. As the control IgG affected CLAN incidence, the data was normalised by subtracting the non-specific value. As the overall reduction in CLAN incidence was 90% upon addition of the specific antibody, and 38% may have been non-specific, the true reduction related to the neutralising of TGF-β2 was 52%.

After establishing that the CLAN inducing influence of rh-TGF-β2 added to cultures could be reduced by neutralisation of the molecule, the same experiments were undertaken with AH. These results showed that CLAN induction by AH could also be reduced by the addition of TGF-β2 neutralising antibody (Figure 5-17). CLAN incidence in AH was 35% but was reduced to 7% ($p=0.0001$) in the presence of the specific antibody representing an overall percentage decrease of 80%. As before the reduction achieved by the addition of an IgG control was taken to represent non-specific binding and was calculated as 40%. Therefore, the overall reduction caused by the specific neutralising of TGF-β2 was 40%.

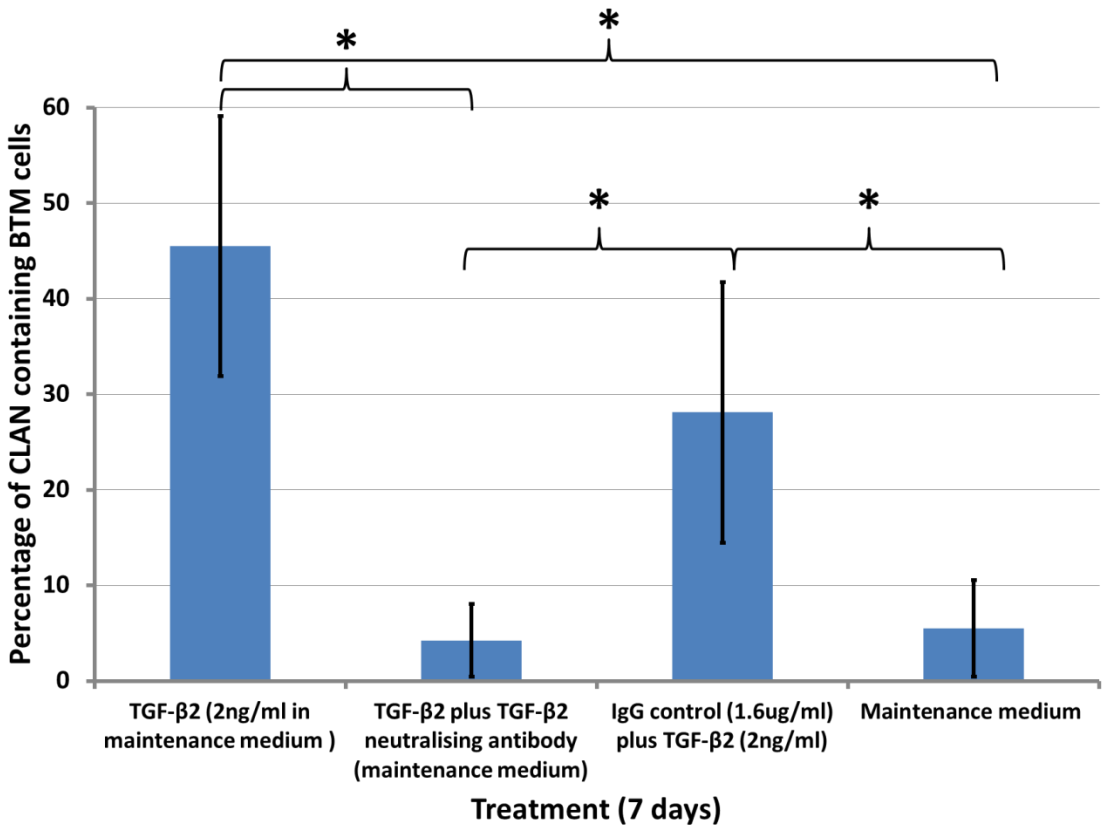

Figure 5-16. CLAN incidence following the neutralisation of TGF-β2.

Bar chart representing the percentage of CLAN containing BTM cells following 7 days exposure to various conditions. Treatment with TGF-β2 resulted in a significant CLAN induction above maintenance media (p<0.0001). Addition of a TGF-β2 specific neutralising antibody resulted in a CLAN incidence of 4%, representing a significant (p=0.0001) percentage decrease of 90%. Addition of the control IgG also resulted in a decrease of CLAN incidence compared to TGF-β2 treatment and so was taken to represent the TGF-β2 negating effect which resulted from non-specific binding. Taking this into account the TGF-β2 antibody was responsible for a specific decrease in CLAN incidence by 52%. Bars represent average values where n=5. Error bars show standard deviation and bars marked with * indicate a value significantly different.

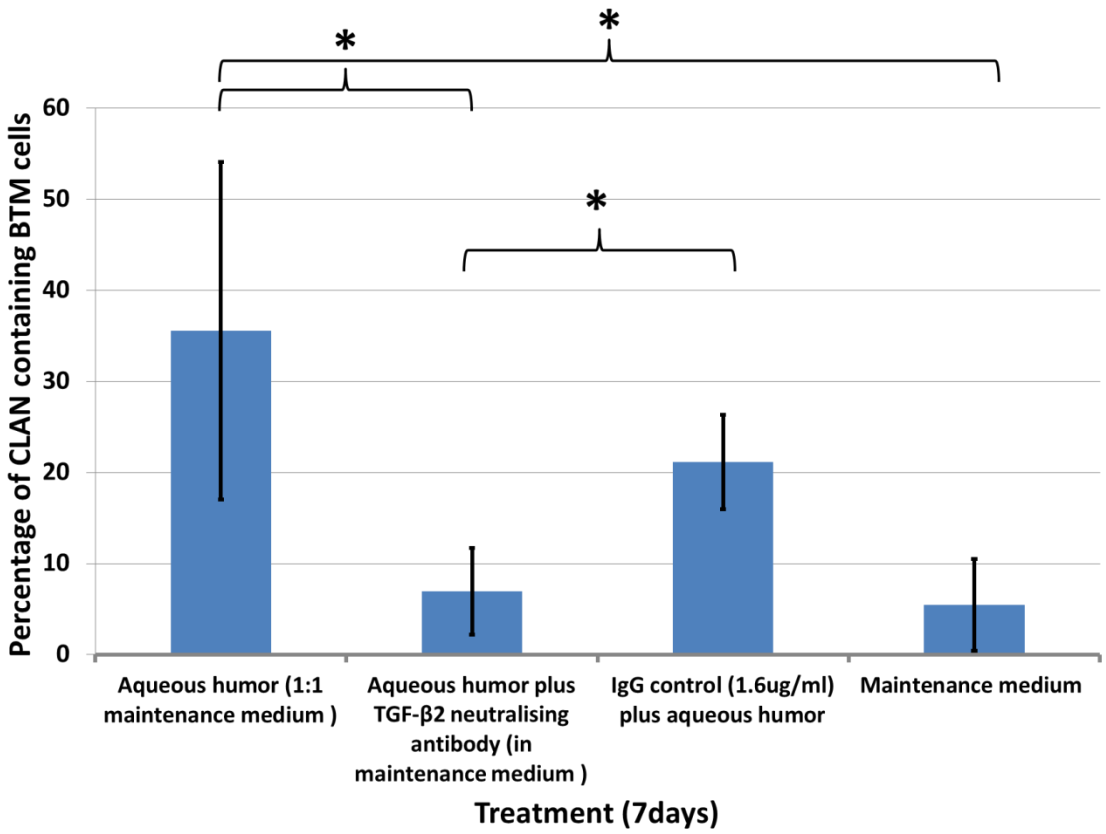

Figure 5-17. CLAN incidence in BTM cells following the neutralisation of TGF-β2 in AH.

A bar chart illustrating the percentage of CLAN containing BTM cells. Treatment with AH resulted in a significantly larger number of CLAN containing cells (35%) compared to maintenance media (p<0.005). Addition of a TGF-β2 specific neutralising antibody to AH resulted in a CLAN incidence of 6.9% which represented a percentage decrease of almost 81%. Compared to TGF-β2 treatment addition of the control IgG also resulted in a decrease of CLAN incidence accounting for 40% of the total decrease. Therefore the TGF-β2 antibody was responsible for a specific decrease in CLAN incidence by 41%. Bars represent average values where n=5. Error bars show standard deviation and bars marked with * indicate where a significant difference was observed.

The CLAN inducing effect of TGF-β2 could also be negated in HTM cells by addition of TGF-β2 specific antibody (Figure 5-18). A panel of 6 HTM donors revealed that addition of TGF-β2 neutralising antibody could reduce CLAN incidence to within baseline levels ($p=0.295$). When the data from the 6 donors was combined the average CLAN containing cells was 2.3% following treatment with the antibody. The decrease from an average incidence of 26% with TGF-β2 represented an average reduction of 91% ($p=0.0001$).

There was some variation between donors (Figure 5-19) and in 2 instances the percentage decrease was found to be 53 and 44%, much lower than in other donors were values ranged from 83-93%. In all cases, however, the reduction in CLAN incidence was significant ($p=0.004$).

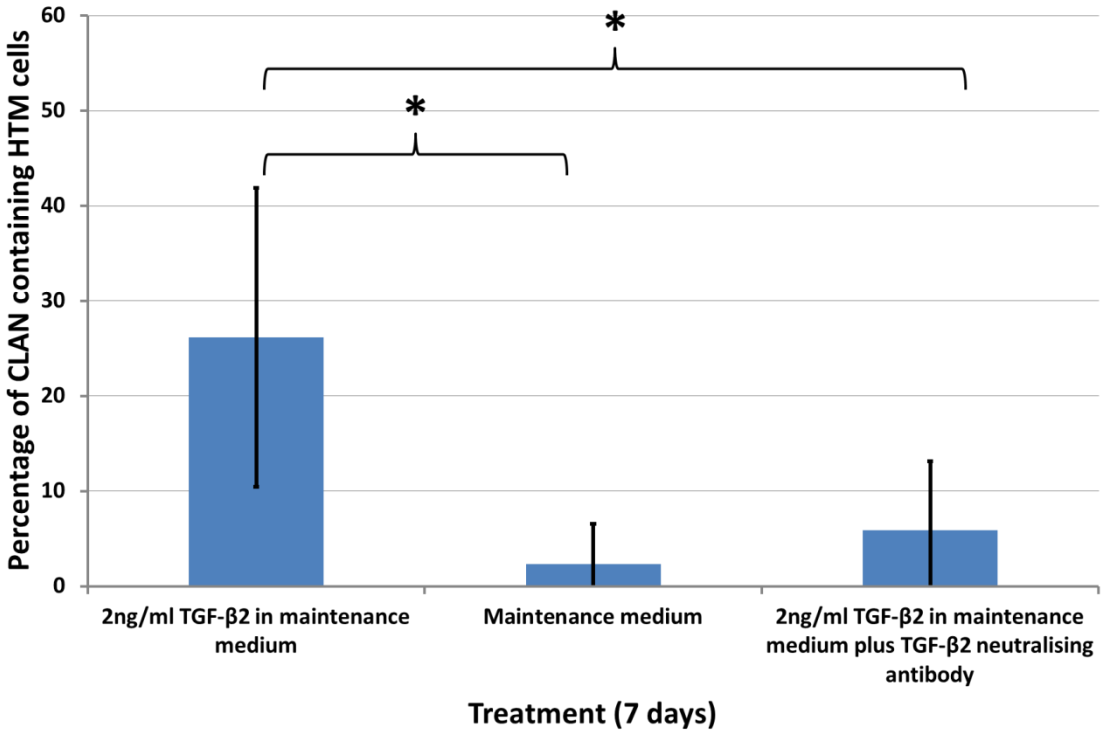

Figure 5-18. Percentage of CLAN containing HTM cells in presence of TGFβ2 neutralising antibody.

Bar chart showing the average percentage of CLANs in HTM cell cultures from 6 donors treated for 7 days. The addition of rh TGF-β2 resulted in a CLAN incidence of 26% a value significantly increased compared to maintenance medium only (p=0.0001). The presence of TGF-β2 neutralising antibody caused a significant reduction in the number of CLANs observed and values were comparable to medium only. Bars represent average values from 6 different donors. Error bars show standard deviation while bars marked with * indicate where a significant difference was observed.

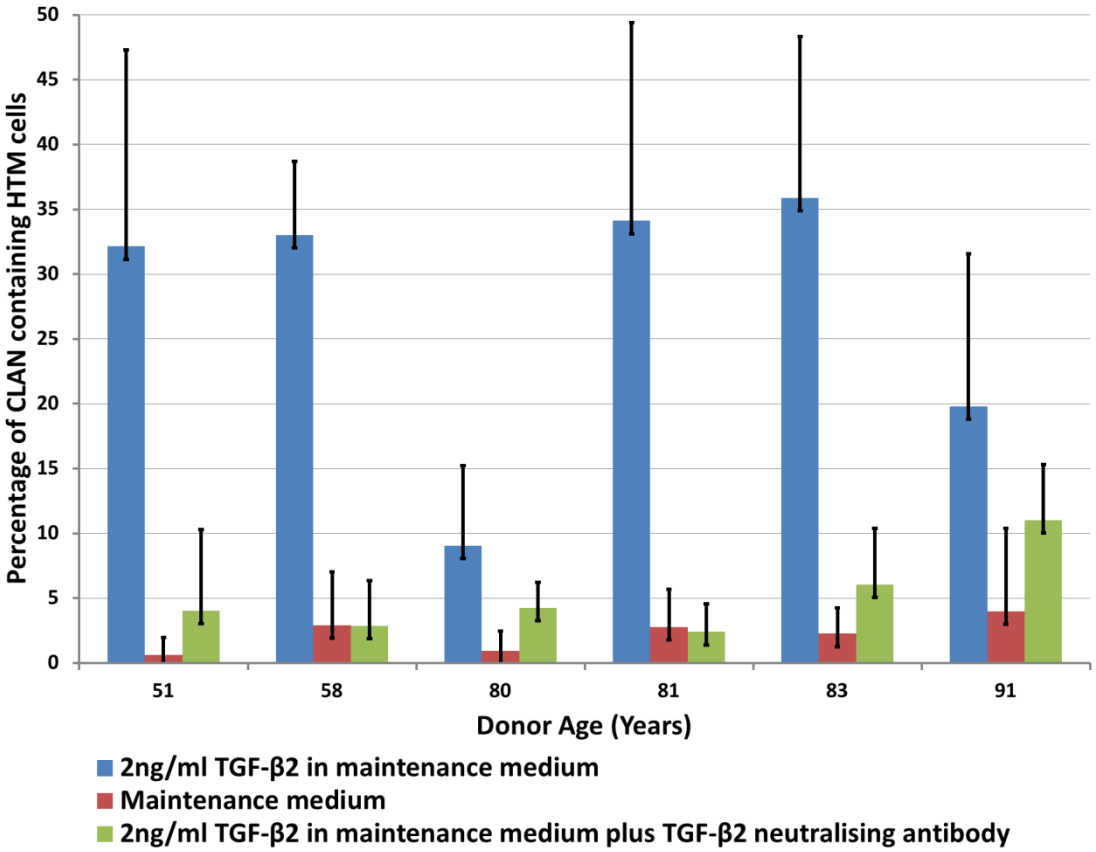

Figure 5-19. Bar chart representing the changes observed in individual HTM cell cultures upon addition of TGF-β2 neutralising antibody.

The data present in figure 5-18 is the average results from the 6 donors shown above. In all donors the presence of TGF-β2 resulted in a significant increase in CLAN containing cells above the maintenance medium only treatment. Treatment with TGF-β2 neutralising antibody also resulted in a significant reduction in CLAN in all donors. The reduction observed was variable accounting for 45-93%. Bars represent average values where n≥2 while error bars show standard deviation.

5.5 Discussion

The established use of TM cell cultures has provided valuable insight into the functioning of TM cells (Alvarado et al., 1982; Grierson et al., 1985b; Polansky et al., 1981; Polansky et al., 1979). TM cells *in vivo* do not undergo proliferation (Alvarado et al., 1981; Grierson and Howes, 1987; Polansky et al., 1979) but the presence of 10% FCS *in vitro* encourages cell to proliferate. Reducing the content of FCS to 1% will maintain cell cultures but proliferation is reduced (Freshney, 1992). In order to investigate the influence of AH on TM cells, cultures needed to be maintained in AH for up to 7 days to be comparable with previous studies. The use of AH as a medium supplement is not common place as it was found, in this study and in others (Fautsch et al., 2005), to be unreliable. Although some batches of undiluted AH were capable of maintaining BTM cells, the unreliable nature over long exposures meant that we investigated mixing AH with medium. Like Fautsch et al we also settled on mixing AH 1 to 1 with medium as cell morphology remained healthy throughout. The initial explanation given for poor survival was that *in vivo* the aqueous is flowing through the TM, so cells are not subject to stagnant aqueous, as is the case in cell culture. A possible solution to this would have been to use a pump which would have allowed us to pass a constant stream of aqueous over the TM cells on the cell culture substrate. However, the volume of AH required for the duration of one experimental run would be large, meaning that having a sufficient quantity of fresh AH for multiple experiments would not be feasible or reproducible. A potential alternative would be the use of a clamped anterior segments model (Johnson, 2005). Under this model system the continual flow of AH (or a supplemented AH) through the TM could reduce cell loss through stagnant AH. This system has the added benefit of the cells remaining *in situ* so that manipulation due to adherence to unnatural substrates is removed and cells would not be artificially aged through passage. While providing a more "natural" environment for the TM cells this model system does throw up a striking difficulty. The ability to view the actin cytoskeleton within TM cells *in situ.*

The variations observed in TM cell health when incubated with AH may be explained by differences in batches caused by the nature of AH itself. The primary AH is continually altered through contact with different ocular tissue and by disease status.

As there is no way to ensure that the AH from each globe is comparable and that each donor is free of ocular pathology there may be large variations in the constituents of the AH itself. As previously explained fresh AH would not always be available for experiments and so frozen stocks would be required. The process of freeze/ thawing the AH could have a detrimental effect on its composition as the enthalpy changes which occur during freezing increase the risk of protein denaturation (Cao et al., 2003). The storage of AH in individual vials reduced the risk of multiple freeze/thaw cycles however others have shown that the activation state of growth factors can be altered when AH is frozen (Maier et al., 2006). Comparison of TM cell morphology and cell number did not note any significant differences between BTM cell cultures treated with fresh or frozen AH. Although protein analysis was not conducted to compare fresh and frozen AH, previous work with frozen AH failed to note any differences (Hogg et al., 1995). Growth curves obtained with AH were comparable to maintenance medium with only a small increase in cell number observed throughout the 14 day experimentation period. This is not an unexpected result as *in vivo* TM cells are not actively proliferating (Alvarado et al., 1981; Grierson and Howes, 1987) but maintained by the delicate mixture of growth factors within the AH. During the course of obtaining the growth curves for AH it was observed that BTM cells re-suspended in AH failed to settle onto the surface of the substrate. In order to assess growth the cells were firstly plated with maintenance media for 24 hours and then treated with AH. A possible explanation may be the migratory stimulation of AH (Hogg et al., 1995; Porter et al., 1991) on TM cells as migration requires changes in cell adhesion which may inhibit the initial substrate attachment process.

Once the use of AH was optimised, treatment of BTM cells began and revealed that AH was a potent inducer of CLANs following 7 days exposure. These findings were mimicked in HTM cells although the percentage of CLAN containing cells was rarely as high in HTM cells as those observed in BTM cells. Given that the actin cytoskeleton is a dynamic structure it seems strange that the formation of CLANs would only reach significance after 7 days, however, this is a finding consistent with previous studies involving TM cells *in vitro* (Clark et al., 1994; Wade et al., 2009). The complex nature of AH provided many possible agents to investigate in search of the CLAN promoting

agent. The composition of the AH changes with different ocular pathologies with alterations in several growth factors (Grierson et al., 2000; Hu and Ritch, 2001), for example increases in TGF-β2 (Inatani et al., 2001; Jampel et al., 1990; Ochiai and Ochiai, 2002; Ozcan et al., 2004; Tripathi et al., 1994) has been linked to the pathogenesis of glaucoma. TGF-β2 has an anti-proliferative influence on TM cells so it is not surprising that growth curves indicate TGF-β2 did not cause TM cells to proliferate. FGF and HGF evoke contrasting results to those of TGF-β2. FGF (250ng/ml) was traditionally added to the medium used in TM cell culture to promote cell growth (Polansky et al., 1979), while HGF also known as scatter factor promoted cell migration (Grierson et al., 2000). Both increased cell numbers across the experimentation period (14 days) consistently higher than maintenance medium. CLAN incidence was always below 10% regardless of the increasing concentrations of FGF or HGF. During cell division the cytoskeleton undergoes rapid changes to allow for the daughter cells to split apart (Heng and Koh, 2010). Rapid alteration in the actin cytoskeleton is also required for cell motility (Mitchison and Cramer, 1996; Olson and Nordheim, 2010), therefore, if the cytoskeleton is organised based on the cells needs it would be unlikely to contain a CLAN that is suspected to restrict remodelling. TGF-β2 on the other hand does not evoke either of these responses and demonstrates a potent induction of CLANs.

The percentage of CLAN containing HTM and BTM cells was found to be statistically similar regardless of whether cells were incubated with AH or 2ng/ml TGF-β2. This made for interesting reading and a series of experiments were conducted in order to investigate whether TGF-β2 was the CLAN inducing agent present in AH. The use of a specific TGF-β2 neutralising antibody was expanded upon within this work, while the use of other agents to negate TGF-β2 activity was explored in our publication (O'Reilly et al., 2011). The addition of the antibody significantly reduced CLAN incidence in cultures treated with rhTGF-β2 thus showing that inhibiting TGF-β2 resulted in fewer CLANs. Addition of the antibody to AH also produced a comparable decrease in the percentage of CLAN containing cells but did not completely eliminate the presence of CLANs in either AH or TGF-β2. The presence of the IgG control clearly interfered with CLAN formation perhaps by non-specific binding to TGF-β2 thus reducing the number

of molecules available to bind to cell surface receptors and produce the cytoskeletal rearrangement. Even with the non-specific reduction the decrease in CLAN incidence observed upon treatment with the specific neutralising antibody was significant. As shown by us in the literature (O'Reilly et al., 2011) the TGF-β2 CLAN inducing properties could be reduced by treating TM cells with TGF-β RI and RII blocking agents, a smad-3 inhibitor, the proteoglycan decorin and mannose-6-phosphate. While the exact mechanisms of action were not investigated these data provide evidence that TGF-β2 is a major CLAN inducing agent which may function via the Smad signalling pathway.

Growth factors do not occur in isolation but are constituents in the complex mixture that is AH making it difficult to attribute actions to just one growth factor given that they are interconnected (Yamamoto et al., 2005). These growth factors were therefore added in combination to investigate how they might interact with each other *in vivo*. Combining HGF, FGF and TGF-β2 resulted in a CLAN incidence significantly lower than TGF-β2 could evoke when added alone. This may indicate that HGF and FGF interfere with TGF-β2 in some manner. The exact manner of this is unknown; because the growth factors do not compete for receptors (may be some non-specific overlap) the inhibitory action must be via another mechanism. Lu et al demonstrated that TGF-β2 could block FGF induced proliferation in corneal endothelium (Lu et al., 2006) while Kroening et al showed (Kroening et al., 2009) CTGF was influenced by HGF. A similar interaction may be taking place in the mix of growth factors under investigation. Alternatively it may be that the balance of growth factors is inducing a specific cell function that favours straight stress fibres. Growth factors are known to alter the actin cytoskeleton (Ridley and Hall, 1992) and the specific balance needed for CLANs may not be met under these circumstances as the signal for straight stress fibres over rides the TGF-β2 signal for CLANs.

This raises an important question as to how TGF-β2 causes CLANs *in vivo*. This work has provided evidence that the main CLAN inducing agent present in AH is TGF-β2. Until other growth factors and constituents of AH are explored it is difficult to claim it is the sole CLAN-producing agent present. However, no literature has shown that TGF-β2 level in AH increases with age although various pathologies which are associated

with ageing, such as cataracts, may alter the growth factor balance. The influence of glaucoma on the presence of CLANs in the TM has already been established; in the next chapter the influence of donor age on CLAN formation is explored both *ex vivo* and in relation to the presence of TGF-β2 *in vitro*.

6 Can donor Age influence CLAN incidence?

This aspect of the research focused on CLAN incidence in relation to donor age and was investigated using *ex vivo* and *in vitro* techniques.

6.1 In vitro experiments

HTM cells from multiple donors of different ages were examined via microscopy following 7 days exposure to control conditions (incubated with maintenance medium) or treatment conditions in the presence of 2ng/ml TGF-β2. HTM cells established from different donors exhibited different cell morphologies and culture patterns under control conditions (this observation was addressed in detail in chapter 4). Cell morphology at the end of the experimentation period was compared to cultures prior to experimentation and revealed no visible alterations in phenotype throughout the 7 day period.

CLAN incidence in most cultures was low, ranging from less than 1% to 10%, with the exception of 2 cultures in which incidence reached 14% (23 year old) and 24% (2 year old). Plotting CLAN incidence against the age of the donor showed no significant change with increasing age, however, there does appear to be a slight decrease but this was not strongly correlated R^2=0.16 (Figure 6-1). For further analysis the donors were divided into two groups; young donors and old donors. Only 2 donors fell between 10 years and 50 years, and for the purpose of this analysis they were removed from both groups as their presence was not sufficient to change the statistical analysis in either group. When values were compared there was no statistically significant change in CLAN incidence between young and old groups p=0.157.

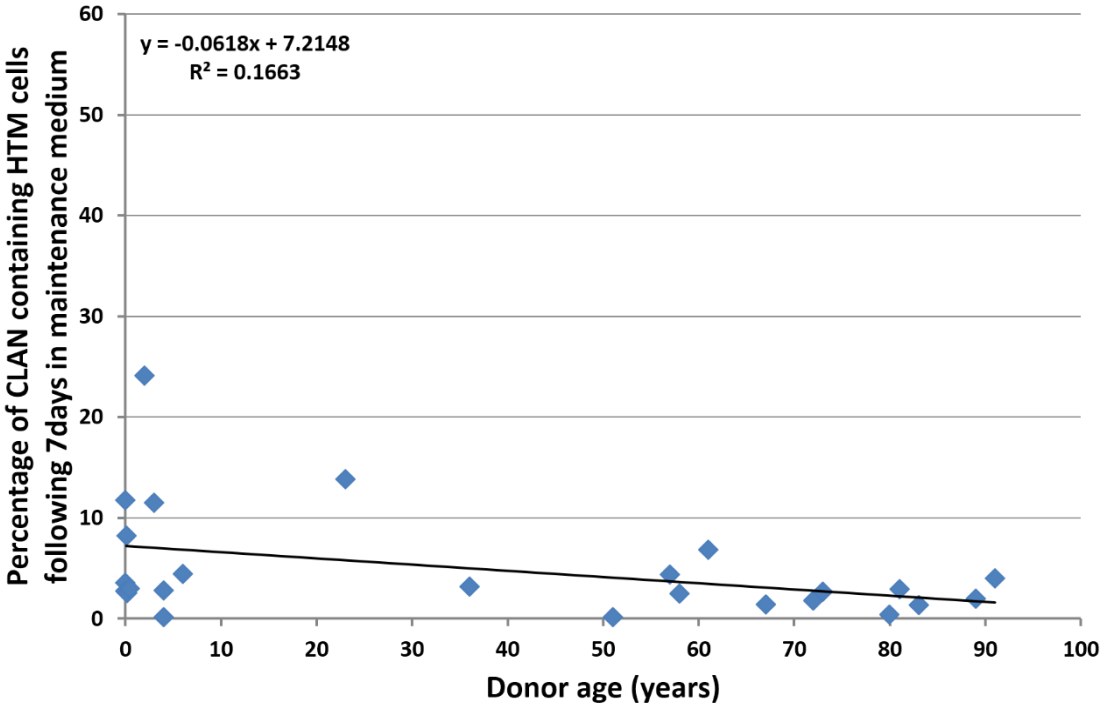

Figure 6-1. CLAN incidence in HTM cells treated for 7 days in maintenance medium.

Scatter plot illustrating the percentage of CLAN containing HTM cells in cultures incubated with maintenance medium for 7 days. CLAN incidence appears relatively stable over the age range available although there does appear to be a slight decrease with increasing age. Each point is the average values obtained from 10 fields of view where n=2. The black line is the linear regression.

Unlike control conditions, HTM cells incubated in the presence of 2ng/ml TGF-β2 were found to have an altered phenotype at the end of the 7 day treatment period with cells becoming more epithelioid. Although this shape change was previously observed with BTM cells, the changes in HTM cells were not uniform. Figure 6-2 provides some examples of HTM cells following 7 days with maintenance medium or in the presence of TGF-β2. The shape change which occurred was not present in all HTM cultures and the extent of the alteration was also found to vary between donors.

TGF-β2 also influenced the cytoskeleton, resulting in an increase in the percentage of CLAN containing cells in all donors to a greater or lesser extent with values ranging from 9% to almost 40%. On first glance of data shown in Figure 6-3a it would seem that no strong correlation could be detected between CLAN incidence and increasing donor age (R^2= 0.1137). Values were found to fluctuate between donors but some values did not follow the general trend of the age cluster providing drastically different values and so they were removed as out layers. Having removed the out layers the strength of the correlation was increased (R^2=0.49), as shown in Figure 6-3b, indicating that CLAN incidence may increase with increasing donor age. As before, results were divided into young and old groups and examined minus the out layers. By doing so it was found that the percentage of CLAN containing cells in old donors was significantly higher than younger donors p=0.03.

Caution must be applied when considering ageing and using primary cultures. This is especially important when using cells such as the TM cells which have very low proliferation rates *in vivo*. While care has been taken to try and reduce the number of cell divisions experienced during experimentation, the number of cell divisions that the cells undergo even during one passage is much higher that they would ever undergo *in vivo*. This will infer stress that would not have been present normally and could artificial age cells.

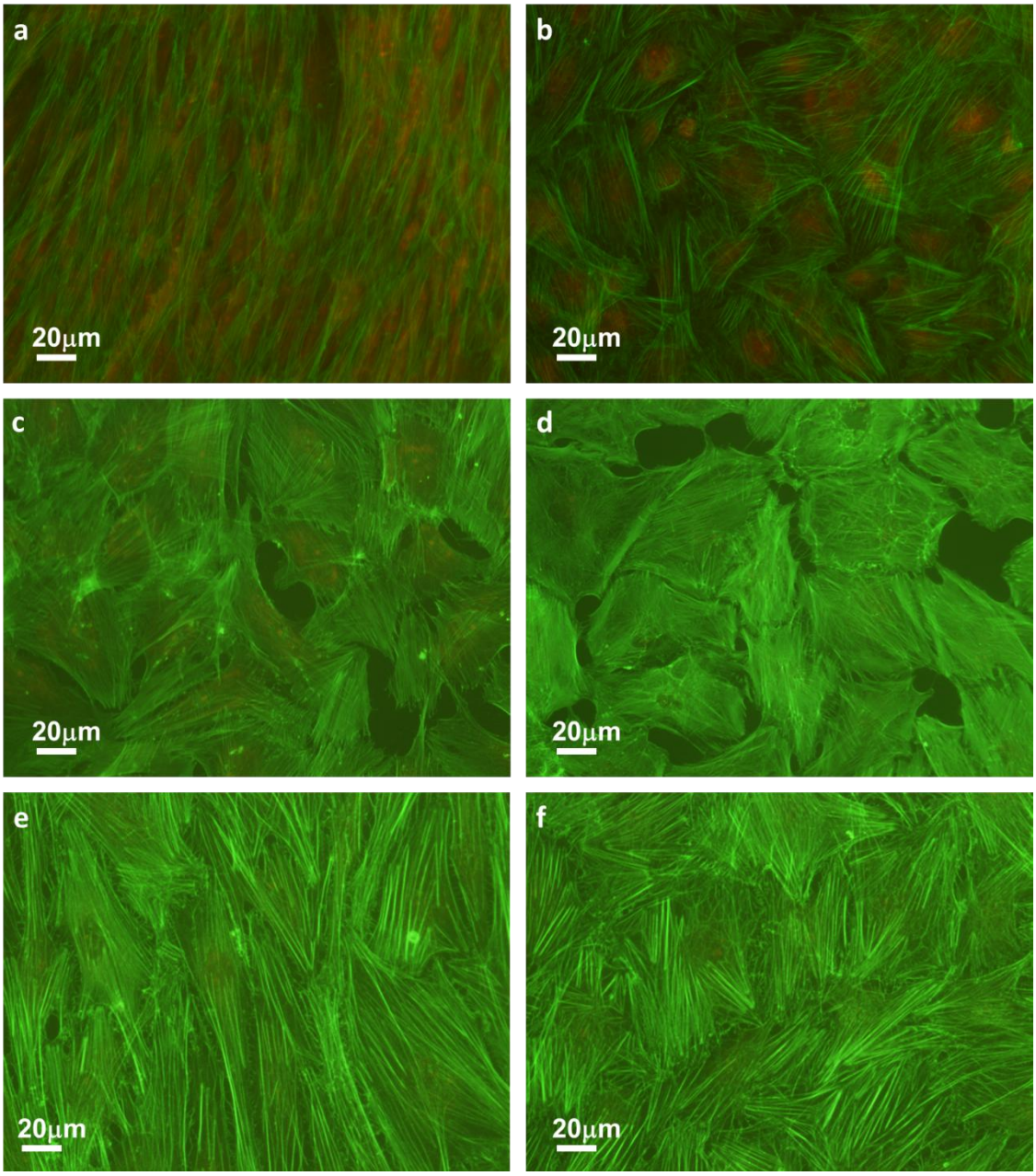

Figure 6-2. Cell shape change in HTM cells with TGF-β2 treatment.

Fluorescent images showing the cell morphology of HTM cells from donors: 010 (a&b), 027 (c&d) and 033 (e&f). Cells in images a,c and e were incubated for 7 days in maintenance medium while those in images b, d and f were treated with 2ng/ml TGF-β2 for 7 days. The most obvious change in shape is between a&b. In images c and d, cells were quite epithelial under control conditions and so little shape difference is observed but the actin arrangements are greatly altered. In the final pair of images the cells show almost no change in shape or actin arrangement.

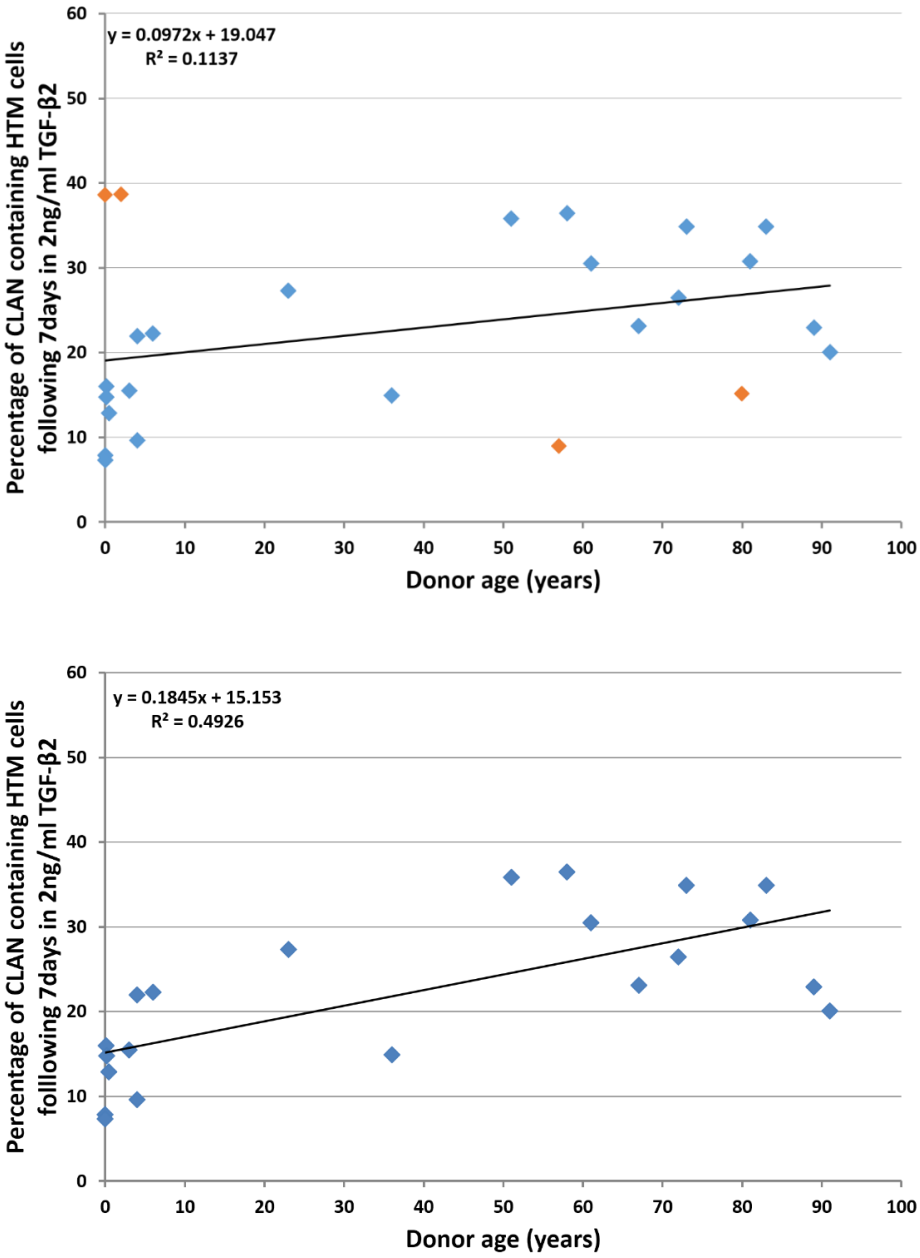

Figure 6-3. The percentage of CLAN containing HTM cells following 7 days incubation in the presence of 2ng/ml TGF-β2.

Both scatter plots illustrate the percentage of CLAN containing HTM cells with TGF-β2 treatment. The top figure shows the CLAN incidence for all 26 donors across the age range, demonstrating a poor linear relationship. The red points are those results which were considered to be out layers and have been removed to produce the bottom scatter plot. With the 4 out layers removed the linear relationship is much stronger (R=0.49) which would suggest that the percentage of CLAN containing HTM cells does increase with age. Coloured points are averaged values where n=2, red points highlight out layers which have been removed for figure b.

As treatment with TGF-β2 produced an increase in CLAN incidence in all donors examined, the percentage to which CLANs could be induced was examined. The data revealed positive correlation between the percentage of CLAN induction and donor age registering an R^2 value of 0.58, as demonstrated in Figure 6-4. Clustering of the data was observed as the values from the older donors did not overlap with the values from the younger donors. Statistical analysis confirmed that the percentage of CLAN induction between the groups was different p=0.009. As stated previously, only 2 donors fell between the ages of 10 and 50 years and so were not considered in earlier evaluations. The current scatter plot provided justification for this decision as both values fell between the clusters.

It would seem from the observations that treatment with TGF-β2 was capable of inducing CLAN formation which was accompanied by a change in cell shape. In experiments lead by Prof. Grierson, BTM cells were categorised following treatment with either DEX or TGF-β2 into each of the three shape categories identified in chapter 4. The fluorescent images of these cells were then used to assign actin staining as either stress fibre or CLAN providing the data in Figure 6-5. From the observations it was clear that CLANs were more common in cells with an epithelioid shape, while spindle cells were more likely to have a stress fibres only pattern.

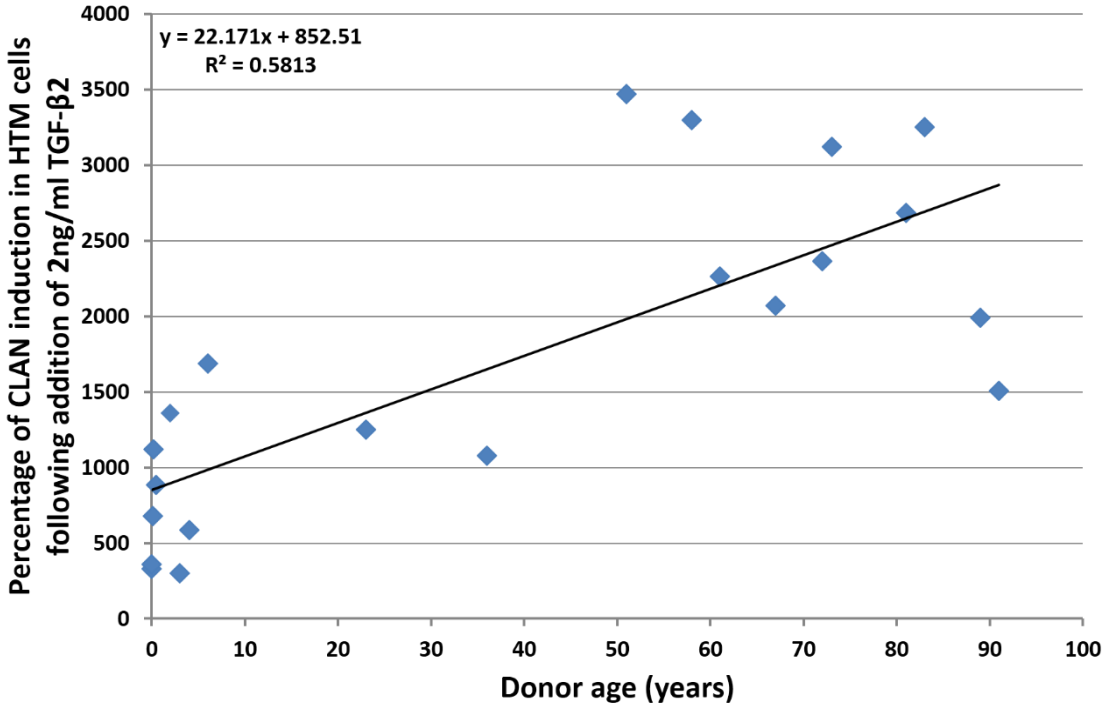

Figure 6-4. Scatter plot of CLAN induction in HTM cells compared to donor age.

The percentage of CLAN induction following 7 days treatment with TGF-β2 compared to control with maintenance medium only revealed a positive linear correlation with an R^2 value of 0.58. This would suggest that HTM cells established from older donors were more susceptible to CLAN induction by treatment with TGF-β2. It is also clear from this scatter plot that there are two distinct clusters with limited overlap. Cells from older donors had a greater percentage of CLAN induction than any of the younger donors. As a group older donors had a significantly higher level of induction than young donors (p=0.009) coloured points are the percentage induction observed by comparing CLAN incidence in control conditions compared to incidence following treatment with TGF-β2. Black line is the linear trend line.

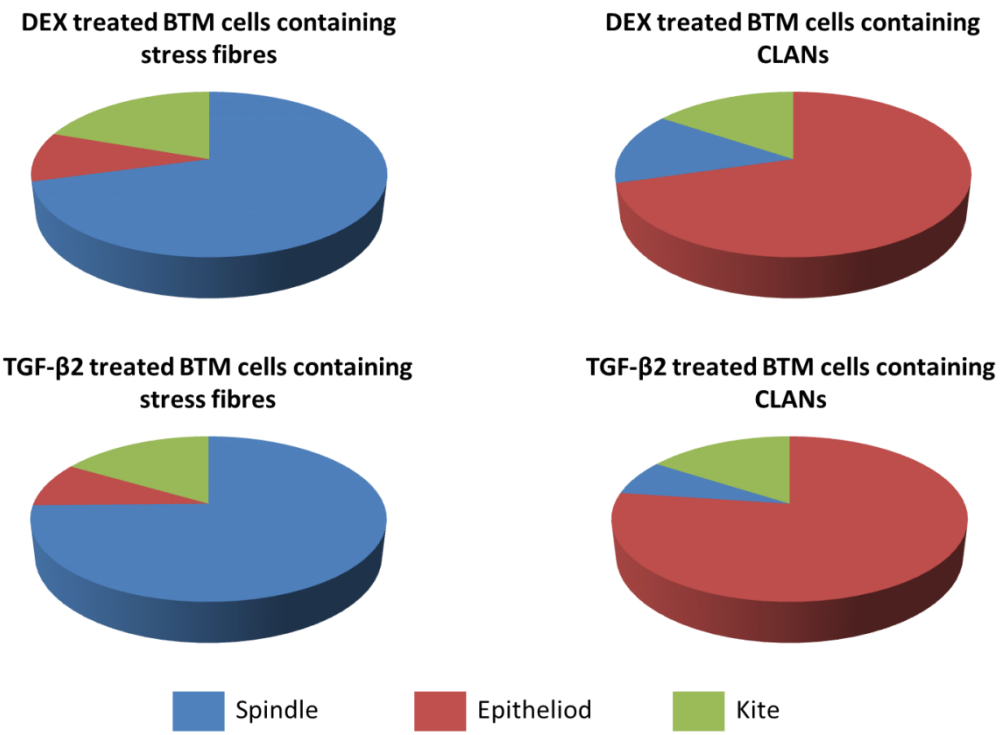

	Cell shape		
	Epitheliod	Spindle	Kite
DEX treated BTM cells containing stress fibre	9.7	70.7	19.6
DEX treated BTM cells containing CLAN	70.4	14.1	15.5
TGF-β2 treated BTM cells containing stress fibre	8.8	74.7	16.5
TGF-β2 treated BTM cells containing CLAN	77.2	7	15.8

Figure 6-5. BTM cell shape and the incidence of CLANs.

The pie charts show that cell shape could be linked to the cytoskeletal arrangement it contained. Stress fibres were more likely to occur in spindle cells while CLANs were most often identified in epithelioid cells. The shift in cell shape from epithelioid to spindle is almost identical ranging from 70-77% while the number of cells classified as kite shaped remains below 20% regardless of cytoskeletal organisation.

6.2 Ex Vivo experiments

Following processing samples of TM tissue obtained from human globes were visualised using confocal microscopy. CLANs had already been identified in TM tissue via this method (Hoare et al., 2009) and we wished to increase the cohort to incorporate a wider age range.

6.2.1 TM Tissue morphology

The flow of AH through the TM is reported as not being uniform around its circumference, (Hann et al., 2005) and so there may be the potential for variation in structure across the TM. As only a portion of the TM was to be examined preliminary work was undertaken by Emma Knight to study CLAN incidence from each dissected quadrant. A number of globes were used in the pilot work and counts carried out in a masked fashion by Emma Knight. The data relating to one globe can be seen in Table 6-1 and demonstrates that the number of CLANs in each quadrant was remarkably similar. The number of nuclei which we took to be an indication of cell numbers (assuming one nucleus per cell), however, was more variable with the highest nuclear count in the inferior quadrant (214) and the lowest in the nasal quadrant. Even so the CLAN/nuclei ratio was reasonably consistent from quadrant to quadrant.

Table 6-1. Variation of CLAN incidence in different quadrants of TM from human globes.

Data generated by Emma Knight revealed that the incidence of CLANs was reasonably consistent between quadrants of the same globe with only minor differences. There was some variation in the number of nuclei counted with the highest values obtained in the inferior quadrant. This data has been collected from counts carried out on one globe.

Quadrant	Total number of CLANs	Total number of nuclei	CLANs per nuclei
superior	155	184	0.84
Inferior	173	214	0.81
Nasal	169	150	1.13
Temporal	161	211	0.76

The previously published technique employed to retrieve the TM was found to produce samples with a suitable depth of TM tissue for analysis without major disruption to the internal structure (Hoare et al., 2009). Several samples also spanned from the epithelial cells of the transition zone to the ciliary muscles (Figure 6-6). While these regions could be used for orientation purposes, care was taken not to obtain images from within these regions as the morphology did not match that of the TM and could bias data. The staining pattern in the transition region revealed actin was most dense around the periphery of the cells which were clearly epithelioid in shape (Figure 6-7). At times it appeared that there were many CLANs present within this region as the actin was highly branched, however, upon closer inspection the spokes were found not to be straight and there were no hub points visible. The muscle area of the tissue was very brightly stained and dominated by straight bundles of actin inserting into the meshwork (Figure 6-8).

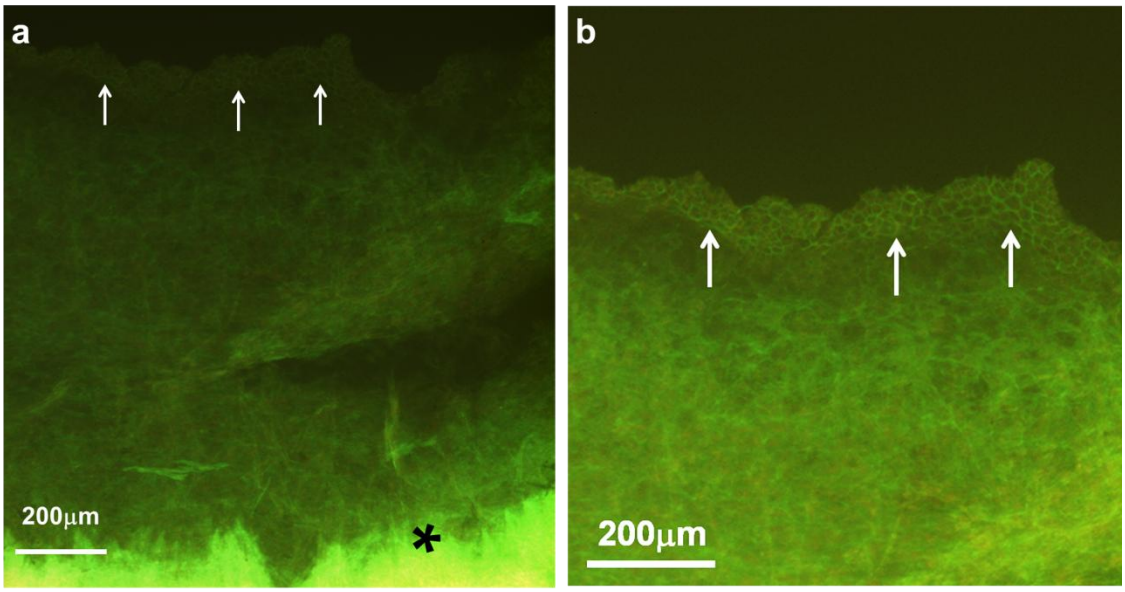

Figure 6-6. Fluorescent image of the tissue removed from human globe spanning from the transition zone to the ciliary muscle.

The process of peeling away the meshwork produced segments with varying degrees of TM tissue and different regions. In the sample above the transition zone has been indicated by the arrows. The epithelioid shape of the cells in this area is visible in the image b. The tangled web of the trabecular meshwork connects the epithelioid cells with the brightly stained smooth muscle (indicated by the asterisk) in image a.

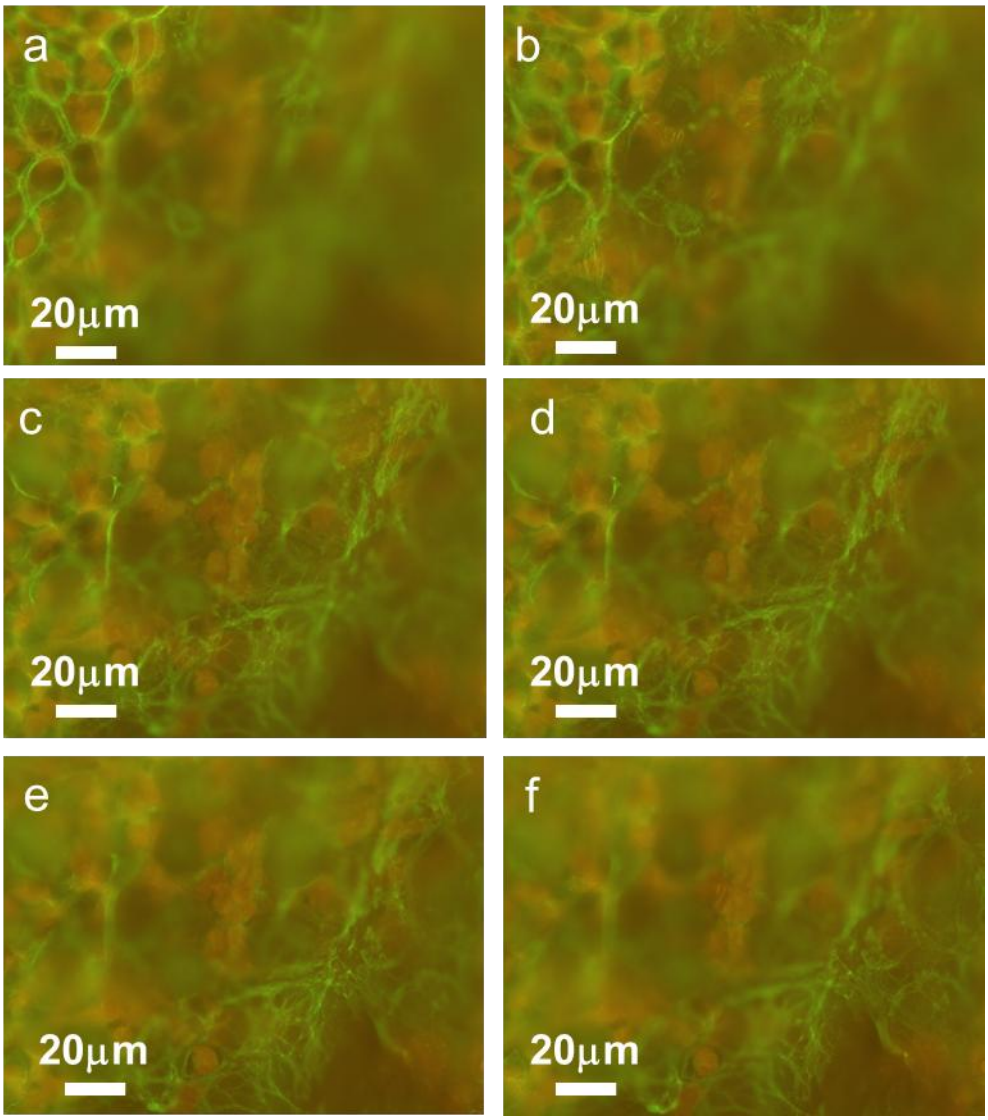

Figure 6-7. Fluorescent images of phalloidin stained tissue through the transition zone.

Although this area of tissue was not used for the purposes of counting CLANs, a series of images were collected via conventional fluorescence microscopy prior to examination via confocal microscopy. The epithelial cells seen in image a. have dense actin staining around the periphery of the cells. As the plane of focus moves the epithelial actin pattern becomes less obvious until the actin is more branched. The branches seen in this area are not the straight actin spokes associated with CLANs.

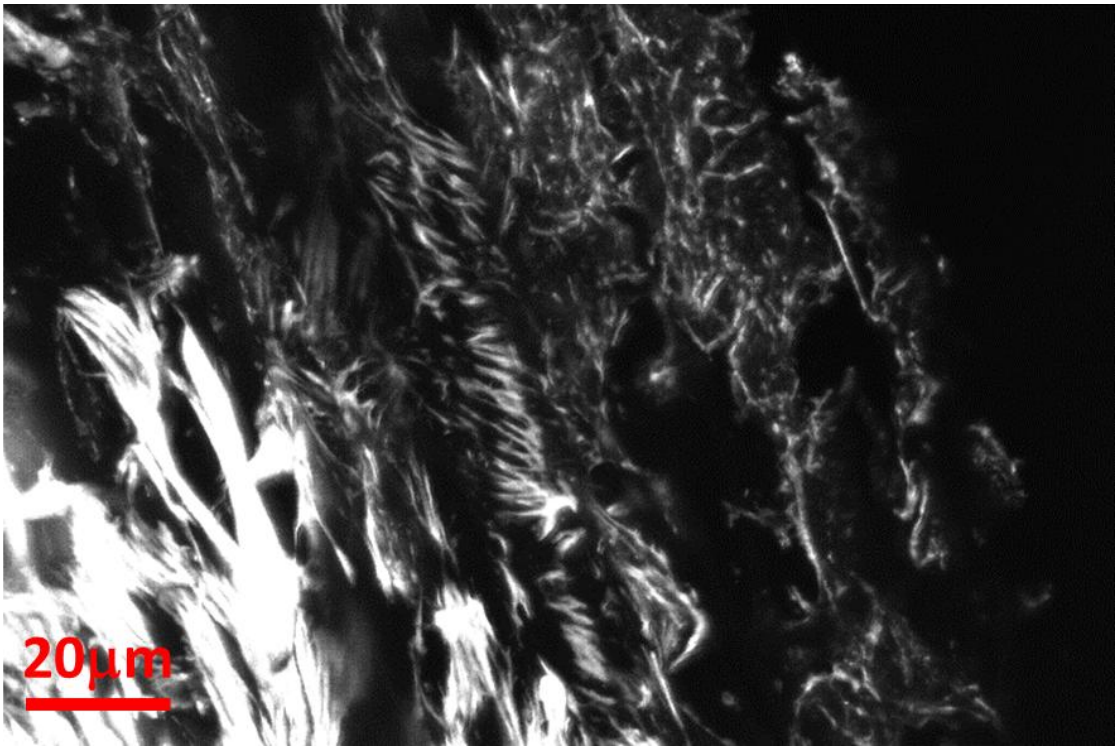

Figure 6-8. Confocal image of TM tissue with saturated staining of smooth muscle.

This confocal image demonstrates the actin staining observed in TM tissue removed from a human globe and stained with phalloidin. The over saturated staining in the bottom left hand corner is smooth muscle which is visible as very straight thick bundles. The actin staining in the tissue around these bundles was also rather straight.

The dissection method did not separate the different layers of the meshwork and while in most sections the uveal and corneoscleral layers of the TM were clearly evident the quantity of the uveal meshwork was variable and there was little evidence of the JCT region. The uveal region of the TM was clearly recognisable as the cellular actin staining was sparse and the trabecular beams were clear due to auto-fluorescence from the collagen beams. This provided a clear image of the trabecular beams and as seen in Figure 6-9 the large intra-trabecular spaces can be identified. Further into the tissue the beams were still visible but the spaces became smaller and the actin staining in the surrounding TM cells became more intense. The clear beams gave way to a more complicated and congested pattern in which pores (Figure 6-10) were observed and depending on the orientation of the tissue the sheets of corneoscleral TM were observed as thin rows of staining (Figure 6-11).

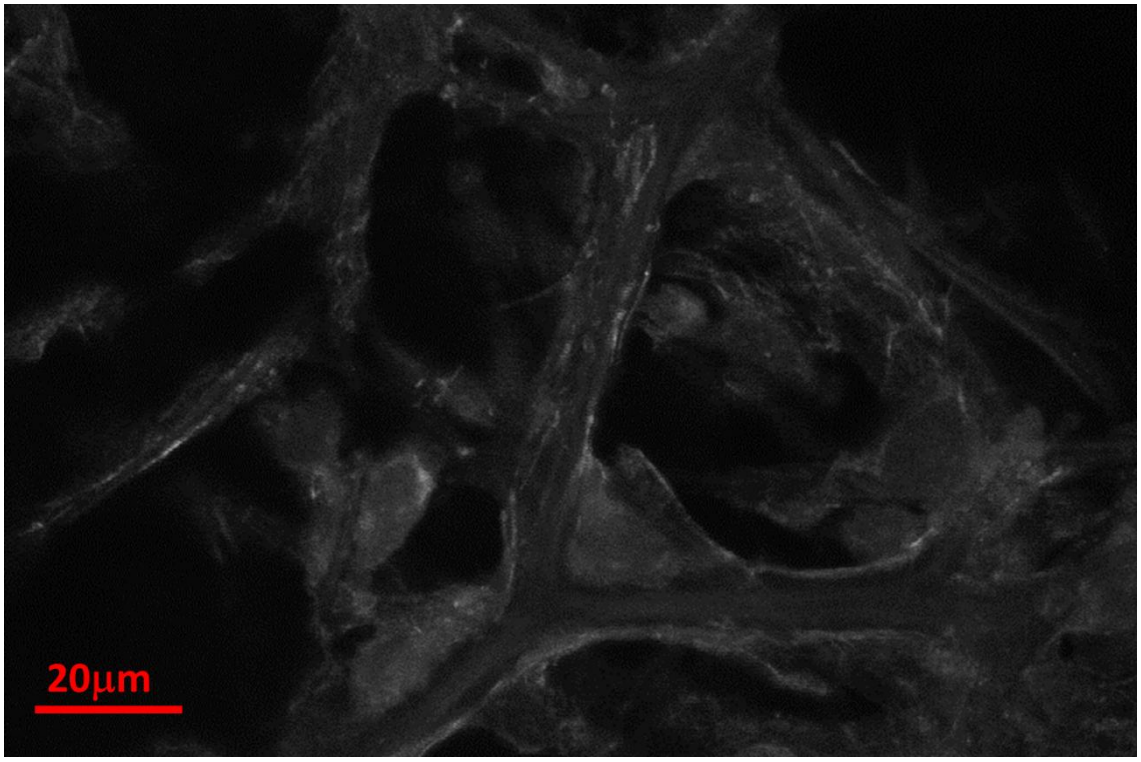

Figure 6-9. Confocal image of uveal meshwork.

The actin staining in the uveal meshwork was not as intense as in other areas of the TM and may indicate a lesser amount of actin. Bleed through from the PI channel and auto fluorescence of the collagen core has results in the visualisation of the nuclei of TM cells resting on top of the trabecular beams. The large intra-trabecular spaces are also visible.

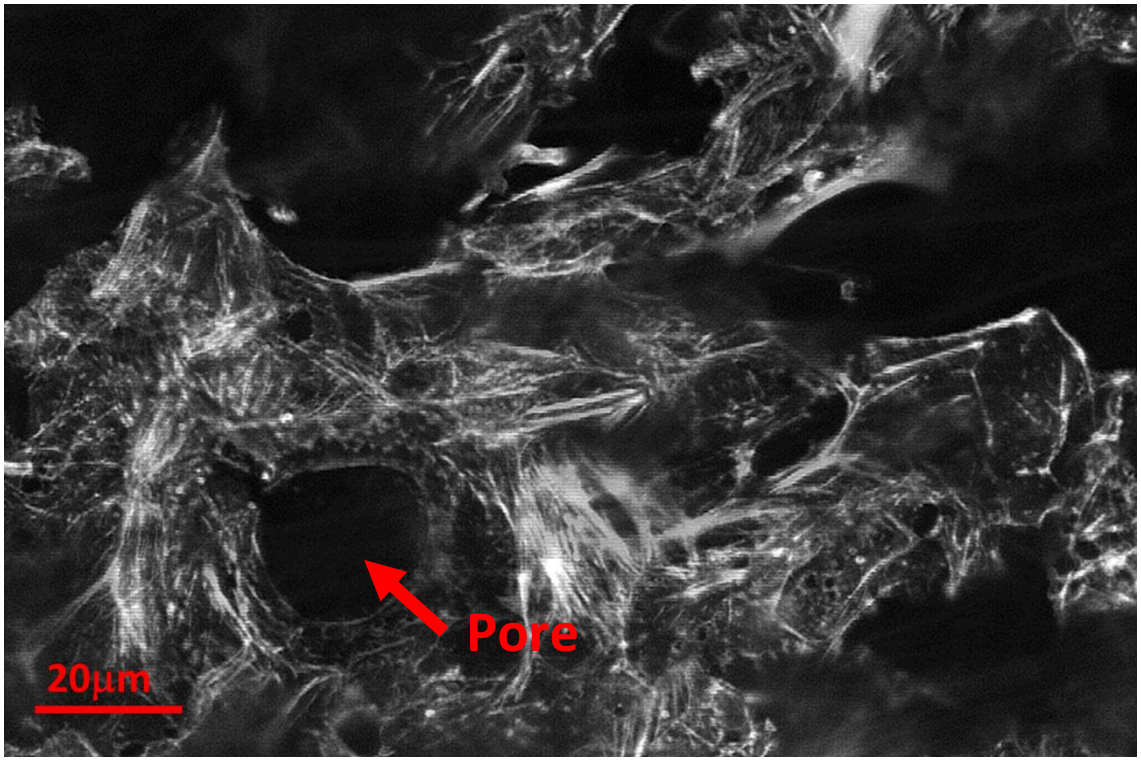

Figure 6-10. Confocal image of the corneoscleral region of the TM.

As the structure of the meshwork changes the level of actin staining increases so that in the corneoscleral region the phalloidin staining is more intense. The actin pattern is more complicated and congested than the uveal. The corneoscleral region of the TM is plate like with fluid flowing through pores like that highlighted by the arrow.

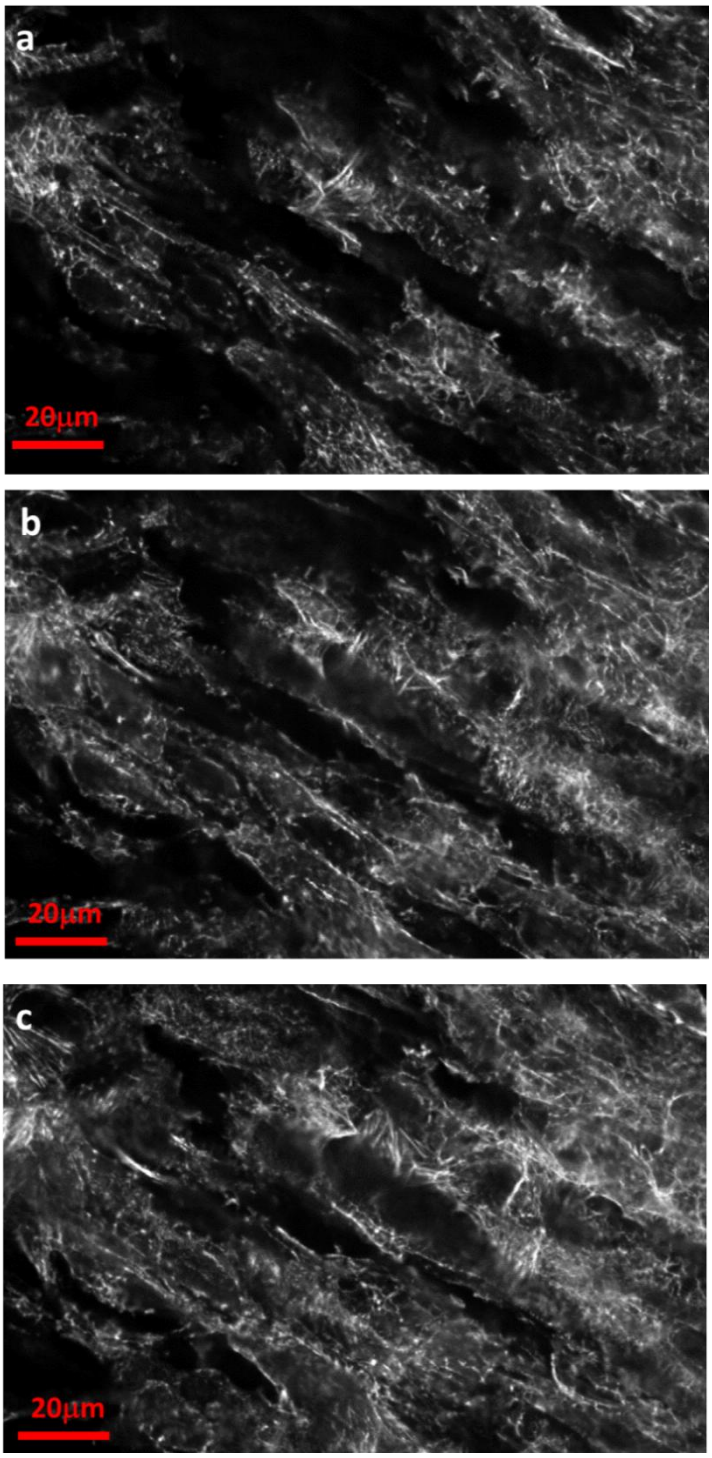

Figure 6-11. Confocal image of corneoscleral sheets.

The sheet-like orientation of the corneoscleral region of the TM is seen in these 3 consecutive images looking through the TM tissue in a flat mount. The flat plate-like structures are stacked on top of one another and orientated away from the viewer. As the view moves deeper within the tissue the actin orientation becomes more dense and complex.

6.2.2 CLAN incidence *Ex Vivo*

Identifying CLANs in the complete architecture of the TM tissue was time consuming as the 3 dimensional nature of the TM meant that at times the full hub and spoke arrangement was not clear in one image of a z-series. Examination of each section revealed the presence of a CLAN that could be linked with hubs and spokes to sections immediately before and/or after. It was found that most CLANs identified spanned 2-3 sections, representing 2-3µm of tissue and were highly variable in shape and size in both planes of view. As shown in Figure 6-12 a complete CLAN is clearly visible when multiple sections were merged.

The images collected from the PI channel were used to count the number of nuclei in each area of tissue available (one nuclei was taken to represent one cell). As can be seen in Figure 6-13, the average number of nuclei decreased with increasing donor age resulting in an R^2 value of 0.6289.

CLANs were identified by mapping their position through the various z-series sections in each area so that one CLAN may occupy multiple sections. In order to account for age-related loss of TM cells and variation in the tissue samples the incidence of CLANs was expressed as a percentage of the total number of nuclei (cells) counted. When expressed as a percentage of the cell population there was positive linear correlation with age (R^2=0.588) showing that CLAN incidence in older tissue tended to be higher than in tissue from younger donors.

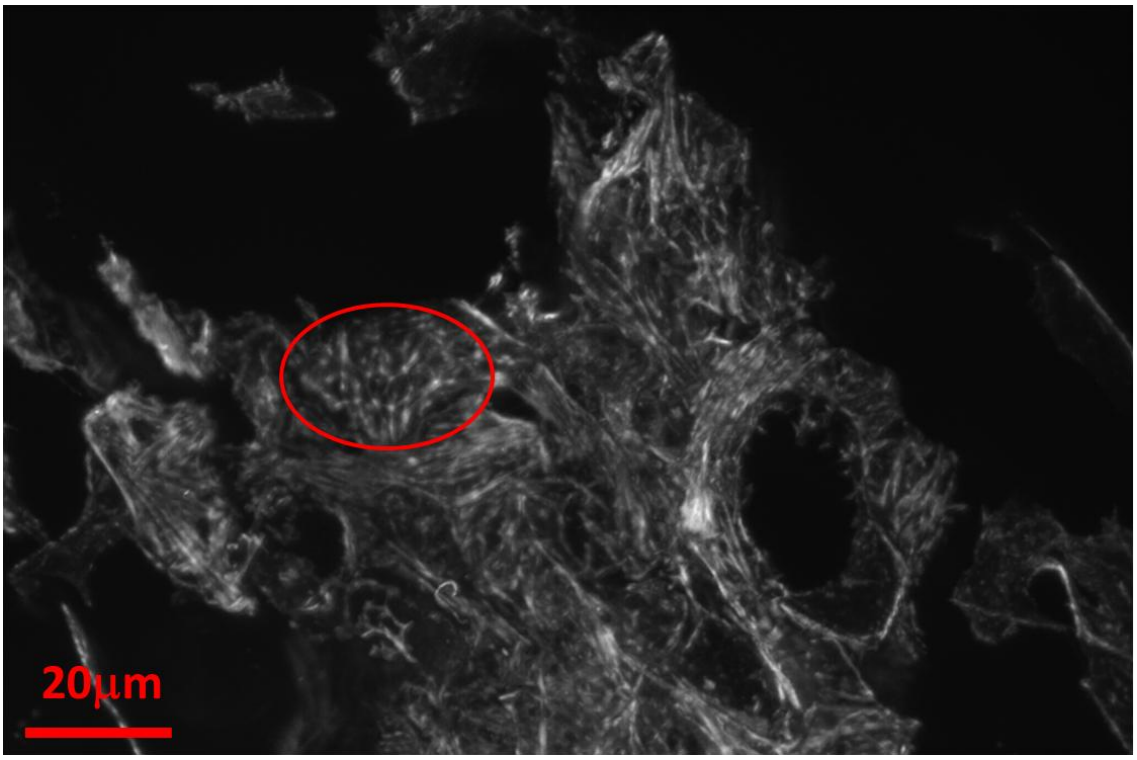

Figure 6-12. Example of a CLAN identified in human TM tissue.

This is an image of human TM tissue captured via confocal microscopy (x60 objective) with fluorescent labelling of actin with Alexa-phalloidin 488. The image has been created by merging 4 separate sequential images of a z-series. The complex nature of the meshwork is clearly visible and the red circle identifies a CLAN with brightly stained hub points.

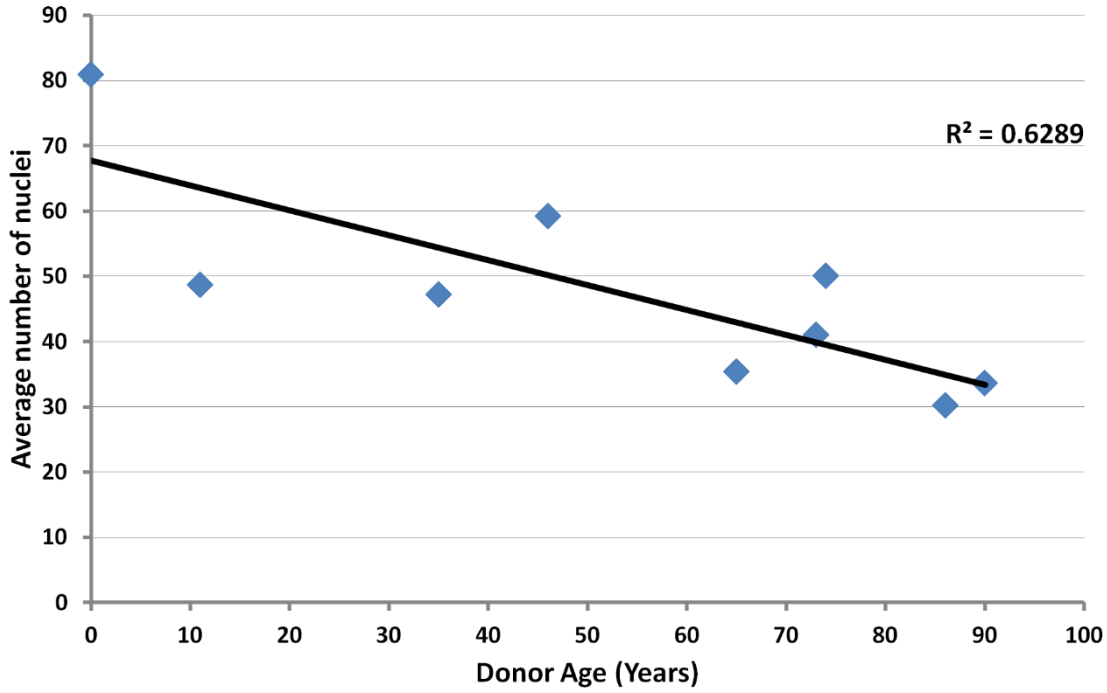

Figure 6-13. Scatter plot showing the average number of nuclei in TM tissue plotted against donor age.

The number of nuclei is seen to decrease with increasing donor age with an R2 value of 0.6289. At 0 years the average number of nuclei counted in the areas analysed was 80 while at around 90 years old, representing our oldest donors, this value had decreased to below 40. Coloured points are the averaged values taken from 20 fields of view.

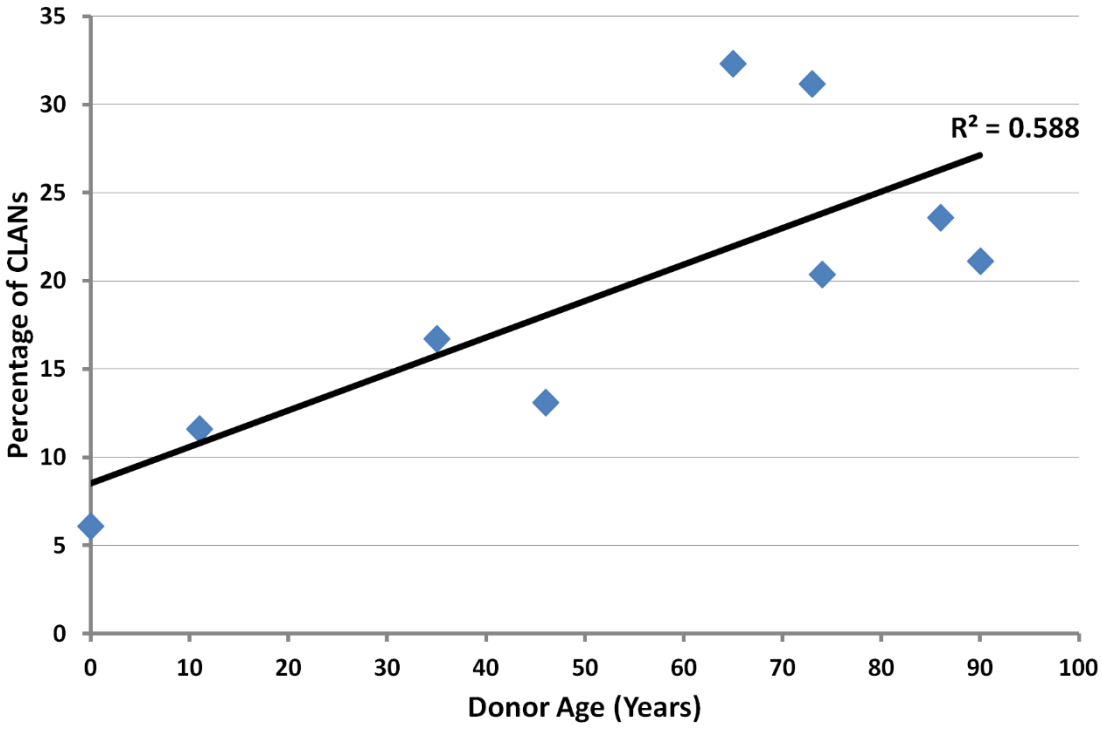

Figure 6-14. Scatter plot showing the average number of CLANs in TM tissue plotted against donor age.

Plotting the percentage of CLANs identified against donor age revealed a strong positive linear correlation R^2=0.588. With increasing donor age there was an increase in the percentage of CLANs identified. Coloured points represent the average values taken from 20 separate areas across the TM tissue available.

Morphological comparison of TM tissue from young and old donors (Figure 6-15) appeared to highlight the differences expressed in graphical form above. Images a & b represent the youngest donor and are noticeably different from images c and d simply by the level of staining present. In image a. there is a lot of phalloidin staining with very little open spaces. The actin itself also appears thin and delicate in comparison to image c, where the phalloidin staining from 90 years old donor appears to be fused into thicker bundles. The numbers of nuclei are also visibly different with counts from image b (young) proving difficult due to overlapping nuclei compared to the sparse arrangement seen in figure d.

The data from this work was applied alongside the previously published data of Hoare et el and is shown in Figure 6-16 (Hoare et al., 2009). It would appear that in the previous study the number of CLANs counted was much higher, so that the values from both studies do not seem to be comparable. In order to test the validity of this difference, the images from a healthy donor used in the previous study were re-evaluated and revealed a final value half that reported in the earlier study. An adjustment was applied to the current data and in doing so brought the values in line with those previously published. As shown in the lower scatter plot of Figure 6-16 values in both studies were now comparable within the older donors and appeared to link well with the slope of the points.

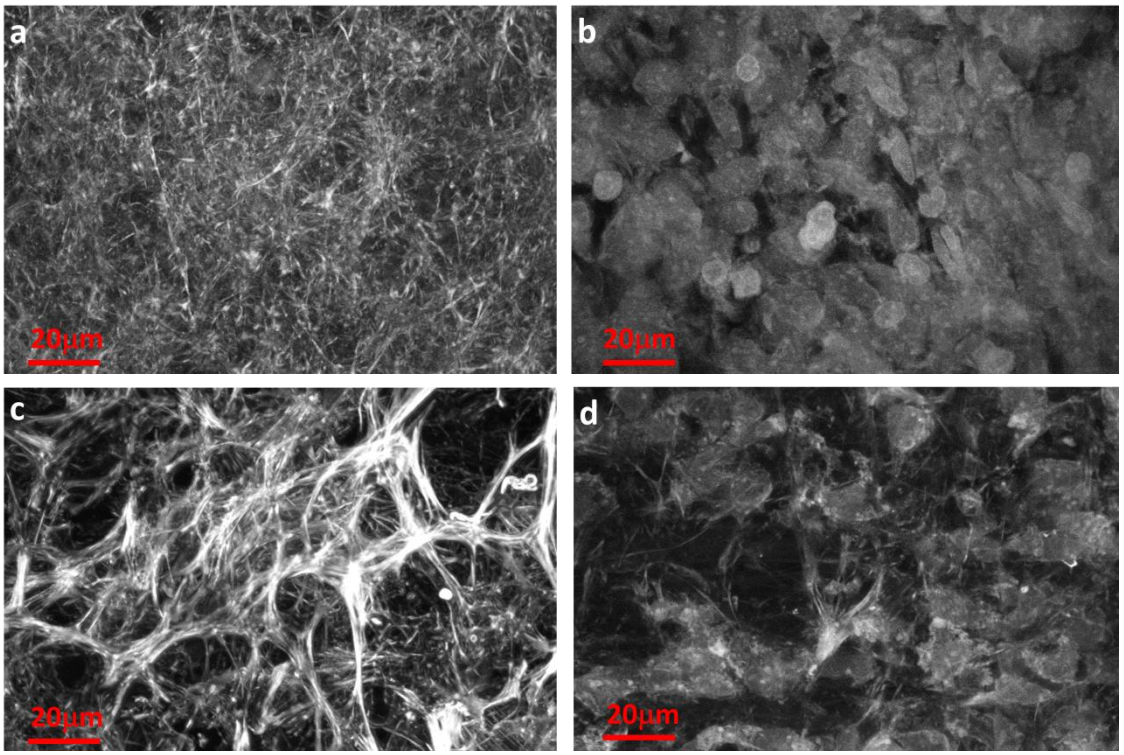

Figure 6-15. Confocal images comparing the actin and nuclei staining in young and old TM tissue.

Images a & b are merged confocal images taken from the TM tissue of our youngest donor. In image a, the fine actin fills the field of view in a complex array of fibres, while image b is the nuclei associated with the tissue. The field of view contains many nuclei, some of which are over lapping. In contrast images c & d are taken from TM tissue of the oldest donor in the cohort. The actin staining in image c forms much thicker bundles than any observed in image a and the number of nuclei present in image d is also visibly less than in image b.

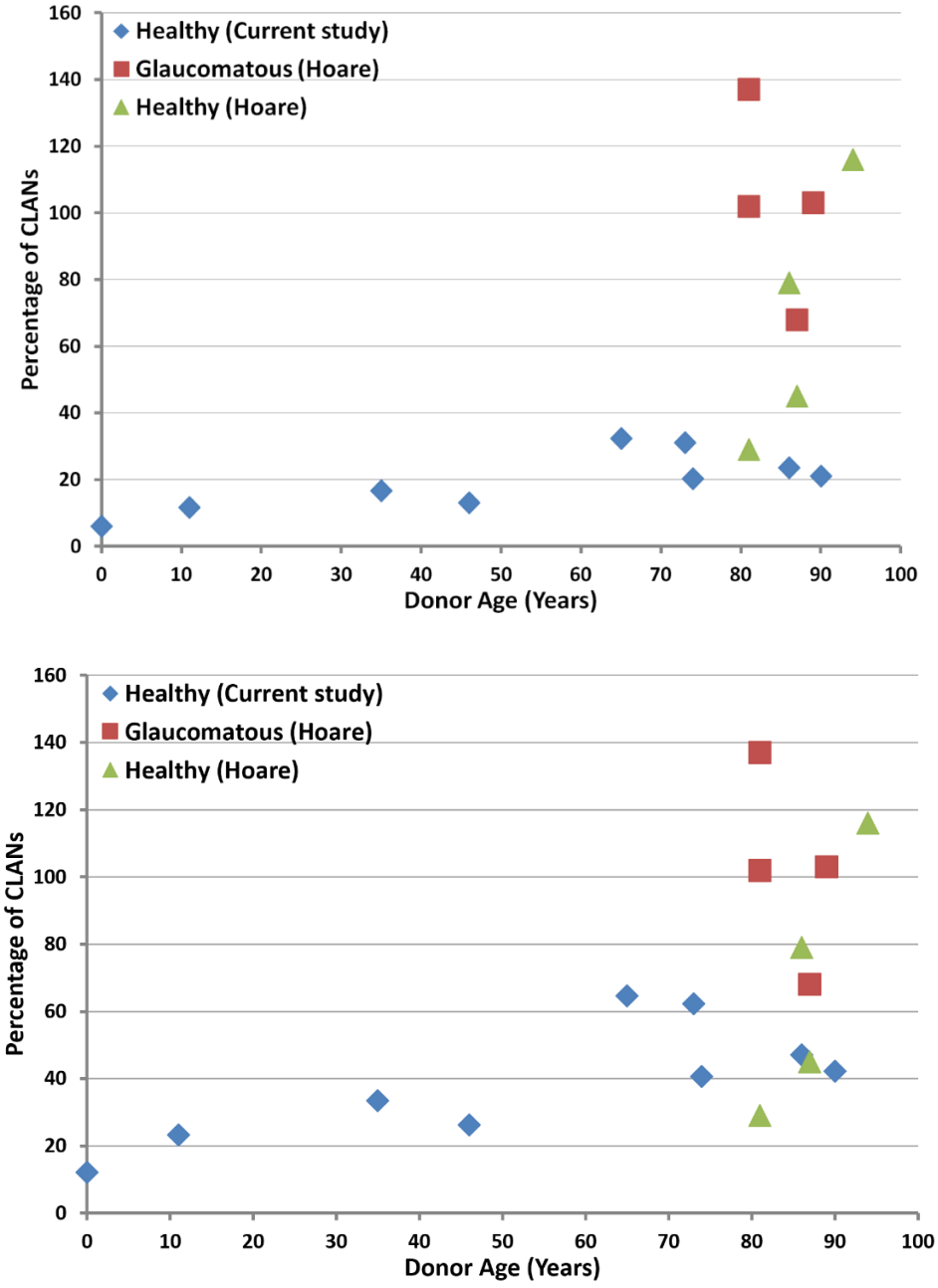

Figure 6-16. Scatter plots of CLANs in donors from the current study and published work of Hoare et al. (Hoare et al., 2009).

Both scatter plots represent the percentage of CLANs counted in relation to donor age from the current study alongside the previously published data of Hoare. In the top plot the values of the current work are much less than in the previous study. In the second plot the values from the current work have been adjusted based on re-evaluation of previous data. Values in older healthy donors are now comparable and demonstrate a linear correlation with increase donor age (R^2=0.4).

6.2.3 Analysis of CLANs

During data collection it was noted that CLANs were not of uniform size. Given this degree of variability it was questioned whether investigating the size of the CLANs present and the total area in which they were present would vary with age. Average CLAN area ranged from 350μm^2 to 780 μm^2 but had no striking relationship to donor age. The area of each CLAN in a z-series were added together to produce the area of tissue in which CLANs were present. This was then taken as a percentage of the total area of the field of view. This analysis was only possible in the plane of images and not through the z-plane as we could not track the CLANs in this dimension. The percentage of tissue taken up by CLANs was found to range from 10-25%, but again was not correlated with donor age (Figure 6-17).

The previously used method of image analysis was applied to CLANs in tissue and by comparing these values to those obtained *in vitro* it was discovered that CLANs observed in organised tissue and in TM cells *in vitro* were similar. There was some difference in the overall area, with CLANs formed *in vitro* seemingly larger than those *ex vivo* (Table 6-2). The basic components of the structure were found to correlate well together, as the number of hubs and spokes and the spokes per hub were almost identical. The only difference was that spoke length *ex vivo* (3.8μm) was slightly shorter than the measurements obtained *in vitro (6μm)*.

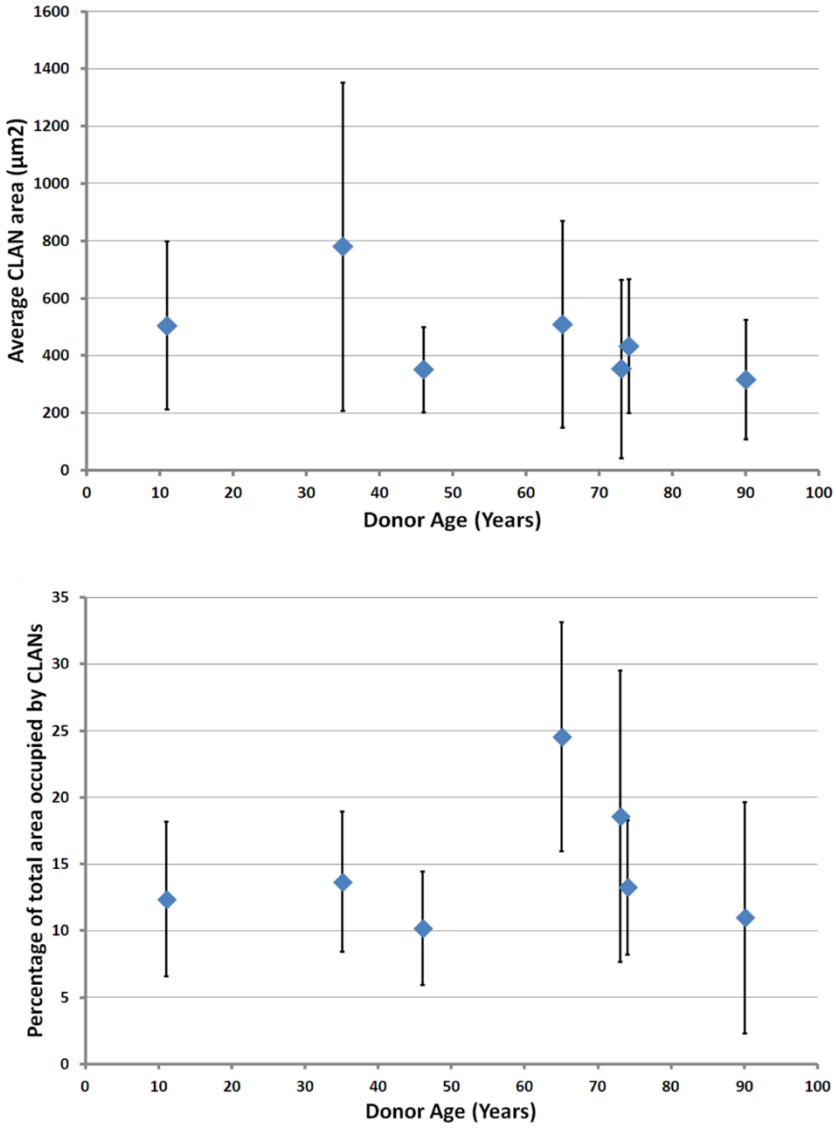

Figure 6-17. Average CLAN area and total area containing CLANs plotted against donor age.

Together these scatter plots provide information on the size of the individual CLANs present in the TM tissue and also to what extent the TM tissue is occupied by CLANs. The Top scatter plot demonstrates the average area of individual CLANs in TM tissue. The average CLAN area ranged from 350-780μm^2 demonstrating some degree of linear correlation associated with donor age (R^2=0.31). The total area of TM tissue occupied by CLANs also demonstrated variation but failed to reveal any correlation with donor age.

Table 6-2. Illustrating the basic measurements of the CLANs observed in the TM tissue ex vivo compared to the in vitro measurements.

Comparison of the various parameters above revealed that the average area of CLANs ex vivo was smaller than those identified in vitro although there was overlap given the variability in CLAN size. The number of hubs and spokes within the CLANs were almost identical as was the incidence of spokes per hub. The length of spokes measured ex vivo was found to be shorter than those in vitro and the overall shape of the CLANs ex vivo were more circular than in vitro.

	Ex Vivo		In Vitro	
	Average	SD	Average	SD
CLAN area (µm2)	471.70	151.78	784.67	271.86
Hub number	27.60	7.56	28.50	11.56
Spoke number	47.10	14.70	55.00	25.73
Spoke per hub	3.60	0.80	3.90	0.36
Spoke length (µm)	3.84	0.96	6.04	0.99
Circularity	0.65	0.15	0.49	0.14

6.3 Discussion

The identification of CLANs in TM cells from human (Clark et al., 1994; O'Reilly et al., 2011) and bovine species (Wade et al., 2009) as well as in TM tissue (Clark et al., 2005; Hoare et al., 2009; Read et al., 2003) from both normal and glaucomatous donors suggested that these structures could be important in normal and pathological TM but until now the relationship with donor age had not been explored.

6.3.1 In Vitro

In vitro cultures of HTM cells were firstly examined in medium only conditions to investigate whether cells derived from donors of different ages exhibited any differences in morphology or cytoskeletal arrangement. Any differences observed in the current cohort may then be inferred as being an age-related feature of cells. There was minimal variation apart from a small decline in CLAN incidence with increasing donor age but it was not considered strong enough to merit a true pattern. Grouping of donors into old and young revealed there was no statistically significant difference, thus confirming the trend. The age range available included tissue from infants under 1 year old and extended to 91 years old. There is limited literature exploring differences of TM cell *in vitro* that have been derived from different donors never mind the potential influence of donor age. Studies using foetal TM cells suggested they make a good model as they have similar ultrastructural features as adults (Lee et al., 2008). It would seem then that the percentage of CLAN containing cells under control conditions at least is influenced solely by the *in vitro* environment.

Given that TFG-β2 was shown to induce CLAN formation in earlier experiments it was also utilised here. As before treatment with 2ng/ml TGF-β2 induced CLANs above medium only levels, however, the induction was variable with the percentage of CLAN containing cell ranging from 9% to 40%. CLAN incidence was found to have some correlation with donor age but there were 4 donors in which the percentage of CLANs did not appear to fit with the pattern of the age range. In an attempt to explain these anomalies cultures were re-evaluated morphologically. In 2 young donors (027 aged 5 days and 031 aged 2 years) CLAN incidence was extremely high, some of the highest observed (approximately 39%). Donor 031 (age 2 years) was also identified as having high CLAN incidence in control cultures. Upon closer inspection it was noted that both

cultures contained cells of a predominantly epithelioid nature even in medium only conditions. In some areas of these cultures a cobblestone-like effect was described with the actin localising to the cell periphery as observed in corneal endothelial cells (Gordon, 1990). Contrasting these results were the strangely low CLAN counts obtained in donors 009 and 010 aged 58 and 80 years respectively. The presence of TGF-β2 resulted in values of 9%, when the same treatment in most other older donors had produced values of 20-37%. Morphological inspection of these cells noted that while they were epithelioid in the presence of TGF-β2, the cells were very spindle shaped and highly aligned in medium only cultures. Even with the TGF-β2 induced change in cell shape the main cytoskeletal arrangement was straight stress fibres. During the re-evaluation of HTM cell shape it was noted that the only other culture above infancy to be reported as highly spindle in medium was 020 aged 36 years. In the presence of TGF-β2 15% of cells were found to contain a CLAN. With donors 009 and 010 excluded this was the lowest CLAN incidence above 10 years old. All other donors above 10 years old were described as being predominantly cigar shaped or epithelioid in medium only conditions.

It has been observed that 3 distinct cell types exist in the outflow pathway; endothelial cells from schlemm's canal, TM cells from the uveal and corneoscleral and TM cells from the cribriform region (Flugel et al., 1991), each with its own primary function (Alvarado et al., 2004). Rohen et al (Rohen et al., 1982) suggested that TM cell cultures derived from explants were likely mainly derived from cribriform layer. If the cells of a particular culture had a different ratio of cell types this might account for some of the difference observed.

Another explanation for the differences observed may be provided by the evaluation of cell shape in relation to donor age. The majority of HTM cells from younger donors were more spindle in shape and could compact close together while cells from older donors tended to be more epithelioid. Experiments using both TGF-β2 and DEX revealed that cell shape is highly indicative of actin arrangement, with epithelioid cells more likely to contain a CLAN.

By removing the 4 out layers based on morphological differences the linear correlation between CLAN incidence and age was much stronger (R^2=0.49). The division of the donors into young and old revealed that in the presence of 2ng/ml TGF-β2 older donors produced significantly more CLANs than younger donors. The increase in the percentage of CLAN containing cells in presence of TGF-β2 was not the only value in which we were interested. It has been stated here that TGF-β2 induced CLAN formation above medium only conditions in all donors regardless of age. When the percentage induction was presented in graphical form it was clear that two distinct groups were visible with young donors having consistently lower CLAN incidence than older donors. The linear regression between donor age and percentage of CLAN induction was 0.58 and when taken together we felt positive that TGF-β2 induces CLAN formation in a greater number of HTM cells from older donors than younger donors. Although this was an extensive study, increasing the number of donors involved may help to cement the trends observed. Special attention to the middle section is most certainly needed, as only 2 donors within the current study fall between 10 and 50 years (23 and 36 years old). Both were closely associated with the much younger donors than the older donors when percentage induction was assessed, however, the percentage of CLAN containing cells in medium and TGF-β2 were variable (donor aged 23 had high CLAN incidence in medium only and TGF-β2 while donor aged 36 had lower than expected values).

As to why HTM cells from older donors are more susceptible to TGF-β2 induction we have examined some of the processes related with ageing in the TM. With increasing age there is a decreased number of TM cells (Alvarado et al., 1981; Grierson and Howes, 1987) which has been attributed to apoptosis (Agarwal et al., 1999; Baleriola et al., 2008; Sibayan et al., 1998). Others have shown that the level of senescence (Liton et al., 2005) is also increased *in vivo*. Increased incidence of senescence and apoptosis are linked to stresses such as ROS. If older cells are already compromised then the addition of TGF-β2 may be sufficient to increase CLAN incidence. In chapter 6 we deal with several age-related changes which have been reported in TM cells, including apoptosis, senescence and ROS.

6.3.2 Ex Vivo

Previously published data from our own group described the identification of CLANs in TM tissue ex vivo (Hoare et al., 2009) and illustrated that the incidence of CLANs in tissue from glaucomatous donors was much higher than values in non-glaucomatous donors. Although only 4 donors were examined in each group, there seemed to be an age-related increase in normal tissue. With this preliminary data and the knowledge that glaucoma is an age-related study we set about the second aspect of this chapter; identifying CLANs in TM tissue from donors of different ages.

During the current analysis it was noted that the technique for removing the TM often provided samples which not only contained meshwork but also the transition zone and muscle fibres from the ciliary muscle inserting into the TM. These provided useful landmarks during orientation as the actin staining was unique to the areas and very different to the TM. In the transition zone the actin was clearly distributed around the periphery of the endothelial cells, as described in the literature (Gordon, 1990). Moving towards the TM the actin staining became more branched and disorganised and CLAN-like structures which did not fit with our definition of TAPAS were observed. Imaging towards the ciliary muscle was also avoided as the phalloidin staining was often saturated due to the high concentrations of actin in the smooth muscle. The saturation itself may influence the observer's ability to visualise some of the actin patterns but also the cellular actin surrounding these fibres appeared much straighter than in other regions.

This method also ensured that uveal and corneoscleral TM were present in every section, although the quantity of uveal meshwork could be variable and the presence of cribriform was not guaranteed. There were differences in the actin staining patterns between the uveal and corneoscleral meshwork. In the uveal the level of actin staining was often poor as the core of the trabecular beams were visible due to auto fluorescence, while the actin staining in the corneoscleral region was much more vibrant and detailed. Straight stress fibres were evident in many different orientations due to the 3D nature of the tissue and depending on the orientation of the tissue the sheets of the corneoscleral meshwork could be seen as flat perforated sheets or stacked plates. An overview of the tissue from our youngest and oldest donors

provided two very different views of the TM tissue. The PI stained nuclei were clearly diminished and the fine actin staining in the younger donor was now imposed upon by thicker actin bundles which seemed fused together.

The identification of CLANs in the complex architecture of the TM tissue would not be possible without the optical sectioning of confocal microscopy (Amos and White, 2003; Baschong et al., 1999; Brotchie et al., 1999). Serial sectioning made it possible to trace the CLANs and get a better idea of their size and structure. The size and structure of CLANs in TM tissue was variable, this is not unexpected as variability has been observed both *in vitro* and in previous *ex vivo* work (Hoare et al., 2009). Most CLANs spanned across 2-3 z-series, representing a depth of 2-3μm and were often easily identified in the corneoscleral region as they spanned between the visible limits of the plates from section to section. In the JCT region identification of CLANs was led by the identification of interconnecting spokes as there were a lot of staining profiles that resembled hub points described by Read et al as focal concentrations of f-actin (Read et al., 2003; Read et al., 2007).

It seemed that the majority of the CLANs identified were in the late uveal (not the isolated branches) and corneoscleral regions of the TM. The CLAN-like structures identified by Hoare and Read were also present throughout but were certainly a dominant feature of the transition zone and the more complex arrangements of the JCT were actin staining was most disorganised. The incidence of CLANs in the tissue was found to increase with increasing donor age as it yielded a strong linear regression value of 0.588. As is common in studies requiring tissue donation there was an abundance of tissue from advanced ages and limited tissue from younger age groups. We do feel however that there is a sufficient spread to make the statement CLANs increase with increasing donor age. CLAN incidence is expressed as a percentage of CLAN containing cells as including the number of nuclei provided us with a means to ensure our tissue was following the previously published trends of cell loss. It was reassuring to find a decrease in TM cell number with age as it fits with the previously published works (Alvarado et al., 1984; Alvarado et al., 1981; Calthorpe et al., 1991; Grierson and Howes, 1987; Grierson et al., 1984) and so allowed the data to be normalised.

The values for CLAN incidence obtained in the current study were compared to the published results of Hoare. There was certainly some disparity between the counts obtained between both sets of counts. By carrying out a small re-evaluation of some of the normal tissue which was examined in the earlier paper it became apparent that the differences observed were due to inter-observer error. This difference may be a result of our determination to establish a more precise definition of a CLAN. The manner in which the counts were conducted varied as the earlier work included much smaller structures which have been excluded from the current work. My re-evaluation of images previous analysed by Hoare et al revealed a reduction in CLAN numbers of almost 50%. Taking this variation into account the values from both studies were much more comparable.

The measurement aspect of this work indicates that CLANs formed *ex vivo* are slightly smaller than those observed *in vitro*. The difference in area measurements was not found to be significant and we believe it may be skewed by the different natures of the environment. On a flat culture plate we can clearly see the entire CLAN structure, however, *ex vivo* analysis adds a further dimension which makes tracing the CLAN more difficult. This complicated orientation may also explain the why spoke length *ex vivo* is seemingly a few μm smaller than *in vitro*. However, it may well be that CLANs in the organised tissue are smaller than those observed *in vitro* as the ECM to which the cells are bound is different and this may influence the size of CLANs.

We are confident that this work strengthens our earlier work stating that CLANs are a feature of TM tissue. We can now add that CLAN incidence is increased with increasing donor age in non-glaucomatous tissue.

7. How do age-related stresses influence CLAN formation?

In the previous chapter the influence of donor age on CLAN incidence was explored. As ageing is a complex process cells may be experiencing differing levels and types of stress. We therefore investigated how different forms of age-related stress influenced CLAN formation. Cells were assessed for the level of senescence and apoptosis without the addition of a potent CLAN inducer to assess baseline levels. The baseline levels were then compared to values with TGF-β2 to evaluate how this factor, known to induce CLAN formation, affected apoptosis and senescence. In order to induce oxidative stress, TM cells were treated with hydrogen peroxide and finally TM cells were grown on AGEd matrigels in an attempt to mimic whether AGEs were associated with CLAN formation.

7.1 Senescence

To assess the number of senescent cells in a culture the numbers of β-gal positive cells present were recorded as a percentage of the total nuclei counted. Cells were also counterstained with phalloidin so that the cytoskeletal pattern of each individual cell could be appreciated in conjunction with the presence or absence of β-gal staining (

Figure 7-1).

BTM cells at a mid-passage (6) and high passage (11) were used to optimise the staining protocol. The BTM cells were maintained on labtek chamber slides for 4 weeks in order to increase the likelihood of senescence in post confluent conditions. As can be seen in Figure 7-2 the β-gal staining was not uniform across all cells. Cells such as those indicated by asterisk were considered β-gal negative because staining was extremely pale in comparison to the majority of other cells in the field of view and therefore taken as background. In contrast some cells such as those indicated by arrows were β-gal positive and exhibited extremely dark staining. The percentage of senescent cells in these BTM cultures was found to be 75% in passage 11 cultures and 54% in passage 6 cultures, while CLAN incidence was found to be higher than baseline level of CLANs with values of 13% at passage 11 and 22% at passage 6 (Figure 7-3).

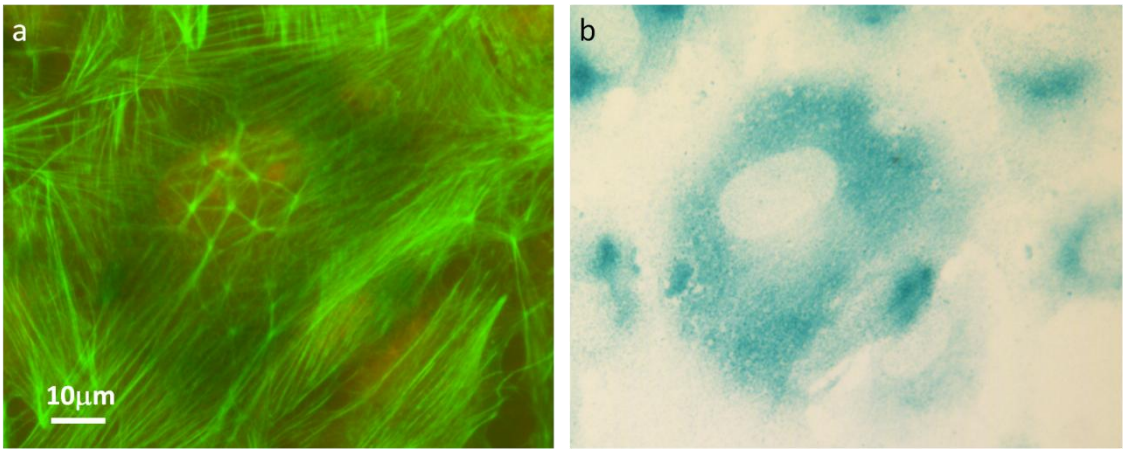

Figure 7-1. BTM cells stained with β-gal, phalloidin and PI.

Image a. is a merged image of a BTM cell stained with β-gal, phalloidin and PI. By examining all the staining it was possible to record the total number of cells in a field of view based on PI staining and then to categorise the cells based on both the β-gal status (seen in image b) and the cytoskeletal arrangement present as viewed using phalloidin. The BTM cell in the image would be classed as β-gal positive and containing a CLAN.

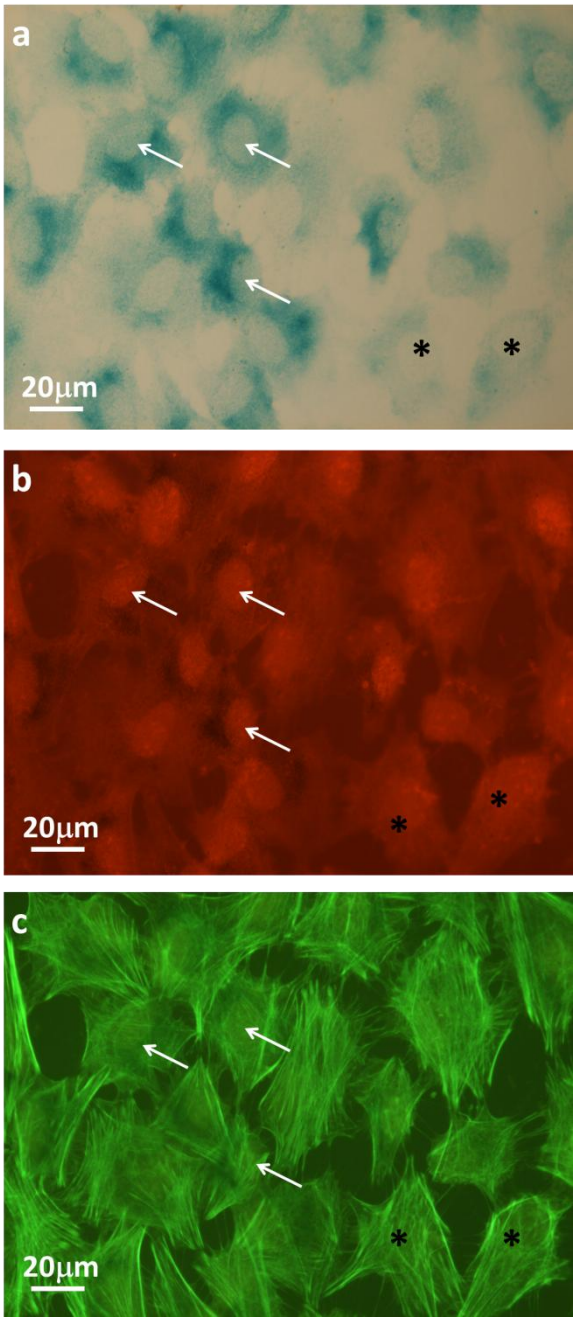

Figure 7-2. β-gal and phalloidin/PI co-staining of BTM cells.

The BTM cells used in this experiment were maintained on the same substrate for 4 weeks post confluence in order to increase the number of senescent cells in the population. Image a. is a phase microscopy image of BTM cells stained with β-gal. The blue colour is localised to the cell cytoplasm but it not uniformly distributed within the cell nor do all cells stain to the same degree. Image b, is the same field of view captured using fluorescence of the same microscope. Here the cell nuclei are stained red with PI and this is used to provide the total cell count, while phalloidin in image c shows the actin staining. The cells marked with arrows have the strongest β-gal staining and would definitely be counted as β-gal positive. The cells marked with an axterix however had faint staining and would be considered β-gal negative.

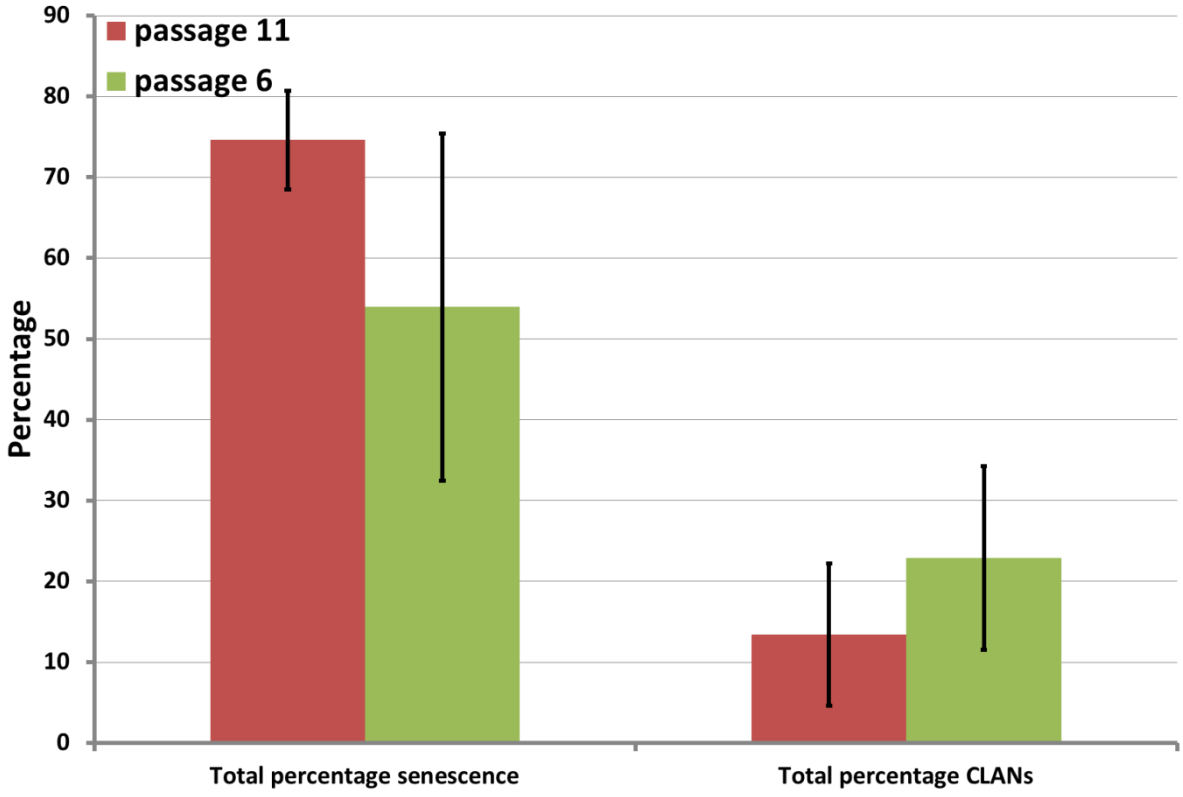

Figure 7-3. Bar chart representing the percentage of β-gal positive cells and the percentage of CLAN containing cells in BTM cell cultures at passage 11 and 6.

The BTM cells used in this experiment were maintained on the same substrate for 4 weeks post confluence in order to increase the number of senescent cells in the population. The percentage of senescent cells in both populations accounted for over half the cells observed, averaging 75% and 55%. The percentage of CLAN containing cells was higher than baseline levels when cells were attached to the substrate for 7 days. CLAN incidence in passage 6 culture was higher (22%) than levels in passage 11 cultures (13%) with a significant difference observed (p=0.032). (Coloured bars are average values from 10 field of views, n=2. Error bars represent standard deviation).

The data collected from BTM cell cultures was further analysed by separating cells into categories based on both β-gal staining and cytoskeletal evaluation. It was discovered that the largest percentage of cells were categorised as β-gal positive without a CLAN, with values of 67% in passage 11 and 41% in passage 6 (Table 7-1). Following from this the next largest group was β-gal negative without a CLAN accounting for 20% and 37% (passage 11 and 6). Unsurprisingly, cells containing CLANs were the smallest groups of cells in the population, accounting for no more than 14% regardless of whether cells were β-gal positive or negative. In both cultures there were more β-gal positive cells that contained CLANs than β-gal negative but this difference did not reach a significant level ($p=0.097$).

Table 7-1. Percentage of BTM cells categorised on the basis of β-gal staining status and the presence or absence of a CLAN.

The largest group identified was senescent cells that did not contain CLANs accounting for more than half the population in passage 11. The second largest category was β-gal negative cells without a CLAN representing 20% and 37%. CLAN containing cells represented the smallest categories and while the CLAN incidence was slightly higher in senescent cells there was no significant difference compared to non-senescent cells that contained a CLAN.

	BTM culture passage 11	BTM culture passage 6
senescent without CLAN	66.67	40.70
non-senescent without CLAN	20.09	37.21
senescent plus CLAN	8.22	13.95
non-senescent plus CLAN	5.02	8.14

HTM cells from 6 donors were also stained with β-gal, phalloidin and PI to assess the level of senescence and to examine the co-incidence of CLANs in both β-gal positive and negative cells. Unlike the BTM cell cultures, the HTM cells were incubated as normal in maintenance medium until confluent then treated with 2ng/ml TGF-β2.

The level of senescence in the HTM cell cultures in maintenance medium was found to vary from 0 to 12% across HTM donors (Figure 7-4), with similar fluctuations observed upon treatment with 2ng/ml TGF-β2 for 7 days. The percentage of β-gal positive cells ranged from 2-14% but did not significantly increase the percentage of β-gal positive cells ($p=0.682$) in any donor. Comparison of β-gal staining to donor age revealed that the percentage of β-gal positive cells was not highly correlated with increasing donor age. Donors aged 36 and 58 were found to contain the highest percentage of β-gal positive cells while donor aged 91 had the lowest percentage of β-gal positive cells. The average number of cells in a field of view was also variable among donors, with older donors tending to have fewer cells on average than younger donors.

In keeping with previous results treatment with TGF-β2 increased the percentage of CLAN containing cells in all donors, however, the largest percentage of cells were categorised as β-gal negative without a CLAN; regardless of the presence of TGF-β2. This group accounted for the majority of the cells observed, with values of 75% in presence of TGF-β2 and 88% in maintenance medium only. The second largest group was non-senescent plus a CLAN and the presence of TGF-β2 did cause a shift as only 6% of cells in maintenance medium fell into this group but reached almost 19% in TGF-β2 treated cultures. The results provided in Table 7-2 are the averaged values obtained from all 6 donors. The percentage of senescence was very low in these cultures and only accounted for approximately 5 % of cells regardless of whether TGF-β2 was present. From the values obtained senescent cells were more likely to have stress fibre arrangements of actin than to contain a CLAN.

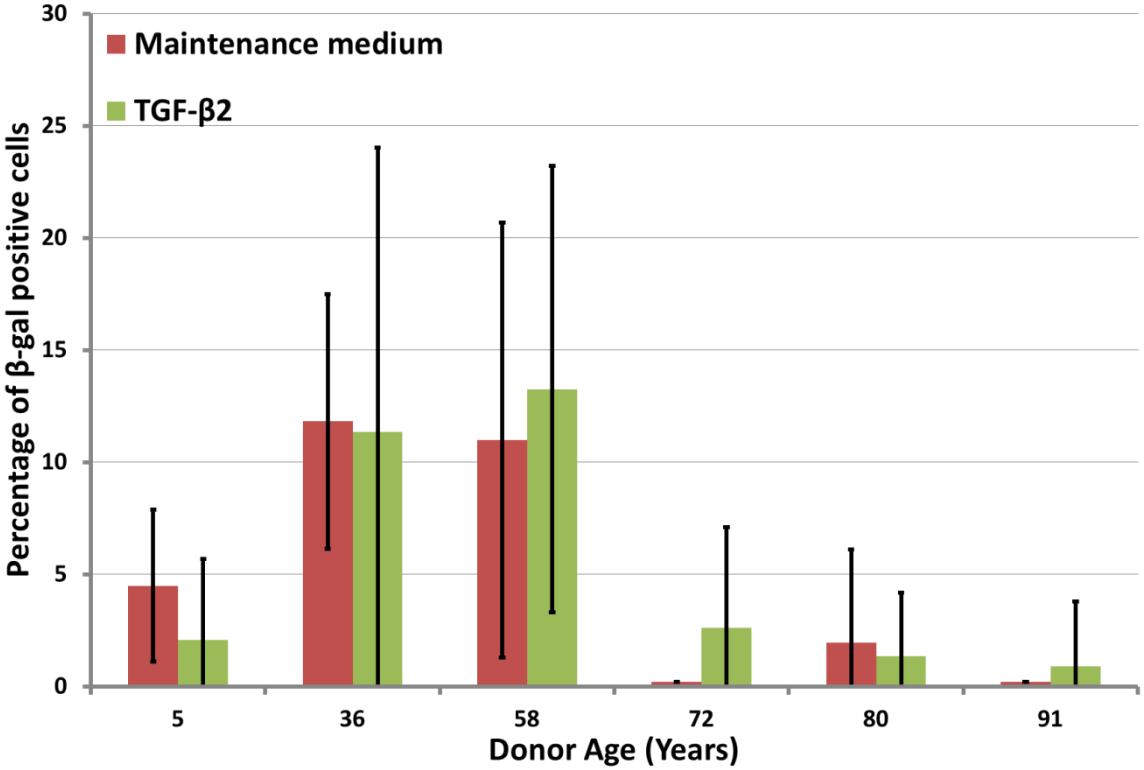

Figure 7-4. Overall percentages of β-gal positive HTM cells in cultures from various donors.

Bar chart illustrating the percentage of β-gal positive cells identified in 6 stable cultures of HTM cells derived from different donors. The percentage of β-gal positive cells was variable ranging from 0-12% following incubation with maintenance medium. Incubation in the presence of TGF-β2 did not significantly increase the level of senescence in any donor. (Values are averaged from 10 fields of view from 2 replicates, error bars represent standard deviation).

Table 7-2. The percentage of HTM categorised on the basis of β-gal staining status and the presence of CLANs.

The majority of HTM cells were categorised as non-senescent and without a CLAN, followed by non-senescent with a CLAN. While maintenance medium and TGF-β2 produced similar results, the presence of TGF-β2 induced CLAN formation and so there were greater numbers of non-senescent plus CLAN. The same shift was not observed in senescent cells with values almost identical. Most senescent cells were found to be without a CLAN. The values are averaged from 6 different donors where counts were taken from separate10 fields of view.

	maintenance medium	2ng/ml TGF-β2 (in maintenance medium)
non-senescent without CLAN	88.18	75.29
non-senescent plus CLAN	6.01	18.97
senescent without CLAN	4.65	4.21
senescent plus CLAN	1.16	1.53

7.1 Apoptosis

The number of BTM cells expressing markers of apoptosis was assessed by staining cells with TUNEL following 7 days exposure to maintenance medium, growth medium or 2ng/ml TGF-β2. Positive experimental controls, shown in Figure 7-5, were created by the addition of DNase to cells to induce DNA breaks. TUNEL staining carried out on BTM cells (regardless of experimental treatment) was found to stain the cell cytoplasm to some degree. This was opposed to the highly nuclei localised pattern observed with induced DNA breaks. Despite the background staining it was still relatively easy to identify positively stained cells as indicated by the arrows in Figure 7-6. It was evident that many of the cells with positive TUNEL staining of their nuclei were intact and did not exhibit as yet cytoplasmic blebbing or evidence of advanced cytoplasmic shrinkage so CLAN and actin cytoskeleton evaluation should be practical and potentially useful.

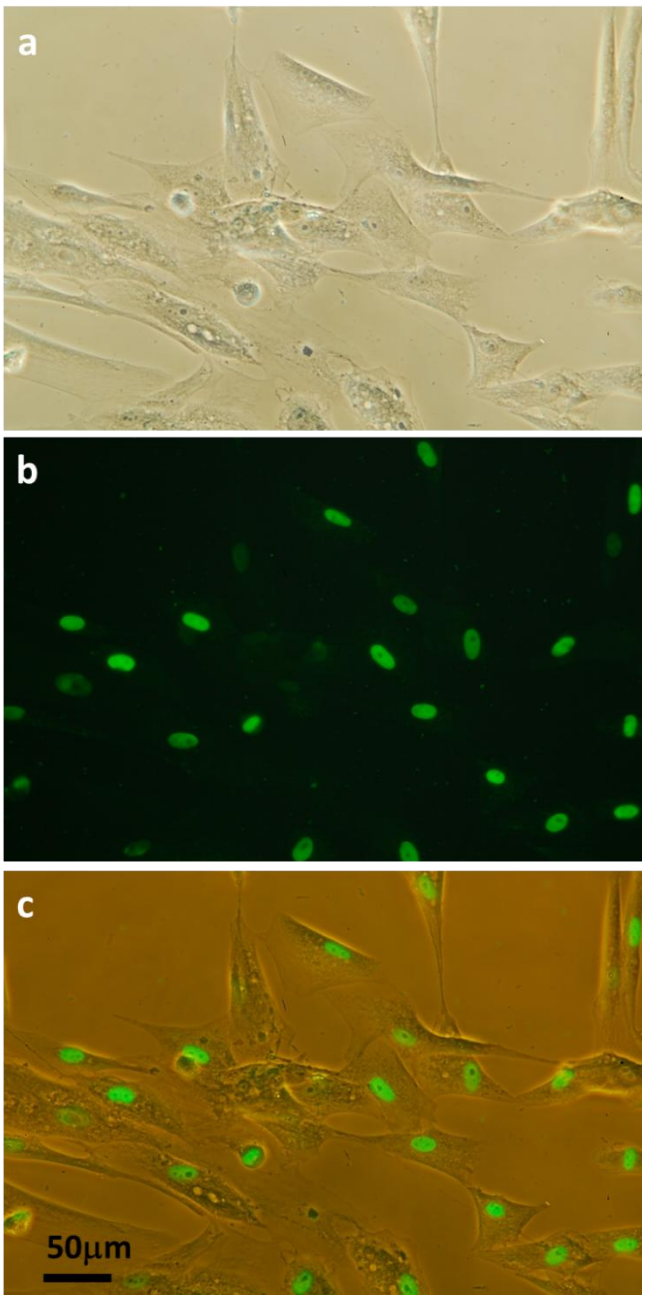

Figure 7-5. Positive TUNEL staining in BTM cells caused by DNase treatment.

The top image is a phase contrast image of BTM cells in culture exhibiting a normal morphology. Cells were treated with DNase to provide positive experimental controls for TUNEL staining and can be seen as green fluorescence in the middle image. The final image was created by merging the phase contrast and fluorescent images demonstrating the localisation of the stain to the nucleus within the TM cells.

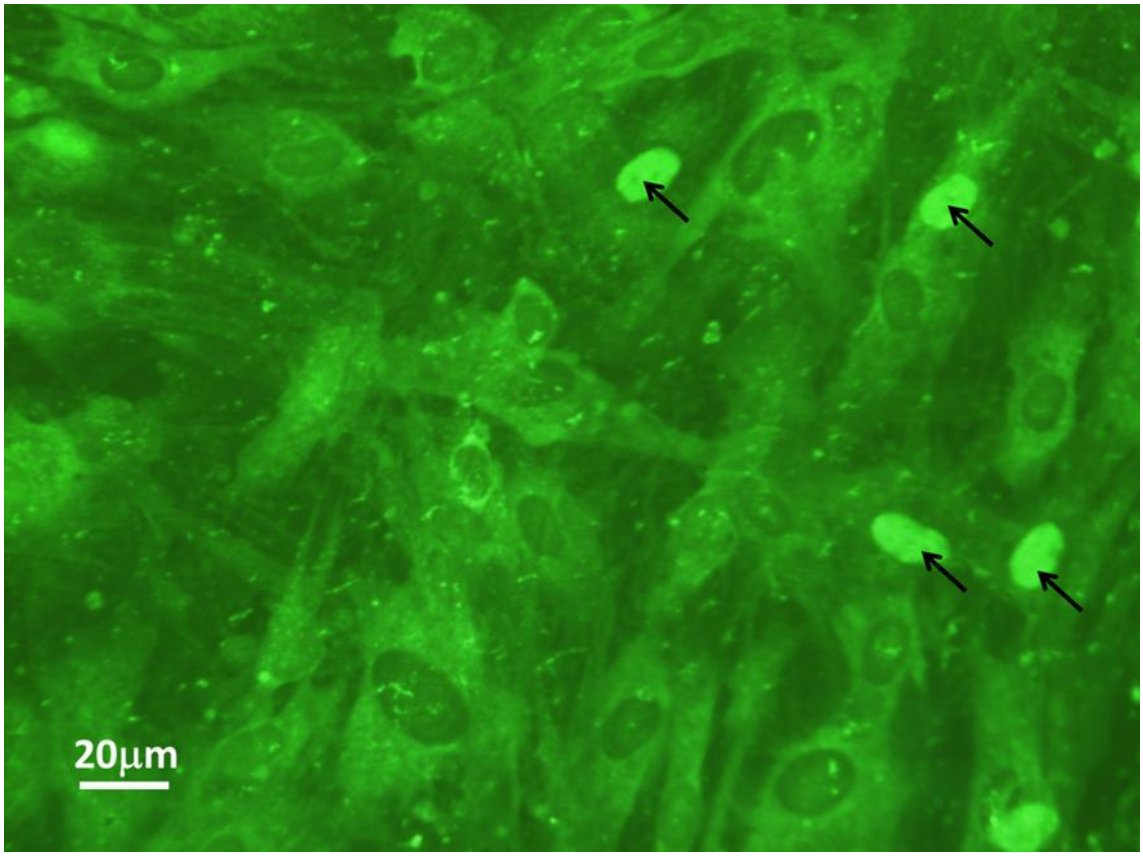

Figure 7-6. Florescent image of HTM cells stained with TUNEL.

In HTM and BTM cells the stain was not localised to the nucleus as observed in control samples but was found to stain the cell cytoplasm also. Despite this it was still possible to observe TUNEL positive cells (as indicated by the arrows) as the stain was very intense within the nucleus.

The percentage of TUNEL positive BTM cells in cultures treated with maintenance medium was found to be 6%. This value did not change significantly in BTM cell cultures treated with either growth medium or 2ng/ml TGF-β2 ($p=0.207$). The maximum percentage of TUNEL positive cells observed occurred in growth medium with a value of around 10% (Figure 7-7).

TUNEL staining was carried out on HTM cells from 6 donors ranging in age from 0-92 years. No treatment was found to induce a significantly higher level of TUNEL staining within the donor cells, however, there was variability with the percentage of TUNEL positive cells ranging from 3-15%, as indicated by Figure 7-8.

As there was no significant difference observed between treatments the average percentage of TUNEL positive cells across all treatments was calculated and compared to donor age. This examination revealed that the youngest donor had the lowest number of TUNEL positive cells (3%) while the oldest donor contained the highest (13%). Despite some fluctuations between the averaged, values were found to have a strong positive linear correlation with increasing donor age ($R^2=0.789$).

Despite the observation that both TUNEL staining and the induction of CLANs increases with age, direct comparison of the percentage of CLAN containing HTM cells (from previous experiments) to the percentage of TUNEL positive cells in each of the six cultures did not provide positive correlation. CLAN incidence in medium only did not change significantly and so no correlation could be drawn from these data. CLAN incidence in the presence of TGF-β2 compared to percentage of TUNEL positive cells returned a R^2 value of only 0.040 as illustrated in Figure 7-8.

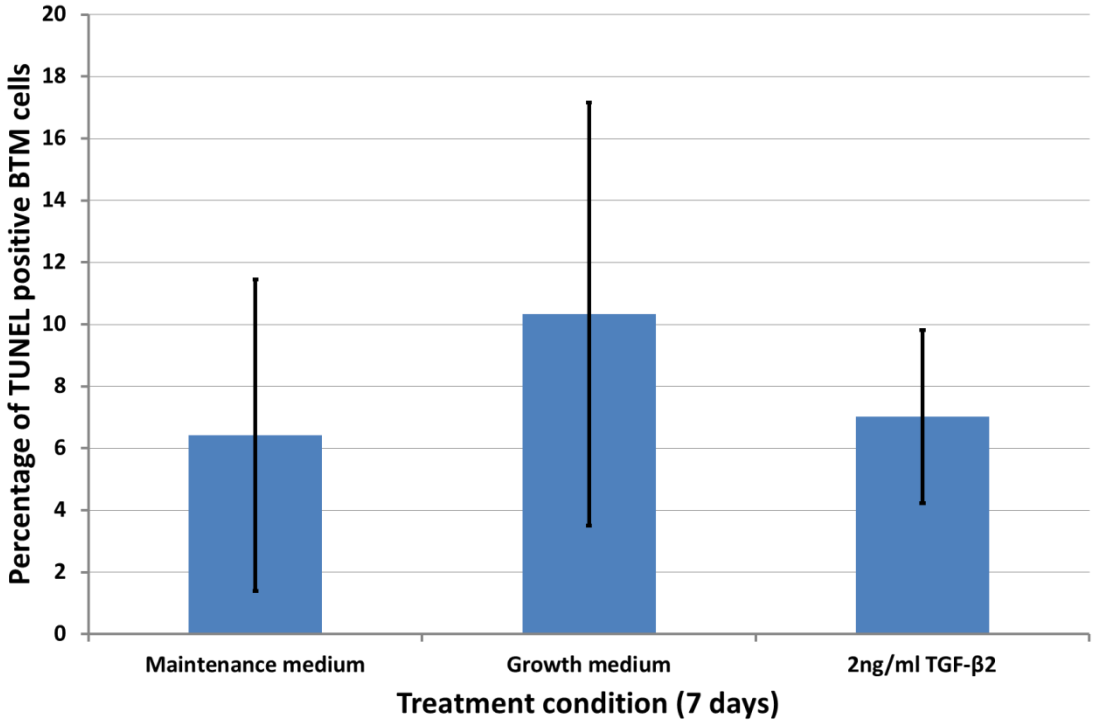

Figure 7-7. The percentage of TUNEL positive BTM cells

Bar chart illustrating the percentage of TUNEL positive BTM cells present in cultures treated for 7days with maintenance medium, growth medium or 2ng/ml TGF-β2.No significant difference was observed between any of the treatments (p=0.207). (Coloured bars are averaged values when n=3, error bars represent standard error).

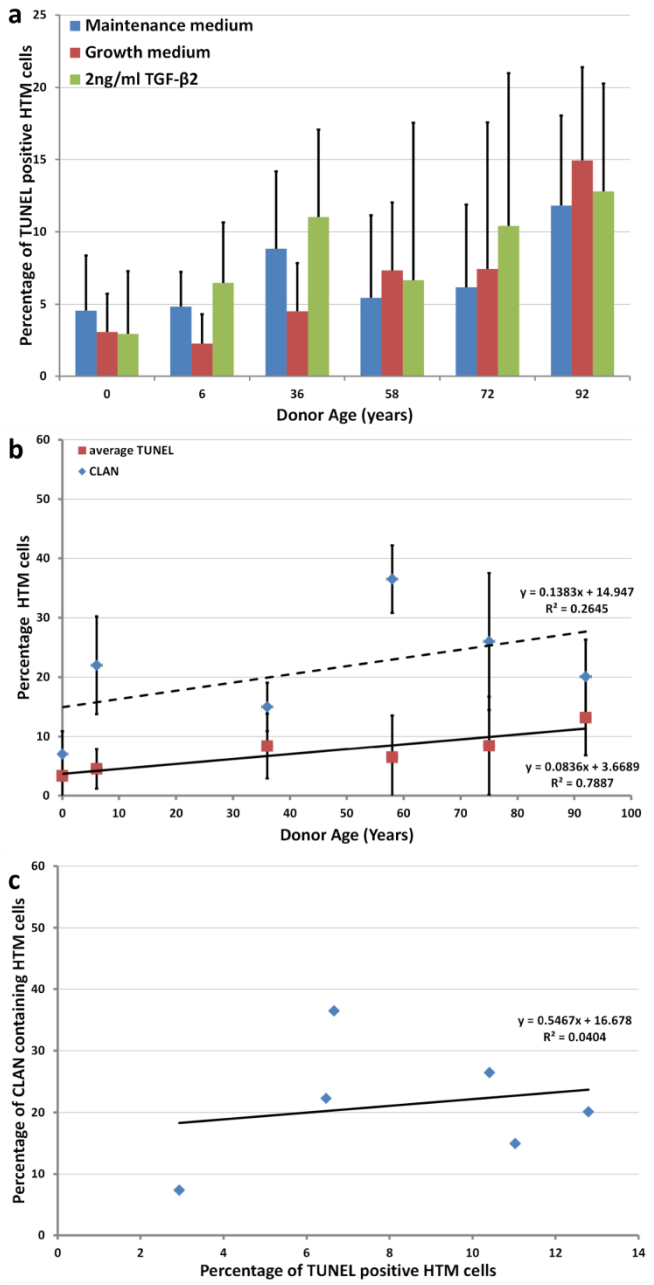

Figure 7-8. Charts illustrating the percentage of TUNEL positive HTM cells compared to percentage of CLANs.

As seen in graph a, the percentage of TUNEL positive HTM cells was variable among donors and between treatments ranging from 3-15%. As no treatment resulted in a statistically significant increase in TUNEL the results were taken together and averaged values are shown in graph b. A positive correlation exists between TUNEL staining and increasing donor age as it exists between CLAN incidence and donor age. However comparing the values obtained in each culture (graph c) demonstrated that increased TUNEL did not always correlate with increased CLAN incidence (coloured bars are averaged results, n=2, error bars demonstrate standard deviation).

7.2 Oxidative stress

In order to provoke oxidative stress in the TM cells they were treated with increasing concentrations of H_2O_2 for 1 hour. Cells were then fixed and examined either immediately following the stress or allowed to recover for 7 days in either fresh maintenance medium or 2ng/ml TGF-β2. These experiments were carried out with BTM cells initially before treatment was used on a small cohort of HTM cells.

BTM cells treated with hydrogen peroxide showed little change in cell morphology with increasing concentrations of H_2O_2 from 200μM to 800μM as seen in Figure 7-9. BTM cells treated with H_2O_2 for 1 hour exhibited a percentage of CLAN containing cells ranging from 14 to 15%, with H_2O_2 concentration of 400μM producing the largest percentage (Figure 7-10). CLAN incidence was further increased in cultures which were treated with H_2O_2 and then allowed to recover in maintenance medium for a further 7 days. Under these conditions CLAN incidence reached approximately 30% with all concentrations of H_2O_2, except 400μM. The baseline level of CLANs in BTM cells incubated with maintenance medium for 7 days is 10%. Pre-treatment with H_2O_2 resulted in a value significantly higher ($p=0.029$) than the baseline of 10%.

Treatment with 2ng/ml TGF-β2 following H_2O_2 pre-treatment consistently induced a CLAN incidence of above 30%. The percentage of CLANs was also seen to increase with higher initial concentrations of H_2O_2, with 400μM or 600μM H_2O_2 CLAN incidence reached 40-45% which was significantly higher than 1 hour treatment ($p=0.001$) but not significantly higher than levels observed with TGF-β2 treatment only ($p=0.293$). Only following pre-treatment with 800μM H_2O_2 followed by TGF-β2 did CLAN incidence (52%) significantly increase above that observed with TGF-β2 treatment ($p=0.001$).

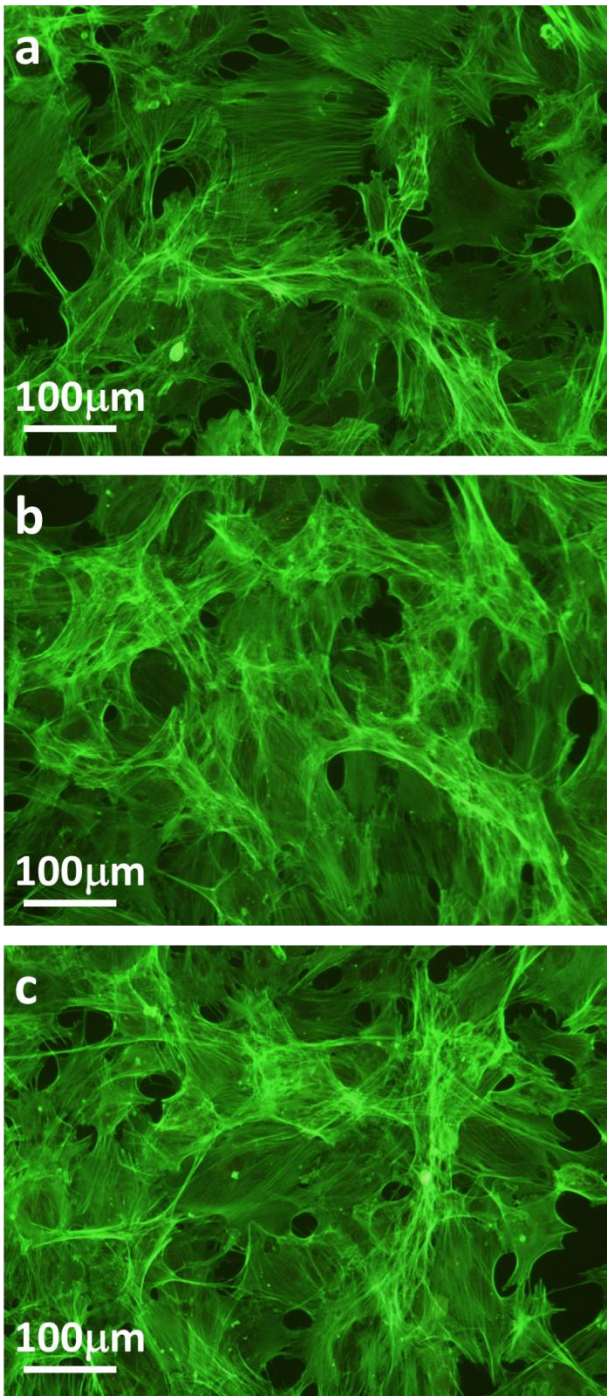

Figure 7-9. Morphology of BTM cells treated with H_2O_2.

Fluorescent images are representative of BTM cells treated for 1 hour with increasing concentrations of H_2O_2 (image a, 200μM, b 400μM, while cells in image c were cultured with 800μM). BTM cell morphology was unchanged throughout; cells exhibited good cell to cell contact and the actin staining was primarily straight stress fibres.

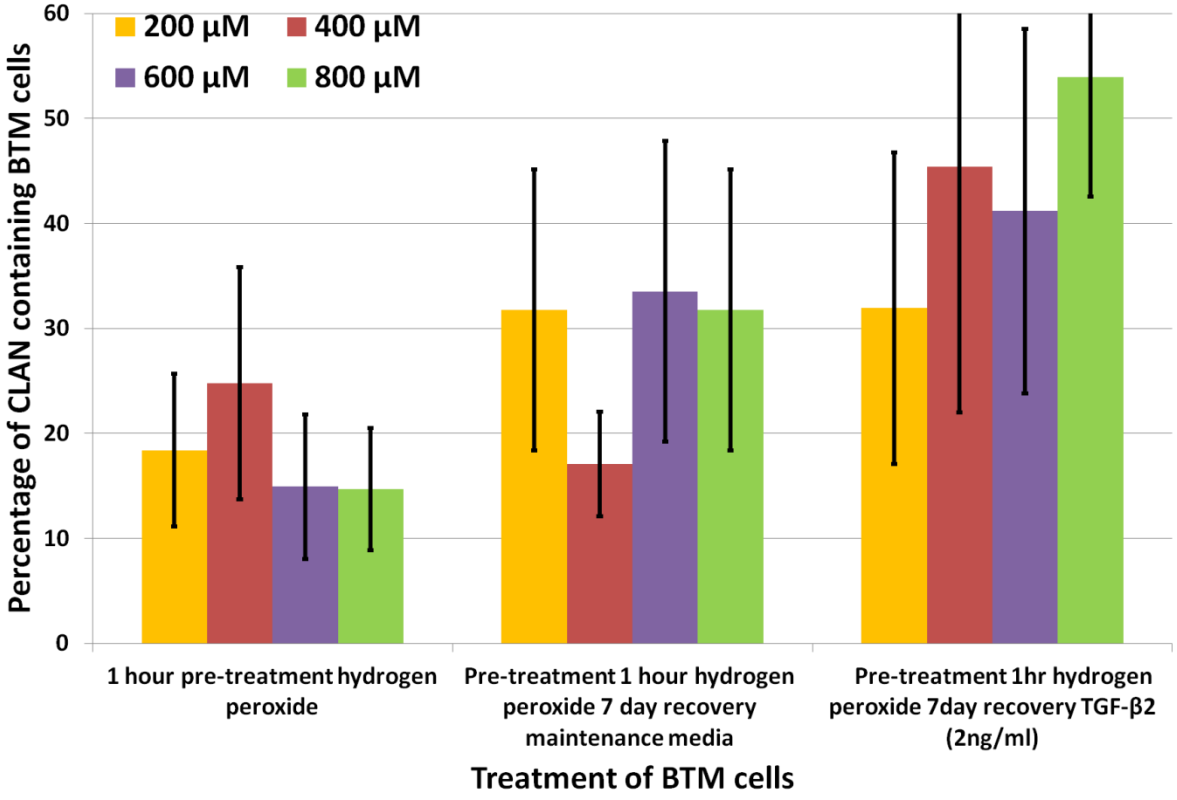

Figure 7-10. CLAN incidence in BTM cells treated with hydrogen peroxide.

Bar charts showing percentage of CLAN containing BTM cells following 1 hour treatment with H_2O_2. CLAN incidence, although high, was not significantly increased above baseline levels following 1 hour treatment. Allowing cells to recover in maintenance medium resulted in a CLAN incidence of approximately 32%, with the exception of 400µM. Recovery in TGF-β2 produced the largest percentage of CLAN containing cells with values reaching 52% with 800µM (coloured bars are averaged values where n=3, error bars represent standard deviation).

The effect of H_2O_2 treatment on HTM cells was not comparable to those observed in BTM cells. Morphological analysis of the cultures revealed that HTM cell health was much more sensitive to H_2O_2 treatment than BTM cells, showing signs of cellular distress at lower concentration than those affecting BTM cells. Cells appeared shrunken with decreased cell-cell contacts and in some cultures there was evidence of cell loss (Figure 7-11). This was most evident following treatment with 800µM H_2O_2 with cultures exhibiting cell rounding and extreme cell shrinkage meaning that CLAN counts were not possible this was particularly evident in donor 020 and 030. However, in many cultures the main body of the cell was still robust enough to observe the cytoskeleton. Treatment for 1 hour with increasing concentrations of H_2O_2 did not induce a significant change in CLAN incidence in any of the donors observed (p-values 015 P=0.090, 020 P=0.582, 026 P=0.164, 028 P=0.851, 030 P=0.137,032 P= 0.072), with values (0.4-4%) failing to significantly increase above experimental controls (0.4-4.6%).CLAN incidence in most of the HTM cells remained low even in the presence of TGF-β2. Donor 015, however, produced high CLAN incidence in a number of the conditions, including the experimental control (28%). When cultures were pre-treated with 200µM H_2O_2 and incubated for 7 days with medium, CLAN incidence was 39% while incubation with TGF-β2 resulted in a CLAN incidence of 42%. These were the largest values obtained in HTM cell cultures, however, the increase failed to reach significance given the unusually high level of CLANs in the experimental controls (p=0.117).

Excluding donor 015 the percentage of CLAN containing cells in the experimental control ranged from 1.8% to 8%. No significant shift was observed with H_2O_2 pre-treatment of any concentration as percentage of CLAN containing cells that did not increase above 7% (P=0.79). Recovery of HTM cells in TGF-β2 following H_2O_2 pre-treatment rarely induced CLANs to levels significantly higher than their experimental controls, with only donor 030 exhibiting a significant increase following 200µM H_2O_2 pre-treatment (p=0.001). Figure 7-12 illustrates the percentage of CLAN containing cells in all 6 donors under the different conditions. No correlation could be drawn between CLAN incidence and donor age in any of the conditions.

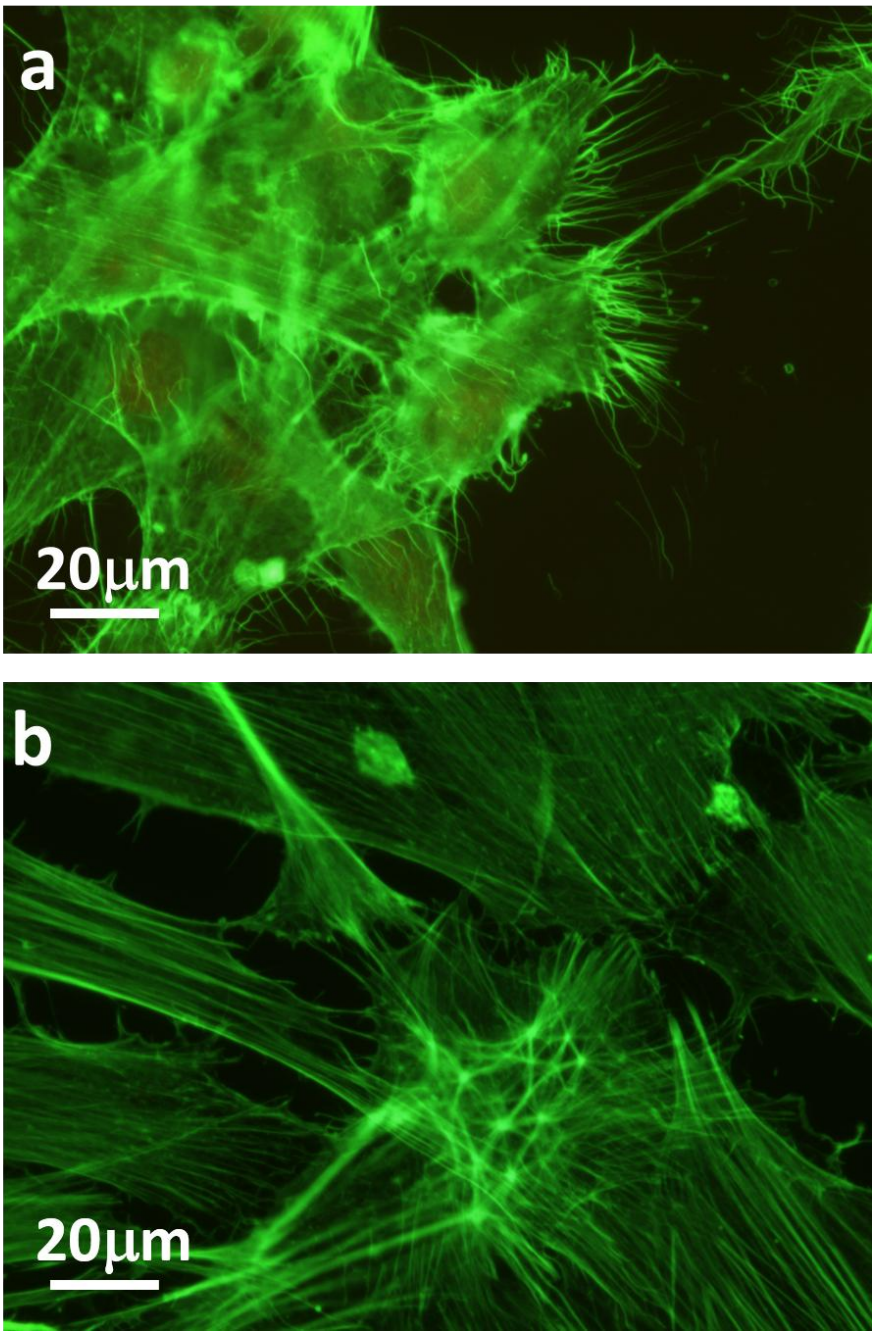

Figure 7-11. Fluorescent images representative of HTM cell morphology following 1 hour treatment with H_2O_2.

HTM cells were affected by H_2O_2 at much lower concentrations compared to BTM cells. As shown in image a, concentrations of 800μM could cause extreme damage to HTM cells, the cells have completely rounded and the actin cytoskeleton cannot be distinguished. At lower concentrations however cell morphology remained unchanged as seen in image b and the actin cytoskeleton is clearly visible. While the predominant actin pattern was straight stress fibres CLANs were clear in the cytoplasm of some HTM cells treated with lower concentrations of H_2O_2.

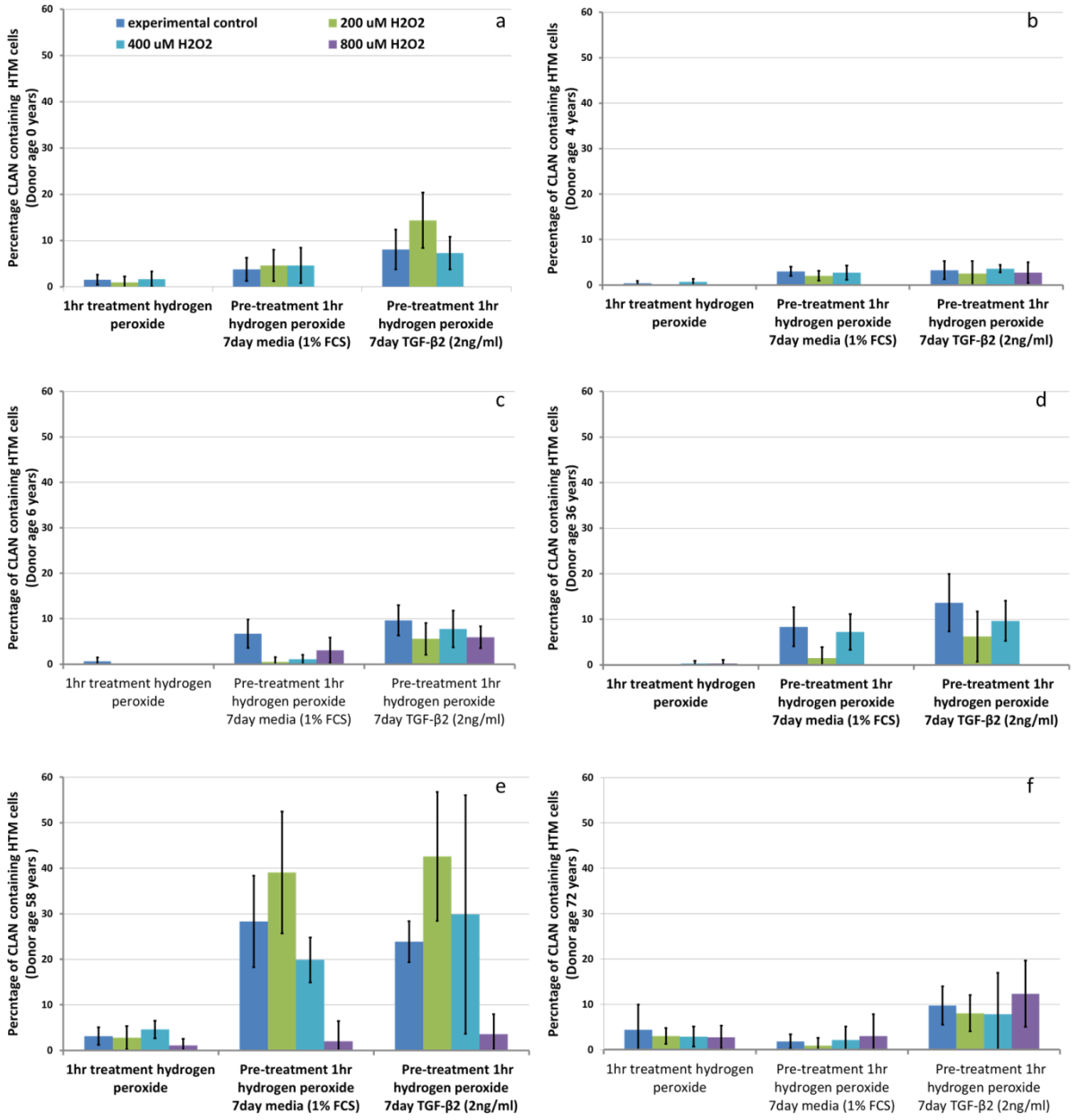

Figure 7-12. Graphs showing CLAN incidence in HTM cells from 6 donors treated with varying concentrations of H_2O_2.

HTM cells cultures pre-treated with 200μM, 400μM or 800μM H_2O_2 for 1 hour were either fixed immediately or allowed to recovery for 7 days in maintenance medium or 2ng/ml TGF-β2 (in maintenance medium). CLAN incidence was variable throughout but failed to be significantly increased above experimental controls by any of the conditions. (Coloured bars represent average values for the experimental controls and each concentration of H_2O_2. Error bars demonstrate standard error, n=2).

BTM cells were stained with a general ROS stain (H_2DCFDA) following 1 hour treatment with increasing concentrations of H_2O_2. The cells were then imaged via fluorescence microscopy to illustrate that our H_2O_2 treatment was inducing oxidative stress in the TM cells. Fluorescent images were taken at the same time points and the intensity of the fluorescence was observed to be greater in H_2O_2 treatment cells than the medium only cultures (Figure 7-13). This increase in fluorescence represented an increased level of ROS. BTM cells in medium only had only faint staining, while treatment with 200μM resulted in intense nuclear staining with dye visible in the cell cytoplasm. Increasing the concentration to 400μm resulted in almost complete uniform cell staining and the level of fluorescence was quickly saturated. There was little visual difference between cultures treated with 400μm or 800μm.

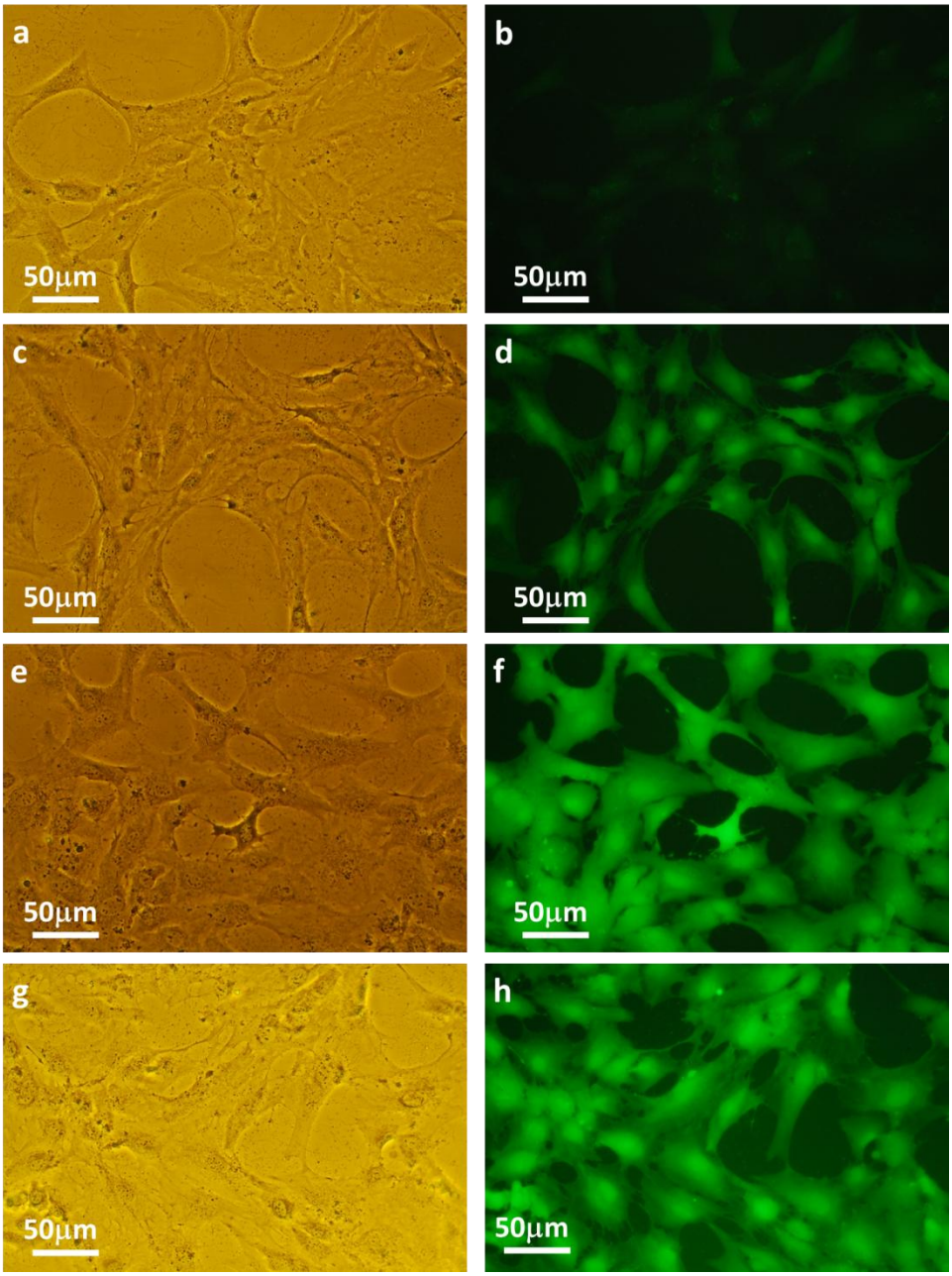

Figure 7-13. BTM cells stained with H2DCFDA (a general ROS stain) following treatment with increasing concentrations of H_2O_2.

Phase contrast images on the left correspond to the fluorescent images on the right. Cultures were stained with H2DCFDA a general ROS stain following 1 hour incubation with either medium only (control) or 200μM, 400μM or 800μM H_2O_2. Increasing intensity of the fluorescence corresponded to increase ROS as it cleaved the probe into its fluorescent form. BTM cell cultures incubated with medium only (a&b) demonstrated minimal fluorescence, while incubation with H_2O_2 resulted in increased fluorescence as seen in c&d representing 200μM H_2O_2, increasing the concentration of H_2O_2 to400μM (e&f) or 800μM (g&h) increased the intensity of the staining compared to 200μM but appeared similar to each other.

7.3 AGE-modified substrate

In vitro models using AGE modified matrigels are a commonly used method for investigating the influence of accumulating cellular adducts on cell behaviour (Glenn et al., 2009; Kuzuya et al., 1996; Stitt et al., 2004). As the external environment can affect cell behaviour (Park et al., 2011; Russell et al., 2008; Schlunck et al., 2008) the influence of substrate on cell morphology and the presence of CLANs was investigated before beginning any experimentation. As all previous experiments were conducted on rigid TC substrates these were investigated first in order to normalise any differences found in matrigel.

Morphological analysis of TM cells grown on either glass or plastic labtek chamber slides under identical conditions revealed that both substrates were capable of maintaining cell growth and producing adequate monolayers. No obvious phenotypic differences were observed, however, it was noted that on occasion the growth of cells on glass was slower than cells from the same population on plastic. Any individual differences were not sufficient to produce significant differences when multiple experiments were analysed. The morphological assessment of BTM cells grown for 7 days on both substrates was confirmed by nuclei counts which showed no significant differences ($p=0.556$) between the average number of cells per field of view in cultures grown on glass or plastic, with averaged values across all treatments of 47-52%.

Assessment of CLAN incidence revealed that BTM cell cultures grown on either glass or plastic TC ware did not significantly alter CLAN incidence ($p=0.18$). BTM cells incubated with growth or maintenance media showed almost identical levels of CLANs (Figure 7-14). Although no significant difference was observed with TGF-β2 treatment, it must be noted that CLAN incidence was lower than might have been expected in the presence of TGF-β2. Identical incubations have repeatedly shown TGF-β2 to be a potent CLAN inducing agent but values in the current experiment reached only 22%.

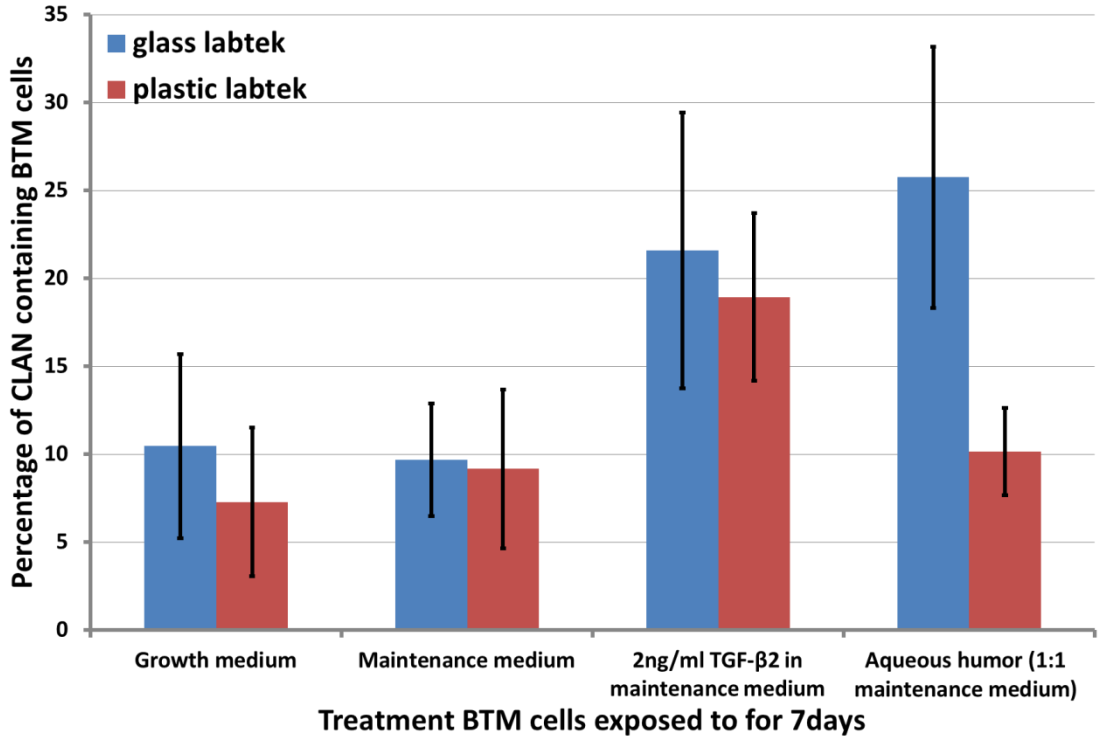

Figure 7-14. Histograms showing the influence of glass and plastic substrates on CLAN formation in BTM cells under various treatments.

The incidence of CLAN containing BTM cells grown on either glass or plastic chamber slides remained largely unchanged regardless of substrate. As shown CLAN incidence was comparable between cultures grown on both substrates indicating their formation was not significantly affected by growth of TM cells on glass or plastic. Coloured bars represent averaged values taken from 2 separate BTM cell cultures, error bars demonstrate standard deviation.

BTM cells were then grown on unmodified matrigels and subsequent examination by phase contrast microscopy revealed that BTM cells exhibited a normal phenotype matching that seen when cells were grown on culture treated plastic and glass (Figure 7-15). Cells were evenly spread across the surface of the matrigels and had reached a starting level of confluence within 7 days. Treatment with either maintenance medium or TGF-β2 for 7 days did not result in any gross changes in morphology and cell number at the end of the experimental period were comparable. When treated with maintenance medium the average cell number was 39.9 per field of view and 34.8 per field of view in the presence of TGF-β2.

Examination of the actin cytoskeleton revealed that the prominent actin arrangement was straight stress fibres which exhibited limited alignment between neighbouring cells. Upon analysis the percentage of CLAN containing cells was 8% in maintenance medium when grown on unmodified matrigels (Figure 7-16). While this value was comparable with the values obtained on both glass and plastic ($p=0.292$), treatment with TGF-β2 failed to reach values produced by the same treatment on glass or plastic ($p=0.010$). The percentage of CLAN containing cells grown on matrigel was only 14% compared to values of approximately 20% when treated with TGF-β2 on glass or plastic. The percentage of CLAN containing cells was however increased above values obtained with maintenance medium.

BTM cells grown on AGE-modified matrigels were found to proliferate at a slower rate than on TC treated substrates or unmodified matrigels, an observation made within our lab with multiple cell types (data not shown). The phenotype of the BTM cells was not found to be altered compared to unmodified matrigels (Figure 7-15) despite the slower rate at which cells reached the starting level of confluence. It was however noted that the cells were more confluent in the centre of the well than towards its periphery. The number of CLAN containing cells following 7 days treatment with maintenance medium on AGE-modified matrigels was 7%, a value comparable to that observed following growth on culture plastic and glass ($p=0.164$) or unmodified matrigel ($p=0.306$). Treatment with TGF-β2 resulted in a significant increase in CLAN incidence compared to maintenance medium, increasing from 7% to 20% ($p=0.001$).

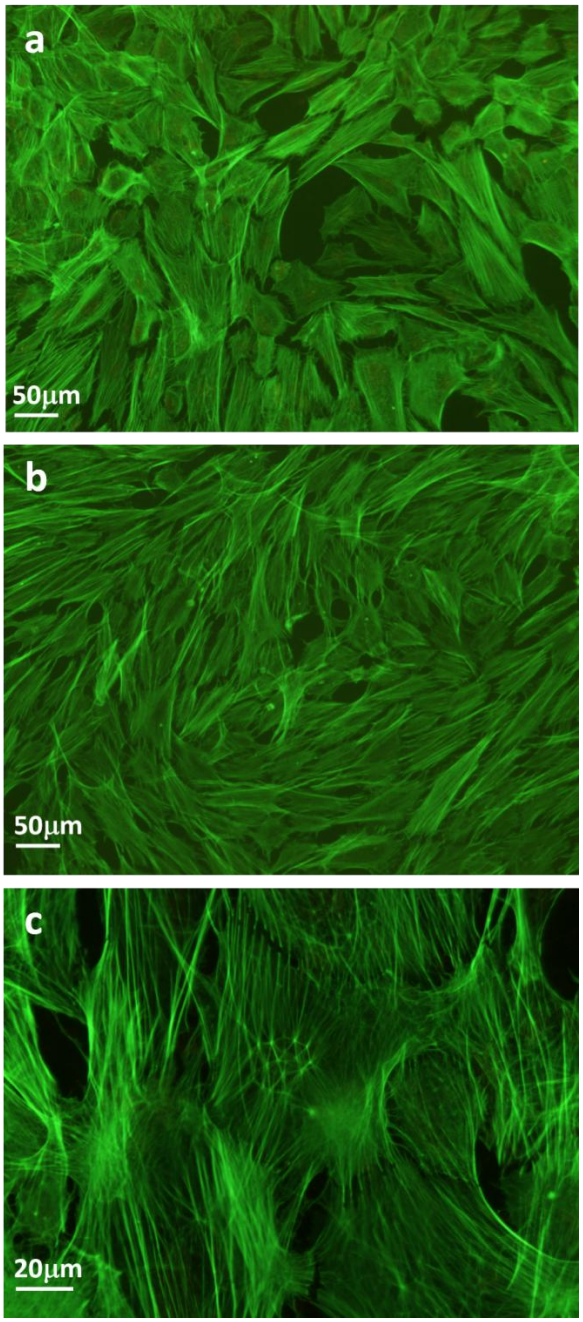

Figure 7-15. Fluorescent images of BTM cells grown on unmodified and AGE-modified matrigels.

BTM cells grown on either a. unmodified matrigels or b. AGE modified matrigels were imaged following 7 days exposure to maintenance medium. BTM cells are characteristically elongated in shape in both images although cell-cell contact is limited in places. Upon addition of TGF-β2 the presence of CLANs was observed in some BTM cells as illustrated by image c. The actin cytoskeleton has been stained green using Alexa-488 phalloidin.

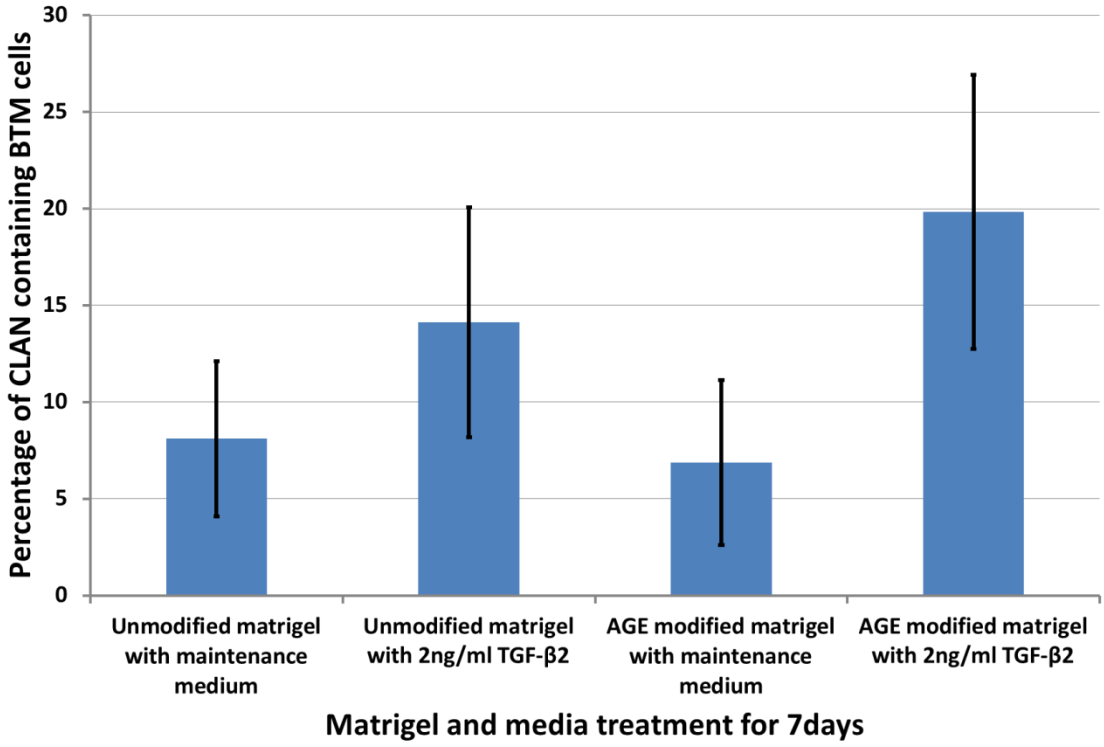

Figure 7-16. Bar chart demonstrating the percentage of CLAN containing BTM cells grown on unmodified and AGE-modified matrigels.

The percentage of CLAN containing BTM cells grown on unmodified matrigels was significantly increased (p=0.001) by the presence of 2ng/ml TFG-β2 with values increasing from 7% to 14%. A similar pattern was observed on the AGE modified matrigels with CLAN incidence significantly increased by the presence of TGF-β2 (p=0.001) from 6% to 20%. (Coloured bars are averaged values, n=3 and error bars are representative of standard deviation).

7.4 Discussion

7.4.1 Senescence

The loss of cells with increased age is well-documented among many cells types within the eye including corneal endothelium, RPE (Wang et al., 2010) and TM (Alvarado et al., 1981; Grierson and Howes, 1987). The loss of TM cells is more pronounced in glaucoma and studies have also demonstrated an increase in the number of senescent cells (Liton et al., 2005a).

β-gal staining is a commonly used marker for senescence (Dimri et al., 1995) which produces a blue precipitate through interaction with increased levels of lysosomal β-galactosidase in senescent cells. Staining BTM cells which had been maintained post confluence served as optimisation for the combined staining. It also provided positively stained cells which could be used to grade future β-gal staining. Cells incubated in maintenance medium on the same substrate post-confluence were more likely to exhibit markers of senescence as the cells are no longer provided with proliferation factors nor do they have sufficient space (Freshney, 1992; Joyce et al., 1998). Some cells were found to stain very well for β-gal and served as positive controls by which to compare other cells. Even under these extended post-confluent conditions some BTM cells stained very faintly and were considered to be β-gal negative. Analysis revealed the percentage of senescent cells was high, accounting for 50-75% of the population. Although no direct comparison could be made with BTM cells that were not treated in this manner, the percentage of senescent cells expected in normal proliferating cultures would be less than 5% (Yu et al., 2010).

It was interesting to observe a CLAN incidence of 13-22% in these BTM cells cultures as these values are increased over baseline values following our normal experimental protocol. This increased percentage of CLANs has led us to question whether pro-longed attachment to substrate increased CLAN incidence. TM cells secrete ECM and growth factors and so condition their environment (Alexander et al., 1998; Faralli et al., 2009; Rhee et al., 2009; Shifera et al., 2010; Tane et al., 2007; Yun et al., 1989). It is possible that the longer the cells are attached the more ECM is laid down which would lead to an alteration in the cytoskeleton (Filla et al., 2006; Schlunck et al., 2008), in this

instance CLAN formation. The high level of senescence in the post-confluent BTM cells made it unsurprising that the largest group of cells was classified as senescent without a CLAN. From this data it would seem that prolonged attachment to the substrate resulted in an increased number of CLAN containing cells.

Because HTM cells were not subject to extended culturing on the same substrate the level of senescence was much lower reaching a maximum of 13%, but remaining below 5% in most cultures. This was an encouraging result as it indicated that the cells under our cell culture conditions were proliferating as expected in the presence of FCS. It is therefore unsurprising that without TGF-β2 stimulation, the largest group was non-senescent with no CLAN. Treatment with TGF-β2 did not increase the percentage of senescent cells in any of the HTM cell cultures to a significant level. This was contradictory to the finding of Yu who showed that TGF-β2 increased senescence from 3.5% to approximately 30% after only 24-48 hours (Yu et al., 2010).

As TGF-β2 did not increase senescence in these cultures, the order of the groups remained unchanged from medium treated cultures but it did increase the percentage of CLAN containing cells. The increase in CLAN incidence was reflected in the increase of non-senescent cells containing a CLAN. This shift did not occur from the senescent group to non-senescent group but rather more of the non-senescent cells developed a CLAN with TGF-β2 treatment. The proportion of senescent cells with a CLAN present did not change, indicating senescent cells are not responsive to TGF-β2 stimulation. Donor age did not appear to have any correlation with the percentage of senescent cells or on how senescent cells responded to TGF-β2. Our work would suggest that senescent cells are less likely to contain CLANs than the rest of the non-senescent population. Loss of cytoskeleton rearrangement with senescence has been reported elsewhere (Hwang et al., 2009). As cells are no longer capable of cell division the cytoskeleton becomes somewhat static, it would therefore be incapable of forming CLANs even in the presence of stimulus.

7.4.2 Apoptosis

The initial aim of TUNEL staining was to assess whether cells were apoptotic and simultaneously observe the actin cytoskeleton. This was not possible as staining TM

cells with TUNEL and rhodamine phalloidin was not compatible. Rather than abandon this area entirely the cells were stained with TUNEL to investigate whether HTM cell cultures had variable percentages of apoptotic cells in the population. While it was not possible compare the presence of apoptosis to cytoskeletal pattern directly the percentage of CLANs from different experimental runs could be compared to apoptosis values. We were confident in making this comparison having previously shown the reproducibility of CLAN incidence.

TUNEL staining detects DNA damage in cells, staining the nucleus (Hall, 1999) as demonstrated by the positive experimental control using DNase. Regardless of treatment no more than 10% of BTM cells were found to contain positive TUNEL staining illustrating that treatment with TGF-β2 did not induce apoptosis in BTM or HTM cells. Cao et al reported that TGF-β2 could increase TUNEL staining in HTM cells but even at higher concentrations than those used in the current study the percentage of apoptotic cells was less than 10% (Cao et al., 2004).

The age-related decrease in the number of TM cells *in vivo* is believed to occur at least in some measure by apoptosis (Agarwal et al., 1999). From this preliminary work, cells from older donors seem to have a larger population of cells in apoptosis compared to cells from younger donors. This may account for the difficulty of culturing TM cells from older donors. In the small cohort of HTM cells investigated the increased number of TUNEL positive cells did not correlate to the culture with the greatest CLAN incidence. However, both CLAN induction and the number of apoptotic cells increase with increasing donor age.

The current work would suggest it is the non-apoptotic cells that contain CLANs. As there is a decline in cell number but the number of CLANs increases, then it would stand to reason that CLANs must exist in non-apoptotic cells otherwise the level of CLANs would remain unchanged as not even half of TM cells are found to contain CLANs with TGF-β2 treatment (Figure 7-17).

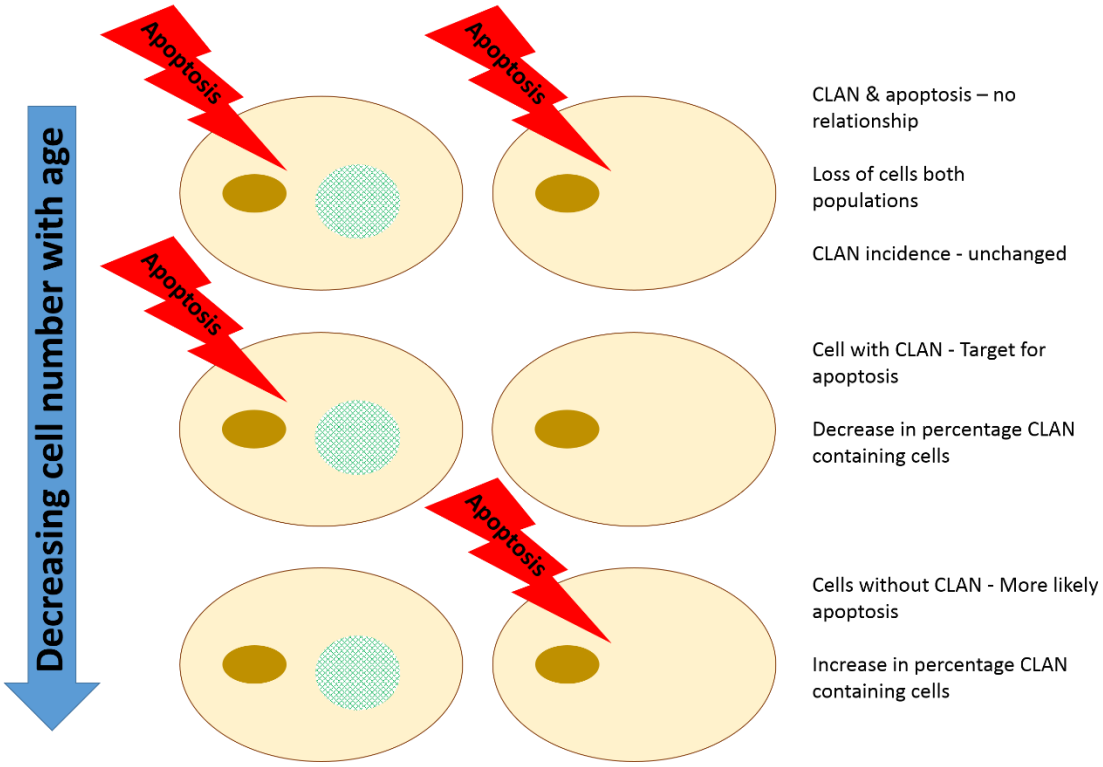

Figure 7-17. Potential relationships between CLAN incidence and apoptosis.

There is a known loss of TM cells with age and the current work has demonstrated that CLANs increase with age. The diagram above illustrates the potential relationship between loss of cells via apoptosis and CLAN incidence. It would seem likely that CLANs occur in cells that are not undergoing apoptosis.

Investigating CLANs and apoptosis by another method, such as annexin V staining, may allow simultaneous comparison of apoptotic state and cytoskeletal pattern and may help shed light on whether it is apoptotic cells which contain CLANs or the non-apoptotic. Further experiments in which TM cells are forced into apoptosis are also needed to expand the current work. Treatment of BTM cells with staurosporine in the current work proved too potent for the cells and resulted in complete loss of the cytoskeleton so that no further analysis was possible.

7.4.3 Oxidative stress

The role of oxidative stress in glaucoma has been receiving increased interest as it has been linked with loss of TM cells (Lin et al., 2010). Several published works have initiated oxidative stress by the addition of H_2O_2 (Yu et al., 2008) and following this methodology in the current work provided some interesting results. One hour treatment with concentrations of H_2O_2 ranging from 200-800μM was sufficient to increase ROS staining in BTM cells as shown by the live cells imaging, while BTM cell morphology was not greatly altered. Cytoskeletal assessment revealed a high percentage of CLAN containing cells (15-25%) in BTM cells treated with H_2O_2. Given that the baseline levels of 10% are recorded after 7 days it was rather high after only 1 hour treatment, indicating that pre-treatment was sufficient to induce CLAN formation. Experiments with chronic sub-toxic concentration of H_2O_2 have shown that the influence is sustained (Li et al., 2007). Although the percentage of CLAN containing cells did not reach the values of TGF-β2; the rate of CLAN formation was much faster.

As most of our studies involved chronic (7 day) experiments cells were allowed to recover in either maintenance medium or TGF-β2. Any difference in CLAN incidence between the pre-treated cells and those without could be attributed to H_2O_2. Interestingly, recovery in maintenance medium resulted in CLAN incidence of approximately 30% compared to 10% without pre-treatment. These values were significantly higher than 7 days medium and statistically similar to those values obtained following treatment with TGF-β2 for 7 days. The increase in CLAN incidence observed following recovery in medium was a significant finding. The presence of H_2O_2 is clearly capable of inducing CLAN formation, a state which persists even when cells have been allowed to recover for 7 days. It would have been interesting to have

carried out counts at various time points leading to 7 days, as this would have provided a view of how H_2O_2 affected the cytoskeleton throughout time. Cytoskeletal re-arrangement can occur very rapidly, while CLANs in the presence of DEX and TGF-β take several days to reach a significant level above baseline. It would be interesting to observe whether CLANs formed quickly after this initial insult or whether they occurred largely during recovery.

Recovery of stressed BTM cells in TGF-β2 showed even higher values in which 30-53% of cells contained CLANs. These values were some of the highest CLAN incidence observed throughout any of this work. While the highest concentration of H_2O_2 produced a significantly increased CLAN incidence than TGF-β2, other concentrations failed to reach significance. No experiment has been capable of inducing CLANs in more than 60% of the TM cells, with most ranging from 30-45%. We have previously shown that senescent cells are not capable of being induced to form CLANs in the presence of TGF-β2 and that it is likely cells entering into apoptosis do not contain CLANs. Work with growth factors has also pointed out that cells undergoing proliferation or migration may also not contain CLANs, as their cytoskeleton is already in a conformational form suited to the function. Therefore it may be that it is not possible to induce CLANs in all TM cells at the same time. Work by others has identified that TM cells are heterogeneous in cultures (Coroneo et al., 1991) while flugel et al highlighted a sub-population of cells that had different actin staining (Flugel et al., 1991). It may be that only certain cells within the TM are capable of CLAN formation.

The results obtained upon the treatment of HTM cells with H_2O_2 were varied and did not mimic those results observed when BTM cells were treated in the same manner. The differences observed between the species may be related to the culture conditions. This conclusion has been based on the observations in other experiments relating to depleted serum concentrations. Under these conditions HTM cells were found to be more susceptible to damage and in some cultures there was evidence of cell rounding and detachment. Both BTM and HTM cells are maintain under identical culture conditions, however, if HTM cells were already in a sub-optimum environment in comparison to BTM cells, then the addition of a regent such as H_2O_2 could have a

deleterious influence on cell health. As discussed previously this sub-optimum culture environment could be due to the use of FCS not human serum. Future work focussing on lower concentrations of H_2O_2 may be more useful.

There are several assays which can be used to assess oxidative stress (Mehanna et al., 2011). The use of commercially available H2DCFDA is well documented for both microscopy and flow cytometry (He et al., 2008b; Lin et al., 2010). It was utilised in the current work as it is a general ROS stain which can enter cells, were the molecule is cleaved by ROS and the resulting product is fluorescent. The initial use of the compound in live cell imaging was to assess cell morphology and cytoskeletal patterns alongside ROS staining compared not only to donor age but also directly to the percentage of CLANs. During this process any basal differences in ROS would be detected via flow cytometry. Use of this technique would also examine whether TGF-β2 treatment influenced ROS staining to a greater or lesser extent in HTM.

Unfortunately, several problems were encountered during this process which made it difficult to assess. High levels of background fluorescence meant that it was more difficult to identify where true staining was present. More worryingly, upon examination with the fluorescence microscope the level of intensity would continue to change until a point after which the molecule failed to fluoresce further. Both problems indicated that the molecule may be unstable. Personal communication with the manufacturer indicated that this may have occurred due to the presence of esterases in FCS. As this fluorescent compound is cleaved in order to produce the fluorescence, any esterases in the medium could lead to premature cleavage. If this occurs then the compound cannot pass the cell membrane and instead becomes fluorescent in the medium until all molecules are cleaved. Given this instability only ROS staining of BTM cells was undertaken as a point of principle that H_2O_2 was increasing ROS in our cells. The data obtained from flow cytometry has been negated from this work due to variable results.

7.4.4 AGE-modified substrate

Growth of BTM cells on unmodified matrigels did not appear to influence the gross morphology of TM cells, nor did it significantly affect CLAN incidence when cultures were incubated with maintenance medium. The addition of TGF-β2, although resulting in a significant increase above medium only, failed to reach levels expected from previous experiments with TGF-β2. The story here is, however, compounded by the unusually low number of CLANs in the glass and plastic control dishes for this experiment. The average CLAN incidence following 7 days in the presence of TGF-β2 on glass or plastic TC-ware was 36%, a value obtained from multiple donors and experimental replicates. However, in the control (no matrigels), CLAN incidence was found to be 19-22%. Although the average values are low they are brought down by a particularly low CLAN incidence in 1 of the donors. In AGE-modified matrigels, CLAN incidence with maintenance medium was slightly decreased but statistically unchanged, again illustrating that there is a baseline level of CLANs regardless of the extracellular environment. The percentage of CLAN containing cells was increased to 20% in the presence TGF-β2 treatment, a value comparable to the experimental control glass and plastic.

Read et al suggested that the in vitro environment would influence TM cells and questioned whether drawing conclusions from such studies was a true reflection of *in vivo* functioning (Read et al., 2007). Work to assess the cytoskeleton of cells grown on different substrates demonstrated not only does the substrate influence TM cells in the presence of medium (Schlunck et al., 2008), but also how TGF-β2 influences the cells (Han et al., 2011). In their work Han et al demonstrated F-actin staining was much greater on more rigid substrates and gene expression was altered. Our current work has shown that fewer CLANs form on matrigels which are more pliable than glass or plastic when treated with medium only. Therefore, while TGF-β2 is capable if inducing CLAN incidence the alterations of the extracellular environment are influential in the degree to which it influence TM cells (Han et al., 2011). The presence of AGE in the ECM can greatly influence cell function (Glenn and Stitt, 2009; Kuzuya et al., 1996) in the current work it attenuated the depression in CLAN incidence to some extent, perhaps by altering the elasticity of the matrigels.

The potential influence of AGEs on cells has been greatly investigated in various cells and tissues throughout the body. Work by Stitt et al has been vital in linking the accumulation of these adducts to diseases such as diabetes (Stitt, 2001, 2010). While the initial focus was on diabetes the theory could be applied to any tissue and especially cells which are long lived. Within the eye work on AGE's remains limited, work by Tezel et al investigated the presence of AGE and RAGE in relation to open angle glaucoma, however, the work was entirely focussed on the lamina cribosa (Tezel et al., 2007). The use of immunological techniques to show AGE and RAGE localisation in the tissue was an area which we hoped to replicate in the TM; however, this was never achieved in our own work. Identifying whether AGE and RAGE were present in the TM would have provided supporting evidence for our *in vitro* work.

A proportion of this work represents preliminary data, but does however provide useful insights and strong indicators for future research directions. Taking these findings together it would seem that while increased senescence and apoptosis occur alongside increased CLAN formation, cells undergoing these changes are not likely to contain a CLAN. The influence of oxidative stress has been shown to be an exciting area of research in glaucoma and it would seem that the formation of CLANs is a part of this process. Combining increased oxidative stress and TGF-β2 produced the highest incidence of CLANs observed across all of the current work. Although TGF-β2 has not been shown to increase with age, protective mechanisms are depleted and so oxidative stress is increased. Both oxidative stress and TGF-β2 increase with glaucoma and may account for the increased incidence of CLANs. The role of the extracellular environment has been shown to influence CLAN formation in the current work and by others (Filla et al., 2006).

8. Discussion

8.1 CLANs in the outflow system

CLANs were first identified as one of many steroid induced changes observed in the TM cells (Clark et al., 1994). Glucocorticoids, such as DEX, are used as topical anti-inflammatory agents and have been associated with elevated IOP since the work of Armaly and Becker and Francois in the 1960's (quoted from Wordinger and Clark, 1999). The hypertension induced by DEX can lead to structural damage resembling that associated with glaucoma (Clark and Wordinger, 2009; Jones and Rhee, 2006; Kersey and Broadway, 2006). DEX is known to induce various changes in TM cells (Wordinger and Clark, 1999) including decreased phagocytosis (Matsumoto and Johnson, 1997; Zhang et al., 2007), increased ECM deposition (Lutjen-Drecoll et al., 1986; Rohen et al., 1993) as well as mediating alterations in gene expression (Clark et al., 2013) and disrupting intercellular junctions (Zhuo et al., 2010) and altering the cell cytoskeleton (O'Brien et al., 1996). The formation of CLANs has been expanded upon within our lab moving away from steroids.

Much work has been published in relation to CLANs since they were first identified in TM cells (Clark et al., 1994), however, some discrepancies exist with regards to CLAN formation. In our earlier publications we defined CLANs as a polygonal structure formed in confluent cell cultures, consisting of at least 5 hub points connected in 3 triangulations by straight actin spokes. We were convinced that the structurally similar polygonal structures identified during settlement (Ireland and Voon, 1981; Lazarides, 1976; Maguire et al., 2007) were different to the structures we identified in confluent cultures. While our current definition was unable to distinguish between these structures we still question the usefulness of studying structures which we have found to dissociate quickly after settling. Our current definition does however distinguish between polygonal structures and the actin tangles/ aggregates which were observed in tissue (Read et al., 2007).

The cells of the TM have contractile properties (Lepple-Wienhues et al., 1991; Luna et al., 2012) attributed to the organisation of the cytoskeleton into straight stress fibres (Gipson and Anderson, 1979; Grierson and Rahi, 1979; Ryder and Weinreb, 1986),

allowing for muscle-like contractions (Pellegrin and Mellor, 2007; Stricker et al., 2010) which can directly influence AH outflow (Wiederholt, 1998). The presence of different cytoskeletal patterns was postulated to influence outflow by making TM cells more rigid (Clark et al., 2005) which would result in increased outflow resistance (Ericksonlamy et al., 1992; Rao et al., 2001; Tian et al., 2000). Modelling of the cytoskeletal structures present in TM cells was undertaken by my student Andrew Heath and considers how the presence of geodesic structures could influence the cell's response to fluid flow and shear stress (Figure 8-1). Taken together, the presence of CLANs in larger quantities in glaucomatous TM (Hoare et al., 2009) could, at least in part, explain the increased resistance to outflow. Data from the current work also suggests a similar but lesser alteration occurs with age.

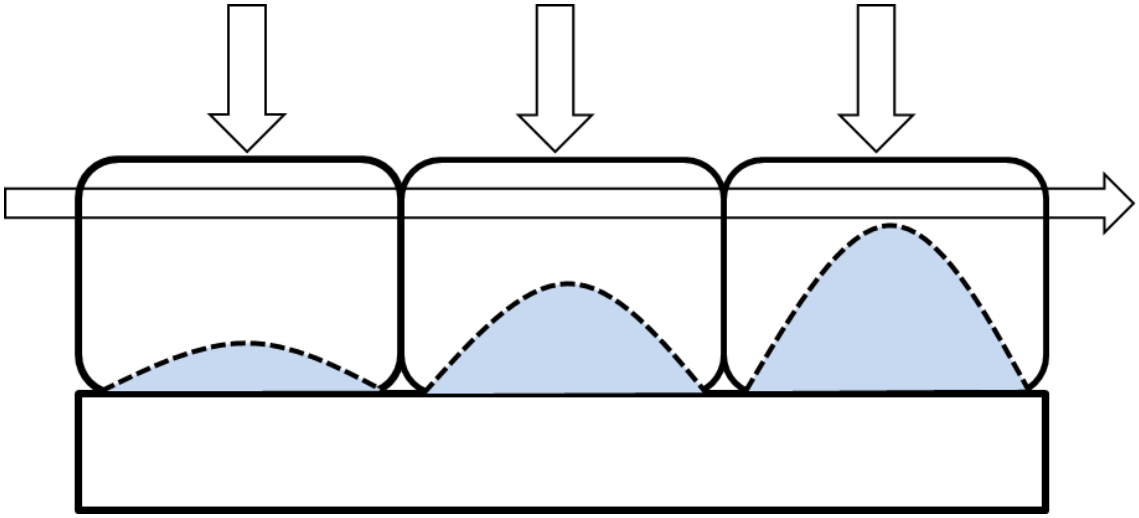

Figure 8-1. The presence of a geodesic structure within the cell.

The presence of a geodesic actin structure in the TM cell is postulated to influence how the cell responds to changes in the extracellular environment. TM cells are subject to shear flow forces as AH flows past, they are influenced by the composition and therefore rigidity of the ECM and to changes in IOP. The level of deformation experienced by the cells will be greatly influenced by the presence (and extent) of the CLAN in the cytoplasm. (Diagram provided by Laura Currie)

When work with CLANs first began it was assumed that their presence in TM cells was a unique feature of these cells and was linked with glaucomatous changes, including those induced by DEX (Clark et al., 2005). If this was the case then targeting the formation of CLANs may serve as a therapeutic target. Although there are several treatment options available for glaucoma patients (Marquis and Whitson, 2005), the search for new glaucoma therapies continues as the current options are still less than ideal (Bagnis et al., 2011) because they mostly work by either reducing the formation of AH or by increasing outflow via the uveoscleral outflow pathway (Kaufman and Rasmussen, 2012). In order to target CLAN formation we had to identify how CLANs formed in TM cells. The identification of CLANs in untreated, non-glaucomatous TM tissue pointed towards a physiological inducer. Published work from this thesis (O'Reilly et al., 2011), identified that AH was capable of inducing CLAN formation in TM cells *in vitro* and that TGF-β2 was the main inducing agent present in AH.

8.2 TGF-β2 influence

TGF-β is known to elicit many responses linked with disease progression in several tissues including ocular tissues such as the lens (Hales et al., 1995). In TM cells, TGF-β2 induces several changes many of these responses are similar to DEX responses and both lead to reduced outflow and damage similar to glaucomatous (reviewed in Bollinger et al., 2011; Clark, 2012; Fuchshofer and Tamm, 2012).

A re-occurring observation throughout this work has been a change in cell shape upon the addition of TGF-β2, and to some extent with AH. In pre-confluent BTM cell cultures, 3 distinct cell shapes were identified and linked to cell motility (O'Reilly, 2010). TGF-β2 treatment in BTM cells consistently produced a change in cell shape from spindle to epithelial which proved important when cell shape was compared to the cytoskeleton arrangement. Weinreb et al demonstrated the importance of actin filaments on regulation of cell shape in TM cells from monkeys (Ryder et al., 1988; Weinreb et al., 1986) and we have shown that epithelial cells tended to be more likely to contain a CLAN, while spindle cells were more likely to contain straight stress fibres. This observation was mirrored in HTM cells, although the shift in cell shape was variable.

The cell cytoskeleton is responsible for mediating cell function, and cell function can be associated with cell shape. HGF and FGF did not induce CLAN formation above baseline levels or a change in cell shape towards the epitheliod, but these growth factors are known to induce proliferation and migration (Coutu and Galipeau, 2011; Gherardi and Stoker, 1991; Nakamura and Mizuno, 2010; Polansky et al., 1979; Ridley et al., 1995). If these cells are committed to migration then they will have a predominantly spindle appearance, as straight stress fibres which allow for the contraction of the cell (Dominguez and Holmes, 2011; Pellegrin and Mellor, 2007), are the most prominent actin arrangement in spindle cells. Similarly cells undergoing proliferation will have adopted a specific cytoskeletal arrangement which is not likely to contain a CLAN (Heng and Koh, 2010). On the other hand, TGF-β2 does not promote proliferation or migration in TM cells, but instead activates the secretion of ECM components and reduces ECM degrading enzymes (Fuchshofer et al., 2003; Roberts et al., 1990b; Sethi et al., 2011a; Sethi et al., 2011b; Tovar-Vidales et al., 2011; Tovar-Vidales et al., 2008) which may be linked with the more epithelial phenotype more likely to contain a CLAN. TGF-β2 alteration of gene and protein expression have been shown to alter actin binding proteins and Bollinger et al suggested these may promote CLANs (Bollinger et al., 2011).

Much work is currently on going to uncover exactly what leads to TM cell dysfunction and ultimately to the increase in AH outflow resistance, with many paths converging on TGF-β2 (Shepard et al., 2010). The scope of the current work did not extend to investigate the pathway through which TGF-β2 acts to induce CLANs, although earlier work by our group indicated that it may proceed via Smad signalling (O'Reilly et al., 2011). There is much literature on the interactions of TGF-β2 mainly concentrating its influence on ECM components (Fuchshofer and Tamm, 2012; Fuchshofer et al., 2003). TGF-β2 influences several aspects of ECM and is modulated by the secretion of antagonising factors such as BMPs (Fuchshofer et al., 2007) and modulating factors such as MMP's (Fuchshofer et al., 2003) creating a self-regulating system. With increased concentrations of TGF-β in glaucoma this system becomes unbalanced and leads to increased ECM deposition. Connective tissue growth factor (CTGF) has been implicated in the signalling of TGF-β2 in these pathways (Fuchshofer et al., 2007) with

studies showing that CTGF is induced by TGF-β2 and that in mouse models overexpression of CTGF resulted in increased deposition of ECM (Junglas et al., 2009).

CTGF was also shown to lead to modification of the actin cytoskeleton (Junglas et al., 2012) and has been noted as a mediator of TGF-β2 effects (reviewed by Taylor, 2012). The direct alteration of the cytoskeleton is mediated by Rho signalling which is vital for cell motility and cell contraction (Hall, 1998; Ridley, 1996) and is known to influence TM cells (Mettu et al., 2004) and outflow (Kumar and Epstein, 2011). In 3T3 cells TGF-β is shown to induce long-term actin reorganisation by smad and Rho GTPases (Vardouli et al., 2008). *In vitro* the cells undergo alterations in shape, motility and attachment (Honjo et al., 2001a; Honjo et al., 2001b; Koga et al., 2006; Rao et al., 2001) through changes in cytoskeleton which leads to increased outflow facility (Kameda et al., 2012; Tian et al., 2000; Tian and Kaufman, 2005) and can be activated by DEX treatment (Fujimoto et al., 2012). Regardless of the pathway, the influence of TGF-β2 on TM cells is well established and we are confident to add induction of CLANs to its repertoire of actions which makes it a very interesting target when investigating glaucoma.

8.3 Therapeutic target

Potential treatments in glaucoma are being taken from the evolving knowledge of these signalling pathways that influence the ECM and cytoskeleton (Kaufman and Rasmussen, 2012). Current drugs in clinical trials include Latrunculin-B (Thomasy et al., 2012) and Rho kinase inhibitors, ROCK inhibitors are in clinical trials (Tanihara et al., 2008; Williams et al., 2011). Both act on the cytoskeleton demonstrating that this is a potential target for therapy. This work may have provided a means of targeting CLANs through TGF-β2.

TGF-β2 has previously been considered as a therapeutic target in glaucoma treatment aimed at reducing postoperative scarring following glaucoma filtration surgery which is a major failing of the surgery (Mead et al., 2003). Neutralisation of TGF-β2 using CAT-152 antibody was found to reduce scarring and work with this drug was continued into phase III clinical trials (Group et al., 2007a; Group et al., 2007b; Siriwardena et al., 2001). The use of a TGF-β2 neutralising antibody in the current work was found to reduce CLAN incidence and for a time may have seemed a potential and specific IOP

lowering treatment. This was however based on the assumption that CLANs were unique to TM cells; this assumption can no longer be up-held in light of recent work conducted in our group. In previous work by Clark et al, the presence of CLANs in other cells was explored and found to be negative. However, the cells used were cell lines and work conducted by Laura Currie in our laboratory has since shown that transformed cell lines are not as good at forming polygonal actin structures. It also demonstrated that CLANs were present in other ocular cells including, optic nerve cells (Job et al., 2010) and RPE (in house data not yet published). These finding may make CLAN treatment targeted to the TM is problematic but may have expanded the role of CLANs into other pathologies.

8.4 CLANs and ageing

The age-related changes observed within the eye are a complex web of known and unknown converging pathways (as discussed by Gabelt and Kaufman, 2005). The findings of Hoare et al identified CLANs in tissue and demonstrated more CLANs in glaucomatous tissue (Hoare et al., 2009). The identification of TGF-β2 as a CLAN inducing agent in AH may account for the presence of CLANs in non-glaucomatous tissue and because TGF-β2 is increased in glaucoma it may also explain the increase in CLANs. The current work highlighted a relationship between donor age and CLAN incidence within tissue from non-glaucomatous donors. Our *in vitro* studies suggest that TGF-β2 is a potent CLAN inducing agent, which preferentially influences cells from older donors. Under medium only conditions no difference could be detected, however, the *ex vivo* investigations demonstrated that CLAN incidence increased with increasing donor age. The general explanation for the difference is that one is an *ex vivo* model while the other is *in vitro* and involves selection of proliferating cells and may not be representative of donor population (Freshney, 1992). There are several manipulations which may influence cell behaviour including; the presence of factors which induce the cells to proliferate when *in vivo* they do not ready do so (Polansky et al., 1981; Polansky et al., 1979). As discussed earlier, cells which are undergoing proliferation are less likely to contain a CLAN and it is noteworthy that CLANs are sparse in cell lines (highly proliferative) compared to primary TM cell cultures. The influence of the extracellular environment must again be considered. Read et al (Read

et al., 2007) and others (Gasiorowski and Russell, 2009; Thomasy et al., 2012) have highlighted that TM cells grown on culture dishes may not be true representations of *in vivo* functions. TM cells *in vivo* grow on a 3D matrix of specific composition that is under continual alteration not a topologically flat rigid surface.

The concentration of TGF-β2 is known to be increased in glaucoma (Inatani et al., 2001; Jampel et al., 1990; Ochiai and Ochiai, 2002; Tripathi et al., 1994c; Yamamoto et al., 2005) but this is not the only alteration(Hu and Ritch, 2001; Hu et al., 2002; Klenkler and Sheardown, 2004; Takai et al., 2012). In the current work treatment of BTM cells with TGF-β2 accompanied by FGF and HGF resulted in smaller induction of CLANs compared to TGF-β2 only. Ocular disease and or age-related changes of other ocular tissue, such as the lens and cornea, may upset the balance of growth factors present in the TM. Alterations in the relative quantities of these growth factors could result in altered cellular responses (Imanishi et al., 2000; Klenkler and Sheardown, 2004; Welge-Lussen et al., 2001) in this instance, increased CLAN incidence in the TM. There is limited data on the potentially inhibitory influence of different growth factors (Gohda et al., 1992; Kroening et al., 2009; Lu et al., 2006) and most data relating to the concentration of growth factors in the anterior chamber is taken from analysis of whole AH. Freddo et al highlighted that the concentrations of proteins vary and suggested that many proteins may enter the anterior chamber near to the chamber angle so that concentrations may vary within the microenvironment of specific tissues (Freddo, 2001, 2013). Although TGF-β2 has been shown in TM there is debate as to its concentrations (Pasquale et al., 1993; Tovar-Vidales et al., 2011) and so there remains no direct evidence as to how concentrations of growth factors in TM are altered by age or disease.

There is little evidence to suggest an alteration in the concentration of TGF-β2 with age other than Yamamoto et al who reported a decrease with age but these were all cataract patients (Yamamoto et al., 2005). Hales et al showed that while lens from all ages underwent TGF-β2 induced changes, the susceptibility was greater in older rats (Hales et al., 2000). It may be possible that the differences observed upon treatment with TGF-β2 were physiological. In the current investigations, attention was placed on

whether processes involved with age related changes within the TM were linked with the induction of CLANs either with or without stimulation with TGF-β2.

HTM cell cultures derived from donors of various ages were used in multiple experiments. Based upon the previous observations of cell shape change in the presence of TGF-β2 and the subsequent increase in CLANs, the cell morphology of HTM cells from donors of different ages were examined. It was observed that the majority of cells from younger donors had a more spindle appearance while cells from older donors were more epithelioid under medium only conditions. The addition of TGF-β2 induced an increase in the percentage of CLANs in all cells, although the degree of shape change was variable. It would seem that the initial morphological status of the cell determines the degree to which it is influenced by TGF-β2

Oxidative DNA damage has been shown to be increased in POAG (Izzotti, 2003; Izzotti et al., 2006) and has been related to IOP and visual field damage (Sacca and Izzotti, 2008). TM cells are in constant contact with H_2O_2 in AH and are capable of eliminating substantial amounts (Nguyen et al., 1988; Spector et al., 1998) due to the presence of antioxidants (Finkel, 2003; Rose et al., 1998). These mechanisms have however been shown to decrease with age leaving cells vulnerable to damage by ROS (Ferreira et al., 2004; Izzotti et al., 2006; Li et al., 2007; Majsterek et al., 2011). Although results from HTM cells was variable, our work in BTM cells has shown H_2O_2 is capable of inducing CLANs which persist at elevated levels even after H_2O_2 is removed this seems to tie in with Yu et al who concluded that H_2O_2 induced characteristic glaucomatous changes *in vitro* (Yu et al., 2008). Exactly how the H_2O_2 is influencing the TM cells is under debate at this time as ROS can attack many sites including the actin cytoskeleton (Zhou et al., 1999b) and DNA (Izzotti, 2003; Sacca et al., 2005). ROS is known to cause further dysfunction of the mitochondria and induce damage to nucleic acids (Abu-Amero et al., 2006; Brennan and Kantorow, 2009; He et al., 2008a; He et al., 2008b; Indo et al., 2007; Izzotti et al., 2010).

TGF-β2 did not appear to induce apoptosis in this study, nor could CLAN incidence be linked with apoptotic cells identified by TUNEL staining. It would seem likely that CLANs occur primarily in non-apoptotic cells as this would account for the increase in

CLANs observed in tissue from older donors. The loss of cell number may be preferentially occurring in non-CLAN containing cells and indicate that further work examining the cell survival value of CLAN formation may be informative. Cells are not only lost from the TM but there is also an increase in the percentage of senescent cells with age (Liton et al., 2005a). Senescent cells in this investigation and others have been reported as being more strongly attached to the substrate as they produce increased quantities of ECM (Campisi, 2011; Yamazaki et al., 2007) and have been shown to have decreased migration (Hwang et al., 2009). Given our previous findings it might have been expected therefore that senescent cells were more likely to contain a CLAN, however, this was not the case. The relationship between senescence and the actin cytoskeleton is unclear, with contradictory results from multiple investigations in different tissues (reviewed in Hwang et al., 2009). The lack of CLANs may be explained by the observation that senescent TM cells are no longer undergoing proliferation and Ca^{2+} induced changes in cell volume are arrested (Chow et al., 2007). As dynamic changes in the actin cytoskeleton are vital for these processes it may indicate that mechanisms controlling cytoskeletal arrangements are compromised so CLANs cannot form even in presence of an inducer. The interplay of different growth factors is brought to light again by Coutu & Galipeau which showed that FGF, a potent mitogen, inhibits senescence in many tissues (Coutu and Galipeau, 2011). In the current work TGF-β2 failed to induce increased senescence, which is contrary to the findings of Yu et al (Yu et al., 2010). We have no explanation for this discrepancy other than possible experimental design and tissue culture difference between the two labs.

AGE's are another avenue of research which may impact on TM cells. AGE's have already been associated with glaucoma in the optic nerve head (Tezel et al., 2007) but as yet there are no studies investigating their presence in the TM. AGE's are known to slowly accumulate on long-lived molecules and lead to progressive dysfunction (Stitt, 2001). The current work used AGE-modified matrigels to investigate whether AGEs could influence CLAN formation. Although the influence of AGE-modified matrigels appeared negligible on CLAN formation it did slow proliferation as seen in other studies (McCarthy et al., 1997). An interesting finding which arose from this study was

that modulating the rigidity of the substrate on which cells were adhered could influence CLAN formation.

8.5 Interaction of ECM and cytoskeleton

The cytoskeleton and ECM are not separate systems but are interconnected via integrin's (Brakebusch and Fassler, 2003; Faralli et al., 2011; Filla et al., 2005). Mechano-regulation of the TM induces changes in both ECM and cytoskeleton (Schwartz and DeSimone, 2008) and it is becoming clear that the interactions between these systems is important (Clark, 2012; Kaufman and Rasmussen, 2012; Stamer and Acott, 2012). The influence of substrate on the actin cytoskeleton and cell behaviour has been demonstrated in many cell types (Park et al., 2011; Schlunck et al., 2008), including HTM cells (Han et al., 2011; Park et al., 2011; Russell et al., 2008; Thomasy et al., 2012; Zhou et al., 1996). The ECM is not simply a mechanical support but is a dynamic structure and changes in ECM are among the most highly investigated aspects of TM dysfunction in both age and glaucoma (Acott and Kelley, 2008; Keller et al., 2009; Yue, 1996). Recent work would suggest that ECM becomes stiffer with age and glaucoma (Last et al., 2011) due to increased accumulation of ECM components and cross-linking (Sethi et al., 2011b; Tovar-Vidales et al., 2008), some of which is mediated by TGF-β2.

As the substrate influences cell shape (McKee et al., 2011; Russell et al., 2008) the observation that HTM cell cultures from older donors tended to have more epithelial shaped cells in comparison to younger donors may be linked to this increased stiffness. TM cells have also been shown to respond to TGF-β2 treatment in different manners depending on the substrate to which they are adherent (Han et al., 2011). These findings may also be correlated with the observation that the overall stiffness of the TM can influence outflow (Camras et al., 2012). It is interesting that CLANs (associated with cellular stiffness) are more prevalent on rigid substrate. The combined stiffness of TM cells and trabecular ECM may confound meshwork pliability in age and glaucoma where outflow resistance is high.

Much research has been carried out by Filla et al relating to the role of integrin's, in the formation of TAPAS (Filla et al., 2004a; Filla et al., 2004b; Filla et al., 2005). Recent

publication by Clark et al set out to analyse changes in cytoskeletal and integrin signalling pathways associated with DEX induced CLAN formation (Clark et al., 2013). Less than 5% of cytoskeletal proteins were affected significantly but the investigation did identify filamin B, which is co-localised with actin in CLANs, as a potential regulator of CLAN formation. They also confirmed that β3 integrin and PI-3 Kinase are involved but concluded that the influence is likely a complex assortment of changes.

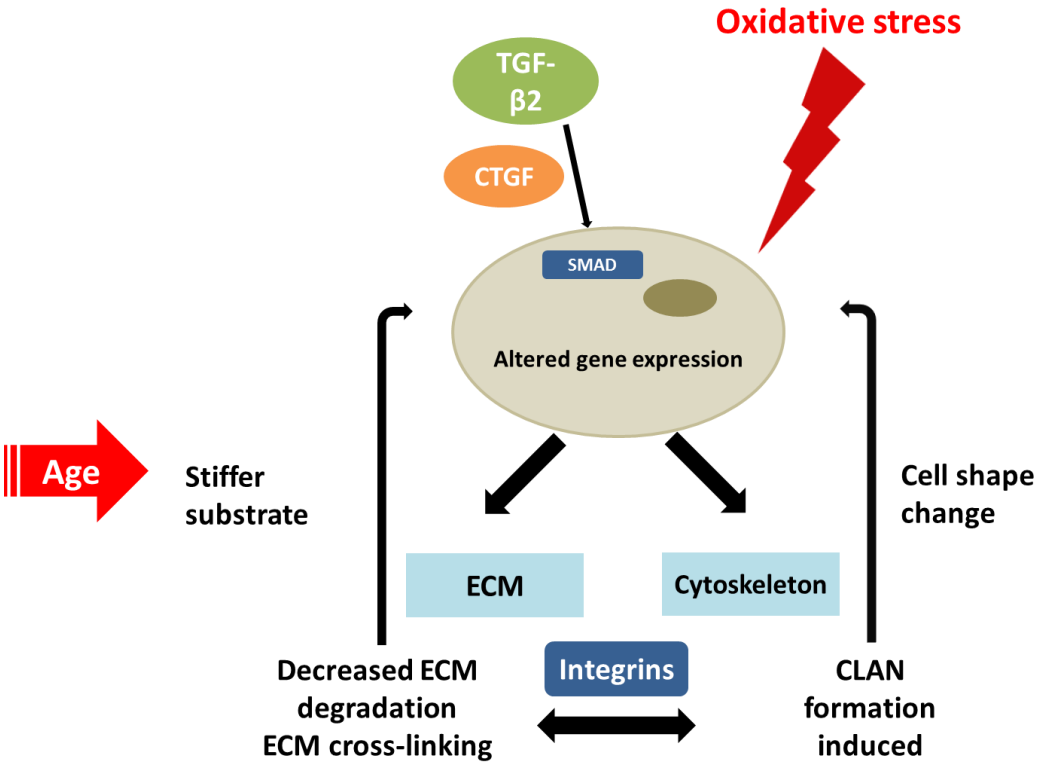

Figure 8-2. Diagram illustrating our current knowledge of how different aspects regulate TM cells

The ability of the TM cells to respond to changes in their environment is dependent on the dynamic and inter-related changes of the ECM and cytoskeleton. The presence of TGF-β2 can influence both ECM and the cytoskeleton. As yet it is unclear the exact mechanism that leads to these changes, alterations in the turnover of the ECM could influence the cytoskeleton leading to the change in cell shape observed. The presence of oxidative stress may make the cells more susceptible to TGF-β2 induced CLANs. With age, changes in the ECM could make the substrate stiffer which feeds back to the cell which will in turn alters the cytoskeleton and this may be the induction of CLANs.

8.6 Baseline CLANs

Of interest, was the finding that no healthy culture was completely void of CLANs, so establishing a baseline of 5% in HTM cells and 10% in BTM cells after 7 days in culture. The presence of CLANs without the stimulation of TGF-β2 could be alluding to another process of CLAN induction leading to the question could something present in our culture environment be capable of inducing CLANs? The identification of CLANs in non-glaucomatous tissue demonstrated that the presence of CLANs without stimulation was not simply an artefact of the culture environment (Hoare et al., 2009). As TM cells are capable of secreting a wide range of substances, including ECM components and soluble growth factors (Shifera et al., 2010), they can "condition" their environment. The modulation of the environment by the TM cells themselves may lead to CLAN formation and may explain why in our senescent studies cells attached to the substrate for extended periods of time contained more CLANs than expected as increasing the length of time on the substrate increases ECM deposition and leads to more stiff matrix (Antia et al., 2008).

8.7 Future work

While this work is adding to the picture of CLAN existence and what changes may lead to their formation, the functional significance of CLANs within a cell is still unclear. Tumminia et al and O'Reilly (O'Reilly, 2010) demonstrated that stretch was capable of inducing CLANs (Tumminia et al., 1998). Functional work is difficult due largely to the heterogeneous nature of the CLAN induction; even our most potent inducers could not induce CLAN formation in greater than 50% of cells. Modelling of TAPAS based on our measurements is currently being undertaken within the group. Others have used modelling techniques (Dalhaimer et al., 2007) in similar manners and we hope that they will provide data as to how these structures respond to different stresses and in the future may demonstrate how their presence influences outflow. A practical approach to testing the influence of CLANs in cells is the use of atomic force microscopy as demonstrated by Maguire et al (Maguire et al., 2007). The resistance provided by the cells can be measured in single cells so that the heterogeneity of the culture does not influence the results. Our plans to use this method were complicated by the need to be able to identify which cells contained a CLAN.

Although most of the work relating to the molecular structure of TAPAS is taken from works which we consider to investigate PAAs it would seem from our own work with measurements that the basic make-up of these structures could be the same. Unlike stress fibres which are bound at focal adhesion sites Filla's work has shown that although the presence of TAPAS is increased in the presence of integrin's they do not associate with focal adhesion sites. They are instead associated via their hub points with alpha-actinin, Syndecan 4 and PIP2 on the apical surface. What "holds" the CLANs in this position has yet to be demonstrated but investigating the role of GAGs would be interesting. TM cells do not exist in a 3D matrix *in vivo* but rather are attached to the trabecular beams via interactions on the basal membrane only with the apical surface coated in GAGs. The presence and potential significance of fibronectin in the outflow system appears repeatedly within the literature and seems to be linked with CLAN formation (Antia et al., 2008). The interaction between integrins and fibronectin were found to drive CLAN formation in Fillas work (Filla et al., 2006) and may help to explain the baseline level of CLANs observed. As the TM cells condition their environment with various secreted molecules they may serve to stabilise the cytoskeleton.

The signalling pathway that leads to CLAN formation remains elusive. CLANs unlike stress fibres are known to form via Arp2/3 independent means. Integrins activate cdc42 and Rac1 during cell spreading while stress fibre formation proceeds via Rho signalling which is activated independently (Price et al., 1998). Filla's group has suggested that the TAPAS formed under their experimental conditions form through Rac1 pathway (Filla et al., 2011). This is known to be involved in the formation of lamellopodia and so may be linked to the cytoplasmic position of these TAPAS.

Due to the dynamic nature of the cytoskeleton and the outflow system it is difficult to assess cause and effect. Do CLANs form with increased pressure or does pressure increase due to the presence of CLANs? Understanding these structures may require live cell imaging to understand how and when they form. The use of GFP tagging of actin has been reported in other fields of research (Ballestrem et al., 1998; Schafer et al., 1998; Small et al., 1999; Wang et al., 2008), but was not continued from the work of wade (Wade and University of, 2010) given poor transfection which has been

attributed to the phagocytic abilities of TM cells (Hoffman et al., 2005). However, as the field of microscopy expands perhaps another method will become available in the future, such as quantum dots (Yoo et al., 2008). Treatment of cells with inducers such as TGF-β2 under time lapse would demonstrate how these structures form and whether they are dynamic or fixed.

The use of perfusion systems in the future would allow for the controlled regulation of pressure within the anterior chamber. It would provide an ideal environment in which to study CLAN formation, by mimicking the *in vivo* environment. The TM cells would be subject not just to CLAN inducing agents but the cells would also be experiencing fluid flow and would be attached to dynamic ECM. A means of visualising the cytoskeleton within live TM cells would provide important information relating to CLAN dynamics. Indicating how quickly the actin cytoskeleton can re-arrange into CLAN and how the CLANs form, whether via enucleation from preformed hub points or by re-organisation of the existing stress fibres present. The ability to regulate and change the pressure would allow the relationship between CLANs and pressure could be better understood. Although high power live cell imaging under these conditions is not currently available it remains an exciting goal for future research. Given the technology currently available there may be more achievable versions of this idea. By fixing the tissue under a set perfusion rate then the influence of pressure on CLAN formation could be explored. The tissue which was received during this study would have been subject to unknown pressure changes. The IOP at the time of fixation is likely to be variable and may influence data. The possibility of getting a 3D image of the TM cell cytoskeleton while the cells are *in situ* would be a great achievement and although difficult in the perfusion systems may be possible in our *ex vivo* work. Careful removal of the TM with some of the surrounding tissue, in order to retain the TM structure, and use of confocal microscopy with 3D imaging capabilities would allow for reconstruction.

Further analysis of senescence and apoptosis markers in relation to the cytoskeleton may allow for areas of this research to be explored in more detail, however, the influence of oxidative stress would appear to be the most appealing area based on data of this thesis. The use of flow cytometry for quantification of ROS with CMH2FDA

has been successfully used elsewhere (He et al., 2008b; Lin et al., 2010) and could be applied to HTM cells from different donors to assess the baseline levels of ROS. Preliminary experiments in the current work were applied to measure any baseline differences observed in HTM cells from donors of different ages. Although the data obtained was a variable comparing the relative level of stress to the percentage of CLAN induction may provide important insights into this area.

8.8 Final summary

The current research has extended work that demonstrated the presence of CLANs in non-glaucomatous TM tissue ex vivo. The age range of donors has shown that the percentage of CLAN containing cells increases with increasing donor age in ex vivo model while *in vitro work* with both primary BTM and HTM cells has shown that the major CLAN inducing agent in AH is TGF-β2. The CLAN induction by TGF-β2 can be attenuated by the presence of other growths factors (HGF and FGF) and is correlated with the extracellular environment and cell shape. HTM cells derived from donors of different ages did not differ in CLAN incidence without stimulation. However, in the presence of TGF-β2, CLANs were induced to a greater extent in HTM cells established from older donors compared to younger donors. While exploring a potential mechanism for this difference it would seem that increased oxidative stress may make cells more susceptible to CLAN induction by TGF-β2.

CLAN inducing agents are now known to include;

Glucocorticoid -DEX	(Clark et al., 2005; Clark et al., 1994; Wade et al., 2009)
Fibronectin mediated by integrin's	(Filla et al., 2005; Filla et al., 2006)
Cyclic Stretch	(Tumminia et al., 1998) (O'Reilly, 2010)
AH mediated by TGF-β2	Current work published (O'Reilly et al., 2011)
Oxidative stress	Current work

9 References

Abu-Amero, K.K., Morales, J., Bosley, T.M., 2006. Mitochondrial abnormalities in patients with primary open-angle glaucoma. Investigative Ophthalmology & Visual Science 47, 2533-2541.

Acott, T.S., Kelley, M.J., 2008. Extracellular matrix in the trabecular meshwork. Experimental Eye Research 86, 543-561.

Adler, F.H., 1965. Physiology of the Eye. Clinical application ... With ... illustrations ... Fourth edition. C. V. Mosby Co., Saint Louis.

Adler, F.H., Alm, A., Kaufman, P.F., 2002. Adlers physiology of the eye : clinical application, 10th ed. Mosby, St. Louis, Mo.

Agarwal, R., Agarwal, P., 2010. Future Target Molecules in Antiglaucoma Therapy: TGF-beta May Have a Role to Play. Ophthalmic Research 43, 1-10.

Agarwal, R., Gupta, S.K., Agarwal, P., Saxena, R., Agrawal, S.S., 2009. Current concepts in the pathophysiology of glaucoma. Indian Journal of Ophthalmology 57, 257-266.

Agarwal, R., Lambert, W., Clark, A.F., Wilson, S.E., Wordinger, R.J., 1997. Expression of transforming growth factor beta isoforms (TGF-beta 1-3) and receptors (TGF beta RI-RIII) in cultured human trabecular meshwork cells. Investigative Ophthalmology & Visual Science 38, 2620-2620.

Agarwal, R., Talati, M., Lambert, W., Clark, A.F., Wilson, S.E., Agarwal, N., Wordinger, R.J., 1999. Fas-activated apoptosis and apoptosis mediators in human trabecular meshwork cells. Experimental Eye Research 68, 583-590.

Alberts, B., National Center for Biotechnology, I., 2002. Molecular biology of the cell, 4th / Bruce Alberts ... et al. . ed. Garland Science, New York.

Alexander, J.P., Samples, J.R., Acott, T.S., 1998. Growth factor and cytokine modulation of trabecular meshwork matrix metalloproteinase and TIMP expression. Current Eye Research 17, 276-285.

Alexander, J.P., Samples, J.R., Van Buskirk, E.M., Acott, T.S., 1991. Expression of matrix metalloproteinases and inhibitor by human trabecular meshwork. Investigative Ophthalmology & Visual Science 32, 172-180.

Allen, J.B., Davidson, M.G., Nasisse, M.P., Fleisher, L.N., McGahan, M.C., 1998. The lens influences aqueous humor levels of transforming growth factor-beta 2. Graefes Archive for Clinical and Experimental Ophthalmology 236, 305-311.

Allingham, R.R., 2005. Shields' textbook of glaucoma, 5th / R. Rand Allingham ... et al. ; M. Bruce Shields, emeritus senior author. ed. Lippincott Willliams & Wilkins, Philadelphia Pa. ; London.

Allingham, R.R., de Kater, A.W., Ethier, C.R., Anderson, P.J., Hertzmark, E., Epstein, D.L., 1992. The relationship between pore density and outflow facility in human eyes. Investigative Ophthalmology & Visual Science 33, 1661-1669.

Allingham, R.R., Liu, Y.T., Rhee, D.J., 2009. The genetics of primary open-angle glaucoma: A review. Experimental Eye Research 88, 837-844.

Alm, A., Nilsson, S.F.E., 2009. Uveoscleral outflow - A review. Experimental Eye Research 88, 760-768.

Alvarado, J., Murphy, C., Juster, R., 1984. Trabecular Meshwork Cellularity in Primary Open-Angle Glaucoma and Nonglaucomatous Normals. Ophthalmology 91, 564-579.

Alvarado, J., Murphy, C., Polansky, J., Juster, R., 1981. Age-Related-Changes in Trabecular Meshwork Cellularity. Investigative Ophthalmology & Visual Science 21, 714-727.
Alvarado, J.A., Betanzos, A., Franse-Carman, L., Chen, J., Gonzalez-Mariscal, L., 2004. Endothelia of Schlemm's canal and trabecular meshwork: distinct molecular, functional, and anatomic features. American Journal of Physiology-Cell Physiology 286, C621-C634.
Alvarado, J.A., Wood, I., Polansky, J.R., 1982. Human trabecular cells. II. Growth pattern and ultrastructural characteristics. Investigative Ophthalmology & Visual Science 23, 464-478.
Anderson, P.J., Wang, J., Epstein, D.L., 1980. Metabolism of calf trabecular (reticular) meshwork. Investigative Ophthalmology & Visual Science 19, 13-20.
Annes, J.P., Munger, J.S., Rifkin, D.B., 2003. Making sense of latent TGF beta activation. Journal of Cell Science 116, 217-224.
Antia, M., Baneyx, G., Kubow, K.E., Vogel, V., 2008. Fibronectin in aging extracellular matrix fibrils is progressively unfolded by cells and elicits an enhanced rigidity response. Faraday Discussions 139, 229-249; discussion 309-225, 419-220.
Araki-Sasaki, K., Danjo, S., Kawaguchi, S., Hosohata, J., Tano, Y., 1997. Human hepatocyte growth factor (HGF) in the aqueous humor. Japanese Journal of Ophthalmology 41, 409-413.
Aslan, M., Dogan, S., Kucuksayan, E., 2013. Oxidative stress and potential applications of free radical scavengers in glaucoma. Redox Report : Communications in Free Radical Research 18, 76-87.
Attisano, L., Wrana, J.L., Lopezcasillas, F., Massague, J., 1994. Tgf-Beta Receptors and Actions. Biochimica Et Biophysica Acta-Molecular Cell Research 1222, 71-80.
Aydin, E., Cumurca, T., Ozugurlu, F., Ozyurt, H., Sahinoglu, S., Mendil, D., Hasdemir, E., 2005. Levels of iron, zinc, and copper in aqueous humor, lens, and serum in nondiabetic and diabetic patients - Their relation to cataract. Biological Trace Element Research 108, 33-41.
Babizhayev, M.A., Yegorov, Y.E., 2011. Senescent Phenotype of Trabecular Meshwork Cells Displays Biomarkers in Primary Open-Angle Glaucoma. Current Molecular Medicine 11, 528-552.
Bachmann, B., Birke, M., Kook, D., Eichhorn, M., Lutjen-Drecoll, E., 2006. Ultrastructural and biochemical evaluation of the porcine anterior chamber perfusion model. Investigative Ophthalmology & Visual Science 47, 2011-2020.
Bagnis, A., Papadia, M., Scotto, R., Traverso, C.E., 2011. Current and emerging medical therapies in the treatment of glaucoma. Expert Opinion on Emerging Drugs 16, 293-307.
Baird, D.T., Collins, J., Egozcue, J., Evers, L.H., Gianaroli, L., Leridon, H., Sunde, A., Templeton, A., Van Steirteghem, A., Cohen, J., Crosignani, P.G., Devroey, P., Diedrich, K., Fauser, B.C.J.M., Fraser, J., Glasier, A., Liebaers, I., Mautone, G., Penney, G., Tarlatzis, B., Grp, E.C.W., 2005. Fertility and ageing. Human Reproduction Update 11, 261-276.
Baleriola, J., Garcia-Feijoo, J., Martinez-de-la-Casa, J.M., Fernandez-Cruz, A., de la Rosa, E.J., Fernandez-Durango, R., 2008. Apoptosis in the trabecular meshwork of glaucomatous patients. Molecular Vision 14, 1513-1516.

Ballestrem, C., Wehrle-Haller, B., Imhof, B.A., 1998. Actin dynamics in living mammalian cells. Journal of Cell Science 111 (Pt 12), 1649-1658.
Barany, E., 1959. Pore size and passage of particulate matter through the trabecular meshwork. Documenta ophthalmologica. Advances in ophthalmology 13, 41-55.
Batterbury, M., Bowling, B., Murphy, C., 2009. Ophthalmology : an illustrated colour text, 3rd ed. Elsevier/Churchill Livingstone, Edinburgh ; New York.
Benezra, D., Sachs, U., 1974. Growth factors in aqueous humor of normal and inflamed eyes of rabbits. Investigative Ophthalmology 13, 868-870.
Bhargava, M., Joseph, A., Knesel, J., Halaban, R., Li, Y., Pang, S., Goldberg, I., Setter, E., Donovan, M.A., Zarnegar, R., et al., 1992. Scatter factor and hepatocyte growth factor: activities, properties, and mechanism. Cell growth & differentiation : the molecular biology journal of the American Association for Cancer Research 3, 11-20.
Bikfalvi, A., Klein, S., Pintucci, G., Rifkin, D.B., 1997. Biological roles of fibroblast growth factor-2. Endocrine Reviews 18, 26-45.
Bill, A., 1975. Blood circulation and fluid dynamics in the eye. Physiological Reviews 55, 383-417.
Bill, A., 1993. Some aspects of aqueous humour drainage. Eye (London) 7 (Pt 1), 14-19.
Bill, A., Phillips, C.I., 1971. Uveoscleral Drainage of Aqueous Humour in Human Eyes. Experimental Eye Research 12, 275-&.
Bill, A., Tornquist, P., Alm, A., 1980. Permeability of the intraocular blood vessels. Transactions of the Ophthalmological Societies of the United Kingdom 100, 332-336.
Bito, L.Z., 1977. The physiology and pathophysiology of intraocular fluids. Experimental Eye Research 25 Suppl, 273-289.
Black, A.A., Wood, J.M., Lovie-Kitchin, J.E., 2011. Inferior field loss increases rate of falls in older adults with glaucoma. Optometry and Vision Science 88, 1275-1282.
Boldea, R.C., Roy, S., Mermoud, A., 2001. Ageing of Schlemm's canal in nonglaucomatous subjects. International Ophthalmology 24, 67-77.
Bollinger, K.E., Crabb, J.S., Yuan, X.L., Putliwala, T., Clark, A.F., Crabb, J.W., 2011. Quantitative Proteomics: TGF beta(2) Signaling in Trabecular Meshwork Cells. Investigative Ophthalmology & Visual Science 52, 8287-8294.
Borras, T., 2003. Gene expression in the trabecular meshwork and the influence of intraocular pressure. Progress in Retinal and Eye Research 22, 435-463.
Borras, T., Rowlette, L.L., Tamm, E.R., Gottanka, J., Epstein, D.L., 2002. Effects of elevated intraocular pressure on outflow facility and TIGR/MYOC expression in perfused human anterior segments. Investigative Ophthalmology & Visual Science 43, 33-40.
Bours, J., 1990. The protein distribution of bovine, human and rabbit aqueous humour and the difference in composition before and after disruption of the blood/aqueous humour barrier. Lens and Eye Toxicity Research 7, 491-503.
Bradley, J.M., Kelley, M.J., Zhu, X., Anderssohn, A.M., Alexander, J.P., Acott, T.S., 2001. Effects of mechanical stretching on trabecular matrix metalloproteinases. Investigative Ophthalmology & Visual Science 42, 1505-1513.
Bradley, J.M., Vranka, J., Colvis, C.M., Conger, D.M., Alexander, J.P., Fisk, A.S., Samples, J.R., Acott, T.S., 1998. Effect of matrix metalloproteinases activity on outflow in perfused human organ culture. Investigative Ophthalmology & Visual Science 39, 2649-2658.

Brakebusch, C., Fassler, R., 2003. The integrin-actin connection, an eternal love affair. The EMBO journal 22, 2324-2333.
Brennan, L.A., Kantorow, M., 2009. Mitochondrial function and redox control in the aging eye: role of MsrA and other repair systems in cataract and macular degenerations. Experimental Eye Research 88, 195-203.
Briggs, M.C., Grierson, I., Hiscott, P., Hunt, J.A., 2000. Active scatter factor (HGF/SF) in proliferative vitreoretinal disease. Investigative Ophthalmology & Visual Science 41, 3085-3094.
Bronnum-Hansen, H., Petersen, I., Jeune, B., Christensen, K., 2009. Lifetime according to health status among the oldest olds in Denmark. Age and Ageing 38, 47-51.
Brubaker, R.F., Bourne, W.M., Bachman, L.A., McLaren, J.W., 2000. Ascorbic acid content of human corneal epithelium. Investigative Ophthalmology & Visual Science 41, 1681-1683.
Buller, C., Johnson, D.H., Tschumper, R.C., 1990. Human Trabecular Meshwork Phagocytosis - Observations in an Organ-Culture System. Investigative Ophthalmology & Visual Science 31, 2156-2163.
Burgess, W.H., Friesel, R., Winkles, J.A., 1994. Structure-function studies of FGF-1: dissociation and partial reconstitution of certain of its biological activities. Molecular Reproduction and Development 39, 56-60; discussion 60-51.
Caballero, M., Liton, P.B., Challa, P., Epstein, D.L., Gonzalez, P., 2004. Effects of donor age on proteasome activity and senescence in trabecular meshwork cells. Biochemical and biophysical research communications 323, 1048-1054.
Caballero, M., Liton, P.B., Epstein, D.L., Gonzalez, P., 2003. Proteasome inhibition by chronic oxidative stress in human trabecular meshwork cells. Biochemical and biophysical research communications 308, 346-352.
Cai, S., Liu, X.Y., Glasser, A., Volberg, T., Filla, M., Geiger, B., Polansky, J.R., Kaufman, P.L., 2000. Effect of latrunculin-A on morphology and actin-associated adhesions of cultured human trabecular meshwork cells. Molecular Vision 6, 132-143.
Calthorpe, C.M., Grierson, I., 1988. Invitro Study of the Migration of Bovine Trabecular Meshwork Cells. Ophthalmic Research 20, 73-73.
Calthorpe, C.M., Grierson, I., Hitchings, R.A., 1991. Chemoattractants Produced by Ocular Cells Induce Trabecular Meshwork Cell-Migration. International Ophthalmology 15, 185-191.
Campisi, J., 2011. Cellular senescence: putting the paradoxes in perspective. Current Opinion in Genetics & Development 21, 107-112.
Camras, L.J., Stamer, W.D., Epstein, D., Gonzalez, P., Yuan, F., 2012. Differential Effects of Trabecular Meshwork Stiffness on Outflow Facility in Normal Human and Porcine Eyes. Investigative Ophthalmology & Visual Science 53, 5242-5250.
Canning, C.R., Greaney, M.J., Dewynne, J.N., Fitt, A.D., 2002. Fluid flow in the anterior chamber of a human eye. IMA J Math Appl Med Biol 19, 31-60.
Cao, Y., Wei, H., Pfaffl, M., Da, B., Li, Z., 2004. Apoptosis of human trabecular meshwork cells induced by transforming growth factor-beta2 in vitro. Journal of Huazhong University of Science and Technology. Medical sciences 24, 87-89, 94.
Cao, Y., Wei, H., Zhang, Y., Da, B., Lu, Y., 2002. Effect of transforming growth factor-beta(2) on extracellular matrix synthesis in bovine trabecular meshwork cells. Chinese Journal of Ophthalmology (Zhonghua Yan Ke Za Zhi) 38, 429-432.

Chow, J., Liton, P.B., Luna, C., Wong, F., Gonzalez, P., 2007. Effect of cellular senescence on the P2Y-receptor mediated calcium response in trabecular meshwork cells. Molecular Vision 13, 1926-1933.
Chowdhury, U.R., Madden, B.J., Charlesworth, M.C., Fautsch, M.P., 2010. Proteome Analysis of Human Aqueous Humor. Investigative Ophthalmology & Visual Science 51, 4921-4931.
Christensen, K., Doblhammer, G., Rau, R., Vaupel, J.W., 2009. Ageing populations: the challenges ahead. Lancet 374, 1196-1208.
Civan, M.M., Macknight, A.D., 2004. The ins and outs of aqueous humour secretion. Experimental Eye Research 78, 625-631.
Clark, A.F., 2012. The Cell and Molecular Biology of Glaucoma: Biomechanical Factors in Glaucoma. Investigative Ophthalmology & Visual Science 53, 2473-2475.
Clark, A.F., Brotchie, D., Read, A.T., Hellberg, P., English-Wright, S., Pang, I.H., Ethier, C.R., Grierson, I., 2005. Dexamethasone alters F-actin architecture and promotes cross-linked actin network formation in human trabecular meshwork tissue. Cell Motility and the Cytoskeleton 60, 83-95.
Clark, A.F., McLaughlin, M.A., Tuttle, L., Chandler, M.L., 1996. Corticosteroid-induced ocular hypertension in cynomolgus monkeys. Investigative Ophthalmology & Visual Science 37, 937-937.
Clark, A.F., Wilson, K., Dekater, A.W., Allingham, R.R., Mccartney, M.D., 1995. Dexamethasone-Induced Ocular Hypertension in Perfusion-Cultured Human Eyes. Investigative Ophthalmology & Visual Science 36, 478-489.
Clark, A.F., Wilson, K., McCartney, M.D., Miggans, S.T., Kunkle, M., Howe, W., 1994. Glucocorticoid-induced formation of cross-linked actin networks in cultured human trabecular meshwork cells. Investigative Ophthalmology & Visual Science 35, 281-294.
Clark, A.F., Wordinger, R.J., 2009. The role of steroids in outflow resistance. Experimental Eye Research 88, 752-759.
Clark, R., Nosie, A., Walker, T., Faralli, J.A., Filla, M.S., Barrett-Wilt, G., Peters, D.M., 2013. Comparative Genomic and Proteomic Analysis of Cytoskeletal Changes in Dexamethasone-Treated Trabecular Meshwork Cells. Molecular & Cellular Proteomics 12, 194-206.
Coleman, A.L., Cummings, S.R., Yu, F., Kodjebacheva, G., Ensrud, K.E., Gutierrez, P., Stone, K.L., Cauley, J.A., Pedula, K.L., Hochberg, M.C., Mangione, C.M., Study Group of Osteoporotic, F., 2007. Binocular visual-field loss increases the risk of future falls in older white women. Journal of the American Geriatrics Society 55, 357-364.
Coleman, A.L., Miglior, S., 2008. Risk factors for glaucoma onset and progression. Survey of Ophthalmology 53 Suppl1, S3-10.
Coroneo, M.T., Korbmacher, C., Flugel, C., Stiemer, B., Lutjendrecoll, E., Wiederholt, M., 1991. Electrical and Morphological Evidence for Heterogeneous Populations of Cultured Bovine Trabecular Meshwork Cells. Experimental Eye Research 52, 375-388.
Costarides, A.P., Riley, M.V., Green, K., 1991. Roles of catalase and the glutathione redox cycle in the regulation of anterior-chamber hydrogen peroxide. Ophthalmic Research 23, 284-294.
Coudrillier, B., Tian, J., Alexander, S., Myers, K.M., Quigley, H.A., Nguyen, T.D., 2012. Biomechanics of the human posterior sclera: age- and glaucoma-related changes measured using inflation testing. Investigative Ophthalmology & Visual Science 53, 1714-1728.

Cousins, S.W., Mccabe, M.M., Danielpour, D., Streilein, J.W., 1991. Identification of Transforming Growth-Factor-Beta as an Immunosuppressive Factor in Aqueous-Humor. Investigative Ophthalmology & Visual Science 32, 2201-2211.
Coutu, D.L., Galipeau, J., 2011. Roles of FGF signaling in stem cell self-renewal, senescence and aging. Aging-Us 3, 920-933.
Cracknell, K.P.B., Grierson, I., 2009. Prostaglandin analogues in the anterior eye: Their pressure lowering action and side effects. Experimental Eye Research 88, 786-791.
Cracknell, K.P.B., Grierson, I., Hogg, P., Majekodunmi, A.A., Watson, P., Marmion, V., 2006. Melanin in the trabecular meshwork is associated with age, POAG but not Latanoprost treatment. A masked morphometric study. Experimental Eye Research 82, 986-993.
Cramer, L.P., Siebert, M., Mitchison, T.J., 1997. Identification of novel graded polarity actin filament bundles in locomoting heart fibroblasts: implications for the generation of motile force. Journal of Cell Biology 136, 1287-1305.
Crawford Downs, J., Roberts, M.D., Sigal, I.A., 2011. Glaucomatous cupping of the lamina cribrosa: a review of the evidence for active progressive remodeling as a mechanism. Experimental Eye Research 93, 133-140.
Crimmins, E.M., 2004. Trends in the health of the elderly. Annual Review of Public Health 25, 79-98.
Cuervo, A.M., Dice, J.F., 2000. When lysosomes get old. Experimental Gerontology 35, 119-131.
Dalhaimer, P., Discher, D.E., Lubensky, T.C., 2007. Crosslinked actin networks show liquid crystal elastomer behaviour, including soft-mode elasticity. Nature Physics 3, 354-360.
David, M., Petit, D., Bertoglio, J., 2012. Cell cycle regulation of Rho signaling pathways. Cell Cycle 11, 3003-3010.
Davson, H., 1969. The Eye, 2nd ed. Academic Press, New York ; London.
de Boer, J.H., Limpens, J., Orengo-Nania, S., de Jong, P.T., La Heij, E., Kijlstra, A., 1994. Low mature TGF-beta 2 levels in aqueous humor during uveitis. Investigative Ophthalmology & Visual Science 35, 3702-3710.
De La Paz, M.A., Epstein, D.L., 1996. Effect of age on superoxide dismutase activity of human trabecular meshwork. Investigative Ophthalmology & Visual Science 37, 1849-1853.
Dekater, A.W., Shahsafaei, A., Epstein, D.L., 1992. Localization of Smooth-Muscle and Nonmuscle Actin Isoforms in the Human Aqueous Outflow Pathway. Investigative Ophthalmology & Visual Science 33, 424-429.
Dernouchamps, J.P., 1982. The proteins of the aqueous humour. Documenta ophthalmologica. Advances in ophthalmology 53, 193-248.
Derynck, R., Zhang, Y., Feng, X.H., 1998. Smads: transcriptional activators of TGF-beta responses. Cell 95, 737-740.
Derynck, R., Zhang, Y.E., 2003. Smad-dependent and Smad-independent pathways in TGF-beta family signalling. Nature 425, 577-584.
Dimri, G.P., Lee, X., Basile, G., Acosta, M., Scott, G., Roskelley, C., Medrano, E.E., Linskens, M., Rubelj, I., Pereira-Smith, O., et al., 1995. A biomarker that identifies senescent human cells in culture and in aging skin in vivo. Proceedings of the National Academy of Sciences of the United States of America 92, 9363-9367.

Dolinis, J., Harrison, J.E., Andrews, G.R., 1997. Factors associated with falling in older Adelaide residents. Australian and New Zealand journal of public health 21, 462-468.
Dominguez, R., Holmes, K.C., 2011. Actin structure and function. Annu Rev Biophys 40, 169-186.
dos Remedios, C.G., Chhabra, D., Kekic, M., Dedova, I.V., Tsubakihara, M., Berry, D.A., Nosworthy, N.J., 2003. Actin binding proteins: regulation of cytoskeletal microfilaments. Physiological Reviews 83, 433-473.
Duan, X., Xue, P., Wang, N., Dong, Z., Lu, Q., Yang, F., 2010. Proteomic analysis of aqueous humor from patients with primary open angle glaucoma. Molecular Vision 16, 2839-2846.
Epstein, D.L., Freddo, T.F., Anderson, P.J., Patterson, M.M., Bassett-Chu, S., 1986. Experimental obstruction to aqueous outflow by pigment particles in living monkeys. Investigative Ophthalmology & Visual Science 27, 387-395.
Epstein, D.L., Rowlette, L.L., Roberts, B.C., 1999. Acto-myosin drug effects and aqueous outflow function. Investigative Ophthalmology & Visual Science 40, 74-81.
Ericksonlamy, K., Rohen, J.W., Grant, W.M., 1991. Outflow Facility Studies in the Perfused Human Ocular Anterior Segment. Experimental Eye Research 52, 723-731.
Ericksonlamy, K., Schroeder, A., Epstein, D.L., 1992. Ethacrynic-Acid Induces Reversible Shape and Cytoskeletal Changes in Cultured-Cells. Investigative Ophthalmology & Visual Science 33, 2631-2640.
Ethier, C.R., 2002. The inner wall of Schlemm's canal. Experimental Eye Research 74, 161-172.
Ethier, C.R., Coloma, F.M., de Kater, A.W., Allingham, R.R., 1995. Retroperfusion studies of the aqueous outflow system. Part 2: Studies in human eyes. Investigative Ophthalmology & Visual Science 36, 2466-2475.
Ethier, C.R., Coloma, F.M., Sit, A.J., Johnson, M., 1998. Two pore types in the inner-wall endothelium of Schlemm's canal. Investigative Ophthalmology & Visual Science 39, 2041-2048.
Ethier, C.R., Johnson, M., Ruberti, J., 2004a. Ocular biomechanics and biotransport. Annual Review of Biomedical Engineering 6, 249-273.
Ethier, C.R., Read, A.T., Chan, D., 2004b. Biomechanics of Schlemm's canal endothelial cells: Influence on F-actin architecture. Biophysical Journal 87, 2828-2837.
Ethier, C.R., Read, A.T., Chan, D.W.H., 2006. Effects of latrunculin-B on outflow facility and trabecular meshwork structure in human eyes. Investigative Ophthalmology & Visual Science 47, 1991-1998.
Fanger, B.O., Wakefield, L.M., Sporn, M.B., 1986. Structure and Properties of the Cellular Receptor for Transforming Growth-Factor Type-Beta. Biochemistry 25, 3083-3091.
Faralli, J.A., Newman, J.R., Sheibani, N., Dedhar, S., Peters, D.M., 2011. Integrin-linked kinase regulates integrin signaling in human trabecular meshwork cells. Investigative Ophthalmology & Visual Science 52, 1684-1692.
Faralli, J.A., Schwinn, M.K., Gonzalez, J.M., Filla, M.S., Peters, D.M., 2009. Functional properties of fibronectin in the trabecular meshwork. Experimental Eye Research 88, 689-693.
Ferreira, S.M., Lerner, S.F., Brunzini, R., Evelson, P.A., Llesuy, S.F., 2004. Oxidative stress markers in aqueous humor of glaucoma patients. American Journal of Ophthalmology 137, 62-69.

Ferrer, E., 2006. Trabecular meshwork as a new target for the treatment of glaucoma. Drug News Perspect 19, 151-158.
Filla, M.S., Clark, A.F., Kaufman, P.L., Peters, D.M., 2004a. Vertices of cross-linked actin networks (CLANs) in Human Trabecular Meshwork (HTM) cells spread on various extracellular matrix proteins contain specific signaling molecules. Investigative Ophthalmology & Visual Science 45, U440-U440.
Filla, M.S., David, G., Weinreb, R.N., Kaufman, P.L., Peters, D.M., 2004b. Distribution of syndecans 1-4 within the anterior segment of the human eye: expression of a variant syndecan-3 and matrix-associated syndecan-2. Experimental Eye Research 79, 61-74.
Filla, M.S., Kaufman, P.L., Peters, D.M., 2005. b1 and b3 integrins cooperate to induce cross-linked actin networks (CLANs) in human trabecular meshwork (HTM) cells. Investigative Ophthalmology & Visual Science 46, -.
Filla, M.S., Schwinn, M.K., Nosie, A.K., Clark, R.W., Peters, D.M., 2011. Dexamethasone-Associated Cross-Linked Actin Network Formation in Human Trabecular Meshwork Cells Involves beta 3 Integrin Signaling. Investigative Ophthalmology & Visual Science 52, 2952-2959.
Filla, M.S., Woods, A., Kaufman, P.L., Peters, D.M., 2006. Beta1 and beta3 integrins cooperate to induce syndecan-4-containing cross-linked actin networks in human trabecular meshwork cells. Investigative Ophthalmology & Visual Science 47, 1956-1967.
Finkel, T., 2003. Oxidant signals and oxidative stress. Current Opinion in Cell Biology 15, 247-254.
Finkel, T., Holbrook, N.J., 2000. Oxidants, oxidative stress and the biology of ageing. Nature 408, 239-247.
Fleenor, D.L., Shepard, A.R., Hellberg, P.E., Jacobson, N., Pang, I.H., Clark, A.F., 2006. TGF beta 2-induced changes in human trabecular meshwork: Implications for intraocular pressure. Investigative Ophthalmology & Visual Science 47, 226-234.
Fletcher, D.A., Mullins, R.D., 2010. Cell mechanics and the cytoskeleton. Nature 463, 485-492.
Flugel-Koch, C., Ohlmann, A., Fuchshofer, R., Welge-Lussen, U., Tamm, E.R., 2004. Thrombospondin-1 in the trabecular meshwork: localization in normal and glaucomatous eyes, and induction by TGF-beta 1 and dexamethasone in vitro. Experimental Eye Research 79, 649-663.
Flugel, C., Tamm, E., Lutjendrecoll, E., 1991. Different Cell-Populations in Bovine Trabecular Meshwork - an Ultrastructural and Immunocytochemical Study. Experimental Eye Research 52, 681-690.
Forrester, J.V., 2008. The eye : basic sciences in practice, 3rd ed. Saunders Elsevier, Edinburgh ; New York.
Foster, A., Resnikoff, S., 2005. The impact of Vision 2020 on global blindness. Eye (London) 19, 1133-1135.
Foster, P.J., Buhrmann, R., Quigley, H.A., Johnson, G.J., 2002. The definition and classification of glaucoma in prevalence surveys. British Journal of Ophthalmology 86, 238-242.
Franco, O.H., Kirkwood, T.B., Powell, J.R., Catt, M., Goodwin, J., Ordovas, J.M., van der Ouderaa, F., 2007. Ten commandments for the future of ageing research in the UK: a vision for action. BMC Geriatrics 7, 10.

Franke, R.P., Grafe, M., Schnittler, H., Seiffge, D., Mittermayer, C., Drenckhahn, D., 1984. Induction of human vascular endothelial stress fibres by fluid shear stress. Nature 307, 648-649.
Freddo, T.F., 2001. Shifting the paradigm of the blood-aqueous barrier. Experimental Eye Research 73, 581-592.
Freddo, T.F., 2013. A contemporary concept of the blood-aqueous barrier. Progress in Retinal and Eye Research 32, 181-195.
Freddo, T.F., Raviola, G., 1982. Freeze-fracture analysis of the interendothelial junctions in the blood vessels of the iris in Macaca mulatta. Investigative Ophthalmology & Visual Science 23, 154-167.
Freeman, E.E., Munoz, B., Rubin, G., West, S.K., 2007. Visual field loss increases the risk of falls in older adults: the Salisbury eye evaluation. Investigative Ophthalmology & Visual Science 48, 4445-4450.
Freshney, R.I., 1992. Animal Cell Culture : Practical Approach, 2Rev. ed. I. R. L. P.
Fuchshofer, R., Stephan, D.A., Russell, P., Tamm, E.R., 2009. Gene expression profiling of TGF beta 2-and/or BMP7-treated trabecular meshwork cells: Identification of Smad7 as a critical inhibitor of TGF-beta 2 signaling. Experimental Eye Research 88, 1020-1032.
Fuchshofer, R., Tamm, E.R., 2009. Modulation of extracellular matrix turnover in the trabecular meshwork. Experimental Eye Research 88, 683-688.
Fuchshofer, R., Tamm, E.R., 2012. The role of TGF-beta in the pathogenesis of primary open-angle glaucoma. Cell and Tissue Research 347, 279-290.
Fuchshofer, R., Welge-Lussen, U., Lutjen-Drecoll, E., 2003. The effect of TGF-beta 2 on human trabecular meshwork extracellular proteolytic system. Experimental Eye Research 77, 757-765.
Fuchshofer, R., Welge-Lussen, U., Lutyen-Drecoll, E., Birke, M., 2006. Biochemical and morphological analysis of basement membrane component expression in corneoscleral and cribriform human trabecular meshwork cells. Investigative Ophthalmology & Visual Science 47, 794-801.
Fuchshofer, R., Yu, A.H.L., Welge-Lussen, U., Tamm, E.R., 2007. Bone morphogenetic protein-7 is an antagonist of transforming growth factor-beta 2 in human trabecular meshwork cells. Investigative Ophthalmology & Visual Science 48, 715-726.
Fujimoto, T., Inoue, T., Kameda, T., Kasaoka, N., Inoue-Mochita, M., Tsuboi, N., Tanihara, H., 2012. Involvement of RhoA/Rho-Associated Kinase Signal Transduction Pathway in Dexamethasone-Induced Alterations in Aqueous Outflow. Investigative Ophthalmology & Visual Science 53, 7097-7108.
Furlong, R.A., Takehara, T., Taylor, W.G., Nakamura, T., Rubin, J.S., 1991. Comparison of biological and immunochemical properties indicates that scatter factor and hepatocyte growth factor are indistinguishable. Journal of Cell Science 100 (Pt 1), 173-177.
Gaasterland, D.E., Pederson, J.E., MacLellan, H.M., Reddy, V.N., 1979. Rhesus monkey aqueous humor composition and a primate ocular perfusate. Investigative Ophthalmology & Visual Science 18, 1139-1150.
Gabelt, B.T., Gottanka, J., Lutjen-Drecoll, E., Kaufman, P.L., 2003. Aqueous humor dynamics and trabecular meshwork and anterior ciliary muscle morphologic changes with age in rhesus monkeys. Investigative Ophthalmology & Visual Science 44, 2118-2125.

Gabelt, B.T., Kaufman, P.L., 2005. Changes in aqueous humor dynamics with age and glaucoma. Progress in Retinal and Eye Research 24, 612-637.
Gasiorowski, J.Z., Russell, P., 2009. Biological properties of trabecular meshwork cells. Experimental Eye Research 88, 671-675.
Gerometta, R., Escobar, D., Candia, O.A., 2011. An hypothesis on pressure transmission from anterior chamber to optic nerve. Medical Hypotheses 77, 827-831.
Gerometta, R., Podos, S.M., Candia, O.A., Wu, B., Malgor, L.A., Mittag, T., Danias, J., 2004. Steroid-induced ocular hypertension in normal cattle. Archives of Ophthalmology 122, 1492-1497.
Gherardi, E., Stoker, M., 1991. Hepatocyte growth factor--scatter factor: mitogen, motogen, and met. Cancer Cells 3, 227-232.
Gipson, I.K., Anderson, R.A., 1979. Actin-Filaments in Cells of Human Trabecular Meshwork and Schlemms Canal. Investigative Ophthalmology & Visual Science 18, 547-561.
Glenn, J.V., Mahaffy, H., Wu, K.Q., Smith, G., Nagai, R., Simpson, D.A.C., Boulton, M.E., Stitt, A.W., 2009. Advanced Glycation End Product (AGE) Accumulation on Bruch's Membrane: Links to Age-Related RPE Dysfunction. Investigative Ophthalmology & Visual Science 50, 441-451.
Glenn, J.V., Stitt, A.W., 2009. The role of advanced glycation end products in retinal ageing and disease. Biochimica et Biophysica Acta: Protein Structure and Molecular Enzymology 1790, 1109-1116.
Gohda, E., Matsunaga, T., Kataoka, H., Yamamoto, I., 1992. TGF-beta is a potent inhibitor of hepatocyte growth factor secretion by human fibroblasts. Cell biology international reports 16, 917-926.
Gong, H., Underhill, C.B., Freddo, T.F., 1994. Hyaluronan in the bovine ocular anterior segment, with emphasis on the outflow pathways. Investigative Ophthalmology & Visual Science 35, 4328-4332.
Gong, H.Y., Trinkaus-Randall, V., Freddo, T.F., 1989. Ultrastructural immunocytochemical localization of elastin in normal human trabecular meshwork. Current Eye Research 8, 1071-1082.
Gordon, S.R., 1990. Changes in Extracellular-Matrix Proteins and Actin during Corneal Endothelial Growth. Investigative Ophthalmology & Visual Science 31, 94-101.
Gottanka, J., Chan, D., Eichhorn, M., Lutjen-Drecoll, E., Ethier, C.R., 2004. Effects of TGF-beta2 in perfused human eyes. Investigative Ophthalmology & Visual Science 45, 153-158.
Gould, D.B., Smith, R.S., John, S.W.M., 2004. Anterior segment development relevant to glaucoma. International Journal of Developmental Biology 48, 1015-1029.
Grant, W.M., 1963. Experimental aqueous perfusion in enucleated human eyes. Archives of Ophthalmology 69, 783-801.
Green, K., Sherman, S.H., Laties, A.M., Pederson, J.E., Gaasterland, D.E., MacLellan, H.M., 1977. Fate of anterior chamber tracers in the living rhesus monkey eye with evidence for uveo-vortex outflow. Transactions of the Ophthalmological Societies of the United Kingdom 97, 731-739.
Grierson, I., 1987. The outflow system in health and disease. Bulletin de la Societe belge d'Ophtalmologie 225 Pt 2, 1-43.

Grierson, I., Day, J., Unger, W.G., Ahmed, A., 1986. Phagocytosis of Latex Microspheres by Bovine Meshwork Cells in Culture. Graefes Archive for Clinical and Experimental Ophthalmology 224, 536-544.
Grierson, I., Heathcote, L., Hiscott, P., Hogg, P., Briggs, M., Hagan, S., 2000. Hepatocyte growth factor/scatter factor in the eye. Progress in Retinal and Eye Research 19, 779-802.
Grierson, I., Howes, R.C., 1987. Age-Related Depletion of the Cell-Population in the Human Trabecular Meshwork. Eye-Transactions of the Ophthalmological Societies of the United Kingdom 1, 204-210.
Grierson, I., Howes, R.C., Wang, Q., 1984. Age-Related-Changes in the Canal of Schlemm. Experimental Eye Research 39, 505-512.
Grierson, I., Kissun, R., Ayad, S., Phylactos, A., Ahmed, S., Unger, W.G., Day, J.E., 1985a. The Morphological Features of Bovine Meshwork Cells-Invitro and Their Synthetic Activities. Graefes Archive for Clinical and Experimental Ophthalmology 223, 225-236.
Grierson, I., Lee, W.R., 1973. Effect of Increased Intraocular-Pressure on Endothelium of Schlemms Canal. Experimental Eye Research 17, 398-399.
Grierson, I., Lee, W.R., 1974. Junctions between Cells of Trabecular Meshwork. Albrecht Von Graefes Archiv Fur Klinische Und Experimentelle Ophthalmologie 192, 89-104.
Grierson, I., Lee, W.R., 1977. Pressure Effects on Distribution of Extracellular Materials in Rhesus-Monkey Outflow Apparatus. Albrecht Von Graefes Archiv Fur Klinische Und Experimentelle Ophthalmologie 203, 155-168.
Grierson, I., Marshall, J., Robins, E., 1983. Human Trabecular Meshwork in Primary Culture - a Morphological and Autoradiographic Study. Experimental Eye Research 37, 349-365.
Grierson, I., Rahi, A.H.S., 1979. Microfilaments in the Cells of the Human Trabecular Meshwork. British Journal of Ophthalmology 63, 3-8.
Grierson, I., Robins, E., Unger, W., Millar, L., Ahmed, A., 1985b. The Cells of the Bovine Outflow System in Tissue-Culture. Experimental Eye Research 40, 35-46.
Group, C.A.T.T.S., Grehn, F., Hollo, G., Khaw, P., Overton, B., Wilson, R., Vogel, R., Smith, Z., 2007a. Factors affecting the outcome of trabeculectomy: an analysis based on combined data from two phase III studies of an antibody to transforming growth factor beta2, CAT-152. Ophthalmology 114, 1831-1838.
Group, C.A.T.T.S., Khaw, P., Grehn, F., Hollo, G., Overton, B., Wilson, R., Vogel, R., Smith, Z., 2007b. A phase III study of subconjunctival human anti-transforming growth factor beta(2) monoclonal antibody (CAT-152) to prevent scarring after first-time trabeculectomy. Ophthalmology 114, 1822-1830.
Gryzunov, Y.A., Deev, A.I., Kurysheva, N.I., Komarova, M.N., 1999. Fluorescent method for albumin assay in human aqueous humour and tear fluid. Bulletin of Experimental Biology and Medicine 128, 1179-1181.
Hales, A.M., Chamberlain, C.G., McAvoy, J.W., 1995. Cataract induction in lenses cultured with transforming growth factor-beta. Investigative Ophthalmology & Visual Science 36, 1709-1713.
Hales, A.M., Chamberlain, C.G., McAvoy, J.W., 2000. Susceptibility to TGF beta 2-induced cataract increases with aging in the rat. Investigative Ophthalmology & Visual Science 41, 3544-3551.
Hall, A., 1998. Rho GTPases and the actin cytoskeleton. Science 279, 509-514.

Hall, P.A., 1999. Assessing apoptosis: a critical survey. Endocrine-Related Cancer 6, 3-8.
Han, H., Wecker, T., Grehn, F., Schlunck, G., 2011. Elasticity-Dependent Modulation of TGF-beta Responses in Human Trabecular Meshwork Cells. Investigative Ophthalmology & Visual Science 52, 2889-2896.
Harman, D., 1992. Role of free radicals in aging and disease. Annals of the New York Academy of Sciences 673, 126-141.
Hayflick, L., 2000. The future of ageing. Nature 408, 267-269.
He, Y., Ge, J., Tombran-Tink, J., 2008a. Mitochondrial Defects and Dysfunction in Calcium Regulation in Glaucomatous Trabecular Meshwork Cells. Investigative Ophthalmology & Visual Science 49, 4912-4922.
He, Y., Leung, K.W., Zhang, Y.H., Duan, S., Zhong, X.F., Jiang, R.Z., Peng, Z., Tombran-Tink, J., Ge, J., 2008b. Mitochondrial complex I defect induces ROS release and degeneration in trabecular meshwork cells of POAG patients: Protection by antioxidants. Investigative Ophthalmology & Visual Science 49, 1447-1458.
Heng, Y.W., Koh, C.G., 2010. Actin cytoskeleton dynamics and the cell division cycle. International Journal of Biochemistry & Cell Biology 42, 1622-1633.
Hoare, M.J., Grierson, I., Brotchie, D., Pollock, N., Cracknell, K., Clark, A.F., 2009. Cross-Linked Actin Networks (CLANs) in the Trabecular Meshwork of the Normal and Glaucomatous Human Eye In Situ. Investigative Ophthalmology & Visual Science 50, 1255-1263.
Hoffman, E.A., Conley, S.M., Stamer, W.D., McKay, B.S., 2005. Barriers to productive transfection of trabecular meshwork cells. Molecular Vision 11, 869-875.
Hogan, M.J., Alvarado, J.A., Weddell, J.E., 1971. Histology of the human eye : an atlas and textbook. Saunders, Philadelphia ; London.
Hogg, P., Calthorpe, M., Ward, S., Grierson, I., 1995. Migration of Cultured Bovine Trabecular Meshwork Cells to Aqueous-Humor and Constituents. Investigative Ophthalmology & Visual Science 36, 2449-2460.
Honjo, M., Inatani, M., Kido, N., Sawamura, T., Yue, B.Y., Honda, Y., Tanihara, H., 2001a. Effects of protein kinase inhibitor, HA1077, on intraocular pressure and outflow facility in rabbit eyes. Archives of Ophthalmology 119, 1171-1178.
Honjo, M., Tanihara, H., Inatani, M., Kido, N., Sawamura, T., Yue, B.Y., Narumiya, S., Honda, Y., 2001b. Effects of rho-associated protein kinase inhibitor Y-27632 on intraocular pressure and outflow facility. Investigative Ophthalmology & Visual Science 42, 137-144.
Howell, G.R., Libby, R.T., John, S.W., 2008. Mouse genetic models: an ideal system for understanding glaucomatous neurodegeneration and neuroprotection. Progress in Brain Research 173, 303-321.
Hu, D.N., Ritch, R., 2001. Hepatocyte growth factor is increased in the aqueous humor of glaucomatous eyes. Journal of Glaucoma 10, 152-157.
Hu, D.N., Ritch, R., Liebmann, J., Liu, Y., Cheng, B., Hu, M.S., 2002. Vascular endothelial growth factor is increased in aqueous humor of glaucomatous eyes. Journal of Glaucoma 11, 406-410.
Hwang, E.S., Yoon, G., Kang, H.T., 2009. A comparative analysis of the cell biology of senescence and aging. Cellular and Molecular Life Sciences 66, 2503-2524.
Imanishi, J., Kamiyama, K., Iguchi, I., Kita, M., Sotozono, C., Kinoshita, S., 2000. Growth factors: importance in wound healing and maintenance of transparency of the cornea. Progress in Retinal and Eye Research 19, 113-129.

Inatani, M., Tanihara, H., Katsuta, H., Honjo, M., Kido, N., Honda, Y., 2001. Transforming growth factor-beta(2) levels in aqueous humor of glaucomatous eyes. Graefes Archive for Clinical and Experimental Ophthalmology 239, 109-113.
Indo, H.P., Davidson, M., Yen, H.C., Suenaga, S., Tomita, K., Nishii, T., Higuchi, M., Koga, Y., Ozawa, T., Majima, H.J., 2007. Evidence of ROS generation by mitochondria in cells with impaired electron transport chain and mitochondrial DNA damage. Mitochondrion 7, 106-118.
Ingber, D.E., 2003. Tensegrity II. How structural networks influence cellular information processing networks. Journal of Cell Science 116, 1397-1408.
Inomata, H., Bill, A., 1977. Exit Sites of Uveoscleral Flow of Aqueous-Humor in Cynomolgus Monkey Eyes. Experimental Eye Research 25, 113-118.
Inomata, H., Smelser, G.K., Bill, A., 1972. Aqueous Humor Pathways through Trabecular Meshwork and into Schlemms Canal in Cynomolgus Monkey (Macaca Irus). American Journal of Ophthalmology 73, 760-&.
Inoue, T., Pattabiraman, P.P., Epstein, D.L., Vasantha Rao, P., 2010a. Effects of chemical inhibition of N-WASP, a critical regulator of actin polymerization on aqueous humor outflow through the conventional pathway. Experimental Eye Research 90, 360-367.
Inoue, T., Pecen, P., Maddala, R., Skiba, N.P., Pattabiraman, P.P., Epstein, D.L., Rao, P.V., 2010b. Characterization of cytoskeleton-enriched protein fraction of the trabecular meshwork and ciliary muscle cells. Investigative Ophthalmology & Visual Science 51, 6461-6471.
Ireland, G.W., Voon, F.C.T., 1981. Polygonal Networks in Living Chick Embryonic-Cells. Journal of Cell Science 52, 55-69.
Ishibashi, T., Murata, T., Hangai, M., Nagai, R., Horiuchi, S., Lopez, P.F., Hinton, D.R., Ryan, S.J., 1998. Advanced glycation end products in age-related macular degeneration. Archives of Ophthalmology 116, 1629-1632.
Itoh, N., Ornitz, D.M., 2011. Fibroblast growth factors: from molecular evolution to roles in development, metabolism and disease. Journal of Biochemistry 149, 121-130.
Izzotti, A., 2003. DNA damage and alterations of gene expression in chronic-degenerative diseases. Acta Biochimica Polonica 50, 145-154.
Izzotti, A., Bagnis, A., Sacca, S.C., 2006. The role of oxidative stress in glaucoma. Mutation Research-Reviews in Mutation Research 612, 105-114.
Izzotti, A., Sacca, S.C., Longobardi, M., Cartiglia, C., 2010. Mitochondrial Damage in the Trabecular Meshwork of Patients With Glaucoma. Archives of Ophthalmology 128, 724-730.
Jacob, T.J.C., Civan, M.M., 1996. Role of ion channels in aqueous humor formation. American Journal of Physiology-Cell Physiology 271, C703-C720.
Jahn, C.E., Leiss, O., Vonbergmann, K., 1983. Lipid-Composition of Human Aqueous-Humor. Ophthalmic Research 15, 220-224.
Jampel, H.D., Roche, N., Stark, W.J., Roberts, A.B., 1990. Transforming Growth-Factor-Beta in Human Aqueous-Humor. Current Eye Research 9, 963-969.
Job, R., Raja, V., Grierson, I., Currie, L., O'Reilly, S., Pollock, N., Knight, E., Clark, A.F., 2010. Cross-linked actin networks (CLANs) are present in lamina cribrosa cells. British Journal of Ophthalmology 94, 1388-1392.

Johnson, D.H., 1997. The effect of cytochalasin D on outflow facility and the trabecular meshwork of the human eye in perfusion organ culture. Investigative Ophthalmology & Visual Science 38, 2790-2799.
Johnson, D.H., 2005. Trabecular meshwork and uveoscleral outflow models. Journal of Glaucoma 14, 308-310.
Johnson, M., 2006. 'What controls aqueous humour outflow resistance?'. Experimental Eye Research 82, 545-557.
Johnson, M., Chan, D., Read, A.T., Christensen, C., Sit, A., Ethier, C.R., 2002. The pore density in the inner wall endothelium of Schlemm's canal of glaucomatous eyes. Investigative Ophthalmology & Visual Science 43, 2950-2955.
Johnson, M., Gong, H., Freddo, T.F., Ritter, N., Kamm, R., 1993. Serum proteins and aqueous outflow resistance in bovine eyes. Investigative Ophthalmology & Visual Science 34, 3549-3557.
Johnson, M., Shapiro, A., Ethier, C.R., Kamm, R.D., 1992. Modulation of outflow resistance by the pores of the inner wall endothelium. Investigative Ophthalmology & Visual Science 33, 1670-1675.
Jones, R., 3rd, Rhee, D.J., 2006. Corticosteroid-induced ocular hypertension and glaucoma: a brief review and update of the literature. Current Opinion in Ophthalmology 17, 163-167.
Joyce, N.C., 2003. Proliferative capacity of the corneal endothelium. Progress in Retinal and Eye Research 22, 359-389.
Joyce, N.C., Harris, D.L., Zieske, J.D., 1998. Mitotic inhibition of corneal endothelium in neonatal rats. Investigative Ophthalmology & Visual Science 39, 2572-2583.
Junglas, B., Kuespert, S., Seleem, A.A., Struller, T., Ullmann, S., Bosl, M., Bosserhoff, A., Kostle, J., Wagner, R., Tamm, E.R., Fuchshofer, R., 2012. Connective Tissue Growth Factor Causes Glaucoma by Modifying the Actin Cytoskeleton of the Trabecular Meshwork. American Journal of Pathology 180, 2386-2403.
Junglas, B., Yu, A.H.L., Welge-Lussen, U., Tamm, E.R., Fuchshofer, R., 2009. Connective tissue growth factor induces extracellular matrix deposition in human trabecular meshwork cells. Experimental Eye Research 88, 1065-1075.
Kaji, Y., Amano, S., Usui, T., Oshika, T., Yamashiro, K., Ishida, S., Suzuki, K., Tanaka, S., Adamis, A.P., Nagai, R., Horiuchi, S., 2003. Expression and function of receptors for advanced glycation end products in bovine corneal endothelial cells. Investigative Ophthalmology & Visual Science 44, 521-528.
Kameda, T., Inoue, T., Inatani, M., Fujimoto, T., Honjo, M., Kasaoka, N., Inoue-Mochita, M., Yoshimura, N., Tanihara, H., 2012. The effect of Rho-associated protein kinase inhibitor on monkey Schlemm's canal endothelial cells. Investigative Ophthalmology & Visual Science 53, 3092-3103.
Kaufman, P.L., 2008. Enhancing trabecular outflow by disrupting the actin cytoskeleton, increasing uveoscleral outflow with prostaglandins, and understanding the pathophysiology of presbyopia: Interrogating Mother Nature: asking why, asking how, recognizing the signs, following the trail. Experimental Eye Research 86, 3-17.
Kaufman, P.L., Barany, E.H., 1977a. Cytochalasin B reversibly increases outflow facility in the eye of the cynomolgus monkey. Investigative Ophthalmology & Visual Science 16, 47-53.

Kaufman, P.L., Barany, E.H., 1977b. Recent observations concerning the effects of cholinergic drugs on outflow facility in monkeys. Experimental Eye Research 25 Suppl, 415-418.
Kaufman, P.L., Rasmussen, C.A., 2012. Advances in Glaucoma Treatment and Management: Outflow Drugs. Investigative Ophthalmology & Visual Science 53, 2495-2500.
Keller, K.E., Aga, M., Bradley, J.M., Kelley, M.J., Acott, T.S., 2009. Extracellular matrix turnover and outflow resistance. Experimental Eye Research 88, 676-682.
Keller, K.E., Bradley, J.M., Kelley, M.J., Acott, T.S., 2008. Effects of modifiers of glycosaminoglycan biosynthesis on outflow facility in perfusion culture. Investigative Ophthalmology & Visual Science 49, 2495-2505.
Keller, K.E., Sun, Y.Y., Yang, Y.F., Bradley, J.M., Acott, T.S., 2012. Perturbation of hyaluronan synthesis in the trabecular meshwork and the effects on outflow facility. Investigative Ophthalmology & Visual Science 53, 4616-4625.
Kerr, J.F., Wyllie, A.H., Currie, A.R., 1972. Apoptosis: a basic biological phenomenon with wide-ranging implications in tissue kinetics. British journal of cancer 26, 239-257.
Kerrigan-Baumrind, L.A., Quigley, H.A., Pease, M.E., Kerrigan, D.F., Mitchell, R.S., 2000. Number of ganglion cells in glaucoma eyes compared with threshold visual field tests in the same persons. Investigative Ophthalmology & Visual Science 41, 741-748.
Kerrigan, L.A., Zack, D.J., Quigley, H.A., Smith, S.D., Pease, M.E., 1997. TUNEL-positive ganglion cells in human primary open-angle glaucoma. Archives of Ophthalmology 115, 1031-1035.
Kersey, J.P., Broadway, D.C., 2006. Corticosteroid-induced glaucoma: a review of the literature. Eye 20, 407-416.
Khaw, P.T., Elkington, A.R., 1999. ABC of eyes, 3rd ed. BMJ Pub. Group, London.
Khurana, R.N., Deng, P.F., Epstein, D.L., Rao, P.V., 2003. The role of protein kinase C in modulation of aqueous humor outflow facility. Experimental Eye Research 76, 39-47.
Kiffin, R., Bandyopadhyay, U., Cuervo, A.M., 2006. Oxidative stress and autophagy. Antioxidants and Redox Signaling 8, 152-162.
Kim, K.S., Lee, B.H., Kim, I.S., 1992. The measurement of fibronectin concentrations in human aqueous humor. Korean Journal of Ophthalmology : KJO 6, 1-5.
Kinsey, V.E., 1951. The chemical composition and the osmotic pressure of the aqueous humor and plasma of the rabbit. Journal of General Physiology 34, 389-402.
Kirkwood, T.B.L., Austad, S.N., 2000. Why do we age? Nature 408, 233-238.
Klenkler, B., Sheardown, H., 2004. Growth factors in the anterior segment: role in tissue maintenance, wound healing and ocular pathology. Experimental Eye Research 79, 677-688.
Knisely, T.L., Hosoi, J., Nazareno, R., Granstein, R.D., 1994. The Presence of Biologically Significant Concentrations of Glucocorticoids but Little or No Cortisol Binding Globulin within Aqueous-Humor - Relevance to Immune Privilege in the Anterior-Chamber of the Eye. Investigative Ophthalmology & Visual Science 35, 3711-3723.
Koga, T., Koga, T., Awai, M., Tsutsui, J., Yue, B.Y., Tanihara, H., 2006. Rho-associated protein kinase inhibitor, Y-27632, induces alterations in adhesion, contraction and motility in cultured human trabecular meshwork cells. Experimental Eye Research 82, 362-370.
Konz, D.D., Flugel-Koch, C., Ohlmann, A., Tamm, E.R., 2009. Myocilin in the trabecular meshwork of eyes with primary open-angle glaucoma. Graefe's archive for clinical and

experimental ophthalmology = Albrecht von Graefes Archiv fur klinische und experimentelle Ophthalmologie.
Kroening, S., Solomovitch, S., Sachs, M., Wullich, B., Goppelt-Struebe, M., 2009. Regulation of connective tissue growth factor (CTGF) by hepatocyte growth factor in human tubular epithelial cells. Nephrology, dialysis, transplantation : official publication of the European Dialysis and Transplant Association - European Renal Association 24, 755-762.
Kuchle, M., Ho, T.S., Nguyen, N.X., Hannappel, E., Naumann, G.O., 1994. Protein quantification and electrophoresis in aqueous humor of pseudoexfoliation eyes. Investigative Ophthalmology & Visual Science 35, 748-752.
Kumar, J., Epstein, D.L., 2011. Rho GTPase-Mediated Cytoskeletal Organization in Schlemm's Canal Cells Play a Critical Role in the Regulation of Aqueous Humor Outflow Facility. Journal of Cellular Biochemistry 112, 600-606.
Kuzuya, M., Satake, S., Miura, H., Hayashi, T., Iguchi, A., 1996. Inhibition of endothelial cell differentiation on a glycosylated reconstituted basement membrane complex. Experimental Cell Research 226, 336-345.
Last, J.A., Pan, T.R., Ding, Y.Z., Reilly, C.M., Keller, K., Acott, T.S., Fautsch, M.P., Murphy, C.J., Russell, P., 2011. Elastic Modulus Determination of Normal and Glaucomatous Human Trabecular Meshwork. Investigative Ophthalmology & Visual Science 52, 2147-2152.
Lazarides, E., 1976. Actin, Alpha-Actinin, and Tropomyosin Interaction in Structural Organization of Actin-Filaments in Nonmuscle Cells. Journal of Cell Biology 68, 202-219.
Lee, B.L., Bathija, R., Weinreb, R.N., 1998. The definition of normal-tension glaucoma. Journal of Glaucoma 7, 366-371.
Lee, S.H., Dominguez, R., 2010. Regulation of actin cytoskeleton dynamics in cells. Molecules and Cells.
Lepple-Wienhues, A., Stahl, F., Wiederholt, M., 1991. Differential smooth muscle-like contractile properties of trabecular meshwork and ciliary muscle. Experimental Eye Research 53, 33-38.
Li, G., Luna, C., Liton, P.B., Navarro, I., Epstein, D.L., Gonzalez, P., 2007. Sustained stress response after oxidative stress in trabecular meshwork cells. Molecular Vision 13, 2282-2288.
Li, G., Luna, C., Qiu, J., Epstein, D.L., Gonzalez, P., 2011. Role of miR-204 in the regulation of apoptosis, endoplasmic reticulum stress response, and inflammation in human trabecular meshwork cells. Investigative Ophthalmology & Visual Science 52, 2999-3007.
Li, J.P., Tripathi, B.J., Tripathi, R.C., 2000. Modulation of pre-mRNA splicing and protein production of fibronectin by TGF-ss 2 in porcine trabecular cells. Investigative Ophthalmology & Visual Science 41, 3437-3443.
Li, Q., Weng, J., Mohan, R.R., Bennett, G.L., Schwall, R., Wang, Z.F., Tabor, K., Kim, J., Hargrave, S., Cuevas, K.H., Wilson, S.E., 1996. Hepatocyte growth factor and hepatocyte growth factor receptor in the lacrimal gland, tears, and cornea. Investigative Ophthalmology & Visual Science 37, 727-739.
Lin, Y.Z., Epstein, D.L., Liton, P.B., 2010. Intralysosomal Iron Induces Lysosomal Membrane Permeabilization and Cathepsin D-Mediated Cell Death in Trabecular

Meshwork Cells Exposed to Oxidative Stress. Investigative Ophthalmology & Visual Science 51, 6483-6495.
Liton, P.B., Challa, P., Stinnett, S., Luna, C., Epstein, D.L., Gonzalez, P., 2005a. Cellular senescence in the glaucomatous outflow pathway. Experimental Gerontology 40, 745-748.
Liton, P.B., Gonzalez, P., Epstein, D.L., 2009. The role of proteolytic cellular systems in trabecular meshwork homeostasis. Experimental Eye Research 88, 724-728.
Liton, P.B., Lin, Y.Z., Luna, C., Li, G.R., Gonzalez, P., Epstein, D.L., 2008. Cultured porcine trabecular meshwork cells display altered lysosomal function when subjected to chronic oxidative stress. Investigative Ophthalmology & Visual Science 49, 3961-3969.
Liton, P.B., Liu, X., Challa, P., Epstein, D.L., Gonzalez, P., 2005b. Induction of TGF-beta1 in the trabecular meshwork under cyclic mechanical stress. Journal of Cellular Physiology 205, 364-371.
Liu, J.H., Gokhale, P.A., Loving, R.T., Kripke, D.F., Weinreb, R.N., 2003a. Laboratory assessment of diurnal and nocturnal ocular perfusion pressures in humans. Journal of ocular pharmacology and therapeutics : the official journal of the Association for Ocular Pharmacology and Therapeutics 19, 291-297.
Liu, X., Agarwal, R., Clark, A.F., Wordinger, R.J., 2003b. Human trabecular meshwork cells from normal and glaucomatous donors respond to TGFb2 and BDNF treatment differently. Investigative Ophthalmology & Visual Science 44, U310-U310.
Liu, X., Wu, Z., Sheibani, N., Brandt, C.R., Polansky, J.R., Kaufman, P.L., 2003c. Low dose latrunculin-A inhibits dexamethasone-induced changes in the actin cytoskeleton and alters extracellular matrix protein expression in cultured human trabecular meshwork cells. Experimental Eye Research 77, 181-188.
Liu, X.Y., Cai, S.P., Glasser, A., Volberg, T., Polansky, J.R., Fauss, D.J., Brandt, C.R., Geiger, B., Kaufman, P.L., 2001. Effect of H-7 on cultured human trabecular meshwork cells. Molecular Vision 7, 145-153.
Lodish, H.F., 2008. Molecular cell biology, 6th ed. W.H. Freeman, New York.
Lopatin, D.E., Vanpoperin, N., Maccallum, D.K., Meyer, R.F., Lillie, J.H., 1989. Changes in Aqueous Immunoglobulin and Albumin Levels Following Penetrating Keratoplasty. Investigative Ophthalmology & Visual Science 30, 122-131.
Lu, J.W., Lu, Z.Y., Reinach, P., Zhang, J.W., Dai, W., Lu, L., Xu, M., 2006. TGF-beta 2 inhibits AKT activation and FGF-2-induced corneal endothelial cell proliferation. Experimental Cell Research 312, 3631-3640.
Lu, Z., Overby, D.R., Scott, P.A., Freddo, T.F., Gong, H., 2008. The mechanism of increasing outflow facility by rho-kinase inhibition with Y-27632 in bovine eyes. Experimental Eye Research 86, 271-281.
Luna, C., Li, G.R., Huang, J.Y., Qiu, J.M., Wu, J., Yuan, F., Epstein, D.L., Gonzalez, P., 2012. Regulation of Trabecular Meshwork Cell Contraction and Intraocular Pressure by miR-200c. Plos One 7.
Luna, C., Li, G.R., Liton, P.B., Epstein, D.L., Gonzalez, P., 2009. Alterations in gene expression induced by cyclic mechanical stress in trabecular meshwork cells. Molecular Vision 15, 534-544.
Lutjen-Drecoll, E., 1999a. Functional morphology of the trabecular meshwork in primate eyes. Progress in Retinal and Eye Research 18, 91-119.
Lutjen-Drecoll, E., 1999b. Morphology of the trabecular meshwork. Pathogenesis and Risk Factors of Glaucoma, 101-107

245.
Lutjen-Drecoll, E., 2000. Importance of trabecular meshwork changes in the pathogenesis of primary open-angle glaucoma. Journal of Glaucoma 9, 417-418.
Lutjen-Drecoll, E., 2005. Morphological changes in glaucomatous eyes and the role of TGF beta(2) for the pathogenesis of the disease. Experimental Eye Research 81, 1-4.
Lutjen-Drecoll, E., Gabelt, B.T., Tian, B.H., Kaufman, P.L., 2001. Outflow of aqueous humor. Journal of Glaucoma 10, S42-S44.
Lutjen-Drecoll, E., Shimizu, T., Rohrbach, M., Rohen, J.W., 1986. Quantitative analysis of 'plaque material' between ciliary muscle tips in normal- and glaucomatous eyes. Experimental Eye Research 42, 457-465.
Lutjendrecoll, E., Futa, R., Rohen, J.W., 1981. Ultrahistochemical Studies on Tangential Sections of the Trabecular Meshwork in Normal and Glaucomatous Eyes. Investigative Ophthalmology & Visual Science 21, 563-573.
Lutz, M., Knaus, P., 2002. Integration of the TGF-beta pathway into the cellular signalling network. Cellular Signalling 14, 977-988.
Macknight, A.D., McLaughlin, C.W., Peart, D., Purves, R.D., Carre, D.A., Civan, M.M., 2000. Formation of the aqueous humor. Clinical and experimental pharmacology & physiology 27, 100-106.
Maguire, P., Kilpatrick, J.I., Kelly, G., Prendergast, P.J., Campbell, V.A., O'Connell, B.C., Jarvis, S.P., 2007. Direct mechanical measurement of geodesic structures in rat mesenchymal stem cells. Hfsp Journal 1, 181-191.
Majsterek, I., Malinowska, K., Stanczyk, M., Kowalski, M., Blaszczyk, J., Kurowska, A.K., Kaminska, A., Szaflik, J., Szaflik, J.P., 2011. Evaluation of oxidative stress markers in pathogenesis of primary open-angle glaucoma. Experimental and Molecular Pathology 90, 231-237.
Mao, W.M., Tovar-Vidales, T., Yorio, T., Wordinger, R.J., Clark, A.F., 2011. Perfusion-Cultured Bovine Anterior Segments as an Ex Vivo Model for Studying Glucocorticoid-Induced Ocular Hypertension and Glaucoma. Investigative Ophthalmology & Visual Science 52, 8068-8075.
Mark, H.H., 2010. Aqueous Humor Dynamics in Historical Perspective. Survey of Ophthalmology 55, 89-100.
Marquis, R.E., Whitson, J.T., 2005. Management of glaucoma: Focus on pharmacological therapy. Drugs & Aging 22, 1-21.
Marshall, G.E., Konstas, A.G., Lee, W.R., 1990. Immunogold localization of type IV collagen and laminin in the aging human outflow system. Experimental Eye Research 51, 691-699.
Marshall, G.E., Konstas, A.G., Lee, W.R., 1991. Immunogold ultrastructural localization of collagens in the aged human outflow system. Ophthalmology 98, 692-700.
Masoro, E.J., 1990. Physiology of ageing: nutritional aspects. Age and Ageing 19, S5-9.
Massague, J., 2000. How cells read TGF-beta signals. Nature Reviews Molecular Cell Biology 1, 169-178.
Massague, J., 2006. The logic of TGF-beta signalling. FEBS Journal 273, 2-2.
Massague, J., 2012. TGF-beta signaling in development and disease. FEBS Letters 586, 1833.
Massague, J., Gomis, R.R., 2006. The logic of TGF beta signaling. FEBS Letters 580, 2811-2820.

Matsumoto, Y., Johnson, D.H., 1997. Dexamethasone decreases phagocytosis by human trabecular meshwork cells in situ. Investigative Ophthalmology & Visual Science 38, 1902-1907.
Matsumura, A., Kubota, T., Taiyoh, H., Fujiwara, H., Okamoto, K., Ichikawa, D., Shiozaki, A., Komatsu, S., Nakanishi, M., Kuriu, Y., Murayama, Y., Ikoma, H., Ochiai, T., Kokuba, Y., Nakamura, T., Matsumoto, K., Otsuji, E., 2013. HGF regulates VEGF expression via the c-Met receptor downstream pathways, PI3K/Akt, MAPK and STAT3, in CT26 murine cells. International Journal of Oncology 42, 535-542.
McAvoy, J.W., Chamberlain, C.G., de Iongh, R.U., Richardson, N.A., Lovicu, F.J., 1991. The role of fibroblast growth factor in eye lens development. Annals of the New York Academy of Sciences 638, 256-274.
McCarthy, A.D., Etcheverry, S.B., Bruzzone, L., Cortizo, A.M., 1997. Effects of advanced glycation end-products on the proliferation and differentiation of osteoblast-like cells. Molecular and Cellular Biochemistry 170, 43-51.
McKee, C.T., Wood, J.A., Shah, N.M., Fischer, M.E., Reilly, C.M., Murphy, C.J., Russell, P., 2011. The effect of biophysical attributes of the ocular trabecular meshwork associated with glaucoma on the cell response to therapeutic agents. Biomaterials 32, 2417-2423.
McLaren, J.W., 2009. Measurement of aqueous humor flow. Experimental Eye Research 88, 641-647.
McLaughlin, C.W., Zellhuber-McMillan, S., Peart, D., Purves, R.D., Macknight, A.D., Civan, M.M., 2001. Regional differences in ciliary epithelial cell transport properties. The Journal of Membrane Biology 182, 213-222.
McMenamin, P.G., Lee, W.R., Aitken, D.A., 1986. Age-related changes in the human outflow apparatus. Ophthalmology 93, 194-209.
Mcmenamin, P.G., Lee, W.R., Grierson, I., Grindle, F.C.J., 1983. Giant Vacuoles in the Lining Endothelium of the Human Schlemm Canal after Topical Timolol Maleate. Investigative Ophthalmology & Visual Science 24, 339-342.
Mcmenamin, P.G., Steptoe, R.J., 1991. Normal Anatomy of the Aqueous-Humor Outflow System in the Domestic Pig Eye. Journal of Anatomy 178, 65-77.
Mead, A.L., Wong, T.T.L., Cordeiro, M.F., Anderson, I.K., Khaw, P.T., 2003. Evaluation of anti-TGF-beta 2 antibody as a new postoperative anti-scarring agent in glaucoma surgery. Investigative Ophthalmology & Visual Science 44, 3394-3401.
Mehanna, C., Baudouin, C., Brignole-Baudouin, F., 2011. Spectrofluorometry assays for oxidative stress and apoptosis, with cell viability on the same microplates: A multiparametric analysis and quality control. Toxicology in Vitro 25, 1089-1096.
Meller, D., Peters, K., Meller, K., 1997. Human cornea and sclera studied by atomic force microscopy. Cell and Tissue Research 288, 111-118.
Mettu, P.S., Deng, P.F., Misra, U.K., Gawdi, G., Epstein, D.L., Rao, P.V., 2004. Role of lysophospholipid growth factors in the modulation of aqueous humor outflow facility. Investigative Ophthalmology & Visual Science 45, 2263-2271.
Mitchison, T.J., Cramer, L.P., 1996. Actin-based cell motility and cell locomotion. Cell 84, 371-379.
Mohammadi, M., Olsen, S.K., Ibrahimi, O.A., 2005. Structural basis for fibroblast growth factor receptor activation. Cytokine & Growth Factor Reviews 16, 107-137.
Mukesh, B.N., McCarty, C.A., Rait, J.L., Taylor, H.R., 2002. Five-year incidence of open-angle glaucoma: the visual impairment project. Ophthalmology 109, 1047-1051.

Munch, G., Schinzel, R., Loske, C., Wong, A., Durany, N., Li, J.J., Vlassara, H., Smith, M.A., Perry, G., Riederer, P., 1998. Alzheimer's disease--synergistic effects of glucose deficit, oxidative stress and advanced glycation endproducts. Journal of Neural Transmission 105, 439-461.
Nakamura, T., Mizuno, S., 2010. The discovery of Hepatocyte Growth Factor (HGF) and its significance for cell biology, life sciences and clinical medicine. Proceedings of the Japan Academy Series B-Physical and Biological Sciences 86, 588-610.
Nakamura, T., Sakai, K., Nakamura, T., Matsumoto, K., 2011. Hepatocyte growth factor twenty years on: Much more than a growth factor. Journal of Gastroenterology and Hepatology 26, 188-202.
Nakasato, Y.R., Carnes, B.A., 2006. Health promotion in older adults. Promoting successful aging in primary care settings. Geriatrics 61, 27-31.
Nelson, P., Aspinall, P., Papasouliotis, O., Worton, B., O'Brien, C., 2003. Quality of life in glaucoma and its relationship with visual function. Journal of Glaucoma 12, 139-150.
Nguyen, K.P., Chung, M.L., Anderson, P.J., Johnson, M., Epstein, D.L., 1988. Hydrogen peroxide removal by the calf aqueous outflow pathway. Investigative Ophthalmology & Visual Science 29, 976-981.
O'Brien, E.T., Perkins, S.L., Roberts, B.C., Epstein, D.L., 1996. Dexamethasone inhibits trabecular cell retraction. Experimental Eye Research 62, 675-688.
O'Reilly, S., Pollock, N., Currie, L., Paraoan, L., Clark, A.F., Grierson, I., 2011. Inducers of cross-linked actin networks in trabecular meshwork cells. Investigative Ophthalmology & Visual Science 52, 7316-7324.
O'Reilly, S.C., 2010. Functional consequences of cross-linked actin networks in bovine trabecular meshwork cells [electronic resource]. University of Liverpool.
Ochiai, Y., Ochiai, H., 2002. Higher concentration of transforming growth factor-beta in aqueous humor of glaucomatous eyes and diabetic eyes. Japanese Journal of Ophthalmology 46, 249-253.
Olshansky, S.J., Carnes, B.A., Desesquelles, A., 2001. Demography. Prospects for human longevity. Science 291, 1491-1492.
Ornitz, D.M., Itoh, N., 2001. Fibroblast growth factors. Genome Biology 2.
Overby, D.R., Stamer, W.D., Johnson, M., 2009. The changing paradigm of outflow resistance generation: Towards synergistic models of the JCT and inner wall endothelium. Experimental Eye Research 88, 656-670.
Oyster, C.W., 1999. The human eye : structure and function. Sinauer Associates, Sunderland, Mass.
Ozcan, A.A., Ozdemir, N., Canataroglu, A., 2004. The aqueous levels of TGF-beta2 in patients with glaucoma. International Ophthalmology 25, 19-22.
Park, J.S., Chu, J.S., Tsou, A.D., Diop, R., Tang, Z.Y., Wang, A.J., Li, S., 2011. The effect of matrix stiffness on the differentiation of mesenchymal stem cells in response to TGF-beta. Biomaterials 32, 3921-3930.
Parker, M.G., Thorslund, M., 2007. Health trends in the elderly population: getting better and getting worse. Gerontologist 47, 150-158.
Pasquale, L.R., Dormanpease, M.E., Lutty, G.A., Quigley, H.A., Jampel, H.D., 1993. Immunolocalization of Tgf-Beta-1, Tgf-Beta-2, and Tgf-Beta-3 in the Anterior Segment of the Human Eye. Investigative Ophthalmology & Visual Science 34, 23-30.
Patil, C.K., Mian, I.S., Campisi, J., 2005. The thorny path linking cellular senescence to organismal aging. Mechanisms of Ageing and Development 126, 1040-1045.

Pederson, J.E., Gaasterland, D.E., Maclellan, H.M., 1977. Uveoscleral Aqueous Outflow in Rhesus-Monkey - Importance of Uveal Reabsorption. Investigative Ophthalmology & Visual Science 16, 1008-1017.
Pellegrin, S., Mellor, H., 2007. Actin stress fibres. Journal of Cell Science 120, 3491-3499.
Polansky, J.R., Weinreb, R., Alvarado, J.A., 1981. Studies on human trabecular cells propagated in vitro. Vision Research 21, 155-160.
Polansky, J.R., Weinreb, R.N., Baxter, J.D., Alvarado, J., 1979. Human trabecular cells. I. Establishment in tissue culture and growth characteristics. Investigative Ophthalmology & Visual Science 18, 1043-1049.
Porter, K.M., Epstein, D.L., Liton, P.B., 2012. Up-Regulated Expression of Extracellular Matrix Remodeling Genes in Phagocytically Challenged Trabecular Meshwork Cells. Plos One 7.
Powers, C.J., McLeskey, S.W., Wellstein, A., 2000. Fibroblast growth factors, their receptors and signaling. Endocrine-Related Cancer 7, 165-197.
Price, L.S., Leng, J., Schwartz, M.A., Bokoch, G.M., 1998. Activation of Rac and Cdc42 by integrins mediates cell spreading. Molecular Biology of the Cell 9, 1863-1871.
Quigley, H.A., 2005. New paradigms in the mechanisms and management of glaucoma. Eye (London) 19, 1241-1248.
Quigley, H.A., 2011. Glaucoma. Lancet 377, 1367-1377.
Quigley, H.A., Addicks, E.M., Green, W.R., Maumenee, A.E., 1981. Optic nerve damage in human glaucoma. II. The site of injury and susceptibility to damage. Archives of Ophthalmology 99, 635-649.
Quigley, H.A., Broman, A.T., 2006. The number of people with glaucoma worldwide in 2010 and 2020. British Journal of Ophthalmology 90, 262-267.
Quigley, H.A., Brown, A., Dorman-Pease, M.E., 1991. Alterations in elastin of the optic nerve head in human and experimental glaucoma. British Journal of Ophthalmology 75, 552-557.
Quigley, H.A., Enger, C., Katz, J., Sommer, A., Scott, R., Gilbert, D., 1994. Risk factors for the development of glaucomatous visual field loss in ocular hypertension. Archives of Ophthalmology 112, 644-649.
Ramos, R.F., Stamer, W.D., 2008. Effects of cyclic intraocular pressure on conventional outflow. Investigative Ophthalmology & Visual Science 49, 275-281.
Rao, P.V., Deng, P.F., Kumar, J., Epstein, D.L., 2001. Modulation of aqueous humor outflow facility by the rho kinase-specific inhibitor Y-27632. Investigative Ophthalmology & Visual Science 42, 1029-1037.
Raviola, G., 1974. Effects of paracentesis on the blood-aqueous barrier: an electron microscope study on Macaca mulatta using horseradish peroxidase as a tracer. Investigative Ophthalmology & Visual Science 13, 828-858.
Raviola, G., 1977. The structural basis of the blood-ocular barriers. Experimental Eye Research 25 Suppl, 27-63.
Read, A.T., Chan, D.W.H., Ethier, C.R., 2007. Actin structure in the outflow tract of normal and glaucomatous eyes (vol 82, pg 974, 2006). Experimental Eye Research 84, 213-226.
Resch, Z.T., Hann, C.R., Cook, K.A., Fautsch, M.P., 2010. Aqueous humor rapidly stimulates myocilin secretion from human trabecular meshwork cells. Experimental Eye Research 91, 901-908.

Resnikoff, S., Pascolini, D., Etya'ale, D., Kocur, I., Pararajasegaram, R., Pokharel, G.P., Mariotti, S.P., 2004. Global data on visual impairment in the year 2002. Bulletin of the World Health Organization 82, 844-851.
Rhee, D.J., Haddadin, R.I., Kang, M.H., Oh, D.J., 2009. Matricellular proteins in the trabecular meshwork. Experimental Eye Research 88, 694-703.
Ridley, A.J., 1996. Rho: theme and variations. Current Biology 6, 1256-1264.
Ridley, A.J., Comoglio, P.M., Hall, A., 1995. Regulation of scatter factor/hepatocyte growth factor responses by Ras, Rac, and Rho in MDCK cells. Molecular and Cellular Biology 15, 1110-1122.
Ridley, A.J., Hall, A., 1992. The small GTP-binding protein rho regulates the assembly of focal adhesions and actin stress fibers in response to growth factors. Cell 70, 389-399.
Rieck, P.W., Cholidis, S., Hartmann, C., 2001. Intracellular signaling pathway of FGF-2-modulated corneal endothelial cell migration during wound healing in vitro. Experimental Eye Research 73, 639-650.
Ringvold, A., Anderssen, E., Kjonniksen, I., 2000. Distribution of ascorbate in the anterior bovine eye. Investigative Ophthalmology & Visual Science 41, 20-23.
Roberts, A.B., Flanders, K.C., Heine, U.I., Jakowlew, S., Kondaiah, P., Kim, S.J., Sporn, M.B., 1990a. Transforming growth factor-beta: multifunctional regulator of differentiation and development. Philosophical transactions of the Royal Society of London. Series B, Biological sciences 327, 145-154.
Roberts, A.B., Heine, U.I., Flanders, K.C., Sporn, M.B., 1990b. Transforming growth factor-beta. Major role in regulation of extracellular matrix. Annals of the New York Academy of Sciences 580, 225-232.
Roberts, A.B., Sporn, M.B., 1992. Differential expression of the TGF-beta isoforms in embryogenesis suggests specific roles in developing and adult tissues. Molecular Reproduction and Development 32, 91-98.
Roberts, M.D., Sigal, I.A., Liang, Y., Burgoyne, C.F., Downs, J.C., 2010. Changes in the biomechanical response of the optic nerve head in early experimental glaucoma. Investigative Ophthalmology & Visual Science 51, 5675-5684.
Robertson, J.V., Golesic, E., Gauldie, J., West-Mays, J.A., 2010. Ocular Gene Transfer of Active TGF-beta Induces Changes in Anterior Segment Morphology and Elevated IOP in Rats. Investigative Ophthalmology & Visual Science 51, 308-318.
Rohen, J.W., Lutjendrecoll, E., Flugel, C., Meyer, M., Grierson, I., 1993. Ultrastructure of the Trabecular Meshwork in Untreated Cases of Primary Open-Angle Glaucoma (Poag). Experimental Eye Research 56, 683-692.
Rose, R.C., Richer, S.P., Bode, A.M., 1998. Ocular oxidants and antioxidant protection. Proceedings of the Society for Experimental Biology and Medicine. Society for Experimental Biology and Medicine 217, 397-407.
Russell, P., Gasiorowski, J.Z., Nealy, P.F., Murphy, C.J., 2008. Response of human trabecular meshwork cells to topographic cues on the nanoscale level. Investigative Ophthalmology & Visual Science 49, 629-635.
Russell, P., Johnson, D.H., 1996. Enzymes protective of oxidative damage present in all decades of life in the trabecular meshwork, as detected by two-dimensional gel electrophoresis protein maps. Journal of Glaucoma 5, 317-324.
Ryder, M.I., Weinreb, R.N., 1986. The cytoskeleton of the cynomolgus monkey trabecular cell. I. General considerations. Investigative Ophthalmology & Visual Science 27, 1305-1311.

Ryder, M.I., Weinreb, R.N., Alvarado, J., Polansky, J., 1988. The Cytoskeleton of the Cultured Human Trabecular Cell - Characterization and Drug Responses. Investigative Ophthalmology & Visual Science 29, 251-260.
Sacca, S.C., Izzotti, A., 2008. Oxidative stress and glaucoma: injury in the anterior segment of the eye. Glaucoma: An Open Window to Neurodegeneration and Neuroprotection 173, 385-407.
Sacca, S.C., Pascotto, A., Camicione, P., Capris, P., Izzotti, A., 2005. Oxidative DNA damage in the human trabecular meshwork: clinical correlation in patients with primary open-angle glaucoma. Archives of Ophthalmology 123, 458-463.
Salom, D., Diaz-Llopis, M., Quijada, A., Garcia-Delpech, S., Udaondo, P., Romero, F.J., Millan, J.M., Arevalo, J.F., 2010. Aqueous Humor Levels of Hepatocyte Growth Factor in Retinitis Pigmentosa. Investigative Ophthalmology & Visual Science 51, 3157-3161.
Salvi, S.M., Akhtar, S., Currie, Z., 2006. Ageing changes in the eye. Postgraduate Medical Journal 82, 581-587.
Santibanez, J.F., Quintanilla, M., Bernabeu, C., 2011. TGF-beta/TGF-beta receptor system and its role in physiological and pathological conditions. Clinical Science 121, 233-251.
Schachtschabel, D.O., Bigalke, B., Rohen, J.W., 1977. Production of Glycosaminoglycans by Cell-Cultures of Trabecular Meshork of Primate Eye. Experimental Eye Research 24, 71-80.
Schachtschabel, D.O., Binninger, E.A., Rohen, J.W., 1989. Invitro Cultures of Trabecular Meshwork Cells of the Human-Eye as a Model System for the Study of Cellular Aging. Archives of Gerontology and Geriatrics 9, 251-262.
Schafer, D.A., Welch, M.D., Machesky, L.M., Bridgman, P.C., Meyer, S.M., Cooper, J.A., 1998. Visualization and molecular analysis of actin assembly in living cells. Journal of Cell Biology 143, 1919-1930.
Schlunck, G., Han, H., Wecker, T., Kampik, D., Meyer-Ter-Vehn, T., Grehn, F., 2008. Substrate rigidity modulates cell-matrix interactions and protein expression in human trabecular meshwork cells. Investigative Ophthalmology & Visual Science 49, 262-269.
Schmidt, A.M., Yan, S.D., Yan, S.F., Stern, D.M., 2000. The biology of the receptor for advanced glycation end products and its ligands. Biochimica et Biophysica Acta: Protein Structure and Molecular Enzymology 1498, 99-111.
Schoeni, R.F., Freedman, V.A., Martin, L.G., 2008. Why is late-life disability declining? Milbank Quarterly 86, 47-89.
Schwartz, M.A., DeSimone, D.W., 2008. Cell adhesion receptors in mechanotransduction. Current Opinion in Cell Biology 20, 551-556.
Seddon, A., Decker, M., Muller, T., Armellino, D., Kovesdi, I., Gluzman, Y., Bohlen, P., 1991. Structure/activity relationships in basic FGF. Annals of the New York Academy of Sciences 638, 98-108.
Sethi, A., Jain, A., Zode, G.S., Wordinger, R.J., Clark, A.F., 2011a. Role of TGFbeta/Smad signaling in gremlin induction of human trabecular meshwork extracellular matrix proteins. Investigative Ophthalmology & Visual Science 52, 5251-5259.
Sethi, A., Mao, W., Wordinger, R.J., Clark, A.F., 2011b. Transforming growth factor-beta induces extracellular matrix protein cross-linking lysyl oxidase (LOX) genes in human trabecular meshwork cells. Investigative Ophthalmology & Visual Science 52, 5240-5250.

Shepard, A.R., Millar, J.C., Pang, I.H., Jacobson, N., Wang, W.H., Clark, A.F., 2010. Adenoviral gene transfer of active human transforming growth factor-{beta}2 elevates intraocular pressure and reduces outflow facility in rodent eyes. Investigative Ophthalmology & Visual Science 51, 2067-2076.
Shi, Y.G., Massague, J., 2003. Mechanisms of TGF-beta signaling from cell membrane to the nucleus. Cell 113, 685-700.
Shields, M.B., Spaeth, G.L., 2012. The glaucomatous process and the evolving definition of glaucoma. Journal of Glaucoma 21, 141-143.
Shifera, A.S., Trivedi, S., Chau, P., Bonnemaison, L.H., Iguchi, R., Alvarado, J.A., 2010. Constitutive secretion of chemokines by cultured human trabecular meshwork cells. Experimental Eye Research 91, 42-47.
Sibayan, S.A.B., Latina, M.A., Sherwood, M.E., Flotte, T.J., White, K., 1998. Apoptosis and morphologic changes in drug-treated trabecular meshwork cells in vitro. Experimental Eye Research 66, 521-529.
Sigal, I.A., Ethier, C.R., 2009. Biomechanics of the optic nerve head. Experimental Eye Research 88, 799-807.
Sigal, L.H., 2012. Basic Science for the Clinician 57 Transforming Growth Factor beta. JCR-Journal of Clinical Rheumatology 18, 268-272.
Singh, R., Barden, A., Mori, T., Beilin, L., 2001. Advanced glycation end-products: a review. Diabetologia 44, 129-146.
Siriwardena, D., Cordeiro, M.F., King, A.J., Donaldson, M.L., Wells, A., Levin, S., Migdal, C.S., Khaw, P.T., 2001. Human anti-TGF beta 2 antibody (CAT-152)as a new modulator of wound healing in glaucoma filtration surgery: longer term follow up data. Investigative Ophthalmology & Visual Science 42, S107-S107.
Small, J.V., Rottner, K., Hahne, P., Anderson, K.I., 1999. Visualising the actin cytoskeleton. Microscopy Research and Technique 47, 3-17.
Snell, R.S., 1981. Clinical anatomy : for medical students, 2nd ed. Beckenham : Little, Boston [Mass.].
Spector, A., Ma, W., Wang, R.R., 1998. The aqueous humor is capable of generating and degrading H2O2. Investigative Ophthalmology & Visual Science 39, 1188-1197.
Sporn, M.B., 2006. The early history of TGF-beta, and a brief glimpse of its future. Cytokine & Growth Factor Reviews 17, 3-7.
Sporn, M.B., Roberts, A.B., Wakefield, L.M., Assoian, R.K., 1986. Transforming growth factor-beta: biological function and chemical structure. Science 233, 532-534.
Srikanth, V., Maczurek, A., Phan, T., Steele, M., Westcott, B., Juskiw, D., Munch, G., 2011. Advanced glycation endproducts and their receptor RAGE in Alzheimer's disease. Neurobiology of Aging 32, 763-777.
Stamer, W.D., Acott, T.S., 2012. Current understanding of conventional outflow dysfunction in glaucoma. Current Opinion in Ophthalmology 23, 135-143.
Steely, H.T., Browder, S.L., Julian, M.B., Miggans, S.T., Wilson, K.L., Clark, A.F., 1992. The Effects of Dexamethasone on Fibronectin Expression in Cultured Human Trabecular Meshwork Cells. Investigative Ophthalmology & Visual Science 33, 2242-2250.
Steller, H., 1995. Mechanisms and Genes of Cellular Suicide. Science 267, 1445-1449.
Stevens, J.A., Corso, P.S., Finkelstein, E.A., Miller, T.R., 2006. The costs of fatal and non-fatal falls among older adults. Injury prevention : journal of the International Society for Child and Adolescent Injury Prevention 12, 290-295.

Stitt, A.W., 2001. Advanced glycation: an important pathological event in diabetic and age related ocular disease. British Journal of Ophthalmology 85, 746-753.
Stitt, A.W., 2005. The maillard reaction in eye diseases. Annals of the New York Academy of Sciences 1043, 582-597.
Stitt, A.W., 2010. AGEs and Diabetic Retinopathy. Investigative Ophthalmology & Visual Science 51, 4867-4874.
Stoker, M., 1989. Effect of scatter factor on motility of epithelial cells and fibroblasts. Journal of Cellular Physiology 139, 565-569.
Stricker, J., Falzone, T., Gardel, M.L., 2010. Mechanics of the F-actin cytoskeleton. Journal of Biomechanics 43, 9-14.
Stuart, K.A., Riordan, S.M., Lidder, S., Crostella, L., Williams, R., Skouteris, G.G., 2000. Hepatocyte growth factor/scatter factor-induced intracellular signalling. International Journal of Experimental Pathology 81, 17-30.
Suzman, R., Riley, M.W., 1985. Introducing the "oldest old". The Milbank Memorial Fund quarterly. Health and society 63, 177-186.
Takai, Y., Tanito, M., Ohira, A., 2012. Multiplex cytokine analysis of aqueous humor in eyes with primary open-angle glaucoma, exfoliation glaucoma, and cataract. Investigative Ophthalmology & Visual Science 53, 241-247.
Takebayashi, T., Iwamoto, M., Jikko, A., Matsumura, T., Enomoto-Iwamoto, M., Myoukai, F., Koyama, E., Yamaai, T., Matsumoto, K., Nakamura, T., et al., 1995. Hepatocyte growth factor/scatter factor modulates cell motility, proliferation, and proteoglycan synthesis of chondrocytes. Journal of Cell Biology 129, 1411-1419.
Tamm, E.R., 2009. The trabecular meshwork outflow pathways: Structural and functional aspects. Experimental Eye Research 88, 648-655.
Tamm, E.R., Baur, A., Lutjendrecoll, E., 1995. Transforming Growth-Factor-Beta-1 Induces Alpha-Smooth-Muscle Actin Expression in Cultured Human and Monkey Trabecular Meshwork. Investigative Ophthalmology & Visual Science 36, S194-S194.
Tan, J.C., Gonzalez, J.M., Jr., Hamm-Alvarez, S., Song, J., 2012. In situ autofluorescence visualization of human trabecular meshwork structure. Investigative Ophthalmology & Visual Science 53, 2080-2088.
Tan, J.C.H., Peters, D.M., Kaufman, P.L., 2006. Recent developments in understanding the pathophysiology of elevated intraocular pressure. Current Opinion in Ophthalmology 17, 168-174.
Tane, N., Dhar, S., Roy, S., Pinheiro, A., Ohira, A., Roy, S., 2007. Effect of excess synthesis of extracellular matrix components by trabecular meshwork cells: possible consequence on aqueous outflow. Experimental Eye Research 84, 832-842.
Tanihara, H., Inatani, M., Honjo, M., Tokushige, H., Azuma, J., Araie, M., 2008. Intraocular pressure-lowering effects and safety of topical administration of a selective ROCK inhibitor, SNJ-1656, in healthy volunteers. Archives of Ophthalmology 126, 309-315.
Taylor, A.W., 2012. Primary Open-Angle Glaucoma: A Transforming Growth Factor-beta Pathway-Mediated Disease. American Journal of Pathology 180, 2201-2204.
Tezel, G., 2006. Oxidative stress in glaucomatous neurodegeneration: Mechanisms and consequences. Progress in Retinal and Eye Research 25, 490-513.
Tezel, G., Luo, C., Yang, X.J., 2007. Accelerated aging in glaucoma: Immunohistochemical assessment of advanced glycation end products in the human

retina and optic nerve head. Investigative Ophthalmology & Visual Science 48, 1201-1211.
Thomasy, S.M., Wood, J.A., Kass, P.H., Murphy, C.J., Russell, P., 2012. Substratum Stiffness and Latrunculin B Regulate Matrix Gene and Protein Expression in Human Trabecular Meshwork Cells. Investigative Ophthalmology & Visual Science 53, 952-958.
Thylefors, B., Negrel, A.D., Pararajasegaram, R., Dadzie, K.Y., 1995. Global data on blindness. Bulletin of the World Health Organization 73, 115-121.
Tian, B., Gabelt, B.T., Geiger, B., Kaufman, P.L., 2009. The role of the actomyosin system in regulating trabecular fluid outflow. Experimental Eye Research 88, 713-717.
Tian, B., Geiger, B., Epstein, D.L., Kaufman, P.L., 2000. Cytoskeletal involvement in the regulation of aqueous humor outflow. Investigative Ophthalmology & Visual Science 41, 619-623.
Tian, B., Kaufman, P.L., 2005. Effects of the Rho kinase inhibitor Y-27632 and the phosphatase inhibitor calyculin A on outflow facility in monkeys. Experimental Eye Research 80, 215-225.
Tian, B.H., Kaufman, P.L., Volberg, T., Gabelt, B.T., Geiger, B., 1998. H-7 disrupts the actin cytoskeleton and increases outflow facility. Archives of Ophthalmology 116, 633-643.
Tinetti, M.E., Williams, C.S., 1997. Falls, injuries due to falls, and the risk of admission to a nursing home. New England Journal of Medicine 337, 1279-1284.
Toris, C.B., 2010. Pharmacotherapies for glaucoma. Current Molecular Medicine 10, 824-840.
Toris, C.B., Yablonski, M.E., Wang, Y.L., Camras, C.B., 1999. Aqueous humor dynamics in the aging human eye. American Journal of Ophthalmology 127, 407-412.
Toussaint, O., Royer, V., Salmon, M., Remacle, J., 2002. Stress-induced premature senescence and tissue ageing. Biochemical pharmacology 64, 1007-1009.
Tovar-Vidales, T., Clark, A.F., Wordinger, R.J., 2011. Transforming growth factor-beta2 utilizes the canonical Smad-signaling pathway to regulate tissue transglutaminase expression in human trabecular meshwork cells. Experimental Eye Research 93, 442-451.
Tovar-Vidales, T., Roque, R., Clark, A.F., Wordinger, R.J., 2008. Tissue transglutaminase expression and activity in normal and glaucomatous human trabecular meshwork cells and tissues. Investigative Ophthalmology & Visual Science 49, 622-628.
Tripathi, B.J., Tripathi, R.C., Li, J., Chan, W.F.A., 1994a. Aqueous-Humor in Glaucomatous Eyes Contains Increased Amounts of Tgf-Beta-2. Investigative Ophthalmology & Visual Science 35, 1848-1848.
Tripathi, R.C., Borisuth, N.S.C., Kolli, S.P., Tripathi, B.J., 1993. Trabecular Cells Express Receptors That Bind Tgf-Beta-1 and Tgf-Beta-2 - a Qualitative and Quantitative Characterization. Investigative Ophthalmology & Visual Science 34, 260-263.
Tripathi, R.C., Borisuth, N.S.C., Tripathi, B.J., 1992. Detection, Quantification, and Significance of Basic Fibroblast Growth-Factor in the Aqueous-Humor of Man, Cat, Dog and Pig. Experimental Eye Research 54, 447-454.
Tripathi, R.C., Chan, W.F.A., Li, J.P., Tripathi, B.J., 1994b. Trabecular Cells Express the Tgf-Beta-2 Gene and Secrete the Cytokine. Experimental Eye Research 58, 523-528.
Tripathi, R.C., Li, J., Chan, W.F., Tripathi, B.J., 1994c. Aqueous humor in glaucomatous eyes contains an increased level of TGF-beta 2. Experimental Eye Research 59, 723-727.

Tripathi, R.C., Millard, C.B., Tripathi, B.J., 1989. Protein-Composition of Human Aqueous-Humor - Sds-Page Analysis of Surgical and Post-Mortem Samples. Experimental Eye Research 48, 117-130.
Tschumper, R.C., Johnson, D.H., Bradley, J.M.B., Acott, T.S., 1990. Glycosaminoglycans of Human Trabecular Meshwork in Perfusion Organ-Culture. Current Eye Research 9, 363-369.
Tumminia, S.J., Mitton, K.P., Arora, J., Zelenka, P., Epstein, D.L., Russell, P., 1998. Mechanical stretch alters thc actin cytoskeletal network and signal transduction in human trabecular meshwork cells. Investigative Ophthalmology & Visual Science 39, 1361-1371.
Turano, K.A., Rubin, G.S., Quigley, H.A., 1999. Mobility performance in glaucoma. Investigative Ophthalmology & Visual Science 40, 2803-2809.
Ueda, J., Wentz-Hunter, K., Yue, B.Y., 2002. Distribution of myocilin and extracellular matrix components in the juxtacanalicular tissue of human eyes. Investigative Ophthalmology & Visual Science 43, 1068-1076.
Ueda, J., Yue, B.Y., 2003. Distribution of myocilin and extracellular matrix components in the corneoscleral meshwork of human eyes. Investigative Ophthalmology & Visual Science 44, 4772-4779.
United Nations. Department of, E., Social Affairs. Population, D., 2005. Population challenges and development goals. United Nations publication. ST/ESA/SER. A/248, New York.
Vardouli, L., Vasilaki, E., Papadimitriou, E., Kardassis, D., Stournaras, C., 2008. A novel mechanism of TGF beta-induced actin reorganization mediated by Smad proteins and Rho GTPases. FEBS Journal 275, 4074-4087.
Vass, J., 2013. AgeUK Agenda for Later Life, Age UK Agenda for Later Life.
Vittitow, J., Borras, T., 2004. Genes expressed in the human trabecular meshwork during pressure-induced homeostatic response. Journal of Cellular Physiology 201, 126-137.
Vlassara, H., Palace, M.R., 2002. Diabetes and advanced glycation endproducts. Journal of Internal Medicine 251, 87-101.
Wade, N.C., Grierson, I., O'Reilly, S., Hoare, M.J., Cracknell, K.P.B., Paraoan, L.I., Brotchie, D., Clark, A.F., 2009. Cross-linked actin networks (CLANs) in bovine trabecular meshwork cells. Experimental Eye Research 89, 648-659.
Wade, N.C., University of, L., 2010. Cross linked actin networks (CLANs) in the trabecular meshwork cells of the outflow system [electronic resource] : their nature and functional significance with respect to glaucoma. University of Liverpool.
Wang, N., Chintala, S.K., Fini, M.E., Schuman, J.S., 2001. Activation of a tissue-specific stress response in the aqueous outflow pathway of the eye defines the glaucoma disease phenotype. Nature Medicine 7, 304-309.
Wang, W., Dean, D.C., Kaplan, H.J., 2010. Age-related macular degeneration. Discovery medicine 9, 13-15.
Wang, Y.S., Yoo, C.M., Blancaflor, E.B., 2008. Improved imaging of actin filaments in transgenic Arabidopsis plants expressing a green fluorescent protein fusion to the C- and N-termini of the fimbrin actin-binding domain 2. The New Phytologist 177, 525-536.
Weber, J.A., Wong, K.B., 2010. Older adults coping with vision loss. Home Health Care Services Quarterly 29, 105-119.

Wei, Y.H., Lee, H.C., 2002. Oxidative stress, mitochondrial DNA mutation, and impairment of antioxidant enzymes in aging. Experimental biology and medicine 227, 671-682.
Weidner, K.M., Sachs, M., Birchmeier, W., 1993. The Met receptor tyrosine kinase transduces motility, proliferation, and morphogenic signals of scatter factor/hepatocyte growth factor in epithelial cells. Journal of Cell Biology 121, 145-154.
Weinreb, R.N., Bloom, E., Baxter, J.D., Alvarado, J., Lan, N., O'Donnell, J., Polansky, J.R., 1981. Detection of glucocorticoid receptors in cultured human trabecular cells. Investigative Ophthalmology & Visual Science 21, 403-407.
Weinreb, R.N., Ryder, M.I., 1990. Insitu Localization of Cytoskeletal Elements in the Human Trabecular Meshwork and Cornea. Investigative Ophthalmology & Visual Science 31, 1839-1847.
Weinreb, R.N., Ryder, M.I., Polansky, J.R., 1986. The cytoskeleton of the cynomolgus monkey trabecular cell. II. Influence of cytoskeleton-active drugs. Investigative Ophthalmology & Visual Science 27, 1312-1317.
Welge-Lussen, U., May, C.A., Lutjen-Drecoll, E., 2000. Induction of tissue transglutaminase in the trabecular meshwork by TGF-beta 1 and TGF-beta 2. Investigative Ophthalmology & Visual Science 41, 2229-2238.
Welge-Lussen, U., May, C.A., Neubauer, A.S., Priglinger, S., 2001. Role of tissue growth factors in aqueous humor homeostasis. Current Opinion in Ophthalmology 12, 94-99.
Weng, J., Liang, Q., Mohan, R.R., Li, Q., Wilson, S.E., 1997. Hepatocyte growth factor, keratinocyte growth factor, and other growth factor-receptor systems in the lens. Investigative Ophthalmology & Visual Science 38, 1543-1554.
Wiederholt, M., 1998. Direct involvement of trabecular meshwork in the regulation of aqueous humor outflow. Current Opinion in Ophthalmology 9, 46-49.
Wiederholt, M., Bielka, S., Schweig, F., Lutjen-Drecoll, E., Lepple-Wienhues, A., 1995. Regulation of outflow rate and resistance in the perfused anterior segment of the bovine eye. Experimental Eye Research 61, 223-234.
Wiederholt, M., Schafer, R., Wagner, U., Lepple-Wienhues, A., 1996. Contractile response of the isolated trabecular meshwork and ciliary muscle to cholinergic and adrenergic agents. German journal of ophthalmology 5, 146-153.
Wiederholt, M., Thieme, H., Stumpff, F., 2000. The regulation of trabecular meshwork and ciliary muscle contractility. Progress in Retinal and Eye Research 19, 271-295.
Williams, R.D., Novack, G.D., van Haarlem, T., Kopczynski, C., Group, A.R.P.A.S., 2011. Ocular hypotensive effect of the Rho kinase inhibitor AR-12286 in patients with glaucoma and ocular hypertension. American Journal of Ophthalmology 152, 834-841 e831.
Wirtz, M.K., Bradley, J.M., Xu, H., Domreis, J., Nobis, C.A., Truesdale, A.T., Samples, J.R., Van Buskirk, E.M., Acott, T.S., 1997. Proteoglycan expression by human trabecular meshworks. Current Eye Research 16, 412-421.
Wolff, E., 1976. Wolff's anatomy of the eye and orbit.
Wolff, E., Tripathi, R.C., Tripathi, B.J., Bron, A.J., Warwick, R., 1997. Wolff's Anatomy of the eye and orbit, 8th ed. Chapman & Hall Medical, London ; New York.
Wood, J.M., Lacherez, P., Black, A.A., Cole, M.H., Boon, M.Y., Kerr, G.K., 2011. Risk of falls, injurious falls, and other injuries resulting from visual impairment among older

adults with age-related macular degeneration. Investigative Ophthalmology & Visual Science 52, 5088-5092.
Wordinger, R.J., Clark, A.F., 1999. Effects of glucocorticoids on the trabecular meshwork: Towards a better understanding of glaucoma. Progress in Retinal and Eye Research 18, 629-667.
Wordinger, R.J., Clark, A.F., Agarwal, R., Lambert, W., McNatt, L., Wilson, S.E., Qu, Z., Fung, B.K.K., 1998. Cultured human trabecular meshwork cells express functional growth factor receptors. Investigative Ophthalmology & Visual Science 39, 1575-1589.
Wordinger, R.J., Fleenor, D.L., Hellberg, P.E., Pang, I.H., Tovar, T.O., Zode, G.S., Fuller, J.A., Clark, A.F., 2007. Effects of TGF-beta2, BMP-4, and gremlin in the trabecular meshwork: implications for glaucoma. Investigative Ophthalmology & Visual Science 48, 1191-1200.
Wrana, J.L., Attisano, L., Carcamo, J., Zentella, A., Doody, J., Laiho, M., Wang, X.F., Massague, J., 1992. TGF beta signals through a heteromeric protein kinase receptor complex. Cell 71, 1003-1014.
Wrana, J.L., Attisano, L., Wieser, R., Ventura, F., Massague, J., 1994. Mechanism of activation of the TGF-beta receptor. Nature 370, 341-347.
Wu, G., Chen, Y.G., Ozdamar, B., Gyuricza, C.A., Chong, P.A., Wrana, J.L., Massague, J., Shi, Y., 2000. Structural basis of Smad2 recognition by the Smad anchor for receptor activation. Science 287, 92-97.
WuDunn, D., 2001. The effect of mechanical strain on matrix metalloproteinase production by bovine trabecular meshwork cells. Current Eye Research 22, 394-397.
WuDunn, D., 2009. Mechanobiology of trabecular meshwork cells. Experimental Eye Research 88, 718-723.
Wyllie, A.H., Kerr, J.F., Currie, A.R., 1980. Cell death: the significance of apoptosis. International review of cytology 68, 251-306.
Yamamoto, N., Itonaga, K., Marunouchi, T., Majima, K., 2005. Concentration of transforming growth factor beta2 in aqueous humor. Ophthalmic Research 37, 29-33.
Yamazaki, Y., Matsunaga, H., Nishikawa, M., Ando, A., Kaneko, S., Okuda, K., Wada, M., Ito, S., Matsumura, M., 2007. Senescence in cultured trabecular meshwork cells. British Journal of Ophthalmology 91, 808-811.
Yang, H., Thompson, H., Roberts, M.D., Sigal, I.A., Downs, J.C., Burgoyne, C.F., 2011. Deformation of the early glaucomatous monkey optic nerve head connective tissue after acute IOP elevation in 3-D histomorphometric reconstructions. Investigative Ophthalmology & Visual Science 52, 345-363.
Yoo, J., Kambara, T., Gonda, K., Higuchi, H., 2008. Intracellular imaging of targeted proteins labeled with quantum dots. Experimental Cell Research 314, 3563-3569.
Yu, A.L., Birke, K., Moriniere, J., Welge-Lussen, U., 2010. TGF-beta 2 Induces Senescence-Associated Changes in Human Trabecular Meshwork Cells. Investigative Ophthalmology & Visual Science 51, 5718-5723.
Yu, A.L., Fuchshofer, R., Kampik, A., Welge-Lussen, U., 2008. Effects of oxidative stress in trabecular meshwork cells are reduced by prostaglandin analogues. Investigative Ophthalmology & Visual Science 49, 4872-4880.
Yue, B.Y., Elner, V.M., Elner, S.G., Davis, H.R., 1987. Lysosomal enzyme activities in cultured trabecular-meshwork cells. Experimental Eye Research 44, 891-897.
Yue, B.Y., Elvart, J.L., 1987. Biosynthesis of glycosaminoglycans by trabecular meshwork cells in vitro. Current Eye Research 6, 959-967.

Yue, B.Y.J.T., 1996. The extracellular matrix and its modulation in the trabecular meshwork. Survey of Ophthalmology 40, 379-390.
Yue, B.Y.J.T., Lin, C.C.L., Fei, P.F., Tso, M.O.M., 1984. Effects of Chondroitin Sulfate on Metabolism of Trabecular Meshwork. Experimental Eye Research 38, 35-44.
Yun, A.J., Murphy, C.G., Polansky, J.R., Newsome, D.A., Alvarado, J.A., 1989. Proteins secreted by human trabecular cells. Glucocorticoid and other effects. Investigative Ophthalmology & Visual Science 30, 2012-2022.
Zhang, J.D., Cousens, L.S., Barr, P.J., Sprang, S.R., 1991. Three-dimensional structure of human basic fibroblast growth factor, a structural homolog of interleukin 1 beta. Proceedings of the National Academy of Sciences of the United States of America 88, 3446-3450.
Zhang, X., Ognibene, C.M., Clark, A.F., Yorio, T., 2007. Dexamethasone inhibition of trabecular meshwork cell phagocytosis and its modulation by glucocorticoid receptor beta. Experimental Eye Research 84, 275-284.
Zhao, X., Ramsey, K.E., Stephan, D.A., Russell, P., 2004. Gene and protein expression changes in human trabecular meshwork cells treated with transforming growth factor-beta. Investigative Ophthalmology & Visual Science 45, 4023-4034.
Zhou, E.H., Krishnan, R., Stamer, W.D., Perkumas, K.M., Rajendran, K., Nabhan, J.F., Lu, Q., Fredberg, J.J., Johnson, M., 2012. Mechanical responsiveness of the endothelial cell of Schlemm's canal: scope, variability and its potential role in controlling aqueous humour outflow. Journal of the Royal Society, Interface / the Royal Society 9, 1144-1155.
Zhou, L., Fukuchi, T., Kawa, J.E., Higginbotham, E.J., Yue, B.Y., 1995. Loss of cell-matrix cohesiveness after phagocytosis by trabecular meshwork cells. Investigative Ophthalmology & Visual Science 36, 787-795.
Zhou, L., Li, Y., Yue, B.Y., 1999a. Alteration of cytoskeletal structure, integrin distribution, and migratory activity by phagocytic challenge in cells from an ocular tissue--the trabecular meshwork. In Vitro Cellular & Developmental Biology - Animal 35, 144-149.
Zhou, L., Zhang, S.R., Yue, B.Y., 1996. Adhesion of human trabecular meshwork cells to extracellular matrix proteins. Roles and distribution of integrin receptors. Investigative Ophthalmology & Visual Science 37, 104-113.
Zhou, L.L., Li, Y.H., Yue, B.Y.J.T., 1999b. Oxidative stress affects cytoskeletal structure and cell-matrix interactions in cells from an ocular tissue: The trabecular meshwork. Journal of Cellular Physiology 180, 182-189.
Zhuo, Y.H., He, Y., Leung, K.W., Hou, F., Li, Y.Q., Chai, F., Ge, J., 2010. Dexamethasone disrupts intercellular junction formation and cytoskeleton organization in human trabecular meshwork cells. Molecular Vision 16, 61-71.
Zong, H., Madden, A., Ward, M., Mooney, M.H., Elliott, C.T., Stitt, A.W., 2010. Homodimerization is essential for the receptor for advanced glycation end products (RAGE)-mediated signal transduction. Journal of Biological Chemistry 285, 23137-23146.